12 SYNTHESIS: GENETIC MODEL FOR THE FORMATION OF THE WATERLOO VHMS DEPOSIT

The polymetallic Waterloo VHMS deposit represents a small, but high-grade base metal resource of 243,500 tonnes ore grading 3.8 % Cu, 13.8 % Zn, 3.0 % Pb, 74 g/t Ag, and 1.2 g/t Au. The deposit is hosted by volcanic rocks belonging to the Seventy Mile Range Group that forms a major relic of Cambro-Ordovician back-arc basin volcanism at the northern end of the Tasman Fold Belt System.

The development of the back-arc basin at the eastern margin of the Australian continent was initiated in response to the subduction of oceanic crust in the Early Cambrian. Initial subsidence of the attenuated Precambrian continental lithosphere was accompanied by the rapid deposition of the Puddler Creek Formation, a thick (maximum stratigraphic thickness of 9,000 m) largely continent-derived volcanic and sedimentary package containing a small volume of basalt and andesite. An increase of the thermal gradient was responsible for the subsequent formation of voluminous crustal melts that erupted as the Mount Windsor Formation rhyolites and dacites (maximum stratigraphic thickness of 3,500 m). Volcanism during the following stage of back-arc basin development was produced by melting of variably modified mantle sources. The mantle-derived volcanism persisted for a relatively long period of time and resulted in the deposition of the Trooper Creek Formation, a thick sequence (maximum stratigraphic thickness of 4,000 m) of compositionally and texturally diverse volcaniclastic lithofacies that are intercalated with coherent volcanic units and non-volcanic sedimentary facies. Ceasing of the volcanic activities during the Lower Ordovician was accompanied by the deposition of the Rollston Range Formation that represents a sequence of volcanic-derived sandstone and mudstone (maximum stratigraphic thickness of 1,000 m).

The formation of VHMS deposits was restricted to the Ordovician (~470 to 475 Ma) period of mantle-derived volcanism resulting in the deposition of the Trooper Creek Formation. This stratigraphic control on mineralisation suggests that base metal deposits only formed at a specific time of the magmatic evolution of the back-arc basin. Moreover, the VHMS deposits of the district occur only in three stratigraphic intervals of the Trooper Creek Formation. The oldest known deposits are located at the contact between the Mount Windsor Formation and the overlying Trooper Creek Formation (Thalanga-West 45 horizon). The central unit of the Trooper Creek Formation (Waterloo horizon) is an additional host to mineralisation. The youngest mineralisation of the district occurs in the upper unit of the Trooper Creek Formation close to the contact to the Rollston Range Formation (Liontown-Highway/Reward horizon). The deposits in the central and upper units of the Trooper Creek Formation appear to be located in the hanging wall of major graben margin faults indicating that mineralisation was bound to specific extensional intrabasinal scale settings.

The marine palaeogeographic setting of volcanism is interpreted to have varied spatially and temporally during deposition of the Trooper Creek Formation and the formation of the massive sulphide deposits. The marine environment was possibly characterised

by scattered shallow-water areas and islands surrounded by relatively deep sea. The Waterloo area itself represented a depocenter at the time of massive sulphide formation that was probably located in a relatively deep marine environment. Sedimentation in the Waterloo area was controlled by derivation of volcanic debris from surrounding topographically higher areas and downslope distribution by gravity-driven subaqueous mass flows.

The Waterloo area was initially dominated by andesitic volcanism as recorded by the non-explosive near-vent andesitic facies association occurring in the stratigraphic footwall of the deposit. The andesite-dominated facies association comprises coherent volcanic units and less abundant *in situ* hyaloclastite. The andesite is interpreted to have formed shallow sub-seafloor intrusions and lavas venting at the ancient seafloor. In total, a considerable volume of lava (>0.04 km^3 constrained by drilling) accumulated before the andesitic volcanism ceased (Figure 12-1a).

The onset of hydrothermal activities in the Waterloo area occurred either after cessation of the andesitic volcanism or at the waning stage of the volcanic activities as evidenced by the absence of unaltered andesitic emplacement units in the immediate footwall to the massive sulphides. The blanket-like mineralisation probably formed at the seafloor by exhalative processes. The massive sulphide accumulations were principally composed of pyrite, sphalerite, and chalcopyrite, minor galena and tennantite, and contained traces of altaite, bornite, calaverite, cassiterite, electrum, hessite, and petzite (Figure 12-1b).

The massive sulphide precipitation was located above a zone of poorly focused discharge because fluid flow through the lava-dominated footwall succession was largely diffuse and initially controlled by small fissures and fractures in the host rocks, contacts between individual andesitic emplacement units, or local brecciated intervals. However, the permeability of the footwall volcanic rocks was modified trough time as a result of the interaction of the volcanic rocks with the aggressive mineralising hydrothermal fluids.

The hydrothermal alteration resulted in substantial textural, mineralogical, and geochemical modifications of the volcanic rocks in the footwall of the Waterloo deposit involving complex reactions of the fluids with the glassy or (partly) crystalline groundmass as well as with the phenocrysts contained in the volcanic rocks. The quantitatively most important changes in the upflow zones of the aggressive hydrothermal fluids were related to the conversion of primary igneous plagioclase to secondary muscovite and quartz by the combined effects of hydrogen and potassium metasomatism. The alteration of the volcanic rocks in the upflow zones of the hydrothermal fluids was, therefore, principally linked to the acidity of the mineralising hydrothermal fluids. Acid alteration in the upflow zones was accompanied by silicification because the hydrothermal fluids cooled during their ascent to the seafloor. Thus, alteration in the upflow zones resulted in the development of the silicic alteration facies (Figure 12-1b).

Outward percolation of hydrothermal fluids into the volcanic rocks surrounding the major upflow zones caused the development of the phyllic alteration facies that envelops the silicic core. Percolation of the hydrothermal fluids into the outer alteration halo was accompanied by neutralisation of the acids,

Figure 12-1: Schematic reconstruction of the evolution of the Waterloo sequence and the hydrothermal system resulting in the formation of the massive sulphide deposit.

(a) Formation of an andesitic-dominated non-explosive, near-vent facies association

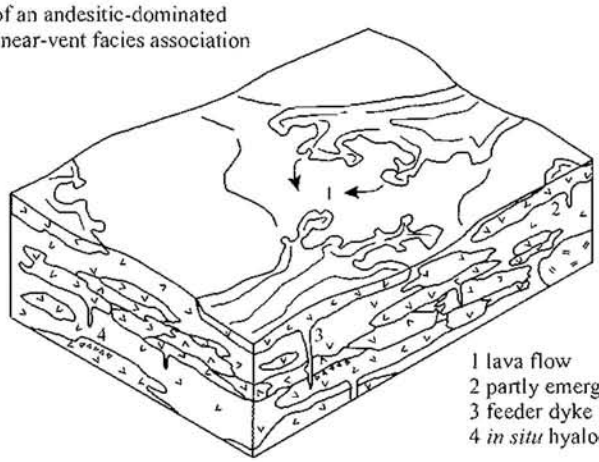

1 lava flow
2 partly emergent sill
3 feeder dyke
4 *in situ* hyaloclastite

(b) Waning of andesitic volcanism and formation of massive sulphides at the seafloor

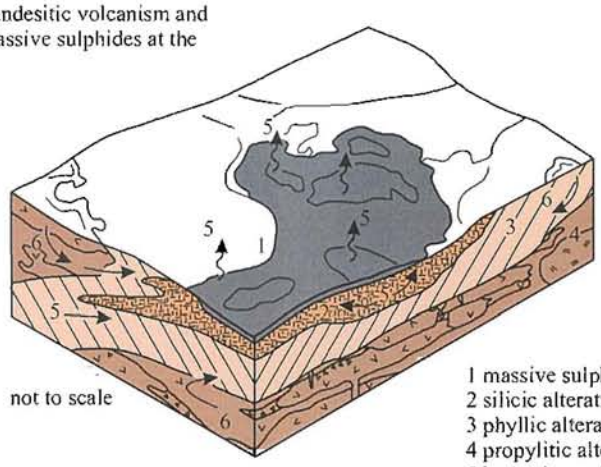

1 massive sulphides
2 silicic alteration facies
3 phyllic alteration facies
4 propylitic alteration facies
5 hydrothermal fluid flow
6 circulation of seawater

(c) Burial of the massive sulphides by mass-flow deposition of the coarse quartz-feldspar crystal-rich sandstone and breccia facies

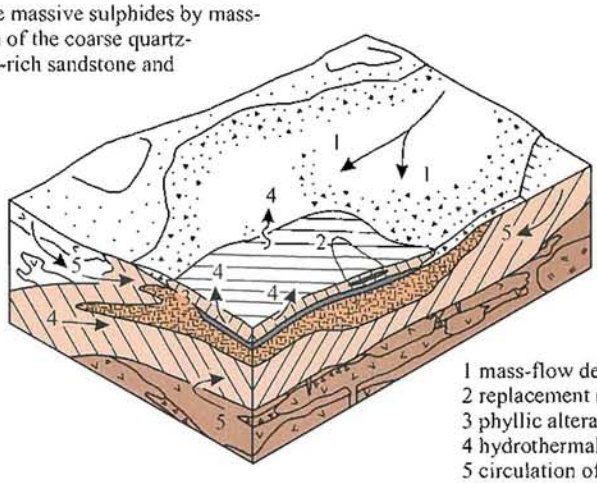

1 mass-flow deposition
2 replacement massive sulphides
3 phyllic alteration
4 hydrothermal fluid flow
5 circulation of seawater

(d) Emplacement of the partially extrusive dacite cryptodome and waning of hydrothermal activities

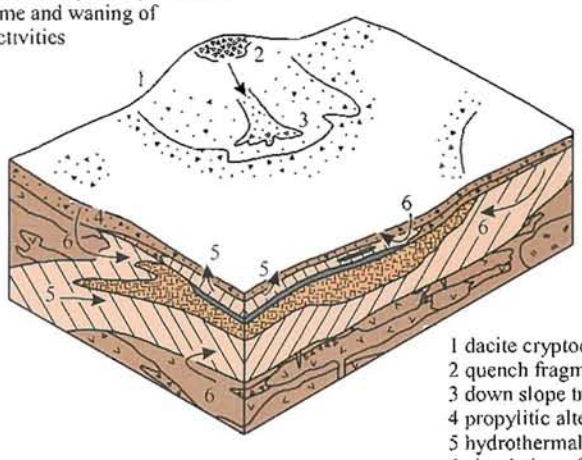

1 dacite cryptodome
2 quench fragmentation
3 down slope transport of fragments
4 propylitic alteration
5 hydrothermal fluid flow
6 circulation of seawater

(e) Period of relatively quite sedimentation and emplacement of syn-sedimentary basaltic to andesitic emplacement units

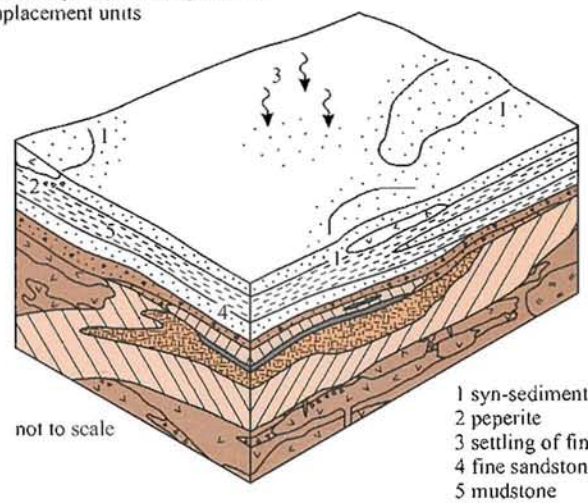

not to scale

1 syn-sedimentary sill
2 peperite
3 settling of fine volcanic detritus
4 fine sandstone
5 mudstone

(f) Mass-flow deposition of the coarse feldspar-quartz sandstone and breccia facies

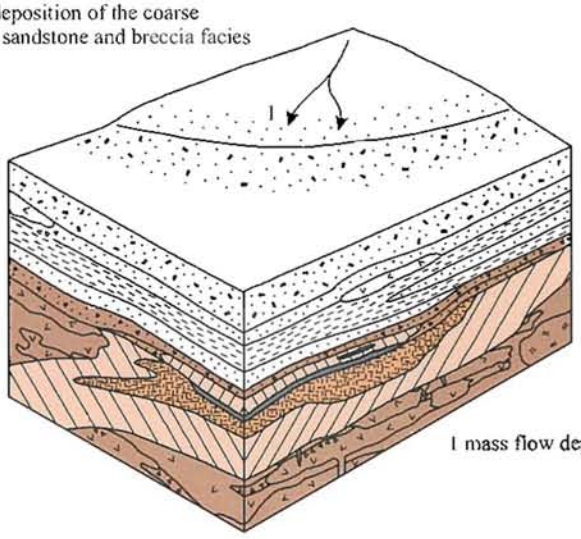

1 mass flow deposition

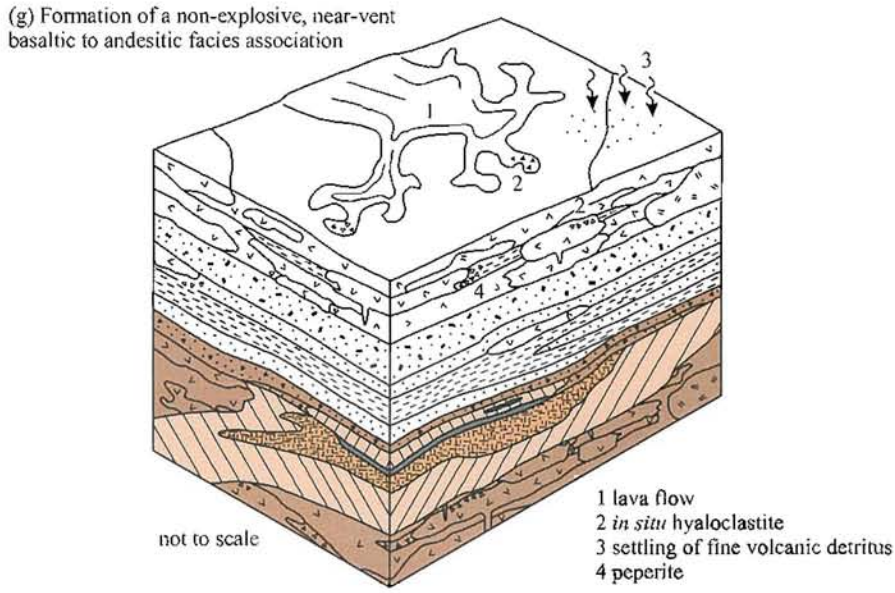

cooling of the hydrothermal fluids, and mixing with seawater percolating into the zones surrounding the thermal upflow. In particular rapid neutralisation of the strong acids must have occurred because chlorite represents a major alteration product in phyllic-altered rocks. Moreover, the reactivity of CO_2 with respect to hydrogen metasomatism increased with increasing distance to the major upflow zones as evidenced by the replacement of primary plagioclase by calcite and the occurrence of REE carbonates in the outer alteration halo (Figure 12-1b). The high H_2S content of the hydrothermal fluids caused a sulphidisation of the volcanic host rocks by converting primary ilmenite and titanomagnetite to secondary pyrite and rutile. Moreover, divalent iron contained in rock-forming silicates and the volcanic glass matrix was redistributed into secondary sulphides.

Mineralogical changes in the alteration halo were not only related to the upflow and outward percolation of aggressive hydrothermal fluids, but also resulted from seawater penetrating downwards into the zones surrounding the thermal upflow. The involvement of seawater in the wall rock alteration caused the conversion of primary plagioclase to albite and resulted in the precipitation of Na-rich micas (paragonite and intermediate Na/K mica) at the expense of previously formed hydrothermal K-rich micas (muscovite and phengitic muscovite). The entrainment of seawater was, therefore, responsible for the pronounced Na metasomatism affecting the volcanic rocks of the outer alteration halo and played an important role in the development of the pronounced mineralogical and geochemical zonation of the alteration halo (Figure 12-1b).

Precipitation of massive sulphides at the seafloor did not occur for a prolonged period of time because the mineralisation was buried by a mass flow-derived coarse volcaniclastic sediment. The coarse quartz-feldspar crystal-rich sandstone and breccia facies records broadly contemporaneous dacitic to rhyolitic volcanism outside the study area (Figure 12-1c).

Volcanism within the study area also shifted to a dacitic composition as evidenced by the

emplacement of a feldspar-porphyritic dacitic cryptodome into the still wet and unconsolidated coarse quartz-feldspar crystal-rich sandstone and breccia overlying the massive sulphides. The dacitic lava locally breached the sediment and emerged at the ancient seafloor. The emerging parts of the dacitic cryptodome were quench fragmented in contact with the ambient cold seawater and fragments of the quenched dacite were transported down slope and incorporated into the surrounding coarse sediments. Collapse and local reworking of jointed and/or quench fragmented dacite also resulted in the formation of talus breccia proximal to the related coherent facies. The cryptodome had a diameter of more than 200 m and was at least 50 m thick (Figure 12-1d).

The hydrothermal system continued to operate after mass flow deposition of the coarse quartz-feldspar crystal-rich sandstone and breccia and the emplacement of the partly emergent cryptodome as indicated by the hydrothermal alteration of the volcanic rocks in the hanging wall of the massive sulphides. However, intense alteration extends only several metres into the hanging wall and fades in intensity with increasing distance to ore indicating that burial of the massive sulphides broadly coincided with the waning stage of the hydrothermal activities (Figure 12-1d).

Burial of the massive sulphides was accompanied by a change in the style of mineralisation because processes of replacement and infilling became important. Replacement and infiltration of the coarse volcaniclastic sediment by impregnation ore was common and tongues of massive sulphides were locally formed by replacement of the permeable rock. Sub-seafloor cooling of the ascending hydrothermal fluids by mixing with seawater entrained into the unconsolidated sediment resulted in the precipitation of secondary minerals within the pore space and also caused the extensive replacement of primary volcaniclastic components. Hanging wall alteration was accompanied by the formation of a wide range of alteration products (*e.g.*, ankerite, barite, celestine, dolomite, fluorite, hematite, and kaolinite) that are typically not present in the upflow zones of the hydrothermal fluids in the footwall of the deposit (Figure 12-c,d).

The hydrothermal activities and the dacitic volcanism in the Waterloo area were followed by a prolonged period of relatively quite sedimentation resulting in the formation of a thick package consisting of fine volcaniclastic material. The occurrence of syn-sedimentary basaltic to andesitic sills in the hanging wall position documents that volcanism within the Waterloo area shifted back to more basic compositions (Figure 12-1e). The period of relatively quite sedimentation was followed by the mass flow deposition of the coarse feldspar-quartz sandstone and breccia facies. The deposition of this coarse volcaniclastic facies records broadly contemporaneous, probably explosive, felsic volcanic activities taking place outside the study area (Figure 12-1f).

The upper part of the hanging wall sequence records the onset of a second period of intense non-explosive, near-vent basaltic to andesitic volcanism in the Waterloo area. As in the case of the footwall proximal facies, a relatively large volume (>0.03 km^3 constrained by drilling) of basic to intermediate lavas was accumulated in a relatively short period of time. However, the observed intercalations of thin layers of mudstone and fine sandstone indicate that background sedimentation occurred (Figure 12-1g).

After deposition of the Waterloo sequence, the volcanic rocks were subject to regional alteration that was caused by the combined effects of devitrification, hydration, burial diagenesis, seawater interaction, regional metamorphism of the lower greenschist facies, and deformation. A regional deforma-

tion event in the Mid- to Late Ordovician tilted the volcanic rocks into a subvertical position. This folding event also resulted in the development of an axial plane cleavage that is particularly well developed in a high strain zone surrounding the massive sulphides. The spatial relationship between the folded bedding plane and the axial plane cleavage as well as the south facing of the bedding of volcaniclastic sediments indicate that the Waterloo sequence is located at the southern limb of a major east-west trending antiform. This antiform has a shallow plunge to the west. The volcanic rocks hosting the massive sulphides were affected by two subsequent faulting events. Early steeply dipping ENE striking faults interpreted to be Silurian or Devonian were accompanied by significant dip-slip normal movement, whereas younger strike-slip faults have no affect to the geometry of the Waterloo sequence.

The results of the present study suggest that the relationships between massive sulphide formation and volcanism can be constrained by integrating volcanological studies on the host rock sequence with mineralogical and geochemical investigations of the hydrothermally altered rocks. The reconstruction of the volcanological evolution has shown that the massive sulphide formation coincided with a relatively short period of felsic volcanism recorded by the deposition of the coarse quartz-feldspar crystal-rich sandstone and breccia facies and the emplacement of the partially emergent dacite cryptodome in the immediate hanging wall of the massive sulphides. The felsic volcanism at the ancient seafloor was associated with magmatic activities at depth that is suggested to have played an important role in the mineralising process by providing heat to drive the hydrothermal system and by possibly contributing chemical components to the mineralising fluids. In particular, the hydrothermal fluids may have contained acidity controlling species of magmatic origin.

REFERENCES

Adamides NG (1987) Diverse modes of occurrence of Cyprus sulphide deposits and comparison with recent analogues. *In* PT Robinson et al. (eds) Cyprus crustal study project: Initial report holes CY-2 and 2a. Geol Surv Can Pap 85-29, pp. 153-168.

Aitchison J (1986) The statistical analysis of compositional data. Chapman and Hall.

Albarède F, Michard A, Minster JF & Michard G (1981) $^{87}Sr/^{86}Sr$ ratios in hydrothermal waters and deposits from the East Pacific Rise at 21°N. Earth Planet Sci Lett 55: 229-236.

Allen RL (1988) False pyroclastic textures in altered silicic lavas, with implications for volcanic-associated mineralization. Econ Geol 83: 1424-1446.

Allen RL (1992) Reconstruction of the tectonic, volcanic, and sedimentary setting of strongly deformed Zn-Cu massive sulfide deposits at Benambra, Victoria. Econ Geol 87: 825-854.

Allen RL (1994) Synvolcanic, subseafloor replacement model for Rosebery and other massive sulphide ores. *In* Contentious issues in Tasmanian geology. Geol Soc Austral Tasm Div, pp. 89-91.

Allen RL & Hunns SR (1990) Excursion Guide E1. The Mount Read Volcanics and related ore deposits. *In* Gondwana: Terranes and resources. Tenth Australian Geological Convention. Geol Soc Austral Abstr 25. Univ of Tasmania, pp. 15-27.

Allen RL, Weihed P & Svenson SA (1996) Setting of Zn-Cu-Au-Ag massive sulfide deposits in the evolution and facies architecture of a 1.9 Ga marine volcanic arc, Skellefte district, Sweden. Econ Geol 91: 1022-1053.

Almodóvar GR, Sáez R, Pons JM, Maestre A, Toscano M & Pascual E (1998) Geology and genesis of the Aznalcóllar massive sulphide deposits, Iberian Pyrite Belt, Spain. Mineral Deposita 33: 111-136.

Alt JC (1994) A sulfur isotopic profile through the Troodos ophiolite, Cyprus: Primary composition and the effects of seawater hydrothermal alteration. Geochim Cosmochim Acta 58: 1825-1840.

Alt JC (1995) Subseafloor processes in mid-ocean ridge hydrothermal systems. Geophys Monogr Ser 91: 85-114.

Alt JC & Anderson TF (1991) Mineralogy and isotopic composition of sulfur in layer 3 gabbros from the Indian Ocean, hole 735B. Proc ODP Sci Res 118: 113-125.

Alt JC, Anderson TF & Bonnell L (1989) The geochemistry of sulphur in a 1.3 km section of hydrothermally altered oceanic crust, DSDP hole 504B. Geochim Cosmochim Acta 53: 1011-1023.

Alt JC, Zuleger E & Erzinger J (1995) Mineralogy and stable isotopic composition of the hydrothermally altered lower sheeted dike complex, Hole 504B, Leg 140. Proc ODP Sci Res 140: 155-166.

Aoki M, Matsumoto T, Kimura M & Fujioka K (1993) Hydrothermal activity and topographic features in the western part of the Minami-Ensei Knoll, northern Okinawa Trough. Proc JAMSTEC Symp Deep Sea Res 9: 309-320.

Appel PWU (1979) Stratabound copper sulfides in a banded iron-formation and in basaltic tuffs in the Early Precambrian Isua supracrustal belt, West Greenland. Econ Geol 74: 45-52.

Arribas A, Jr (1995) Characteristics of high-sulfidation epithermal deposits, and their relation to magmatic fluid. Mineral Ass Can Short Course Ser 23: 419-454.

Bain JHC & Draper JJ (1997) North Queensland geology. AGSO Bull 240. Austral Geol Surv Organ. Paragon Printers.

Baker ET & Lupton JE (1990) Changes in submarine hydrothermal ^{3}He/heat ratios as an indicator of magmatic/tectonic activity. Nature 346: 556-558.

Baker ET, Lavelle JW, Feely RA, Massoth GJ, Walker SL & Lupton JE (1989) Episodic venting of hydrothermal fluids from the Juan de Fuca Ridge. J Geophys Res 94: 9237-9250.

Baker ET, Feely RA, Mottl MJ, Sansone FT, Wheat CG, Resing JA & Lupton JE (1994) Hydrothermal plumes along the East Pacific Rise, 8°40' to 11°50'N: Plume distribution and relationship to the apparent magmatic budget. Earth Planet Sci Lett 128: 1-17.

Baker ET, German CR & Elderfield H (1995) Hydrothermal plumes over spreading-center axes: Global distribution and geological inferences. Geophys Monogr Ser 91: 47-71.

Barley ME (1992) A review of Archean volcanic-hosted massive sulfide and sulfate mineralization in western Australia. Econ Geol 87: 855-872.

Barrett TJ, Cattalani S & MacLean WH (1993) Volcanic lithogeochemistry and alteration at the Delbridge massive sulfide deposit, Noranda, Quebec. J Geochem Expl 48: 135-173.

Barrett TJ, MacLean WH & Tennant SC (2001) Volcanic sequence and alteration at the Parys Mountain volcanic-hosted massive sulfide deposit, Wales, United Kingdom: Applications of immobile element lithogeochemistry. Econ Geol 96: 1279-1305.

Barrie CT & Hannington MD (1999) Classification of volcanic-associated massive sulfide deposits based on host-rock composition. Rev Econ Geol 8: 1-11.

Barrie CT, Ludden JN & Green TH (1993) Geochemistry of volcanic rocks associated with Cu-Zn and Ni-Cu deposits in the Abitibi subprovince. Econ Geol 88: 1341-1358.

Beams SD (1993) Polymetallic massive sulphide exploration case histories Mt. Windsor Volcanic Belt, North Queensland. *In* RA Henderson (ed) Guide to the economic geology of the Charters Towers region, northeastern Queensland. Geol Soc Austral Field Excursion Guidebook. James Cook Univ, pp. 75-79.

Beams SD & Dronseika EV (1995) The exploration history, geology and geochemistry of the polymetallic Reward and Highway deposits, Mt Windsor Subprovince. *In* 17th International Geochemical Exploration Symposium. Mineral deposits of northeast Queensland: Geology and geochemistry. James Cook Univ, pp. 137-153.

Beams SD & Hartley JS (1990) Geology and mineralisation of the Mt Windsor volcanic belt, North Queensland. *In* Gondwana: Terranes and resources. Tenth Australian Geological Convention. Geol Soc Austral Abstr 25. Univ of Tasmania, p. 37.

Beams SD, Laing WP & O'Neill DM (1989) The exploration history and geology of the polymetallic Reward deposit, Mt Windsor Volcanic Belt, North Queensland. *In* North Queensland Gold'89 Conference. Austral Inst Mining Metallurgy, pp. 95-102.

Beams SD, Laurie JP & O'Neill DM (1990) Reward polymetallic sulphide deposit. *In* FE Hughes (ed) Geology of the mineral deposits of Australia and Papua New Guinea. Austral Inst Mining Metallurgy, pp. 1539-1543.

Beams SD, Dronseika EV & Doyle MG (1998) The exploration history, geology and geochemistry of the polymetallic Highway-Reward deposit, Mt Windsor Subprovince. *In* SD Beams (ed) Economic geology of northeast Queensland, the 1998 perspective. Geol Soc Austral, pp. 189-206.

Bell H (1982) Strata-bound sulfide deposits, wall-rock alteration, and associated tin-bearing minerals in the Carolina Slate Belt, South Carolina and Georgia. Econ Geol 77: 294-311.

Bergman Weihed J, Bergström U, Billström K & Weihed P (1996) Geology, tectonic setting, and origin of the Paleoproterozoic Boliden Au-Cu-As deposit, Skellefte district, northern Sweden. Econ Geol 91: 1073-1097.

Bergmann J & Kleeberg R (1998) Rietveld analysis of disordered layer silicates. *In* R Delhez & EJ Mittemeijer (eds) Proc Eur Powder Diff Conf EPDIC 5. Mat Sci Forum 278-281. Trans Tech Pub, pp. 300-305.

Bergmann J, Kleeberg R & Taut T (1994) A new structure refinement and quantitative phase analysis method basing on predetermined true peak profiles. Z Kristallogr Suppl 8: 580.

Bergmann J, Kleeberg R, Taut T & Haase A (1997) Quantitative phase analysis using a new Rietveld algorithm - Assisted by improved stability and convergence behavior. Advances X-Ray Anal 40: 425.

Bergmann J, Friedel P & Kleeberg R (1998) BGMN - A new fundamental parameters based Rietveld program for laboratory X-ray sources, its use in quantitative analysis and structure investigations. CPD Newslett 20: 5-8.

Bergmann J, Friedel P & Kleeberg R (2000a) Handling of unusual instrumental profiles by the BGMN Rietveld program. *In* R Delhez & EJ Mittemeijer (eds) Proc Eur Powder Diff Conf EPDIC 6. Mat Sci Forum 321-324. Trans Tech Pub, pp. 192-197.

Bergmann J, Kleeberg R, Haase A & Breidenstein B (2000b) Advanced fundamental parameters model for improved profile analysis. *In* R Delhez & EJ Mittemeijer (eds) Proc Eur Powder Diff Conf EPDIC 6. Mat Sci Forum 347-349. Trans Tech Pub, pp. 303-308.

Bergmann J, Monecke T & Kleeberg R (2001) Alternative algorithm for the correction of preferred orientation in Rietveld analysis. J Appl Cryst 34: 16-19.

Berry RF (1989) Structure of the Mount Windsor sub-province. Initial report - September 1989. *In* J Pongratz & RR Large (eds) Mount Windsor Volcanics project. Report. CODES. Univ of Tasmania, pp. 51-73.

Berry RF (1991) Structure of the Mount Windsor subprovince. *In* J Pongratz & RR Large (eds) Geological controls on VMS mineralisation in the Mt Windsor Volcanic Belt. Report. CODES. Univ of Tasmania, pp. 1-22.

Berry RF & Crawford AJ (1988) The tectonic significance of Cambrian allochthonous mafic-ultramafic complexes in Tasmania. Austral J Earth Sci 35: 523-533.

Berry RF, Huston DL, Stolz AJ, Hill AP, Beams SD, Kuronen U & Taube A (1992) Stratigraphy, structure, and volcanic-hosted mineralization of the Mount Windsor Subprovince, North Queensland, Australia. Econ Geol 87: 739-763.

Bettison-Varga L & MacKinnon IDR (1997) The role of randomly mixed-layered chlorite/smectite in the transformation of smectite to chlorite. Clays Clay Minerals 45: 506-516.

Bettison-Varga L, Varga RJ & Schiffman P (1992) Relation between ore-forming hydrothermal systems and extensional deformation in the Solea Graben spreading center, Troodos ophiolite, Cyprus. Geology 20: 987-990.

Bettison-Varga L, Schiffman P & Janecky DR (1995) Fluid-rock interaction in the hydrothermal upflow zone of the Solea graben, Troodos ophiolite, Cyprus. Geol Soc Amer Spec Pap 296: 81-100.

Bi X, Cornell DH & Hu R (2002) REE composition of primary and altered feldspar from the mineralized alteration zone of alkaline intrusive rocks, western Yun-

nan Province, China. Ore Geol Rev 19: 69-78.

Binns RA & Scott SD (1993) Actively forming polymetallic sulfide deposits associated with felsic volcanic rocks in the eastern Manus back-arc basin, Papua New Guinea. Econ Geol 88: 2226-2236.

Bischoff JL & Seyfried WE (1978) Hydrothermal chemistry of seawater from 25° to 350°C. Amer Jour Sci 278: 838-860.

Bish DL & Howard SA (1988) Quantitative phase analysis using the Rietveld method. J Appl Cryst 21: 86-91.

Bish DL & Post JE (1993) Quantitative mineralogical analysis using the Rietveld full-pattern fitting method. Amer Mineral 78: 932-940.

Bish DL & Von Dreele RB (1989) Rietveld refinement of non-hydrogen atomic positions in kaolinite. Clays Clay Minerals 37: 289-296.

Black LP, Seymour DB, Corbett KD, Cox SE, Streit JE, Bottrill RS, Calver CR, Everard JL, Green GR, McClenaghan MP, Pemberton J, Taheri J & Turner NJ (1997) Dating Tasmania's oldest geological events. Record 1997/15, Tasman Develop Resources. Tasman Geol Surv.

Blake RL, Hessevick RE, Zoltai T & Finger LW (1966) Refinement of the hematite structure. Amer Mineral 51: 123-129.

Bodon SB & Valenta RK (1995) Primary and tectonic features of the Currawong Zn-Cu-Pb(-Au) massive sulfide deposit, Benambra, Victoria: Implications for ore genesis. Econ Geol 90: 1694-1721.

Boiron MC, Essarraj S, Sellier E, Cathelineau M, Lespinasse M & Poty B (1992) Identification of fluid inclusions in relation to their host microstructural domains in quartz by cathodoluminescence. Geochim Cosmochim Acta 56: 175-185.

Bostrom K & Peterson MNA (1966) Precipitates from hydrothermal exhalations on the East Pacific Rise. Econ Geol 61: 1258-1265.

Botz R, Winckler G, Bayer R, Schmitt M, Schmidt M, Garbe-Schönberg D, Stoffers P & Kristjansson JK (1999) Origin of trace gases in submarine hydrothermal vents of the Kolbeinsey Ridge, North Iceland. Earth Planet Sci Lett 171: 83-89.

Brauhart CW, Groves DI & Morant P (1998) Regional alteration systems associated with volcanogenic massive sulfide mineralization at Panorama, Pilbara, western Australia. Econ Geol 893: 292-302.

Brauhart CW, Huston DL, Groves DI, Mikucki EJ & Gardoll SJ (2001) Geochemical mass-transfer patterns as indicators of the architecture of a complete volcanic-hosted massive sulfide hydrothermal alteration system, Panorama district, Pilbara, western Australia. Econ Geol 96: 1263-1278.

Brindley GW (1945) The effect of grain or particle size on X-ray reflections from mixed powders and alloys, considered in relation to the quantitative determination of crystalline substances by X-ray methods. Philos Mag 36: 347-369.

Brookfield ME (1993) Neoproterozoic Laurentia-Australia fit. Geology 21: 683-686.

Brostigen G & Kjekshus A (1969) Redetermined crystal structure of FeS_2 (pyrite). Acta Chem Scand 23: 2186-2188.

Browne PRL, Graham IJ, Parker RJ & Wood CP (1992) Subsurface andesite lavas and plutonic rocks in the Rotokawa and Ngatamariki geothermal systems, Taupo Volcanic Zone, New Zealand. J Volcanol Geotherm Res 51: 199-215.

Bull SW & Cas RAF (1989) Volcanic influences in a storm and tide dominated shallow marine depositional system: the Late Permian Broughton Formation, southern Sydney Basin, Kiama, NSW, Australia. Austral J Earth Sci 36: 569-584.

Busby-Spera CJ & White JDL (1987) Variation in peperite textures associated

with differing host-sediment properties. Bull Volcanol 49: 765-775.

Butterfield DA, McDuff RE, Mottl MJ, Lilley MD, Lupton JE & Massoth GJ (1994) Gradients in the composition of hydrothermal fluids from the Endeavour segment vent field: Phase separation and brine loss. J Geophys Res 99: 9561-9583.

Campbell IH, Coad P, Franklin JM, Gorton MP, Scott SD, Sowa J & Thurston PC (1982) Rare earth elements in volcanic rocks associated with Cu-Zn massive sulphide mineralization: A preliminary report. Can J Earth Sci 19: 619-623.

Campbell AC, Bowers TS, Measures CI, Falkner KK, Khadem M & Edmond JM (1988) A time series of vent fluid compositions from 21°N, East Pacific Rise (1979, 1981, 1985), and the Guaymas Basin, Gulf of California (1982, 1985). J Geophys Res 93: 4537-4549.

Cas RAF (1983) Submarine 'crystal-tuffs': Their origin using a Lower Devonian example from southeastern Australia. Geol Mag 120: 471-486.

Cas RAF (1992) Submarine volcanism: Eruption styles, products, and relevance to understanding the host-rock successions to volcanic-hosted massive sulfide deposits. Econ Geol 87: 511-541.

Cathles LM (1993) Oxygen isotope alteration in the Noranda mining district, Abitibi greenstone belt, Quebec. Econ Geol 88: 1483-1511.

Chadwick WW, Jr., Embley RW & Fox CG (1995) SeaBeam depth changes associated with recent lava flows, CoAxial segment, Juan de Fuca Ridge: Evidence for multiple eruptions between 1981-1993. Geophys Res Lett 22: 167-170.

Charlou JL, Fouquet Y, Donval JP, Auzende JM, Jean-Baptiste P, Stievenard M & Michel S (1996) Mineral and gas chemistry of hydrothermal fluids on an ultrafast spreading ridge: East Pacific Rise, 17° to 19°S (Naudur cruise, 1993) phase separation processes controlled by volcanic and tectonic activity. J Geophys Res 101: 15899-15919.

Charlou JL, Donval JP, Douville E, Jean-Baptiste P, Radford-Knoery J, Fouquet Y, Dapoigny A & Stievenard M (2000) Compared geochemical signatures and the evolution of Menez Gwen (37°50'N) and Lucky Strike (37°17'N) hydrothermal fluids, south of the Azores Triple Junction on the Mid-Atlantic Ridge. Chem Geol 171: 49-75.

Chatterjee ND & Flux S (1986) Thermodynamic mixing properties of muscovite-paragonite crystalline solutions at high temperatures and pressures, and their geological applications. J Petrol 27: 677-693.

Chen CTA & Marshall WL (1982) Amorphous silica solubilities IV. Behavior in pure water and aqueous sodium chloride, sodium sulfate, magnesium chloride, and magnesium sulfate solutions up to 350°C. Geochim Cosmochim Acta 46: 279-287.

Chen CH, Lee T, Shieh YN, Chen CH & Hsu WY (1995) Magmatism at the onset of back-arc basin spreading in the Okinawa Trough. J Volcanol Geotherm Res 69: 313-322.

Chiba H, Sakai H, Gamo T, Ishibashi J, Nakashima K, Minami H & Dobashi F (1992) Chemistry and isotopic composition of bubbles emerging from the seafloor at the Minami-Ensei Knoll, Okinawa Trough. Proc JAMSTEC Symp Deep Sea Res 8: 81-87.

Cole JW (1984) Taupo-Rotorua Depression: An ensialic marginal basin of North Island, New Zealand. Geol Soc London Spec Pub 16: 121-135.

Cole JW, Darby DJ & Stern TA (1995) Taupo Volcanic Zone and Central Volcanic Region. Backarc structures of North Island, New Zealand. *In* B Taylor (ed) Backarc basins: Tectonics and magmatism. Plenum Press, pp. 1-28.

Collier J & Sinha M (1990) Seismic images of a magma chamber beneath the Lau

Basin back-arc spreading centre. Nature 346: 646-648.

Comodi P & Zanazzi PF (1995) High-pressure structural study of muscovite. Phys Chem Minerals 22: 170-177.

Converse DR, Holland HD & Edmond JM (1984) Flow rates in the axial hot springs of the East Pacific Rise (21°N): Implications for the heat budget and the formation of massive sulfide deposits. Earth Planet Sci Lett 69: 159-175.

Cook NJ, Halls C & Kaspersen PO (1990) The geology of the Sulitjelma ore field, northern Norway - Some new interpretations. Econ Geol 85: 1720-1737.

Cooper RA (1999) The Ordovician time scale - Calibration of graptolite and conodont zones. Acta Univ Carolinae Geol 43: 1-4.

Corbett KD (1992) Stratigraphic-volcanic setting of massive sulfide deposits in the Cambrian Mount Read Volcanics, Tasmania. Econ Geol 87: 564-586.

Corbett KD (2001) New mapping and interpretations of the Mount Lyell mining district, Tasmania: A large hybrid Cu-Au system with an exhalative Pb-Zn top. Econ Geol 96: 1089-1122.

Corliss JB, Dymond J, Gordon LI, Edmond JM, Von Herzen RP, Ballard RD, Green K, Williams D, Bainbridge A, Crane K & van Andel TH (1979) Submarine thermal springs on the Galápagos Rift. Science 203: 1073-1083.

Craig H, Welhan JA, Kim K, Poreda R & Lupton JE (1994) Geochemical studies of the 21°N EPR hydrothermal fluids. EOS Trans Am Geophys Union 61: 992.

Crawford AJ & Berry RF (1992) Tectonic implications of Late Proterozoic-Early Palaeozoic igneous rock associations in western Tasmania. Tectonophysics 214: 37-56.

Crawford AJ, Corbett KD & Everard JL (1992) Geochemistry of the Cambrian volcanic-hosted massive sulfide-rich Mount Read Volcanics, Tasmania, and some tectonic implications. Econ Geol 87: 597-619.

Dalziel IWD (1991) Pacific margins of Laurentia and East Antarctica-Australia as a conjugate rift pair: Evidence and implications for an Eocambrian supercontinent. Geology 19: 598-601.

Date J, Watanabe Y & Saeki Y (1983) Zonal alteration around the Fukazawa Kuroko deposits, Akita prefecture, northern Japan. Econ Geol Monogr 5: 365-386.

Davidson GJ, Stolz AJ & Eggins SM (2001) Geochemical anatomy of silica iron exhalites: Evidence for hydrothermal oxyanion cycling in response to vent fluid redox and thermal evolution (Mt. Windsor Subprovince, Australia). Econ Geol 96: 1201-1226.

Davis AS & Clague DA (1998) Changes in the hydrothermal system at Loihi Seamount after the formation of Pele's pit in 1996. Geology 26: 399-402.

Day RW, Murray CG & Whitaker WG (1978) The eastern part of the Tasman orogenic zone. Tectonophysics 48: 327-364.

De Jong WF (1927) Marmatit und Christophit. Z Kristallogr 66: 515.

De Ronde CEJ (1995) Fluid chemistry and isotopic characteristics of seafloor hydrothermal systems and associated VMS deposits: Potential for magmatic contributions. Mineral Ass Can Short Course Ser 23: 479-510.

Dear JF (1974) Lower Ordovician graptolites from the Ravenswood area, North Queensland. *In* AK Denmead et al. (eds) The Tasman Geosyncline: A symposium. Geol Soc Austral Queensl Div, pp. 313-317.

Delaney JR, Mogk DW & Mottl MJ (1987) Quartz-cemented breccias from the Mid-Atlantic Ridge: Samples of a high-salinity hydrothermal upflow zone. J Geophys Res 92: 9175-9192.

Des Marais DJ & Moore JG (1984) Carbon and its isotopes in mid-oceanic basaltic glasses. Earth Planet Sci Lett 69: 43-57.

Descarreaux J (1973) A petrochemical study of the Abitibi volcanic belt and its bearing on the occurrences of massive sulphide ores. Can Mining Metallurgical Bull 66: 61-69.

Detrick RS, Harding AJ, Kent GM, Orcutt JA, Mutter JC & Buhl P (1993) Seismic structure of the southern East Pacific Rise. Science 259: 499-503.

Doe BR (1994) Zinc, copper, and lead in mid-ocean ridge basalts and the source rock control on Zn/Pb in ocean-ridge hydrothermal deposits. Geochim Cosmochim Acta 58: 2215-2223.

Dollase WA (1971) Refinement of the crystal structures of epidote, allanite and hancockite. Amer Mineral 56: 447-464.

Doyle MG (1994) Facies architecture of a submarine felsic volcanic centre: Highway-Reward, Mount Windsor Volcanics, Cambro-Ordovician, northern Queensland. *In* RA Henderson & BK Davis (eds) New developments in geology and metallogeny: Northern Tasman orogenic zone. Contrib Econ Geol Res Unit 50. James Cook Univ, pp. 149-150.

Doyle MG (1997) A Cambro-Ordovician submarine volcanic succession hosting massive sulfide mineralisation: Mount Windsor Subprovince, Queensland. Ph.D. Thesis, Univ of Tasmania.

Doyle MG (1998) A syn-sedimentary intrusion-dominated host succession to the Highway-Reward VHMS deposit, Queensland. *In* SD Beams (ed) Economic geology of northeast Queensland, the 1998 perspective. Geol Soc Austral, pp. 207-213.

Doyle MG (2001) Volcanic influences on hydrothermal and diagenetic alteration: Evidence from the Highway-Reward, Mount Windsor Subprovince, Australia. Econ Geol 96: 1133-1148.

Doyle MG & Huston DL (1999) The subsea-floor replacement origin of the Ordovician Highway-Reward volcanic-associated massive sulfide deposit, Mount Windsor Subprovince, Australia. Econ Geol 94: 825-844.

Doyle MG & McPhie J (1994) A silicic submarine syn-sedimentary intrusive-dome-hyaloclastite host sequence to massive sulfide mineralisation: Mount Windsor Volcanics, Cambro-Ordovician, Australia. *In* IAVCEI International Volcanological Congress Ankara, Theme 10.

Doyle MG & McPhie J (2000) Facies architecture of a silicic intrusion-dominated volcanic centre at Highway-Reward, Queensland, Australia. J Volcanol Geotherm Res 99: 79-96.

Doyle MG & McPhie J (2001) Shallow-water microbialite-volcaniclastic facies association in the Cambro-Ordovician Mt Windsor Subprovince, Australia. Austral J Earth Sci 48: 815-831.

Draper JJ & Lang SC (1994) Geology of the Devonian to Carboniferous Burdekin Basin. *In* RA Henderson & BK Davis (eds) New developments in geology and metallogeny: Northern Tasman orogenic zone. Contrib Econ Geol Res Unit 50. James Cook Univ, pp. 47-50.

Duhig NC, Stolz J, Davidson GJ & Large RR (1992) Cambrian microbial and silica gel textures in silica iron exhalites from the Mount Windsor volcanic belt, Australia: Their petrography, chemistry, and origin. Econ Geol 87: 764-784.

Eastoe CJ & Gustin MM (1996) Volcanogenic massive sulfide deposits and anoxia in the Phanerozoic oceans. Ore Geol Rev 10: 179-197.

Eastoe CJ, Solomon M & Walshe JL (1987) District-scale alteration associated with massive sulfide deposits in the Mount Read Volcanics, western Tasmania. Econ Geol 82: 1239-1258.

Edmond JM, Measures C, McDuff RE, Chan LH, Collier R, Grant B, Gordon LI & Corliss JB (1979) Ridge crest hydrothermal activity and the balances of the major and minor elements in the

ocean: The Galapagos data. Earth Planet Sci Lett 46: 1-18.

Edmond JM, Campbell AC, Palmer MR, Klinkhammer GP, German CR, Edmonds HN, Elderfield H, Thompson G & Rona P (1995) Time series studies of vent fluids from the TAG and MARK sites (1986, 1990) Mid-Atlantic Ridge: A new solution chemistry model and a mechanism for Cu/Zn zonation in massive sulphide orebodies. Geol Soc London Spec Pub 87: 77-86.

Effenberger H, Mereiter K & Zemann J (1981) Crystal structure refinements of magnesite, calcite, rhodochrosite, siderite, smithonite, and dolomite, with discussion of some aspects of the stereochemistry of calcite type carbonates. Z Kristallogr 156: 233-243.

Effenberger H, Kirfel A & Will G (1983) Untersuchungen zur Elektronendichteverteilung im Dolomit $CaMg(CO_3)_2$. Tschermaks Mineral Petrogr Mitt 31: 151-164.

Elliott-Meadows SR & Appleyard EC (1991) The alteration geochemistry and petrology of the Lar Cu-Zn deposit, Lynn Lake area, Manitoba, Canada. Econ Geol 86: 486-505.

Embley RW & Chadwick WW, Jr. (1994) Volcanic and hydrothermal processes associated with a recent phase of seafloor spreading at the northern Cleft segment: Juan de Fuca Ridge. J Geophys Res 99: 4741-4760.

Embley RW, Chadwick W, Perfit MR & Baker ET (1991) Geology of the northern Cleft segment, Juan de Fuca Ridge: Recent lava flows, sea-floor spreading, and the formation of megaplumes. Geology 19: 771-775.

Embley RW, Chadwick WW, Jr., Jonasson IR, Butterfield DA & Baker ET (1995) Initial results of the rapid response to the 1993 CoAxial event: Relationships between hydrothermal and volcanic processes. Geophys Res Lett 22: 143-146.

Essene EJ (1989) The current status of thermobarometry in metamorphic rocks. Geol Soc London Spec Pub 43: 1-44.

Eugster HP, Albee AL, Bence AE, Thompson JB, Jr. & Waldbaum DR (1972) The two-phase region and excess mixing properties of paragonite-muscovite crystalline solutions. J Petrol 13: 147-179.

Fabbri O & Fournier M (1999) Extension in the southern Ryukyu arc (Japan): Link with oblique subduction and back arc rifting. Tectonics 18: 486-497.

Fagan TJ & Day HW (1997) Formation of amphibole after clinopyroxene by dehydration reactions: Implications for pseudomorphic replacement and mass fluxes. Geology 25: 395-398.

Feely RA, Gendron JF, Baker ET & Lebon GT (1994) Hydrothermal plumes along the East Pacific Rise, 8°40' to 11°50'N: Particle distribution and composition. Earth Planet Sci Lett 128: 19-36.

Fehn U, Green KE, Von Herzen RP & Cathles LM (1983) Numerical models for the hydrothermal field at the Galapagos Spreading Center. J Geophys Res 88: 1033-1048.

Fisher RV (1960) Classification of volcanic breccias. Geol Soc Amer Bull 71: 973-982.

Fouquet Y, von Stackelberg U, Charlou JL, Erzinger J, Herzig PM, Mühe R & Wiedicke M (1993) Metallogenesis in back-arc environments: The Lau basin example. Econ Geol 88: 2154-2181.

Fournier RO (1983) A method of calculating quartz solubilities in aqueous sodium chloride solutions. Geochim Cosmochim Acta 47: 579-586.

Francheteau J, Needham HD, Choukroune P, Juteau T, Séguret M, Ballard RD, Fox PJ, Normark W, Carranza A, Cordoba D, Guerrero J, Rangin C, Bougault H, Cambon P & Hekinian R (1979) Massive deep-sea sulphide ore deposits discovered on the East Pacific Rise. Nature 277: 523-528.

Franklin JM (1995) Volcanic-associated massive sulphide base metals. *In* OR Eckstrand et al. (eds) Geology of Canadian Mineral deposits. Geology of Canada 8. Geol Surv Canada, pp. 158-183.

Franklin JM, Lydon JW & Sangster DF (1981) Volcanic-associated massive sulfide deposits. *In* BJ Skinner (ed) Econ Geol 75th Anniv Vol. Econ Geol Publ, pp. 485-627.

Galley AG (1993) Characteristics of semi-conformable alteration zones associated with volcanogenic massive sulphide districts. J Geochem Expl 48: 175-200.

Galley AG & Koski RA (1999) Setting and characteristics of ophiolite-hosted volcanogenic massive sulfide deposits. Rev Econ Geol 8: 221-246.

Galloway NM (1991) The geology of the Gydgie prospect, northeastern Queensland. B.Apl.Sci. Thesis, Univ of Technology Sydney.

Gamble JA & Wright IC (1995) The southern Havre Trough. Geological structure and magma petrogenesis of an active backarc rift complex. *In* B Taylor (ed) Backarc basins: Tectonics and magmatism. Plenum Press, pp. 29-62.

Gamble JA, Wright IC & Baker JA (1993) Seafloor geology and petrology in the oceanic to continental transition zone of the Kermadec-Havre-Taupo Volcanic Zone arc system, New Zealand. NZ J Geol Geophys 36: 417-435.

Gamo T, Sakai H, Kim ES, Shitashima K & Ishibashi J (1991a) High alkalinity due to sulfate reduction in the CLAM hydrothermal field, Okinawa Trough. Earth Planet Sci Lett 107: 328-338.

Gamo T, Sakai H, Ishibashi J, Oomori T, Chiba H, Shitashima K, Nakashima K, Tanaka Y & Masuda H (1991b) Growth mechanism of the hydrothermal mounds at the CLAM site, Mid Okinawa Trough, inferred from their morphological, mineralogical, and chemical characteristics. Proc JAMSTEC Symp Deep Sea Res 7: 163-184.

Gamo T, Sakai H, Ishibashi J, Nakayama E, Isshiki K, Matsuura H, Shitashima K, Takeuchi K & Ohta S (1993) Hydrothermal plumes in the eastern Manus Basin, Bismarck Sea: CH_4, Mn, Al and pH anomalies. Deep Sea Res 40: 2335-2349.

Gamo T, Okamura K, Charlou JL, Urabe T, Auzende JM, Ishibashi J, Shitashima K, Chiba H, Binns R, Gena K, Henry K, Matsubayashi O, Matsumoto T, Moss R, Nagaya Y, Naka J & Ruellan E (1997) Acid and sulfate-rich hydrothermal fluids from the Manus back-arc basin, Papua New Guinea. Geology 25: 139-142.

Geisler T & Schleicher H (2000) Improved U–Th–total Pb dating of zircons by electron microprobe using a simple new background modeling procedure and Ca as a chemical criterion of fluid-induced U–Th–Pb discordance in zircon. Chem Geol 163: 269–285.

Geisler T, Ulonska M, Schleicher H, Pidgeon RT & Van Bronswijk W (2001) Leaching and differential recrystallization of metamict zircon under experimental hydrothermal conditions. Contrib Mineral Petrol 141: 53-65.

Gemmell JB & Large RR (1992) Stringer system and alteration zones underlying the Hellyer volcanic-hosted massive sulfide deposit, Tasmania, Australia. Econ Geol 87: 620-649.

Gemmell JB & Fulton R (2001) Geology, genesis, and exploration implications of the footwall and hanging-wall alteration associated with the Hellyer volcanic-hosted massive sulfide deposit, Tasmania, Australia. Econ Geol 96: 1003-1035.

Gemmell JB, Binns RA & Parr JM (1999) Submarine, high sulfidation alteration within DESMOS caldera, Manus Basin, PNG. *In* CJ Stanley et al. (eds) Mineral deposits: Processes to processing. Balkema, pp. 503-506.

Gibson HL & Kerr DJ (1993) Giant volcanic-associated massive sulfide depos-

its: With emphasis on Archean deposits. Econ Geol Spec Pub 2: 319-348.

Gibson HL, Morton RL & Hudak GJ (1999) Submarine volcanic processes, deposits, and environments favorable for the location of volcanic-associated massive sulfide deposits. Rev Econ Geol 8: 13-51.

Gifkins CC & Allen RL (2001) Textural and chemical characteristics of diagenetic and hydrothermal alteration in glassy volcanic rocks: Examples from the Mount Read Volcanics, Tasmania. Econ Geol 96: 973-1002.

Giggenbach WF (1981) Geothermal mineral equilibria. Geochim Cosmochim Acta 45: 393-410.

Giggenbach WF (1987) Redox processes governing the chemistry of fumarolic gas discharges from White Island, New Zealand. Appl Geochem 2: 143-161.

Giggenbach WF (1992) Magma degassing and mineral deposition in hydrothermal systems along convergent plate boundaries. Econ Geol 87: 1927-1944.

Giggenbach WF (1995) Composition of fluids in geothermal systems of the Taupo Volcanic Zone, New Zealand, as a function of source magma. *In* YK Kharaka & OV Chudaev (eds) Water-rock interaction. Balkema, pp. 9-12.

Giggenbach WF & Le Guern F (1976) The chemistry of magmatic gases from Erta'Ale, Ethopia. Geochim Cosmochim Acta 40: 25-30.

Giggenbach WF, Tedesco D, Sulistiyo Y, Caprai A, Cioni R, Favara R, Fischer TP, Hirabayashi JI, Korzhinsky M, Martini M, Menyailov I & Shinohara H (2001) Evaluation of results from the fourth and fifth IAVCEI field workshops on volcanic gases, Vulcano island, Italy and Java, Indonesia. J Volcanol Geotherm Res 108: 157-172.

Giorgetti G, Monecke T, Kleeberg R, Herzig PM (2002) Homogeneous intermediate sodium-potassium mica in hydrothermally altered rocks of the Waterloo deposit, Australia: A combined SEM-EMP-XRD-TEM study. Contrib Mineral Petrol: subm.

Goldfarb MS & Delaney JR (1988) Response of two-phase fluids to fracture configurations within submarine hydrothermal systems. J Geophys Res 93: 4585-4594.

Goodfellow WD & Blaise B (1988) Sulfide formation and hydrothermal alteration of hemipelagic sediment in Middle Valley, northern Juan de Fuca Ridge. Can Mineral 26: 675-696.

Goodfellow WD & Franklin JM (1993) Geology, mineralogy, and chemistry of sediment-hosted clastic massive sulfides in shallow cores, Middle Valley, northern Juan de Fuca Ridge. Econ Geol 88: 2037-2068.

Götze J, Habermann D, Neuser RD & Richter DK (1999) High-resolution spectrometric analysis of rare earth elements-activated cathodoluminescence in feldspar minerals. Chem Geol 153: 81-91.

Götze J, Plötze M & Habermann D (2001a) Origin, spectral characteristics and practical applications of the cathodoluminescence (CL) of quartz - A review. Mineral Petrol 71: 225-250.

Götze J, Plötze M, Götte T, Neuser RD & Richter DK (2001b) Cathodoluminescence of clay minerals. *In* J Götze et al. (eds) Cathodoluminescence in geosciences: New insights from CL in combination with other techniques. TU Bergakademie Freiberg, pp. 42-43.

Govindaraju K (1994) 1994 compilation of working values and sample description for 383 geostandards. Geostandards Newslett Spec Issue 18: 1-158.

Graham IJ, Cole JW, Briggs RM, Gamble JA & Smith IEM (1995) Petrology and petrogenesis of volcanic rocks from the Taupo Volcanic Zone: A review. J Volcanol Geotherm Res 68: 59-87.

Green GR, Solomon M & Walshe JL (1981) The formation of the volcanic-hosted

massive sulfide ore deposit at Rosebery, Tasmania. Econ Geol 76: 304-338.

Gregory PW (1981) Gydgie A. to P. 2197 M Queensland. Report for the period 20.03.81 to 19.09.81. Rep 1506/5. Penarroya (Australia) Pty Ltd.

Gregory RT & Taylor HP, Jr. (1981) An oxygen isotope profile in a section of Cretaceous oceanic crust, Samail ophiolite, Oman: Evidence for δ^{18} O buffering of the oceans by deep (>5 km) seawater-hydrothermal circulation at mid-ocean ridges. J Geophys Res 86: 2737-2755.

Gregory PW, Hartley JS & Wills KJA (1987) The Thalanga massive sulphide deposit. *In* E Brennan (ed) Pacific Rim Congress 87. Austral Inst Mining Metallurgy, pp. 573-577.

Gregory PW, Hartley JS & Wills KJA (1990) Thalanga zinc-lead-copper-silver deposit. *In* FE Hughes (ed) Geology of the mineral deposits of Australia and Papua New Guinea. Austral Inst Mining Metallurgy, pp. 1527-1537.

Gregory PW, Hartley JS & Wills KJA (1993) The Thalanga massive sulphide deposit. *In* RA Henderson (ed) Guide to the economic geology of the Charters Towers region, northeastern Queensland. Geol Soc Austral Field Excursion Guidebook. James Cook Univ, pp. 93-98.

Grimes KG (1980) The Tertiary geology of North Queensland. *In* RA Henderson & PJ Stephenson (eds) The geology and geophysics of northeastern Australia. Geol Soc Austral Queensl Div, pp. 329-347.

Guidotti CV, Mazzoli C, Sassi FP & Blencoe JG (1992) Compositional controls on the cell dimensions of $2M_1$ muscovite and paragonite. Eur J Mineral 4: 283-297.

Guirado F, Gali S & Chinchón S (2000) Quantitative Rietveld analysis of aluminous cement clinker phases. Cem Concr Res 30: 1023-1029.

Gulson BL, Large RR & Porritt PA (1987) Base metal exploration of the Mount Read Volcanics, western Tasmania: Pt. III. Application of lead isotopes at Elliott Bay. Econ Geol 82: 308-327.

Güven N (1971) The crystal structures of $2M_1$ phengite and $2M_1$ muscovite. Z Kristallogr 134: 196-212.

Halbach P, Nakamura K, Wahsner M, Lange J, Sakai H, Käselitz L, Hansen RD, Yamano M, Post J, Prause B, Seifert R, Michaelis W, Teichmann F, Kinoshita M, Märten A, Ishibashi J, Czerwinski S & Blum N (1989) Probable modern analogue of Kuroko-type massive sulphide deposits in the Okinawa Trough back-arc basin. Nature 338: 496-499.

Halbach P, Pracejus B & Märten A (1993) Geology and mineralogy of massive sulfide ores from the central Okinawa Trough, Japan. Econ Geol 88: 2210-2225.

Hannington MD, Jonasson IR, Herzig PM & Petersen S (1995) Physical and chemical processes of seafloor mineralization at mid-ocean ridges. Geophys Monogr Ser 91: 115-157.

Hannington MD, Galley AG, Herzig PM & Petersen S (1998) Comparison of the TAG mound and stockwork complex with Cyprus-type massive sulfide deposits. Proc ODP Sci Res 158: 389-415.

Hannington MD, Poulsen KH, Thompson JFH & Sillitoe RH (1999) Volcanogenic gold in the massive sulfide environment. Rev Econ Geol 8: 325-356.

Hanson RE & Schweickert RA (1982) Chilling and brecciation of a Devonian rhyolitic sill intruded into wet sediments, northern Sierra Nevada, California. J Geol 90: 717-724.

Harper GD, Bowman JR & Kuhns R (1988) A field, chemical, and stable isotope study of subseafloor metamorphism of the Josephine ophiolite, California-Oregon. J Geophys Res 93: 4625-4656.

Hartley JS, Peters SG & Beams SD (1989) Current developments in Charters Towers geology and gold mineralisation. *In*

North Queensland Gold'89 Conference. Austral Inst Mining Metallurgy, pp. 7-14.

Hartley JS, Peters SG & Beams SD (1993) Geological context and concepts of mineralisation in the Charters Towers region. *In* RA Henderson (ed) Guide to the economic geology of the Charters Towers region, northeastern Queensland. Geol Soc Austral Field Excursion Guidebook. James Cook Univ, pp. 49-59.

Hashiguchi H, Yamada R & Inoue T (1983) Practical application of low Na_2O anomalies in footwall acid lava for delimiting promising areas around the Kosaka and Fukazawa Kuroko deposits, Akita prefecture, Japan. Econ Geol Monogr 5: 387-394.

Haymon RM, Fornari DJ, Edwards MH, Carbotte S, Wright D & Macdonald KC (1991) Hydrothermal vent distribution along the East Pacific Rise crest (9°09'-54'N) and its relationship to magmatic and tectonic processes on fast-spreading mid-ocean ridges. Earth Planet Sci Lett 104: 513-534.

Heaton THE & Sheppard SMF (1977) Hydrogen and oxygen isotope evidence for sea-water-hydrothermal alteration and ore deposition, Troodos complex, Cyprus. *In* Volcanic processes in ore genesis. Inst Mining Metallurgy, pp. 42-57.

Hedenquist JW (1986) Waiotapu Geothermal Field. Monogr Ser Mineral Dep 26: 65-79.

Hedenquist JW (1987) Mineralization associated with volcanic-related hydrothermal systems in the circum-Pacific basin. *In* MK Horn (ed) Circum-Pacific Energy and Mineral Resources Conference Singapore. Amer Ass Petroleum Geol, pp. 513-524.

Hedenquist JW (1990) The thermal and geochemical structure of the Broadlands-Ohaaki geothermal system. Geothermics 19: 151-185.

Hedenquist JW (1995) The ascent of magmatic fluid: Discharge versus mineralization. Mineral Ass Can Short Course Ser 23: 263-289.

Hedenquist JW & Lowenstern JB (1994) The role of magmas in the formation of hydrothermal ore deposits. Nature 370: 519-527.

Heinrich CA, Günther D, Audétat A, Ulrich T & Frischknecht R (1999) Metal fractionation between magmatic brine and vapor, determined by microanalysis of fluid inclusions. Geology 27: 755-758.

Hekinian R, Fevrier M, Bischoff JL, Picot P & Shanks WC, III (1980) Sulfide deposits from the East Pacific Rise near 21°N. Science 207: 1433-1444.

Hemley JJ & Jones WR (1964) Chemical aspects of hydrothermal alteration with emphasis on hydrogen metasomatism. Econ Geol 59: 538-569.

Henderson RA (1983) Early Ordovician faunas from the Mount Windsor Subprovince, northeastern Queensland. *In* J. Roberts & P.A. Jell (eds), Mem Ass Australas Palaeontols 1. Ass Australas Palaeontols, pp. 145-175.

Henderson RA (1986) Geology of the Mt. Windsor Subprovince - A lower Palaeozoic volcano-sedimentary terrane in the northern Tasman orogenic zone. Austral J Earth Sci 33: 343-364.

Henderson RA & Nind MAP (1994) Tertiary units, landscape and regolith of the Charters Towers region. *In* RA Henderson & BK Davis (eds) New developments in geology and metallogeny: Northern Tasman orogenic zone. Contrib Econ Geol Res Unit 50. James Cook Univ, pp. 17-21.

Hendricks SB & Jefferson ME (1939) Polymorphism of the micas. Amer Mineral 24: 729-771.

Henley RW & McNabb A (1978) Magmatic vapor plumes and ground-water interaction in porphyry copper emplacement. Econ Geol 73: 1-20.

Henley RW & Thornley P (1979) Some geothermal aspects of polymetallic mas-

sive sulfide formation. Econ Geol 74: 1600-1612.

Herrmann W (1994) Immobile element geochemistry of altered volcanics and exhalites at the Thalanga deposit, North Queensland. M. Econ. Geol. Thesis, Univ of Tasmania.

Herrmann W & Hill AP (2001) The origin of chlorite-tremolite-carbonate rocks associated with the Thalanga volcanic-hosted massive sulfide deposit, North Queensland, Australia. Econ Geol 96: 1149-1173.

Herzig PM & Hannington MD (1995) Polymetallic massive sulfides at the modern seafloor: A review. Ore Geol Rev 10: 95-115.

Herzig PM & Hannington MD (2000) Polymetallic massive sulfides and gold mineralization at mid-ocean ridges and in subduction-related environments. *In* DS Cronan (ed) Handbook of marine minerals deposits. CRC Press, pp. 347-368.

Herzig PM, Hannington MD & Arribas A, Jr. (1998) Sulfur isotopic composition of hydrothermal precipitates from the Lau back-arc: Implications for magmatic contributions to seafloor hydrothermal systems. Mineral Deposita 33: 226-237.

Hill RJ (1991) Expanded use of the Rietveld method in studies of phase abundance in multiphase mixtures. Powder Diffraction 6: 74-77.

Hill AP (1996) Structure, volcanic setting, hydrothermal alteration and genesis of the Thalanga massive sulphide deposit. Ph.D. Thesis, Univ of Tasmania.

Hill RJ & Howard CJ (1987) Quantitative phase analysis from neutron powder diffraction data using the Rietveld method. J Appl Cryst 20: 467-474.

Hill RJ, Tsambourakis G & Madsen IC (1993) Improved petrological modal analyses from X-ray powder diffraction data by use of the Rietveld method I. Selected igneous, volcanic, and metamorphic rocks. J Petrol 34: 867-900.

Hillier S (1995) Mafic phyllosilicates in low-grade metabasites. Characterization using deconvolution analysis - Discussion. Clay Minerals 30: 67-73.

Hillier S (2000) Accurate quantitative analysis of clay and other minerals in sandstone by XRD: Comparison of a Rietveld and a reference intensity ratio (RIR) method and the importance of sample preparation. Clay Minerals 35: 291-302.

Höck V (1974) Coexisting phengite, paragonite and margarite in metasediments of the Mittlere Hohe Tauern, Austria. Contrib Mineral Petrol 43: 261-273.

Hodges DJ & Manojlovic PM (1993) Application of lithogeochemistry to exploration for deep VMS deposits in high grade metamorphic rocks, Snow Lake, Manitoba. J Geochem Expl 48: 201-224.

Hölzer G, Fritsch M, Deutsch M, Härtwig J & Förster E (1997) $K\alpha_{1,2}$ and $K\beta_{1,3}$ X-ray emission lines of the 3d transition metals. Phys Rev A56: 4554-4568.

Hongo Y & Nozaki Y (2001) Rare earth element geochemistry of hydrothermal deposits and *Calyptogena* shell from the Iheya Ridge vent field, Okinawa Trough. Geochem J 35: 347-354.

Honma H, Kusakabe M, Kagami H, Iizumi S, Sakai H, Kodama Y & Kimura M (1991) Major and trace element chemistry and D/H, $^{18}O/^{16}O$, $^{87}Sr/^{86}Sr$ and $^{143}Nd/^{144}Nd$ ratios of rocks from the spreading centre of the Okinawa Trough, a marginal back-arc basin. Geochem J 25: 121-136.

Honnorez J & Kirst P (1975) Submarine basaltic volcanism: morphometric parameters for discriminating hyaloclastites from hyalotuffs. Bull Volcanol 39: 441-465.

Honnorez JJ, Alt JC & Humphris SE (1998) Vivisection and autopsy of active and fossil hydrothermal alterations of basalt beneath and within the TAG hydrothermal mound. Proc ODP Sci Res 158: 231-254.

Hopkinson L, Roberts S, Herrington R & Wilkinson J (1999) The nature of crystalline silica from the TAG submarine hydrothermal mound, 26°N Mid Atlantic Ridge. Contrib Mineral Petrol 137: 342-350.

Horikoshi E (1969) Volcanic activity related to the formation of the Kuroko-type deposits in the Kosaka district, Japan. Mineral Deposita 4: 321-345.

Hou Z, Zhang Q & Qu X (1999) Hydrothermal fluid evolution and ore-forming processes of submarine hydrothermal systems in the Okinawa Trough. Explor Mining Geol 8: 257-272.

Hower J, Eslinger EV, Hower ME & Perry EA (1976) Mechanism of burial metamorphism of argillaceous sediment: 1. Mineralogical and chemical evidence. Geol Soc Amer Bull 87: 725-737.

Hughes (1973) Spilites, keratophyres, and the igneous spectrum. Geol Mag 109: 513-527.

Humphris SE & Thompson G (1978) Hydrothermal alteration of oceanic basalts by seawater. Geochim Cosmochim Acta 42: 107-125.

Humphris SE, Herzig PM, Miller DJ, Alt JC, Becker K, Brown D, Brügmann G, Chiba H, Fouquet Y, Gemmell JB, Guerin G, Hannington MD, Holm NG, Honnorez JJ, Iturrino GJ, Knott R, Ludwig R, Nakamura K, Petersen S, Reysenbach AL, Rona PA, Smith S, Sturz AA, Tivey MK & Zhao X (1995) The internal structure of an active sea-floor massive sulphide deposit. Nature 377: 713-716.

Hunns SR & McPhie J (1999) Pumiceous peperite in a submarine volcanic succession at Mount Chalmers, Queensland, Australia. J Volcanol Geotherm Res 88: 239-254.

Huston DL (1990) The stratigraphic and structural setting of the Balcooma volcanogenic massive sulphide lenses, northern Queensland. Austral J Earth Sci 37: 423-440.

Huston DL (1991) Metal zonation and mineralogy of the Waterloo and Agincourt prospects. *In* J Pongratz & RR Large (eds) Geological controls on VMS mineralisation in the Mt Windsor Volcanic Belt. CODES. Univ of Tasmania, pp. 109-145.

Huston DL & Kamprad J (2001) Zonation of alteration facies at Western Tharsis: Implications for the genesis of Cu-Au deposits, Mount Lyell Field, western Tasmania. Econ Geol 96: 1123-1132.

Huston DL & Taylor TW (1990) Dry River copper and lead-zinc-copper deposits. *In* FE Hughes (ed) Geology of the mineral deposits of Australia and Papua New Guinea. Austral Inst Mining Metallurgy, pp. 1519-1526.

Huston DL, Taylor T, Fabray J & Patterson DJ (1992) A comparison of the geology and mineralization of the Balcooma and Dry River South volcanic-hosted massive sulfide deposits, northern Queensland. Econ Geol 87: 785-811.

Huston DL, Kuronen U & Stolz J (1995) Waterloo and Agincourt prospects, northern Queensland: Contrasting styles of mineralization within the same volcanogenic hydrothermal system. Austral J Earth Sci 42: 203-221.

Hutchinson RW (1973) Volcanogenic sulfide deposits and their metallogenic significance. Econ Geol 68: 1223-1246.

Hutchinson RW (1980) Massive base metal sulphide deposits as guides to tectonic evolution. Geol Ass Can Spec Pap 20: 659-684.

Hutton LJ & Crouch SBS (1993) New and revised igneous units in the Charters Towers and Dotswood 1:100000 sheet areas. Queensl Gov Mining J 94: 32-46.

Hutton LJ & Rienks IP (1997) Geology of the Ravenswood Batholith. *In* Queensl Geol 8. Dep Mines Energy.

Hutton LJ, Rienks IP & Wyborn D (1990) A reinterpretation of the Ravenswood Batholith, North Queensland. *In* Proc Pa-

cific Rim Congr 90. Austral Inst Mining Metallurgy, pp. 179-185.

Hutton LJ, Hartley JS & Rienks IP (1993) Geology of the Charters Towers region. *In* RA Henderson (ed) Guide to the economic geology of the Charters Towers region, northeastern Queensland. Geol Soc Austral Field Excursion Guidebook. James Cook Univ, pp. 1-12.

Hutton LJ, Rienks IP, Tenison-Woods K, Hartley JS & Crouch SBS (1994) A geochemical and structurally based reinterpretation of the Ravenswood Batholith, North Queensland. *In* RA Henderson & BK Davis (eds) New developments in geology and metallogeny: Northern Tasman orogenic zone. Contrib Econ Geol Res Unit 50. James Cook Univ, pp. 3-5.

Ishibashi J & Urabe T (1995) Hydrothermal activity related to arc-backarc magmatism in the western Pacific. *In* B Taylor (ed) Backarc basins: Tectonics and magmatism. Plenum Press, pp. 451-495.

Ishibashi J, Grimaud D, Nojiri Y, Auzende JM & Urabe T (1994) Fluctuation of chemical compositions of the phase-separated hydrothermal fluid from the North Fiji Basin Ridge. Marine Geol 116: 215-226.

Ishibashi J, Sano Y, Wakita H, Gamo T, Tsutsumi M & Sakai H (1995) Helium and carbon geochemistry of hydrothermal fluids from the Mid-Okinawa Trough back arc basin, southwest of Japan. Chem Geol 123: 1-15.

Ishikawa Y, Sawaguchi T, Iwaya S & Horiuchi M (1976) Delineation of prospecting targets for Kuroko deposits based on modes of volcanism of underlying dacite and alteration haloes. Mining Geol 26: 105-117.

Ishizuka H, Kawanobe Y & Sakai H (1990) Petrology and geochemistry of volcanic rocks dredged from the Okinawa Trough, an active back-arc basin. Geochem J 24: 75-92.

Izawa E, Motomura Y, Tanaka T & Kimura N (1991) Hydrothermal carbonate chimneys in the Iheya Ridge of the Okinawa Trough. Proc JAMSTEC Symp Deep Sea Res 7: 185-192.

Javoy M & Pineau F (1991) The volatiles record of a 'popping' rock from the Mid-Atlantic Ridge at 14°N: Chemical and isotopic composition of gas trapped in the vesicles. Earth Planet Sci Lett 107: 598-611.

Jiang WT & Peacor DR (1993) Formation and modification of metastable intermediate sodium potassium mica, paragonite, and muscovite in hydrothermally altered metabasites from northern Wales. Amer Mineral 78: 782-793.

Johnson HD & Baldwin CT (1986) Shallow siliciclastic seas. *In* HG Reading (ed) Sedimentary environments and facies. Blackwell, pp. 229-282.

Johnson MC, Anderson AT, Jr. & Rutherford MJ (1994) Pre-eruptive volatile contents of magmas. Rev Mineral 30: 281-330.

Kadko D & Butterfield DA (1998) The relationship of hydrothermal fluid composition and crustal residence time to maturity of vent fields on the Juan de Fuca Ridge. Geochim Cosmochim Acta 62: 1521-1533.

Kadko D & Moore W (1988) Radiochemical constraints on the crustal residence time of submarine hydrothermal fluids: Endeavour Ridge. Geochim Cosmochim Acta 52: 659-668.

Kadko D, Koski R, Tatsumoto M & Bouse R (1985) An estimate of hydrothermal fluid residence times and vent chimney growth rates based on ^{210}Pb/Pb ratios and mineralogic studies of sulfides dredged from the Juan de Fuca Ridge. Earth Planet Sci Lett 76: 35-44.

Kamenetsky VS, Binns RA, Gemmell JB, Crawford AJ, Mernagh TP, Maas R & Steele D (2001) Parental basaltic melts and fluids in eastern Manus backarc Basin: Implications for hydrothermal mineralisation. Earth Planet Sci Lett 184: 685-702.

Kamenetsky VS, Davidson P, Mernagh TP, Crawford AJ, Gemmell JB, Portnyagin MV & Shinjo R (2002) Fluid bubbles in melt inclusions and pillow-rim glasses: High-temperature precursors to hydrothermal fluids? Chem Geol 183: 349-364.

Kawahara A, Ohno M & Takano Y (1972) Structural Study of the amphibole in volcanic tuff. Sci Pap College General Education, Univ Tokyo 22: 67-68.

Kay JR (1987) The Highway gold mine, Charters Towers - Submarine volcanogenic gold-barite stringer mineralization, modified by lateritic weathering. *In* HK Herbert (ed) Proc Symp Gold in Queensland. Pap Dep Geol 12. James Cook Univ, pp. 111-125.

Kempe U, Götze J, Dandar S & Habermann D (1999) Magmatic and metasomatic processes during formation of the Nb-Zr-REE deposits Khaldzan Buregte and Tsakhir (Mongolian Altai): Indications from a combined CL-SEM study. Mineral Mag 63: 165-177.

Kempe U, Gruner T, Nasdala L & Wolf D (2000) Relevance of cathodoluminescence for the interpretation of U-Pb zircon ages, with an example of an application to a study of zircons from the Saxonian Granulite Complex, Germany. *In* M Pagel et al. (eds) Cathodoluminescence in geosciences. Springer, pp. 415-455.

Kent GM, Harding AJ & Orcutt JA (1993) Distribution of magma beneath the East Pacific Rise near the 9°03'N overlapping spreading center from forward modeling of common depth point data. J Geophys Res 98: 13971-13995.

Kent GM, Harding AJ, Orcutt JA, Detrick RS, Mutter JC & Buhl P (1994) Uniform accretion of oceanic crust south of the Garrett transform at 14°15'S on the East Pacific Rise. J Geophys Res 99: 9097-9116.

Kesler SE, Russell N, Seaward M, Rivera J, McCurdy K, Cumming GL & Sutter JF (1981) Geology and geochemistry of sulfide mineralization underlying the Pueblo Viejo gold-silver oxide deposit, Dominican Republic. Econ Geol 76: 1096-1117.

Khin Zaw & Large RR (1992) The precious metal-rich South Hercules mineralization, western Tasmania: A possible subsea-floor replacement volcanic-hosted massive sulfide deposit. Econ Geol 87: 931-952.

King EM, Barrie CT & Valley JW (1997) Hydrothermal alteration of oxygen isotope ratios in quartz phenocrysts, Kidd Creek mine, Ontario: Magmatic values preserved in zircon. Geology 25: 1079-1082.

Klau W & Large DE (1980) Submarine exhalative Cu-Pb-Zn deposits: A discussion of their classification and metallogenesis. Geol Jb D40: 13-58.

Köhler S, Kleeberg R, Monecke T & Renno AD (2000) Quantitative X-ray powder diffraction analyses of basaltic dykes and metabasalts by the Rietveld method. Beih 1 Eur J Mineral 12: 100.

Kohn BP & Glasby GP (1978) Tephra distribution and sedimentation rates in the Bay of Plenty, New Zealand. NZ J Geol Geophys 21: 49-70.

Kokelaar P (1986) Magma-water interactions in subaqueous and emergent basaltic volcanism. Bull Volcanol 48: 275-291.

Komninou A & Sverjensky DA (1995) Pre-ore hydrothermal alteration in an unconformity-type uranium deposit. Contrib Mineral Petrol 121: 99-114.

Kräutner HG (1987) Quantitative modelling of the conversion reactions of plagioclase in albite, zoisite/clinozoisite and calcite (with exemplification on the Argestru metabasite). Dari de Seama ale Sedintelor Inst Geol Geofiz Bucuresti 72-73: 225-252.

Lagerblad B & Gorbatschev R (1985) Hydrothermal alteration as a control of regional geochemistry and ore formation in the central Baltic Shield. Geol Rdsch 74: 33-49.

Laing WP (1986) Preliminary assessment of the structural environment of the Waterloo prospect, North Queensland. *In* JS Hartley & KJA Wills (eds) Progress report on exploration at the Waterloo prospect. Rep 1505/23. Penarroya (Australia) Pty Ltd.

Lalou C, Thompson G, Arnold M, Brichet E, Druffel E & Rona PA (1990) Geochronology of TAG and Snakepit hydrothermal fields, Mid-Atlantic Ridge: Witness to a long and complex hydrothermal history. Earth Planet Sci Lett 97: 113-128.

Lalou C, Reyss JL, Brichet E, Arnold M, Thompson G, Fouquet Y & Rona PA (1993) New age data for Mid-Atlantic Ridge hydrothermal sites: TAG and Snakepit chronology revisited. J Geophys Res 98: 9705-9713.

Lalou C, Reyss JL, Brichet E, Rona PA & Thompson G (1995) Hydrothermal activity on a 10^5-year scale at a slow-spreading ridge, TAG hydrothermal field, Mid-Atlantic Ridge 26°N. J Geophys Res 100: 17855-17862.

Lalou C, Reyss JL & Brichet E (1998) Age of sub-bottom sulfide samples at the TAG active mound. Proc ODP Sci Res 158: 111-117.

Large RR (1977) Chemical evolution and zonation of massive sulfide deposits in volcanic terrains. Econ Geol 72: 549-572.

Large RR (1991) Ore deposit models and exploration criteria for VMS deposits in the Mt Windsor Volcanics. *In* J Pongratz & RR Large (eds) Geological controls on VMS mineralisation in the Mt Windsor Volcanic Belt. CODES. Univ of Tasmania, pp. 181-199.

Large RR (1992) Australian volcanic-hosted massive sulfide deposits: Features, styles, and genetic models. Econ Geol 87: 471-510.

Large RR, Allen RL, Blake MD & Herrmann W (2001a) Hydrothermal alteration and volatile element halos for the Rosebery K lens volcanic-hosted massive sulfide deposit, western Tasmania. Econ Geol 96: 1055-1072.

Large RR, Gemmell JB, Paulick H & Huston DL (2001b) The alteration box plot: A simple approach to understanding the relationship between alteration mineralogy and lithogeochemistry associated with volcanic-hosted massive sulfide deposits. Econ Geol 96: 957-971.

Lasaga AC & Rye DM (1993) Fluid flow and chemical reaction kinetics in metamorphic systems. Amer Jour Sci 293: 361-404.

Lasaga AC, Rye DM, Lüttge A & Bolton EW (2001) Calculation of fluid fluxes in Earth's crust. Geochim Cosmochim Acta 65: 1161-1185.

Leistel JM, Marcoux E, Thiéblemont D, Quesada C, Sánchez A, Almodóvar GR, Pascual E & Sáez R (1998) The volcanic-hosted massive sulphide deposits of the Iberian Pyrite Belt. Mineral Deposita 33: 2-30.

Le Maitre RW, Bateman P, Dudek A, Keller J, Lameyre J, Le Bas MJ, Sabine PA, Schmid R, Sørensen H, Streckeisen A, Woolley AR & Zanettin B (1989) A classification of igneous rocks and glossary of terms. Recommendations of the International Union of Geological Sciences Subcommission on the Systematics of Igneous Rocks. Blackwell.

Lentz DR (1998) Petrogenetic evolution of felsic volcanic sequences associated with Phanerozoic volcanic-hosted massive sulphide systems: The role of extensional geodynamics. Ore Geol Rev 12: 289-327.

Lentz DR (1999) Petrology, geochemistry, and oxygen isotope interpretation of felsic volcanic and related rocks hosting the Brunswick 6 and 12 massive sulfide deposits (Brunswick Belt), Bathurst mining camp, New Brunswick, Canada. Econ Geol 94: 57-86.

Lesher CM, Goodwin AM, Campbell IH & Gorton MP (1986) Trace-element geochemistry of ore-associated and barren, felsic metavolcanic rocks in the Superior

Province, Canada. Can J Earth Sci 23: 222-237.

Letouzey J & Kimura M (1985) Okinawa Trough genesis: Structure and evolution of a backarc basin developed in a continent. Marine Pet Geol 2: 111-130.

Letouzey J & Kimura M (1986) The Okinawa Trough: Genesis of a back-arc developing along a continental margin. Tectonophysics 125: 209-230.

Levingston KR (1972) Ore deposits and mines of the Charters Towers 1:250,000 sheet area, North Queensland. Rep Geol Surv Queensl 57. Queensl Dep Mines.

Levingston KR (1981) Geological evolution and economic geology of the Burdekin River region, Queensland. Bull Bur Mineral Resour Geol Geophys Austral 208.

Lewis KB & Pantin HM (1984) Intersection of a marginal basin with a continent: Structure and sediments of the Bay of Plenty, New Zealand. *In* BP Kokelaar & MF Howells (eds) Marginal basin geology: Volcanic and associated sedimentary and tectonic processes in modern and ancient marginal basins. Geol Soc London Spec Pub 16: 121-135.

Li G, Peacor DR, Merriman RJ & Roberts B (1994) The diagenetic to low-grade metamorphic evolution of matrix white micas in the system muscovite-paragonite in a mudrock from central Wales, United Kingdom. Clays Clay Minerals 42: 369-381.

Lilley MD, Olson EJ, McLaughlin E & Von Damm KL (1991) Methane, hydrogen and carbon dioxide in vent fluids from the 9°N hydrothermal system. EOS Trans Amer Geophys Union 72: 481.

Livi KJT, Veblen DR, Ferry JM & Frey M (1997) Evolution of 2:1 layered silicates in low-grade metamorphosed Liassic shales of central Switzerland. J metamorphic Geol 15: 323-344.

Lowenstern JB (1994) Chlorine, fluid immiscibility, and degassing in peralkaline magmas from Pantelleria, Italy. Amer Mineral 79: 353-369.

Lupton JE (1995) Hydrothermal plumes: Near and far field. Geophys Monogr Ser 91: 317-346.

Lupton JE & Craig H (1981) A major helium-3 source at 15°S on the East Pacific Rise. Science 214: 13-18.

Lupton JE, Baker ET, Mottl MJ, Sansone FJ, Wheat CG, Resing JA, Massoth GJ, Measures CI & Feely RA (1993) Chemical and physical diversity of hydrothermal plumes along the East Pacific Rise, 8°45'N to 11°50'N. Geophys Res Lett 20: 2913-2916.

Lydon JW (1988) Volcanogenic massive sulphide deposits. Geoscience Can Reprint Ser 3: 155-181.

Mackie PE & Young RA (1973) Location of Nd dopant in Fluorapatite, $Ca_5(PO_4)_3$ F:Nd. J Appl Cryst 6: 26-31.

MacLean WH & Barrett TJ (1993) Lithogeochemical techniques using immobile elements. J Geochem Expl 48: 109-133.

MacLean WH & Hoy LD (1991) Geochemistry of hydrothermally altered rocks at the Horne mine, Noranda, Quebec. Econ Geol 86: 506-528.

MacLean WH & Kranidiotis P (1987) Immobile elements as monitors of mass transfer in hydrothermal alteration; Phelps Dodge massive sulfide deposit, Matagami, Quebec. Econ Geol 82: 951-962.

Marquis P, Brown AC, Hubert C & Rigg DM (1990) Progressive alteration associated with auriferous massive sulfide bodies at the Dumagami mine, Abitibi greenstone belt, Quebec. Econ Geol 85: 746-764.

Marumo K (1989) Genesis of kaolin minerals and pyrophyllite in Kuroko deposits of Japan: Implications for the origin of the hydrothermal fluids from mineralogical and stable isotope data. Geochim Cosmochim Acta 53: 2915-2924.

Marumo K & Hattori KH (1999) Seafloor hydrothermal clay alteration at Jade in the back-arc Okinawa Trough: Mineralogy, geochemistry and isotope charac-

teristics. Geochim Cosmochim Acta 63: 2785-2804.

Mattey DP, Carr RH, Wright IP & Pillinger CT (1984) Carbon isotopes in submarine basalts. Earth Planet Sci Lett 70: 196-206.

Mauguin C (1928) Etude des micas au moyen des rayons X. Bull Soc fr Minér Cristallogr 51: 285-332.

McBirney AR (1963) Factors governing the nature of submarine volcanism. Bull Volcanol 26: 455-469.

McClung G (1976) Early Ordovician (Late Arenigian) graptolites from the Cape River Beds in the Rollston Range, Charters Towers district. Queensl Gov Mining J 77: 605-608.

McDuff RE (1995) Physical dynamics of deep-sea hydrothermal plumes. Geophys Monogr Ser 91: 357-368.

McGoldrick PJ & Large RR (1992) Geologic and geochemical controls on gold-rich stringer mineralization in the Que River deposit, Tasmania. Econ Geol 87: 667-685.

McMurtry GM, Sedwick PN, Fryer P, Von der Haar DL & Yeh HW (1993) Unusual geochemistry of hydrothermal vents on submarine arc volcanoes: Kasuga seamounts, northern Mariana arc. Earth Planet Sci Lett 114: 517-528.

McPhie J & Allen RL (1992) Facies architecture of mineralized submarine volcanic sequences: Cambrian Mount Read Volcanics, western Tasmania. Econ Geol 87: 587-596.

McPhie J, Doyle M & Allen R (1993) Volcanic textures: A guide to the interpretation of textures in volcanic rocks. CODES. Univ of Tasmania.

Meagher EP & Lager GA (1979) Polyhedral thermal expansion in the TiO_2 polymorphs: Refinement of the crystal structures of rutile and brookite at high temperature. Can Mineral 17: 77-85.

Merlivat L, Pineau F & Javoy M (1987) Hydrothermal vent waters at 13°N of the East Pacific Rise: Isotopic composition and gas concentration. Earth Planet Sci Lett 84: 100-108.

Miki M (1995) Two-phase opening model for the Okinawa Trough inferred from paleomagnetic study of the Ryukyu arc. J Geophys Res 100: 8169-8184.

Miki M, Matsuda T & Otofuji Y (1990) Opening mode of the Okinawa Trough: Paleomagnetic evidence from the south Ryukyu Arc. Tectonophysics 175: 335-347.

Miller CR (1996) Geological and geochemical aspects of the Liontown VHMS deposit, north eastern Queensland. M. Econ. Geol. Thesis, Univ of Tasmania.

Miller C (1998a) Waterloo: Drill core examination. *In* SD Beams (ed) Economic geology of northeast Queensland, the 1998 perspective. Geol Soc Austral, p. 229.

Miller C (1998b) Liontown: Drill core examination. *In* SD Beams (ed) Economic geology of northeast Queensland, the 1998 perspective. Geol Soc Austral, pp. 225-228.

Miller C, Halley S, Green G & Jones M (2001) Discovery of the West 45 volcanic-hosted massive sulfide deposit using oxygen isotopes and REE geochemistry. Econ Geol 96: 1227-1237.

Minniti M & Bonavia FF (1984) Copper-ore grade hydrothermal mineralization discovered in a seamount in the Tyrrhenian sea (Mediterranean): Is the mineralization related to porphyry-copper or base metal lodes? Marine Geol 59: 271-282.

Monecke T, Kleeberg R, Herzig P, Bergmann J & Gemmell B (1999) Application of quantitative X-ray diffraction analysis by the Rietveld method to VHMS alteration halo studies. *In* CJ Stanley et al. (eds) Mineral deposits: Processes to processing. Balkema, pp. 555-558.

Monecke T, Herzig PM, Kleeberg R, Köhler S & Gemmell JB (2000) Zonation of dioctahedral true mica species in the footwall alteration halo of the Waterloo VHMS deposit, northern Queensland,

Australia. *In* JB Gemmell & J Pongratz (eds) Volcanic environments and massive sulfide deposits. CODES Spec Pub 3. Univ of Tasmania, pp. 131-133.

Monecke T, Gemmell JB & Herzig PM (2001a) Relationship between volcanism and hydrothermal alteration at the Waterloo VHMS deposit, Australia. Beih 1 Eur J Mineral 13: 125.

Monecke T, Gemmell JB & Monecke J (2001b) Fractal distributions of veins in drill core from the Hellyer VHMS deposit, Australia: Constraints on the origin and evolution of the mineralising system. Mineral Deposita 36: 406-415.

Monecke T, Köhler S, Kleeberg R, Herzig PM & Gemmell JB (2001c) Quantitative phase-analysis by the Rietveld method using X-ray powder-diffraction data: Application to the study of alteration halos associated with volcanic-rock-hosted massive sulfide deposits. Can Mineral 39: 1617-1633.

Monecke T, Kempe U & Götze J (2002) Genetic significance of the trace element content in metamorphic and hydrothermal quartz: A reconnaissance study. Earth Planet Sci Lett (in press).

Montelius C, Allen R, Svenson SÅ & Weihed P (2000) The Maurliden volcanogenic Zn-Cu-Au-Ag massive- and network-sulfide deposits, Skellefte district, Sweden. *In* JB Gemmell & J Pongratz (eds) Volcanic environments and massive sulfide deposits. CODES Spec Pub 3. Univ of Tasmania, pp. 135-136.

Moores EM (1991) Southwest U.S.-East Antarctic (SWEAT) connection: A hypothesis. Geology 19: 425-428.

Mora CI & Ramseyer K (1992) Cathodoluminescence of coexisting plagioclases, Boehls Butte anorthosite: CL activators and fluid flow paths. Amer Mineral 77: 1258-1265.

Morey GW & Chen WT (1955) The action of hot water on some feldspars. Amer Mineral 40: 996-1000.

Morey GW & Fournier RO (1961) The decomposition of microcline, albite and nepheline in hot water. Amer Mineral 46: 688-699.

Morton RL & Franklin JM (1987) Two-fold classification of Archean volcanic-associated massive sulfide deposits. Econ Geol 82: 1057-1063.

Morton JL & Sleep NH (1985) A mid-ocean ridge thermal model: Constraints on the volume of axial hydrothermal heat flux. J Geophys Res 90: 11345-11353.

Morton RL, Walker JS, Hudak GJ & Franklin JM (1991) The early development of an Archean submarine caldera complex with emphasis on the Mattabi ash-flow tuff and its relationship to the Mattabi massive sulfide deposit. Econ Geol 86: 1002-1011.

Mottl MJ (1983) Metabasalts, axial hot springs, and the structure of hydrothermal systems at mid-ocean ridges. Geol Soc Amer Bull 94: 161-180.

Mottl MJ, Sansone FJ, Wheat CG, Resing JA, Baker ET & Lupton JE (1995) Manganese and methane in hydrothermal plumes along the East Pacific Rise, 8°40' to 11°50'N. Geochim Cosmochim Acta 59: 4147-4165.

Mulholland IR (1991) The geology, petrology, and alteration geochemistry of the Magpie volcanogenic massive sulfide prospect, North Queensland, Australia. Econ Geol 86: 1387-1400.

Mumme WG, Tsambourakis G, Madsen IC & Hill RJ (1996) Improved petrological modal analyses from X-ray powder diffraction data by use of the Rietveld method. Part II. Selected sedimentary rocks. J Sed Res 66: 132-138.

Murray CG & Kirkegaard AG (1978) The Thomson orogen of the Tasman orogenic zone. Tectonophysics 48: 299-325.

Nedachi M, Ueno H, Ossaka J, Nogami K, Hashimoto J, Fujikura K & Miura T (1992) Hydrothermal ore deposits on the Minami-Ensei Knoll of the Okinawa Trough - Mineral assemblages. Proc

JAMSTEC Symp Deep Sea Res 8: 95-106.

Nehlig P, Juteau T, Bendel V & Cotten J (1994) The root zones of oceanic hydrothermal systems: Constraints from the Samail ophiolite (Oman). J Geophys Res 99: 4703-4713.

Neuser RD (1995) A new high-intensity cathodoluminescence microscope and its application to weakly luminescing minerals. Bochumer Geol Geotechn Arb 44: 116-118.

Newberry RJ, Crafford TC, Newkirk SR, Young LE, Nelson SW & Duke NA (1997) Volcanogenic massive sulfide deposits of Alaska. Econ Geol Monogr 9: 120-150.

Niu Y & Lesher CM (1991) Hydrothermal alteration of mafic metavolcanic rocks and genesis of Fe-Zn-Cu sulfide deposits, Stone Hill district, Alabama. Econ Geol 86: 983-1001.

Noda Y, Matsumoto K, Ohba S, Saito Y, Toriumi K, Iwata Y & Shibuya I (1987) Temperature dependence of atomic thermal parameters of lead chalcogenides, PbS, PbSe and PbTe. Acta Cryst C43: 1443-1445.

Nojiri Y, Ishibashi J, Kawai T, Otsuki A & Sakai H (1989) Hydrothermal plumes along the North Fiji basin spreading axis. Nature 342: 667-670.

Norrish K & Chappell BW (1977) X-ray fluorescence spectrometry. *In* J Zussman (ed) Physical methods in determinative mineralogy. Academic Press, pp. 201-272.

Offler R & Whitford DJ (1992) Wall-rock alteration and metamorphism of a volcanic-hosted massive sulfide deposit at Que River, Tasmania: Petrology and mineralogy. Econ Geol 87: 686-705.

Ohmoto H (1996) Formation of volcanogenic massive sulfide deposits: The Kuroko perspective. Ore Geol Rev 10: 135-177.

Ohmoto H & Rye RO (1974) Hydrogen and oxygen isotopic compositions of fluid inclusions in the Kuroko deposits, Japan. Econ Geol 69: 947-953.

Ohmoto H, Tanimura S, Date J & Takahashi T (1983) Geologic setting of the Kuroko deposits, Japan. Part I. Geologic history of the Green tuff region. Part II. Stratigraphy and structure of the Hokuroku district. Part III. Submarine calderas and Kuroko genesis. Econ Geol Monogr 5: 9-54.

Orr TH (1994) The Mt Leyshon gold mine: Geology and mineralisation. *In* RA Henderson & BK Davis (eds) New developments in geology and metallogeny: Northern Tasman orogenic zone. Contrib Econ Geol Res Unit 50. James Cook Univ, pp. 29-35.

Osterberg SA, Morton RL & Franklin JM (1987) Hydrothermal alteration and physical volcanology of Archean rocks in the vicinity of the Headway-Coulee massive sulfide occurrence, Onaman area, northwestern Ontario. Econ Geol 82: 1505-1520.

Paulick H & Franz G (2001) Greenschist facies regional and contact metamorphism of the Thalanga volcanic-hosted massive sulfide deposit (northern Queensland, Australia). Mineral Deposita 36: 786-793.

Paulick H & Hermann W (1998) Geology of the Thalanga volcanic-hosted massive sulphide deposit (North Queensland). *In* SD Beams (ed) Economic geology of northeast Queensland, the 1998 perspective. Geol Soc Austral, pp. 215-224.

Paulick H & McPhie J (1999) Facies architecture of the felsic lava-dominated host sequence to the Thalanga massive sulfide deposit, Lower Ordovician, northern Queensland. Austral J Earth Sci 46: 391-405.

Paulick H, Herrmann W & Gemmell JB (2001) Alteration of felsic volcanics hosting the Thalanga massive sulfide deposit (northern Queensland, Australia) and geochemical proximity indicators to ore. Econ Geol 96: 1175-1200.

Peccerillo R & Taylor SR (1976) Geochemistry of Eocene calc-alkaline volcanic rocks from the Kastamonu area, northern Turkey. Contrib Mineral Petrol 58: 63-81.

Perkins C & Kennedy AK (1998) Permo-Carboniferous gold epoch of northeast Queensland. Austral J Earth Sci 45: 185-200.

Perkins C, McDougall I & Walshe JL (1993) Isotopic dating of precious and base metal deposits and their host rocks in eastern Australia. Final Rep AMIRA Project P334. Austral Mineral Industries Res Ass.

Perkins C, Walshe JL & Morrison G (1995) Metallogenic episodes of the Tasman fold belt system, eastern Australia. Econ Geol 90: 1443-1466.

Peters SG (1987) Geology and lode controls of the Charters Towers goldfield, northeastern Queensland. Contrib Econ Geol Res Unit 19. James Cook Univ.

Piché M, Guha J & Daigneault R (1993) Stratigraphic and structural aspects of the volcanic rocks of the Matagami mining camp, Quebec: Implications for the Norita ore deposit. Econ Geol 88: 1542-1558.

Pichler H (1965) Acid hyaloclastites. Bull Volcanol 28: 293-310.

Pisutha-Arnond V & Ohmoto H (1983) Thermal history, and chemical and isotopic compositions of the ore-forming fluids responsible for the Kuroko massive sulfide deposits in the Hokuroku district of Japan. Econ Geol Monogr 5: 523-558.

Poitrasson F (2002) In situ investigations of allanite hydrothermal alteration: Examples from calc-alkaline and anorogenic granites of Corsica (southeast France). Contrib Mineral Petrol 142: 485-500.

Polya DA, Solomon M, Eastoe CJ & Walshe JL (1986) The Murchinson George, Tasmania - A possible cross section through a Cambrian massive sulfide system. Econ Geol 81: 1341-1355.

Prokin VA, Buslaev FP & Nasedkin AP (1998) Types of massive sulphide deposits in the Urals. Mineral Deposita 34: 121-126.

Ramseyer K, Baumann J, Matter A & Mullis J (1988) Cathodoluminescence colours of α-quartz. Mineral Mag 52: 669-677.

Ramseyer K, Boles JR & Lichtner PC (1992) Mechanism of plagioclase albitization. J Sed Petrol 62: 349-356.

Ransom B & Helgeson HC (1993) Compositional end members and thermodynamic components of illite and dioctahedral aluminous smectite solid solution. Clays Clay Minerals 41: 537-550.

Raudsepp M, Pani E & Dipple GM (1999) Measuring mineral abundance in skarn. I. The Rietveld method using X-ray powder-diffraction data. Can Mineral 37: 1-15.

Reeder RJ & Dollase WA (1989) Structural variation in the dolomite-ankerite solid-solution series: An X-ray, Mössbauer, and TEM study. Amer Mineral 74: 1159-1167.

Reynolds RC, Jr. (1985) NEWMOD©, a computer program for the calculation of one-dimensional diffraction patterns of mixed-layered clays. 8 Brook Road, Hanover, NH 03755.

Rhede D & Monecke T (2001) Compositional sector zoning in magmatic and hydrothermal monazite. Beih 1 Eur J Mineral 13: 153.

Richards DNG (1980) Palaeozoic granitoids of northeastern Australia. *In* RA Henderson & PJ Stephenson (eds) The geology and geophysics of northeastern Australia. Geol Soc Austral Queensl Div, pp. 229-246.

Richards HG, Cann JR & Jensenius J (1989) Mineralogical zonation and metasomatism of the alteration pipes of Cyprus sulfide deposits. Econ Geol 84: 91-115.

Richardson CJ, Cann JR, Richards HG & Cowan JG (1987) Metal-depleted root zones of the Troodos ore-forming hy-

drothermal systems, Cyprus. Earth Planet Sci Lett 84: 243-253.

Rieder M, Cavazzini G, D'yakonov YS, Frank-Kamenetskii VA, Gottardi G, Guggenheim S, Koval PV, Müller G, Neiva AMR, Radoslovich EW, Robert JL, Sassi FP, Takeda H, Weiss Z & Wones DR (1999) Nomenclature of the micas. Mineral Mag 63: 267-279.

Rienks IP (1991) New plutonic rock units in the northeastern portion of the Ravenswood Batholith. Queensl Gov Mining J 92: 30-42.

Rienks IP, Tenison-Woods K & Wyborn D (1994) New units in the southeast portion of the Ravenswood Batholith. Queensl Gov Mining J 95: 29-47.

Rietveld HM (1969) A profile refinement method for nuclear and magnetic structures. J Appl Cryst 2: 65-71.

Robinson D & Bevins RE (1994) Mafic phyllosilicates in low-grade metabasites. Characterization using deconvolution analysis. Clay Minerals 29: 223-237.

Robinson D, Bevins RE & Rowbotham G (1993) The characterization of mafic phyllosilicates in low-grade metabasalts from eastern North Greenland. Amer Mineral 78: 377-390.

Rona PA (1980) TAG hydrothermal field: Mid-Atlantic Ridge crest at latitude 26°N. J Geol Soc London 137: 385-402.

Rona PA (1988) Hydrothermal mineralization at oceanic ridges. Can Mineral 26: 431-465.

Rona PA & Scott SD (1993) A special issue on sea-floor hydrothermal mineralization: New perspectives. Econ Geol 88: 1935-1976.

Rona PA, Klinkhammer G, Nelsen TA, Trefry JH & Elderfield H (1986) Black smokers, massive sulphides and vent biota at the Mid-Atlantic Ridge. Nature 321: 33-37.

Rosenberg ND, Spera FJ & Haymon RM (1993) The relationship between flow and permeability field in seafloor hydrothermal systems. Earth Planet Sci Lett 116: 135-153.

Roux J & Hovis GL (1996) Thermodynamic mixing models for muscovite-paragonite solutions based on solution calorimetric and phase equilibrium data. J Petrol 37: 1241-1254.

Rule AC & Bailey SW (1987) Refinement of the crystal structure of a monoclinic ferroan clinochlore. Clays Clay Minerals 35: 129-138.

Rutland RWR, Etheridge MA & Solomon M (1990) The stratigraphic and tectonic setting of the ore deposits of Australia. *In* FE Hughes (ed) Geology of the mineral deposits of Australia and Papua New Guinea. Austral Inst Mining Metallurgy, pp. 15-26.

Sakai H, Gamo T, Kim ES, Tsutsumi M, Tanaka T, Ishibashi J, Wakita H, Yamano M & Oomori T (1990a) Venting of carbon dioxide-rich fluid and hydrate formation in mid-Okinawa Trough backarc basin. Science 248: 1093-1096.

Sakai H, Gamo T, Ishibashi J, Shitashima K, Kim ES, Yanagisawa F, Tsutsumi M, Sano Y, Wakit H, Tanaka T, Matsumoto T, Naganuma T & Mitsuzawa K (1990b) Unique chemistry of the hydrothermal solutions in the mid-Okinawa Trough backarc basin. Geophys Res Lett 17: 2133-2136.

Sangster DF & Brook WA (1977) Primitive lead in an Australian Zn-Pb-Ba deposit. Nature 270: 423.

Sangster DF & Scott SD (1976) Precambrian, strata-bound, massive Cu-Zn-Pb sulfide ores of North America. *In* KH Wolf (ed) Handbook of strata-bound and stratiform ore deposits: II. Regional studies and specific deposits. Vol. 6. Cu, Zn, Pb, and Ag deposits. Elsevier, pp. 129-222.

Sawkins FJ (1976) Massive sulphide deposits in relation to geotectonics. Geol Ass Can Spec Pap 14: 221-240.

Sawkins FJ & Kowalik J (1981) The source of ore metals at Buchans: Magmatic ver-

sus leaching models. Geol Ass Can Spec Pap 22: 255-267.

Schardt C, Cooke DR, Gemmell JB & Large RR (2001) Geochemical modeling of the zoned footwall alteration pipe, Hellyer volcanic-hosted massive sulfide deposit, western Tasmania, Australia. Econ Geol 96: 1037-1054.

Scheetz JW (1991) The geology and alteration of the Brewer gold mine, Jefferson, South Carolina. M.Sc. Thesis. Univ of North Carolina.

Scheibner E (1978) Tasman fold belt system or orogenic system: Introduction. Tectonophysics 48: 153-157.

Schiffman P & Smith BM (1988) Petrology and oxygen isotope geochemistry of a fossil seawater hydrothermal system within the Solea Graben, northern Troodos ophiolite, Cyprus. J Geophys Res 93: 4612-4624.

Schiffman P & Staudigel H (1995) The smectite to chlorite transition in a fossil seamount hydrothermal system: The basement complex of La Palma, Canary islands. J metamorphic Geol 13: 487-498.

Schiffman P, Smith BM, Varga RJ & Moores EM (1987) Geometry, conditions and timing of off-axis hydrothermal metamorphism and ore-deposition in the Solea graben. Nature 325: 423-425.

Schmalzried H (1981) Solid state reactions. Verlag Chemie.

Schmincke HU (1967) Fused tuff and peperite in south central Washington. Geol Soc Amer Bull 78: 319-330.

Schultz A & Strickland R (1990) Electromagnetic instrumentation measures hydrothermal heat flux. Sea Technol 31: 31-38.

Scotney PM, Roberts S, Herrington RJ & First DM (1999) Testing for a magmatic component in a high-sulphidation (VMS) system at Wetar Island, Indonesia. *In* CJ Stanley et al. (eds) Mineral deposits: Processes to processing. Balkema, pp. 581-584.

Scott SD (1985) Seafloor polymetallic sulfide deposits: Modern and ancient. Marine Mining 5: 191-212.

Sedwick PN, McMurtry GM & Macdougall JD (1992) Chemistry of hydrothermal solutions from Pele's vents, Loihi Seamount, Hawaii. Geochim Cosmochim Acta 56: 3643-3667.

Seyfried WE, Jr. & Bischoff JL (1979) Low temperature basalt alteration by seawater: An experimental study at 70°C and 150°C. Geochim Cosmochim Acta 43: 1937-1947.

Seyfried WE, Jr., Berndt ME & Seewald JS (1988) Hydrothermal alteration processes at mid-ocean ridges: Constraints from diabase alteration experiments, hot-spring fluids and composition of the oceanic crust. Can Mineral 26: 787-804.

Shanks WC, III & Bischoff JL (1977) Ore transport and deposition in the Read Sea geothermal system: A geochemical model. Geochim Cosmochim Acta 41: 1507-1519.

Shanks WC, III & Seyfried WE, Jr. (1987) Stable isotope studies of vent fluids and chimney minerals, southern Juan de Fuca Ridge: Sodium metasomatism and seawater sulfate reduction. J Geophys Res 92: 11387-11399.

Shanks WC, III, Bischoff JL & Rosenbauer RL (1981) Seawater sulfate reduction and sulfur isotope fractionation in basaltic systems: Interaction of seawater with fayalite and magnetite at 200-350°C. Geochim Cosmochim Acta 45: 1977-1995.

Shanks WC, III, Böhlke JK & Seal RR, II (1995) Stable isotopes in mid-ocean ridge hydrothermal systems: Interactions between fluids, minerals, and organisms. Geophys Monogr Ser 91: 194-221.

Sharpe R & Gemmell JB (2001) Alteration characteristics of the Archean Golden Grove Formation at the Gossan Hill deposit, western Australia: Induration as a focusing mechanism for mineralizing hy-

drothermal fluids. Econ Geol 96: 1239-1262.

Shepherd AM (1998) Waterloo prospect: Infill diamond drilling report. Period 1/4/97 - 1/2/98. RGC (Thalanga) Pty Ltd.

Shinjo R (1998) Petrochemistry and tectonic significance of the emerged Late Cenozoic basalts behind the Okinawa Troughs Ryukyu arc system. J Volcanol Geotherm Res 80: 39-53.

Shinjo R, Chung SL, Kato Y & Kimura M (1999) Geochemical and Sr-Nd isotopic characteristics of volcanic rocks from the Okinawa Trough and Ryukyu Arc: Implications for the evolution of a young, intracontinental back arc basin. J Geophys Res 104: 10591-10608.

Shinjo R, Woodhead JD & Hergt JM (2000) Geochemical variation within the northern Ryukyu Arc: Magma source compositions and geodynamic implications. Contrib Mineral Petrol 140: 263-282.

Sibuet JC, Letouzey J, Barbier F, Charvet J, Foucher JP, Hilde TWC, Kimura M, Ling-Yun C, Marsset B, Muller C & Stephan JF (1987) Back arc extension in the Okinawa Trough. J Geophys Res 92: 14041-14063.

Sibuet JC, Hsu SK, Shyu CT & Liu CS (1995) Structural and kinematic evolutions of the Okinawa Trough backarc basin. *In* B Taylor (ed) Backarc basins: Tectonics and magmatism. Plenum Press, pp. 343-379.

Sibuet JC, Deffontaines B, Hsu SK, Thareau N, Le Formal JP & Liu CS (1998) Okinawa Trough backarc basin: Early tectonic and magmatic evolution. J Geophys Res 103: 30245-30267.

Sidorenko OV, Zvyagin BB & Soboleva SV (1977) Refinement of the crystal structure of $2M_1$ paragonite by the method of high-voltage electron diffraction. Kristallografiya 22: 971-975.

Sillitoe RH, Hannington MD & Thompson JFH (1996) High sulfidation deposits in the volcanogenic massive sulfide environment. Econ Geol 91: 204-212.

Simmons SF & Browne PRL (2000) Hydrothermal minerals and precious metals in the Broadlands-Ohaaki Geothermal System: Implications for understanding low-sulfidation epithermal environments. Econ Geol 95: 971-999.

Simpson K & McPhie J (2001) Fluidal-clast breccia generated by submarine fire fountaining, Trooper Creek Formation, Queensland, Australia. J Volcanol Geotherm Res 109: 339-355.

Skornyakova IS (1965) Dispersed iron and manganese in Pacific Ocean sediments. Int Geol Rev 7: 2161-2174.

Smith JV & Yoder HS (1956) Experimental and theoretical studies of the mica polymorphs. Mineral Mag 31: 209-235.

Solomon M (1976) 'Volcanic' massive sulphide deposits and their host rocks - A review and an explanation. *In* KH Wolf (ed) Handbook of strata-bound and stratiform ore deposits: II. Regional studies and specific deposits. Vol. 6. Cu, Zn, Pb, and Ag deposits. Elsevier, pp. 21-54.

Solomon M (1981) An introduction to the geology and metallic ore deposits of Tasmania. Econ Geol 76: 194-208.

Sparks RSJ & Wilson CJN (1983) Flowhead deposits in ash turbidites. Geology 11: 348-351.

Spiess FN, Macdonald KC, Atwater T, Ballard R, Carranza A, Cordoba D, Cox C, Diaz Garcia VM, Francheteau J, Guerrero J, Hawkins J, Haymon R, Hessler R, Juteau T, Kastner M, Larson R, Luyendyk B, Macdougall JD, Miller S, Normark W, Orcutt J & Rangin C (1980) East Pacific Rise: Hot springs and geophysical experiments. Science 207: 1421-1433.

Spooner ETC & Fyfe WS (1973) Sub-seafloor metamorphism, heat and mass transfer. Contrib Mineral Petrol 42: 287-304.

Stanton RL (1985) Stratiform ores and geological processes. J Proc Royal Soc New South Wales 118: 77-100.

Stanton RL (1990) Magmatic evolution and the ore type - Lava type affiliations of volcanic exhalative ores. *In* FE Hughes (ed) Geology of the mineral deposits of Australia and Papua New Guinea. Austral Inst Mining Metallurgy, pp. 101-107.

Stern RJ, Lin PN, Morris JD, Jackson MC, Fryer P, Bloomer SH & Ito E (1990) Enriched back-arc basin basalts from the northern Mariana Trough: Implications for the magmatic evolution of back-arc basins. Earth Planet Sci Lett 100: 210-225.

Stoffers P, Hannington M, Wright I, Herzig P, de Ronde C, Arpe T, Battershill C, Botz R, Britten K, Browne P, Cheminée JL, Fricke HW, Garbe-Schönberg D, Hekinian R, Hissman K, Huber R, Robertson J, Schauer J, Schmitt M, Scholten J, Schwarz-Schampera U & Smith I (1999) Elemental mercury at submarine hydrothermal vents in the Bay of Plenty, Taupo volcanic zone, New Zealand. Geology 27: 931-934.

Stolz A (1989) Stratigraphic relationships and geochemistry of the Mt Windsor Volcanics. *In* J Pongratz & RR Large (eds) Mount Windsor Volcanics project. CODES. Univ of Tasmania, pp. 1-50.

Stolz AJ (1991) Stratigraphy and geochemistry of the Mt Windsor Volcanics and associated exhalites. *In* J Pongratz & RR Large (eds) Geological controls on VMS mineralisation in the Mt Windsor Volcanic Belt. CODES. Univ of Tasmania, pp. 23-83.

Stolz AJ (1994) Geochemistry and Nd isotope character of the Mt Windsor Volcanics: Implications for the tectonic setting of Cambro-Ordovician VHMS mineralisation. *In* RA Henderson & BK Davis (eds) New developments in geology and metallogeny: Northern Tasman orogenic zone. Contrib Econ Geol Res Unit 50. James Cook Univ, pp. 13-16.

Stolz AJ (1995) Geochemistry of the Mount Windsor Volcanics: Implications for the tectonic setting of Cambro-Ordovician volcanic-hosted massive sulfide mineralization in northeastern Australia. Econ Geol 90: 1080-1097.

Stolz AJ (1998) Technical report: Review of exploration potential. EPM 10582 Mt Windsor Project. RGC Exploration Ltd.

Stolz J & Large RR (1992) Evaluation of the source-rock control on precious metal grades in volcanic-hosted massive sulfide deposits from western Tasmania. Econ Geol 87: 720-738.

Stolz AJ, Davies GR & Allen RL (1997) The importance of different types of magmatism in VHMS mineralisation: Evidence from the geochemistry of the host volcanic rocks to the Benambra massive sulphide deposits, Victoria, Australia. Mineral Petrol 59: 251-286.

Stuart FM, Harrop PJ, Knott R, Fallick AE, Turner G, Fouquet Y & Rickard D (1995) Noble gas isotopes in 25000 years of hydrothermal fluids from 13°N on the East Pacific Rise. Geol Soc London Spec Pub 87: 113-143.

Sun SS & McDonough WF (1989) Chemical and isotopic systematics of ocean basalts: Implications for mantle composition and processes. Geol Soc London Spec Pub 42: 313-345.

Sverjensky DA, Hemley JJ & D'Angelo WM (1991) Thermodynamic assessment of hydrothermal alkali feldspar-mica-aluminosilicate equilibria. Geochim Cosmochim Acta 55: 989-1004.

Syme EC & Bailes AH (1993) Stratigraphic and tectonic setting of Early Proterozoic volcanogenic massive sulfide deposits, Flin Flon, Manitoba. Econ Geol 88: 566-589.

Symonds RB, Rose WI, Bluth GJS & Gerlach TM (1994) Volcanic-gas studies: Methods, results, and applications. Rev Mineral 30: 1-66.

Tanaka T, Mitsuzawa K & Hotta H (1989) 'SHINKAI2000' diving surveys in the east of Iheya Small ridge in the central Okinawa Trough. Proc JAMSTEC Symp Deep Sea Res. 5: 267-281.

Taut T, Kleeberg R & Bergmann J (1997) The new Seifert Rietveld program and its application to quantitative phase analysis. *In* H Morawiec & D Stróz (eds) Proc XVII Conf Appl Cryst. World Scientific, pp. 87-92.

Taylor M & Brown GE (1976) High-temperature structural study of the $P2_1/a \Leftrightarrow A2/a$ phase transition in synthetic titanite, $CaTiSiO_5$. Amer Mineral 61: 435-447.

Torsvik TH, Smethurst MA, Meert JG & Van der Voo R, McKerrow WS, Brasier MD, Sturt BA, Walderhaug HJ (1996) Continental break-up and collision in the Neoproterozoic and Palaeozoic - A tale of Baltica and Laurentia. Earth Sci Rev 40: 229-258.

Tourigny G, Brown AC, Hubert C & Crépeau R (1989) Synvolcanic and syntectonic gold mineralization at the Bousquet mine, Abitibi greenstone belt, Quebec. Econ Geol 84: 1875-1890.

Tourigny G, Doucet D & Bourget A (1993) Geology of the Bousquet 2 mine: An example of a deformed, gold-bearing, polymetallic sulfide deposit. Econ Geol 88: 1578-1597.

Towsend KJ, Miller CF, D'Andrea JL, Ayers JC, Harrison TM & Coath CD (2000) Low temperature replacement of monazite in the Ireteba granite, southern Nevada: Geochronological implications. Chem Geol 172: 95-112.

Trinkler M & Martin M (1998) Zur Mineralogie und Genese des 'Stockscheiders' von Ehrenfriedersdorf. Z Geol Wiss 26: 293-314.

Tseng HY, Heaney PJ & Onstott TC (1995) Characterization of lattice strain induced by neutron irradiation. Phys Chem Minerals 22: 399-405.

Tsunogai U, Ishibashi J, Wakita H, Gamo T, Watanabe K, Kajimura T, Kanayama S & Sakai H (1994) Peculiar features of Suiyo Seamount hydrothermal fluids, Izu-Bonin Arc: Differences from subaerial volcanism. Earth Planet Sci Lett 129: 289-301.

Tufar W (1991) Paragenesis of complex massive sulfide ores from the Tyrrhenian Sea. Mitt österr geol Ges 84: 265-300.

Ueda A & Sakai H (1984) Sulfur isotope study of Quaternary volcanic rocks from the Japanese island arc. Geochim Cosmochim Acta 48: 1837-1848.

Unrug R (1996) The assembly of Gondwanaland. Episodes 19: 11-20.

Urabe T & Sato T (1978) Kuroko deposits of the Kosaka mine, northeast Honshu, Japan - Products of submarine hot springs on Miocene sea floor. Econ Geol 73: 161-179.

Urabe T & Scott SD (1983) Geology and footwall alteration of the South Bay massive sulphide deposit, northwestern Ontario, Canada. Can J Earth Sci 20: 1862-1879.

Urabe T, Scott SD & Hattori K (1983) A comparison of footwall-rock alteration and geothermal systems beneath some Japanese and Canadian volcanogenic massive sulfide deposits. Econ Geol Monogr 5: 345-364.

Urabe T, Baker ET, Ishibashi J, Feely RA, Marumo K, Massoth GJ, Maruyama A, Shitashima K, Okamura K, Lupton JE, Sonoda A, Yamazaki T, Aoki M, Gendron J, Greene R, Kaiho Y, Kisimoto K, Lebon G, Matsumoto T, Nakamura K, Nishizawa A, Okano O, Paradis G, Roe K, Shibata T, Tennant D, Vance T, Walker SL, Yabuki T & Ytow N (1995) The effect of magmatic activity on hydrothermal venting along the superfast-spreading East Pacific Rise. Science 269: 1092-1095.

Van der Hor F (1986) Structural analysis of drillcore from the Waterloo Prospect, North Queensland. *In* JS Hartley (ed) Progress report on exploration at Waterloo prospect. Rep 1505/25. Penarroya (Australia) Pty Ltd.

Van den Kerkhof AM & Hein UF (2001) Fluid inclusion petrography. Lithos 55: 27-47.

Van Eck M (1994) The geology and lithogeochemistry of the Lower Palaeozoic Seventy Mile Range Group at Mt. Farrenden, Charters Towers, North Queensland. M. Econ. Geol. Thesis, Univ of Tasmania.

Vanko DA & Laverne C (1998) Hydrothermal anorthitization of plagioclase within the magmatic/hydrothermal transition at mid-ocean ridges: Examples from deep sheeted dikes (Hole 504B, Costa Rica Rift) and a sheeted dike root zone (Oman ophiolite). Earth Planet Sci Lett 162: 27-43.

Vennemann TW, Muntean JL, Kesler SE, O'Neil JR, Valley JW & Russell N (1993) Stable isotope evidence for magmatic fluids in the Pueblo Viejo epithermal acid sulfate Au-Ag deposit, Dominican Republic. Econ Geol 88: 55-71.

Von Damm KL (1995) Controls on the chemistry and temporal variability of seafloor hydrothermal fluids. Geophys Monogr Ser 91: 222-247.

Von Damm KL, Edmond JM, Grant B, Measures CI, Walden B & Weiss RF (1985) Chemistry of submarine hydrothermal solutions at 21°N, East Pacific Rise. Geochim Cosmochim Acta 49: 2197-2220.

Von Damm KL, Buttermore LG, Oosting SE, Bray AM, Fornari DJ, Lilley MD & Shanks WC, III (1997) Direct observation of the evolution of a seafloor 'black smoker' from vapor to brine. Earth Planet Sci Lett 149: 101-111.

Walker JR (1993) An introduction to computer modeling of X-ray powder diffraction patterns of clay minerals: A guided tour of NEWMOD©. *In* RC Reynolds, Jr. & JR Walker (eds) CMS Workshop lectures 5. Computer applications to X-ray powder diffraction analysis of clay minerals. The Clay Minerals Society, pp. 2-17.

Walshe JL & Solomon M (1981) An investigation into the environment of formation of the volcanic-hosted Mt. Lyell copper deposits using geology, mineralogy, stable isotopes, and a six-component chlorite solid solution model. Econ Geol 76: 246-284.

Wardle R & Brindley GW (1972) The crystal structures of pyrophyllite, 1Tc, and of its dehydroxylate. Amer Mineral 57: 732-750.

Waters JC & Wallace DB (1992) Volcanology and sedimentology of the host succession to the Hellyer and Que River volcanic-hosted massive sulfide deposits, northwestern Tasmania. Econ Geol 87: 650-666.

Webb AW (1970) Appendix. Isotopic age determinations from the Townsville 1:250000 sheet area. *In* DH Wyatt et al. Geology of the Townsville 1:250000 sheet area, Queensland. Rep Bur Mineral Resour Geol Geophys Austral 127.

Webb AW (1971a) Appendix 2. Isotopic age determination. *In* DH Wyatt et al. Geology of the Charters Towers 1:250000 sheet area, Queensland. Rep Bur Mineral Resour Geol Geophys Austral 137, pp. 79-81.

Webb AW (1971b) Appendix. Isotopic dating of the Lolworth Igneous Complex, Hughenden and Charters Towers sheet areas. *In* AGL Paine et al. Geology of the northeastern part of the Hughenden 1:250,000 sheet area, Queensland. Rep Bur Mineral Resour Geol Geophys Austral 126, pp. 46-48.

Welhan JA (1988a) Origins of methane in hydrothermal systems. Chem Geol 71: 183-198.

Welhan JA (1988b) Methane and hydrogen in mid-ocean-ridge basalt glasses: Analysis by vacuum crushing. Can J Earth Sci 25: 38-48.

Wellman P (1995) Tasman orogenic system: A model for its subdivision and growth history based on gravity and magnetic anomalies. Econ Geol 90: 1430-1442.

White JDL, McPhie J & Skilling I (2000) Peperite: A useful genetic term. Bull Volcanol 62: 65-66.

Whitford DJ, Korsch MJ, Porritt PM & Craven SJ (1988) Rare-earth element mobility around the volcanogenic polymetallic massive sulfide deposit at Que River, Tasmania, Australia. Chem Geol 68: 105-119.

Whitford DJ, Korsch MJ & Solomon M (1992) Strontium isotope studies of barites: Implications for the origin of base metal mineralization in Tasmania. Econ Geol 87: 953-959.

Williams PP & Megaw HD (1964) The crystal structures of low and high albites at -180°C. Acta Cryst 17: 882-890.

Wilson CJN, Houghton BF, McWilliams MO, Lanphere MA, Weaver SD & Briggs RM (1995) Volcanic and structural evolution of Taupo Volcanic Zone, New Zealand: A review. J Volcanol Geotherm Res 68: 1-28.

Winchester JA & Floyd PA (1977) Geochemical discrimination of different magma series and their differentiation products using immobile elements. Chem Geol 20: 325-343.

Withnall IW (1988) Precambrian and Palaeozoic geology of the southeastern Georgetown Inlier, North Queensland. Rep Queensl Dep Mines, pp. 1-102.

Withnall IW, Black LP & Harvey KJ (1991) Geology and geochronology of the Balcooma area: Part of an Early Palaeozoic magmatic belt in North Queensland. Austral J Earth Sci 38: 15-29.

Woodhead JD, Harmon RS & Fraser DG (1987) O, S, Sr, and Pb isotope variations in volcanic rocks from the Northern Mariana Island: Implications for crustal recycling in intra-oceanic arcs. Earth Planet Sci Lett 83: 39-52.

Wormald PJ, Orr TOH & Hodkinson IP (1993) The Mount Leyshon gold mine (NE Queensland), an intrusive breccia and igneous complex. *In* RA Henderson (ed) Guide to the economic geology of the Charters Towers region, northeastern Queensland. Geol Soc Austral Field Excursion Guidebook. James Cook Univ, pp. 61-74.

Wright IC (1992) Shallow structure and active tectonism of an offshore continental back-arc spreading system: The Taupo Volcanic Zone, New Zealand. Marine Geol 103: 287-309.

Wright IC (1993) Southern Havre Trough-Bay of Plenty (New Zealand): Structure and seismic stratigraphy of an active back-arc basin complex. *In* PF Ballance (ed) South Pacific Sedimentary Basins. Sedimentary Basins of the World. Elsevier, pp. 195-211.

Wyatt DH & Jell JS (1980) Devonian and Carboniferous stratigraphy of the northern Tasman orogenic zone in the Townsville hinterland, North Queensland. *In* RA Henderson & PJ Stephenson (eds) The geology and geophysics of northeastern Australia. Geol Soc Austral Queensl Div, pp. 201-228.

Wyatt DH, Paine AGL, Clarke DE & Harding RR (1970) Geology of the Townsville 1:250,000 sheet area, Queensland. Rep Bur Mineral Resour Geol Geophys Austral 127.

Wyatt DH, Paine AGL, Clarke DE, Gregory CM & Harding RR (1971) Geology of the Charters Towers 1:250,000 sheet area, Queensland. Rep Bur Mineral Resour Geol Geophys Austral 137.

Yang K & Scott SD (1996) Possible contribution of a metal-rich magmatic fluid to a sea-floor hydrothermal system. Nature 383: 420-423.

Young GM (1992) Late Proterozoic stratigraphy and the Canada-Australia connection. Geology 20: 215-218.

Young RA & Post B (1962) Electron density and thermal effects in alpha quartz. Acta Cryst 15: 337-346

Zen E & Albee AL (1964) Coexistent muscovite and paragonite in pelitic schists. Amer Mineral 49: 904-925.

Zielinski RA (1979) Uranium mobility during interaction of rhyolitic obsidian, perlite, and felsite with alkaline carbonate

solution: T= 120°C, P= 210 kg/cm^2. Chem Geol 27: 47-63.

Zierenberg RA, Koski RA, Morton JL, Bouse RM & Shanks WC, III (1993) Genesis of massive sulfide deposits on a sediment-covered spreading center, Escanaba Trough, southern Gorda Ridge. Econ Geol 88: 2069-2098.

Zierenberg RA, Fouquet Y, Miller DJ, Bahr JM, Baker PA, Bjerkgård T, Brunner CA, Duckworth RC, Gable R, Gieskes J, Goodfellow WD, Gröschel-Becker HM, Guèrin G, Ishibashi J, Iturrino G, James RH, Lackschewitz KS, Marquez LL, Nehlig P, Peter JM, Rigsby CA, Schultheiss P, Shanks WC, III, Simoneit BRT, Summit M, Teagle DAH, Urbat M & Zuffa GG (1998) The deep structure of a sea-floor hydrothermal deposit. Nature 392: 485-488.

Zuleger E, Alt JC & Erzinger J (1995) Primary and secondary variations in major and trace element geochemistry of the lower sheeted dike complex: Hole 504B, Leg 140. Proc ODP Sci Res 140: pp. 65-80.

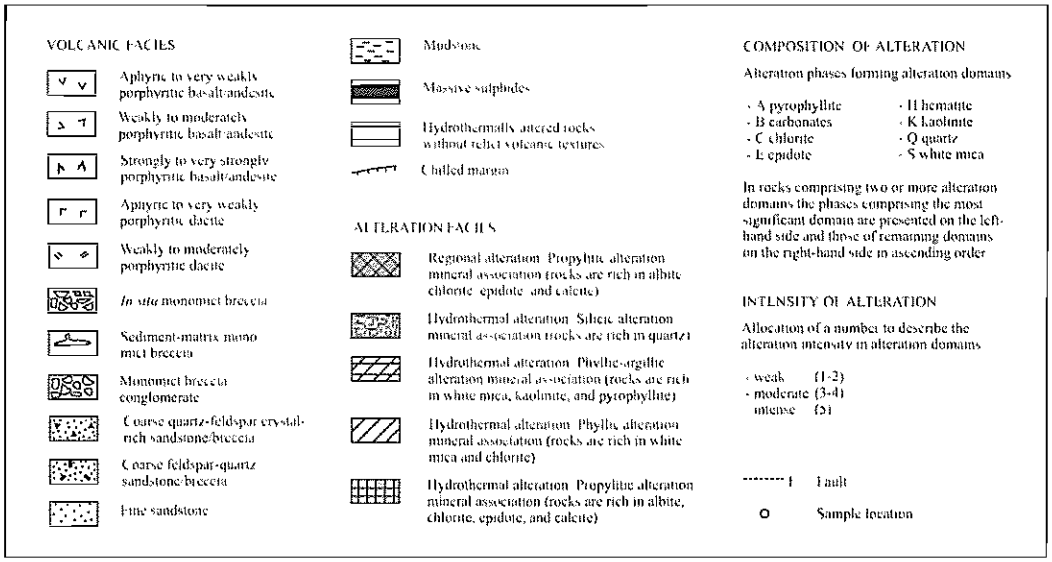
VOLCANIC FACIES
Aphyric to very weakly porphyritic basalt/andesite
Weakly to moderately porphyritic basalt/andesite
Strongly to very strongly porphyritic basalt/andesite
Aphyric to very weakly porphyritic dacite
Weakly to moderately porphyritic dacite
In situ monomict breccia
Sediment-matrix monomict breccia
Monomict breccia conglomerate
Coarse quartz-feldspar crystal-rich sandstone/breccia
Coarse feldspar-quartz sandstone/breccia
Fine sandstone
Mudstone
Massive sulphides
Hydrothermally altered rocks without relict volcanic textures
Chilled margin
ALTERATION FACIES
Regional alteration Propylitic alteration mineral association (rocks are rich in albite chlorite epidote and calcite)
Hydrothermal alteration Silicic alteration mineral association rocks are rich in quartz)
Hydrothermal alteration Phyllic-argillic alteration mineral association (rocks are rich in white mica, kaolinite, and pyrophyllite)
Hydrothermal alteration Phyllic alteration mineral association (rocks are rich in white mica and chlorite)
Hydrothermal alteration Propylitic alteration mineral association (rocks are rich in albite, chlorite, epidote, and calcite)
COMPOSITION OF ALTERATION
Alteration phases forming alteration domains
· A pyrophyllite
· B carbonates
· C chlorite
· E epidote
· H hematite
· K kaolinite
· Q quartz
· S white mica
In rocks comprising two or more alteration domains the phases comprising the most significant domain are presented on the left-hand side and those of remaining domains on the right-hand side in ascending order
INTENSITY OF ALTERATION
Allocation of a number to describe the alteration intensity in alteration domains
· weak (1-2)
· moderate (3-4)
· intense (5)
Fault
Sample location

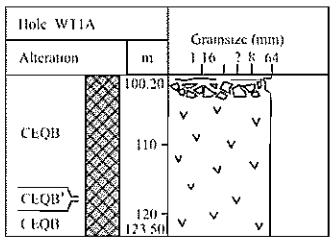
Hole WT1A
Alteration
m
Grainsize (mm)
1/16 2 8 64
CEQB
CEQB'
CEQB
100.20
110
120
123.50

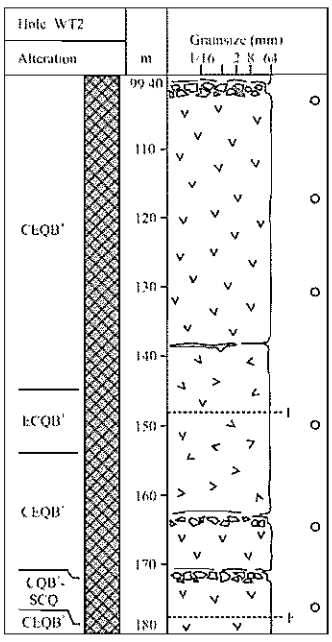
Hole WT2
Alteration
m
Grainsize (mm)
1/16 2 8 64
CEQB'
ECQB'
CEQB'
CQB'-SCQ
CEQB'
99.40
110
120
130
140
150
160
170
180

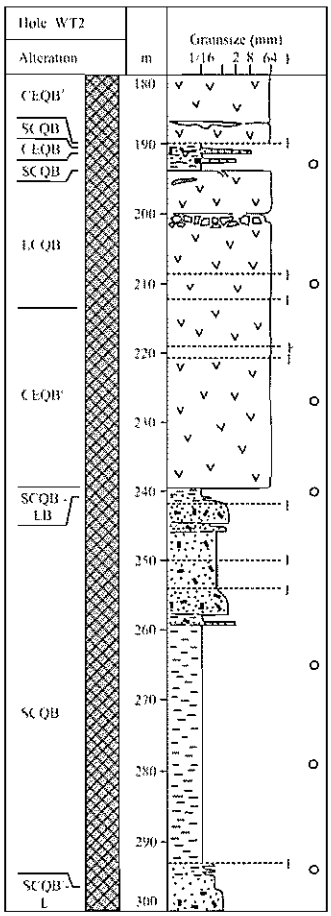
Hole WT2
Alteration
m
Grainsize (mm)
1/16 2 8 64
CEQB'
SCQB
CEQB
SCQB
ECQB
CEQB'
SCQB - LB
SCQB
SCQB - L
180
190
200
210
220
230
240
250
260
270
280
290
300

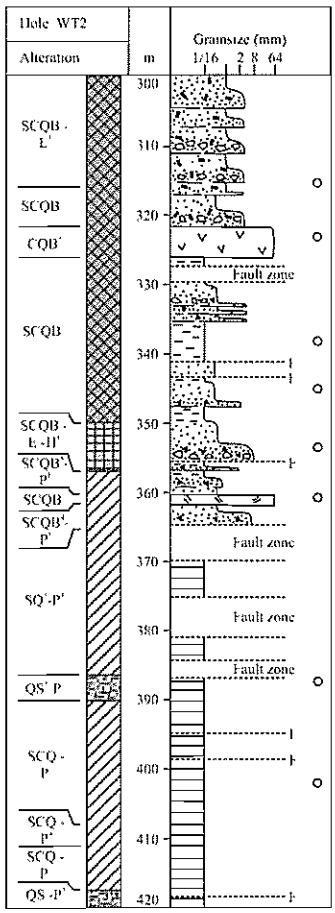
Hole WT2
Alteration
m
Grainsize (mm)
1/16 2 8 64
SCQB - L'
SCQB
CQB'
SCQB
SCQB - E - H'
SCQB' - P'
SCQB
SCQB' - P'
SQ'-P'
QS' P
SCQ - P
SCQ - P'
SCQ - P
QS -P'
Fault zone
Fault zone
Fault zone
Fault zone
300
310
320
330
340
350
360
370
380
390
400
410
420

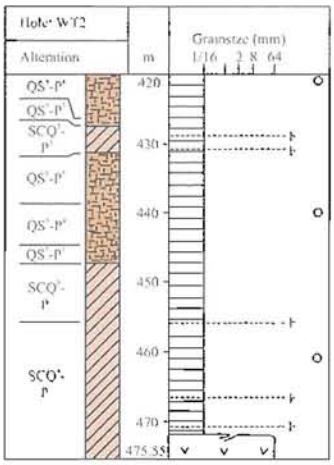
Hole: WT2
Alteration
m
Grainsize (mm)
1/16 2 8 64
420
430
440
450
460
470
475.55

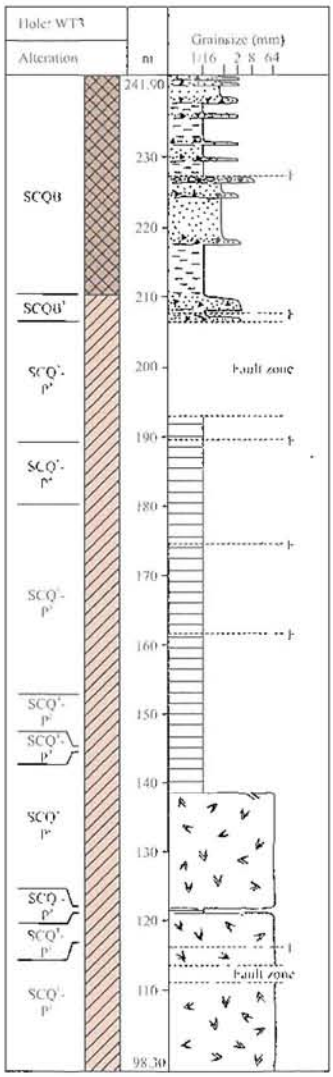
Hole: WT3
Alteration
m
Grainsize (mm)
1/16 2 8 64
241.90
230
220
210
200
190
180
170
160
150
140
130
120
110
98.30
Fault zone
Fault zone

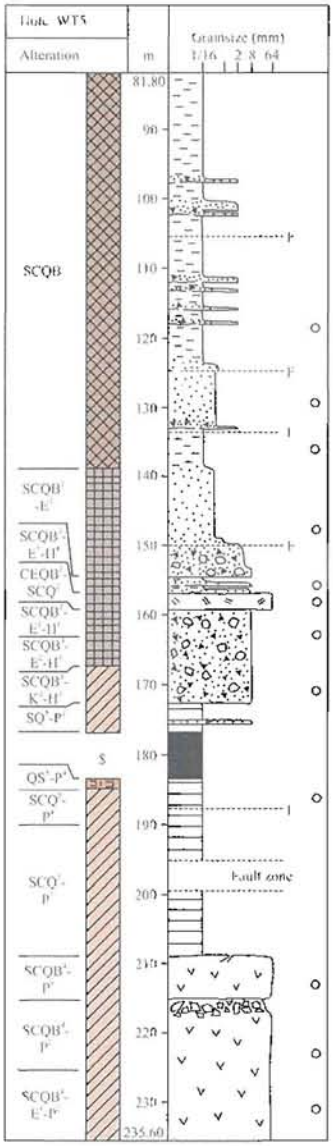
Hole: WT5
Alteration
m
Grainsize (mm)
1/16 2 8 64
81.80
90
100
110
120
130
140
150
160
170
180
190
200
210
220
230
235.60
Fault zone
Fault zone

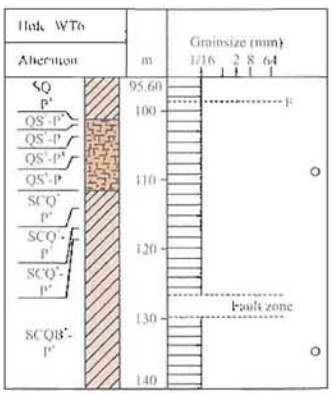
Hole: WT6
Alteration
m
Grainsize (mm)
1/16 2 8 64
95.60
100
110
120
130
140
Fault zone

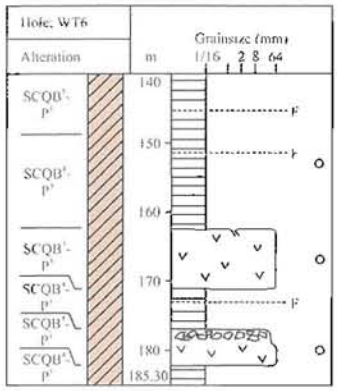
Hole: WT6
Alteration
m
Grainsize (mm)
1/16 2 8 64
140
150
160
170
180
185.30

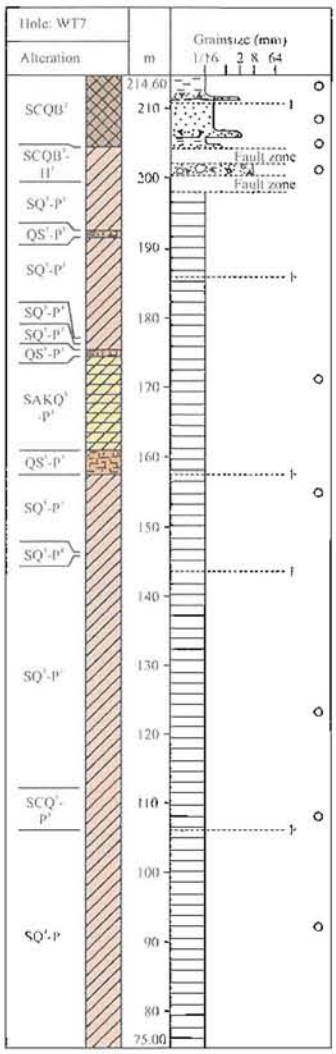
Hole: WT7
Alteration
m
Grainsize (mm)
1/16 2 8 64
214.60
210
200
190
180
170
160
150
140
130
120
110
100
90
80
75.00
Fault zone
Fault zone

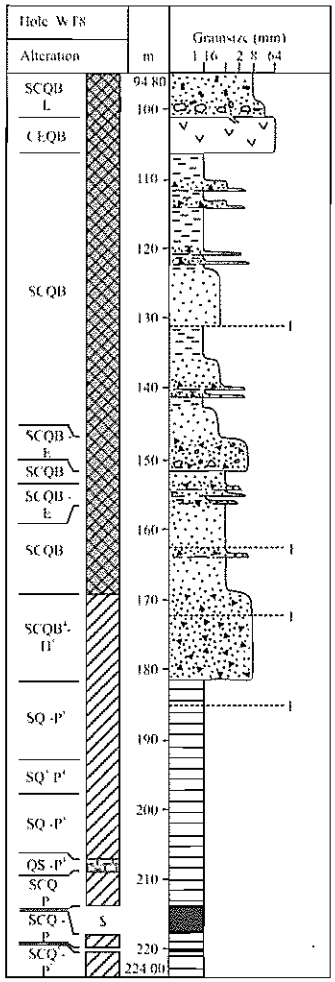
Hole WT8
Alteration
m
Grainsize (mm)
1/16 2 8 64
SCQB
L
CEQB
SCQB
SCQB
E
SCQB
E
SCQB
E
SCQB
SCQB
H'
SQ -P'
SQ' P'
SQ -P'
QS -P'
SCQ
P
SCQ -
P
SCQ -
P
S
94.80
100
110
120
130
140
150
160
170
180
190
200
210
220
224.00

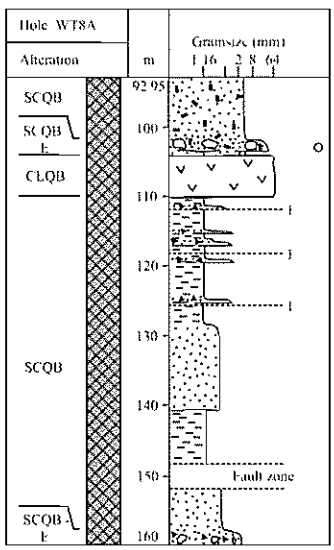
Hole WT8A
Alteration
m
Grainsize (mm)
1/16 2 8 64
SCQB
SCQB
E
CEQB
SCQB
E
92.95
100
110
120
130
140
150
160
Fault zone

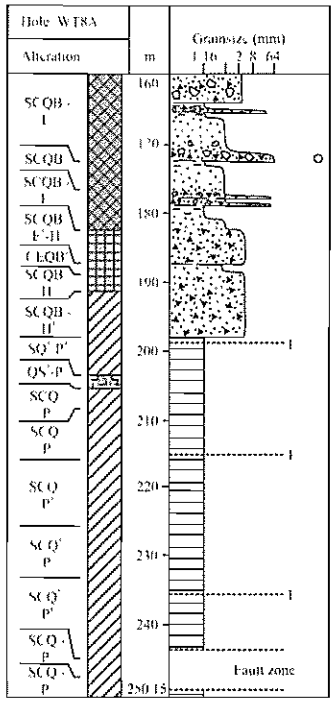
Hole WT8A
Alteration
m
Grainsize (mm)
1/16 2 8 64
SCQB -
I
SCQB
SCQB
I
SCQB
E -H
CEQB
SCQB
H
SCQB -
H'
SQ' P'
QS' -P
SCQ
P
SCQ
P
SCQ
P'
SCQ'
P
SCQ -
P
SCQ -
P
160
170
180
190
200
210
220
230
240
250.15
Fault zone

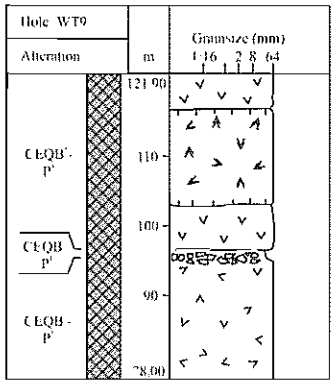
Hole WT9
Alteration
m
Grainsize (mm)
1/16 2 8 64
CEQB'
P'
CEQB
P'
CEQB -
P'
121.00
110
100
90
78.00

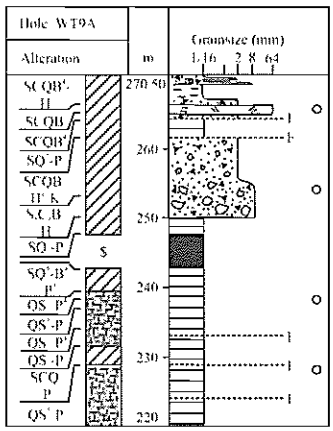
Hole WT9A
Alteration
m
Grainsize (mm)
1/16 2 8 64
SCQB'
H
SCQB
SCQB'
SQ -P
SCQB
H
SCQB
H
SQ -P
SQ' B'
P'
QS P'
QS' -P
QS P'
QS -P
SCQ
P
QS' P
S
270.50
260
250
240
230
220

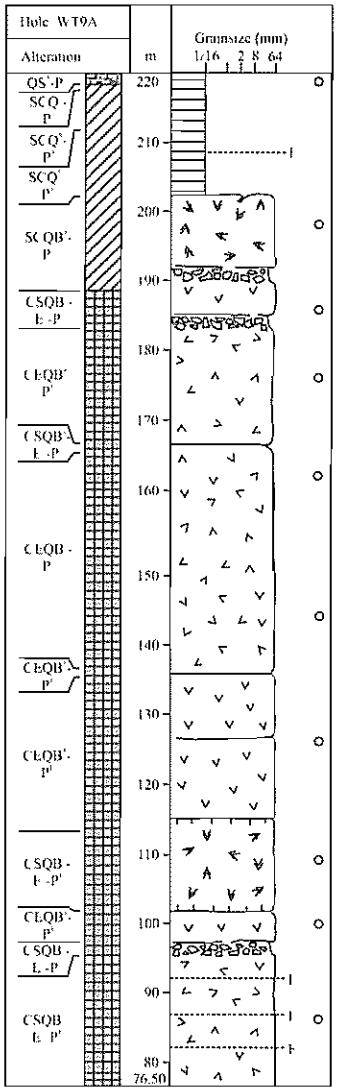
Hole WT9A
Alteration
m
Grainsize (mm)
1/16 2 8 64
QS'-P
SCQ -
P
SCQ'
P'
SCQ'
P'
SCQB'
P
CSQB -
E -P
CEQB'
P'
CSQB
E -P
CEQB -
P
CEQB'
P'
CEQB'
P'
CSQB -
E -P'
CEQB'
P'
CSQB -
E -P
CSQB
E P'
220
210
200
190
180
170
160
150
140
130
120
110
100
90
80
76.50

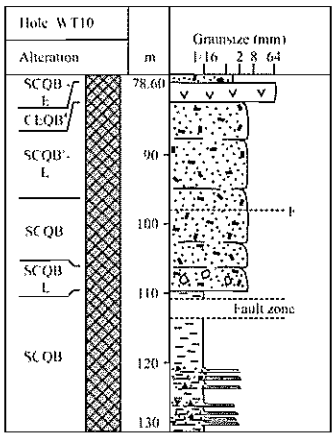
Hole WT10
Alteration
m
Grainsize (mm)
1/16 2 8 64
SCQB -
E
CEQB'
SCQB'
L
SCQB
SCQB
L
SCQB
78.60
90
100
110
120
130
Fault zone

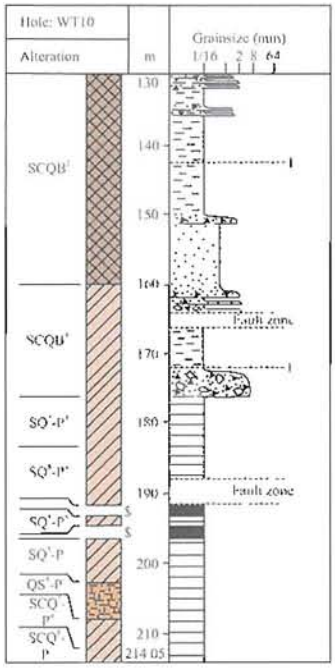
Hole: WT10
Alteration
m
Grainsize (mm)
1/16 2 8 64
130
140
150
160
170
180
190
200
210
214.05
Fault zone
Fault zone

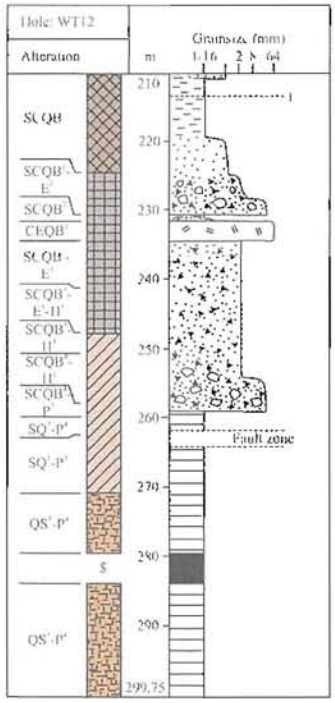
Hole: WT12
Alteration
m
Grainsize (mm)
1/16 2 8 64
210
220
230
240
250
260
270
280
290
299.75
Fault zone

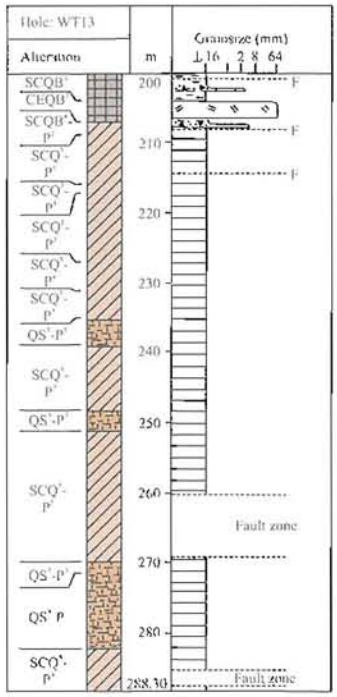
Hole: WT13
Alteration
m
Grainsize (mm)
1/16 2 8 64
200
210
220
230
240
250
260
270
280
288.30
Fault zone
Fault zone

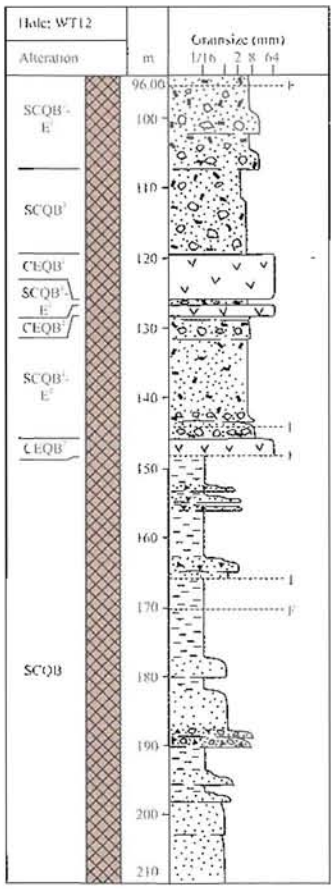
Hole: WT12
Alteration
m
Grainsize (mm)
1/16 2 8 64
96.00
100
110
120
130
140
150
160
170
180
190
200
210

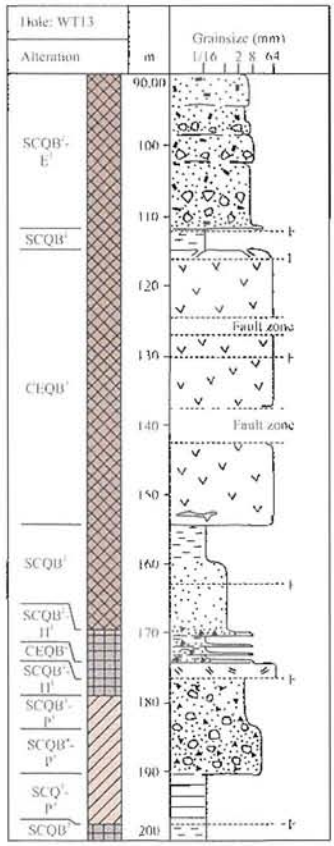
Hole: WT13
Alteration
m
Grainsize (mm)
1/16 2 8 64
90.00
100
110
120
130
140
150
160
170
180
190
200
Fault zone
Fault zone

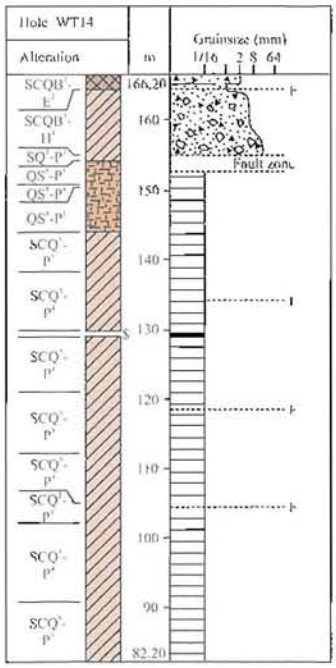
Hole WT14
Alteration
m
Grainsize (mm)
1/16 2 8 64
166.20
160
150
140
130
120
110
100
90
82.20
Fault zone

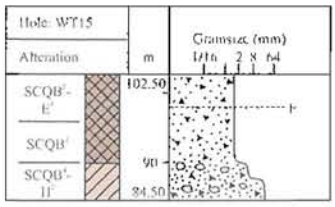
Hole: WT15
Alteration
m
Grainsize (mm)
1/16 2 8 64
102.50
90
84.50

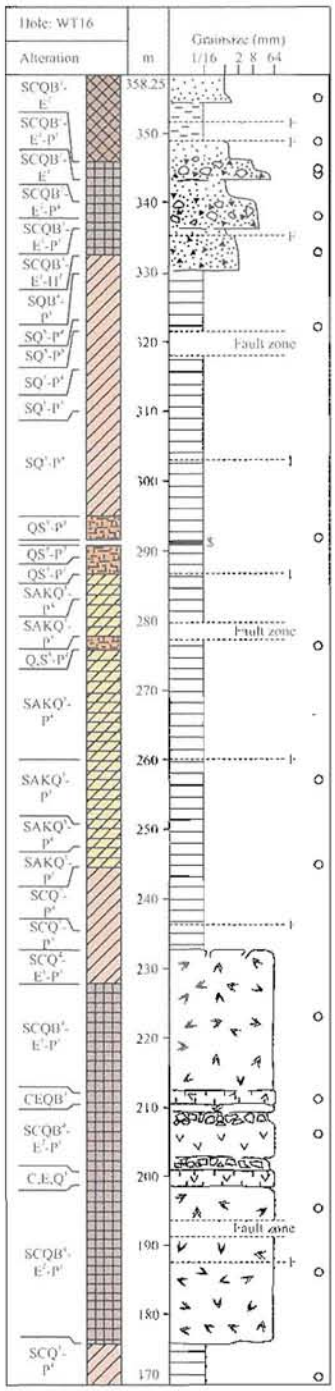
Hole: WT16
Alteration
m
Grainsize (mm)
1/16 2 8 64
358.25
350
340
330
320
310
300
290
280
270
260
250
240
230
220
210
200
190
180
170
Fault zone
Fault zone
Fault zone

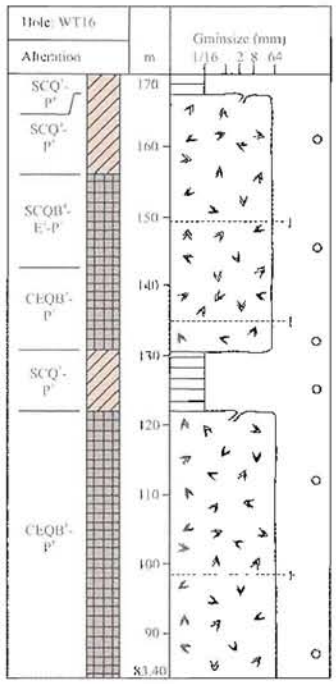
Hole: WT16
Alteration
m
Grainsize (mm)
1/16 2 8 64
170
160
150
140
130
120
110
100
90
83.40

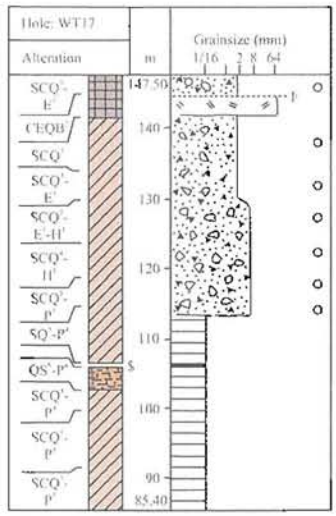
Hole: WT17
Alteration
m
Grainsize (mm)
1/16 2 8 64
147.50
140
130
120
110
100
90
85.40

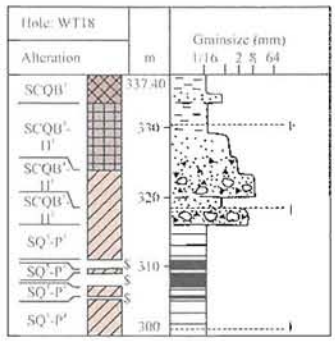
Hole: WT18
Alteration
m
Grainsize (mm)
1/16 2 8 64
337.40
330
320
310
300

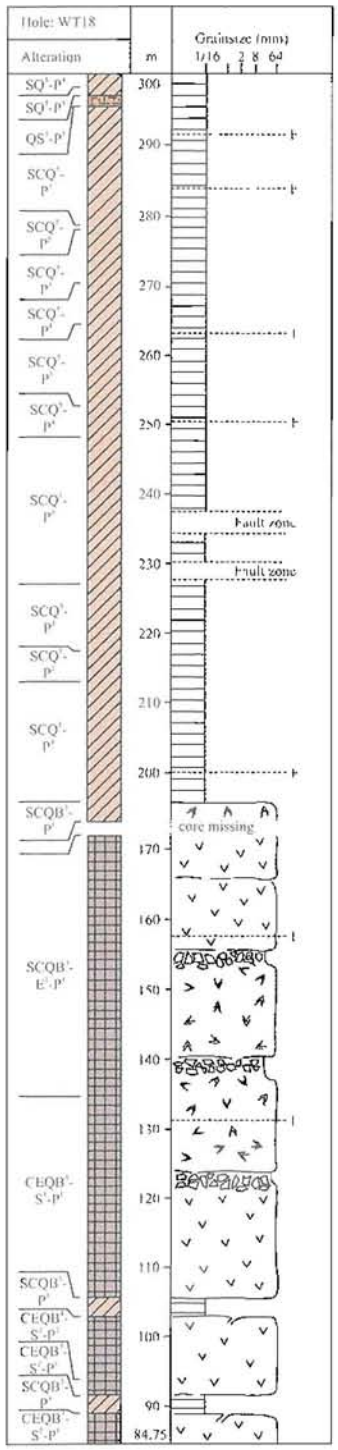
Hole: WT18
Alteration
m
Grainsize (mm)
1/16 2 8 64
300
290
280
270
260
250
240
230
220
210
200
170
160
150
140
130
120
110
100
90
84.75
Fault zone
Fault zone
core missing

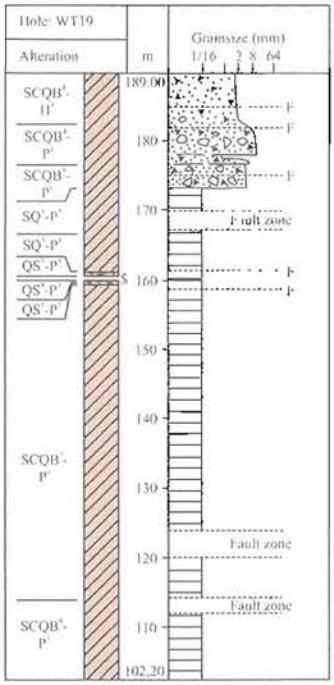
Hole: WT19
Alteration
m
Grainsize (mm)
1/16 2 8 64
189.00
180
170
160
150
140
130
120
110
102.20
Fault zone
Fault zone
SCQB'-P'
SCQB'-II'
SCQB'-P'
SQ'-P'
QS'-P'
SCQB'-P'

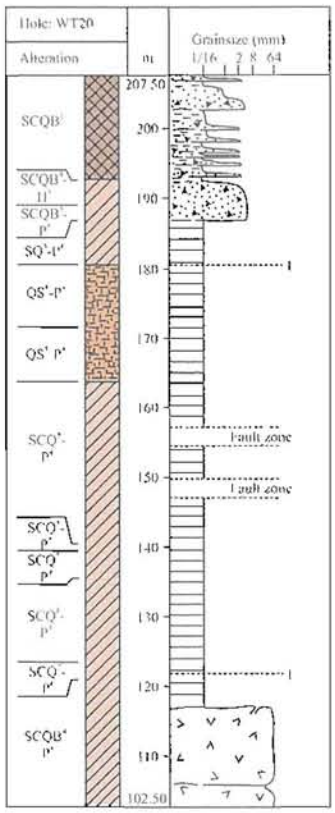
Hole: WT20
Alteration
m
Grainsize (mm)
1/16 2 8 64
207.50
200
190
180
170
160
150
140
130
120
110
102.50
Fault zone
Fault zone
SCQB'
SCQB'-II'
SCQB'-P'
SQ'-P'
QS'-P'
QS' P'
SCQ'-P'
SCQ'-P'
SCQ'-P'
SCQ'-P'
SCQB'-P'

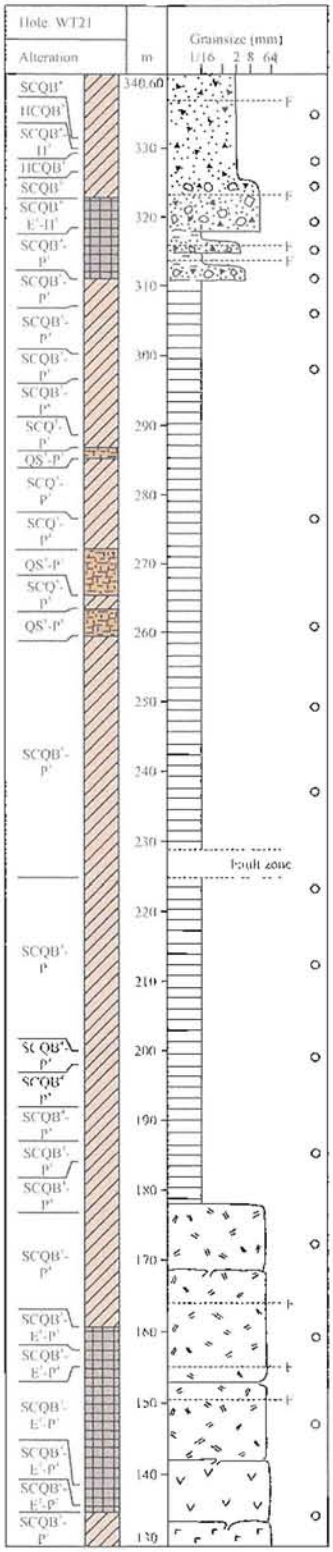
Hole: WT21
Alteration
m
Grainsize (mm)
1/16 2 8 64
340.60
330
320
310
300
290
280
270
260
250
240
230
220
210
200
190
180
170
160
150
140
130
Fault zone
SCQB'
HCQB'
SCQB'-II'
HCQB'
SCQB'
SCQB'-E'-II'
SCQB'-P'
SCQB'-P'
SCQB'-P'
SCQB'-P'
SCQ'-P'
QS'-P'
SCQ'-P'
SCQ'-P'
QS'-P'
SCQB'-P'
Fault zone
SCQB'-P'
SCQB'-P'
SCQB'-P'
SCQB'-P'
SCQB'-P'
SCQB'-E'-P'
SCQB'-E'-P'
SCQB'-E'-P'
SCQB'-E'-P'
SCQB'-E'-P'
SCQB'-P'

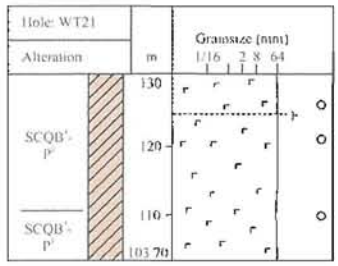
Hole: WT21
Alteration
m
Grainsize (mm)
1/16 2 8 64
130
120
110
103.70
SCQB'-P'
SCQB'-P'

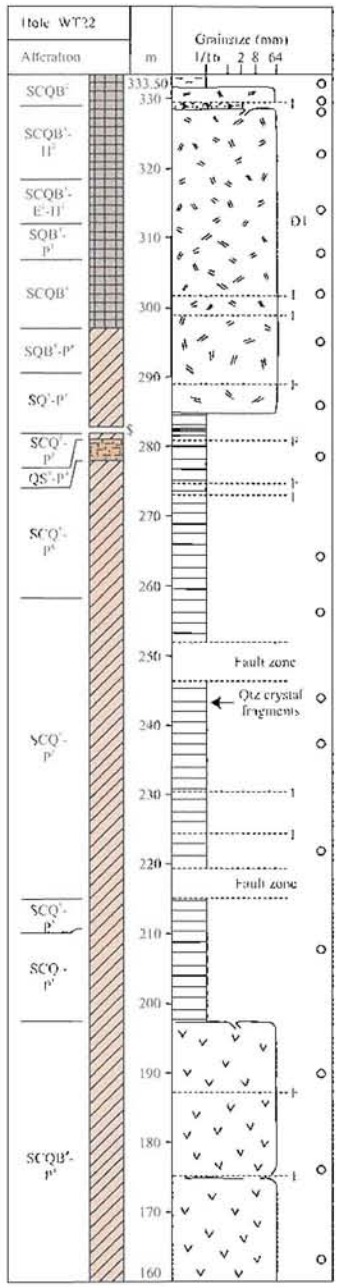
Hole: WT22
Alteration
m
Grainsize (mm)
1/16 2 8 64
333.50
330
320
310
300
290
280
270
260
250
240
230
220
210
200
190
180
170
160
D1
Fault zone
Qtz crystal fragments
Fault zone
SCQB'
SCQB'-II'
SCQB'-E'-II'
SQB'-P'
SCQB'
SQB'-P'
SQ'-P'
SCQ'-P'
QS'-P'
SCQ'-P'
SCQ'-P'
SCQ'-P'
SCQ'-P'
SCQB'-P'

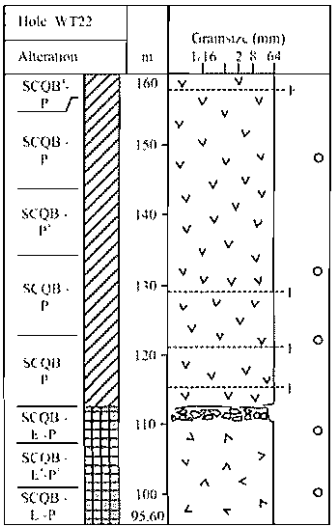
Hole WT22
Alteration
m
Grainsize (mm)
1 16 2 8 64
SCQB'-P
SCQB-P
SCQB-P'
SCQB-P
SCQB-P
SCQB-L-P
SCQB-L'-P'
SCQB-L-P
160
150
140
130
120
110
100
95.60

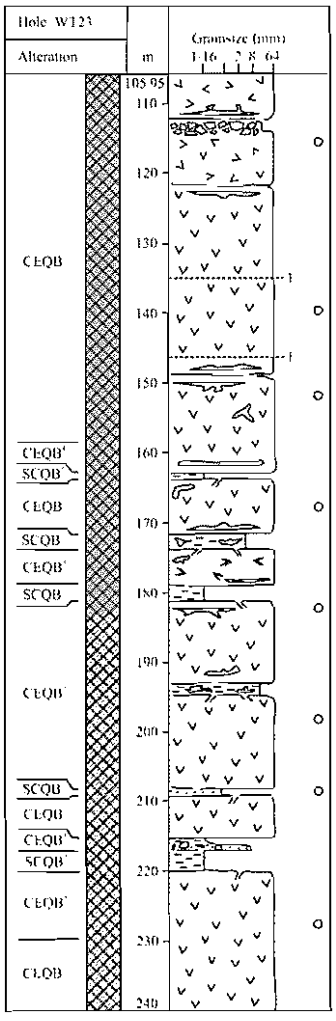
Hole WT23
Alteration
m
Grainsize (mm)
1 16 2 8 64
CEQB
CEQB'
SCQB
CEQB
SCQB
CEQB'
SCQB
CEQB
SCQB
CEQB
SCQB'
CEQB'
CEQB
105.95
110
120
130
140
150
160
170
180
190
200
210
220
230
240

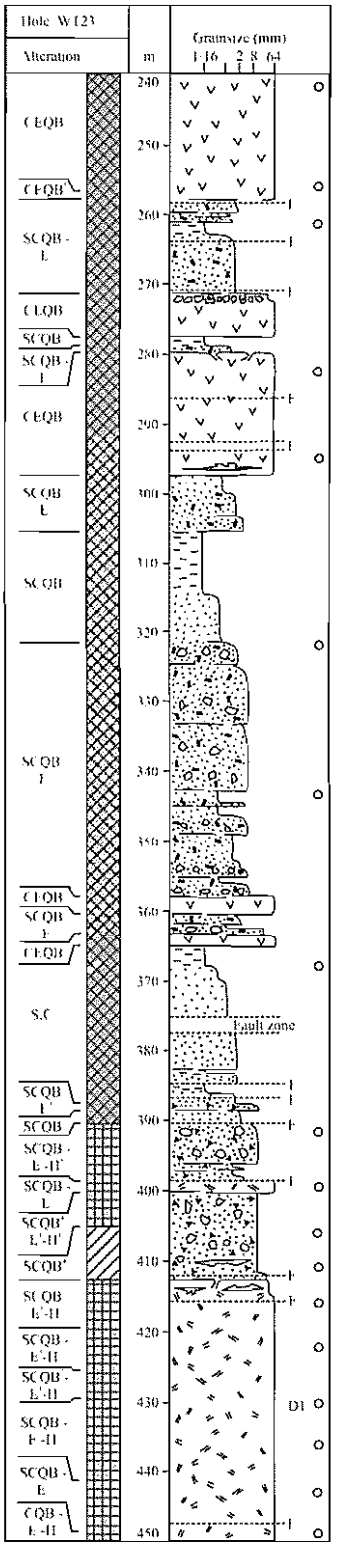
Hole WT23
Alteration
m
Grainsize (mm)
1 16 2 8 64
CEQB
CEQB'
SCQB-L
CEQB
SCQB
SCQB-L
CEQB
SCQB
L
CEQB
SCQB
SCQB
L
SCQB
CEQB
S.C
SCQB
L'
SCQB
SCQB-L-H'
SCQB-L
SCQB'
L'-H'
SCQB'
SCQB
L'-H
SCQB-L'-H
SCQB-L'-H
SCQB-L-H
SCQB-L
CQB-L-H
Fault zone
D1
240
250
260
270
280
290
300
310
320
330
340
350
360
370
380
390
400
410
420
430
440
450

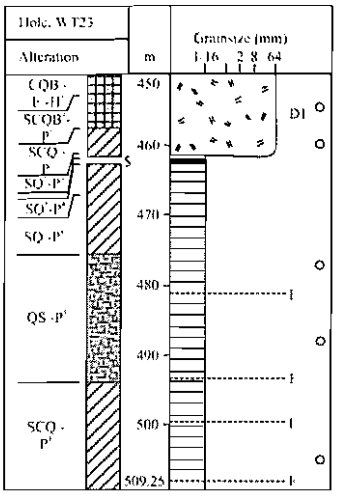
Hole, WT23
Alteration
m
Grainsize (mm)
1 16 2 8 64
CQB-L-H'
SCQB'-P
SCQ-P
SQ-P'
SQ'-P'
SQ-P'
QS-P'
SCQ-P'
D1
450
460
470
480
490
500
509.25

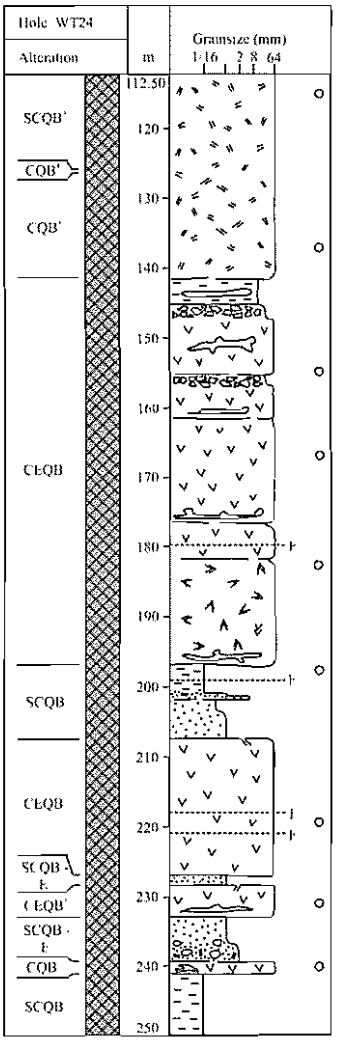
Hole WT24
Alteration
m
Grainsize (mm)
1 16 2 8 64
SCQB'
CQB'
CQB'
CEQB
SCQB
CEQB
SCQB-L
CEQB'
SCQB-L
CQB
SCQB
112.50
120
130
140
150
160
170
180
190
200
210
220
230
240
250

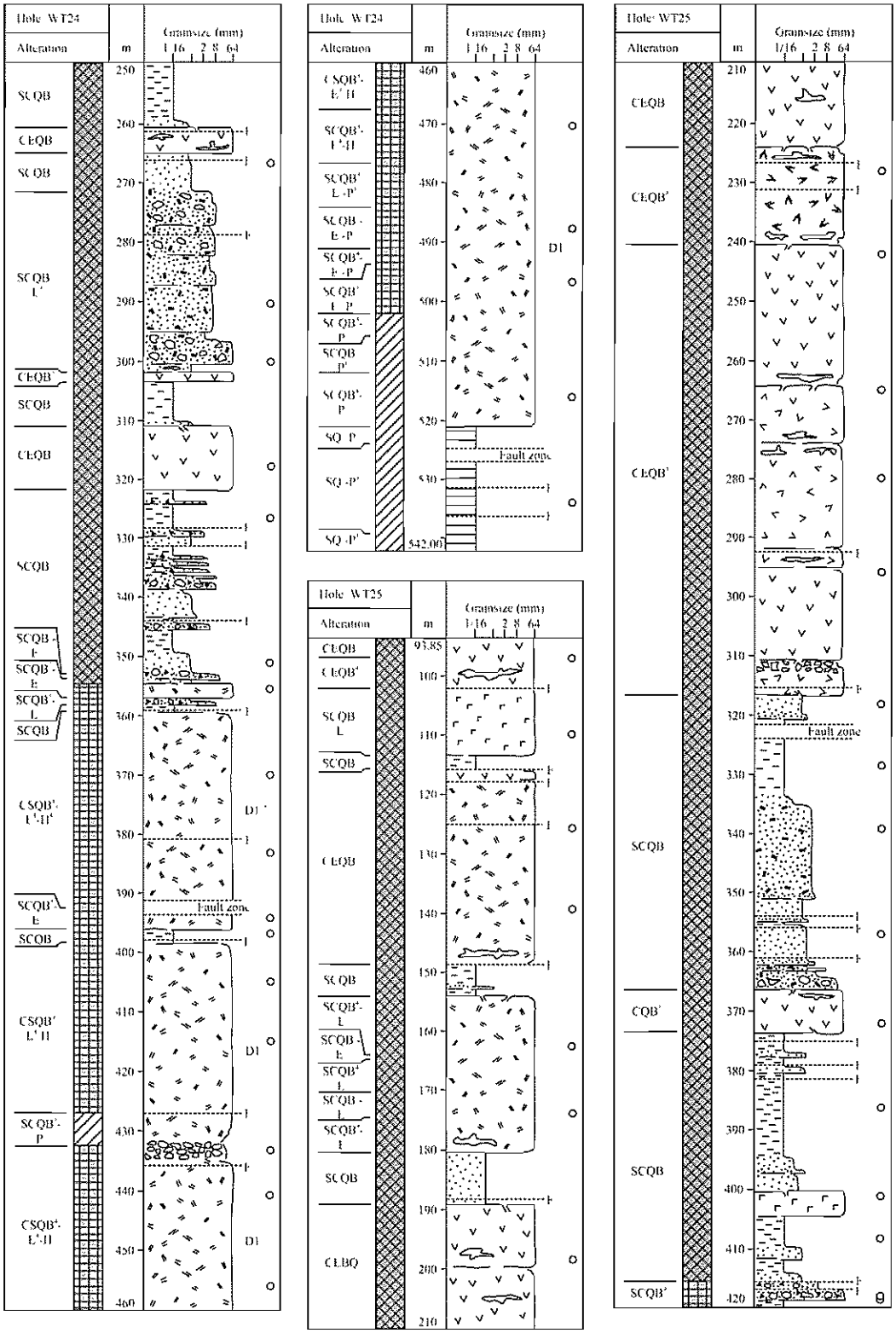
Hole WT24
Alteration
m
Grainsize (mm)
1/16 2 8 64
SCQB
CEQB
SCQB
SCQB L'
CEQB
SCQB
CEQB
SCQB
SCQB - E
SCQB - E
SCQB' - L
SCQB
CSQB' L'-H'
SCQB' E
SCQB
CSQB' L'-H
SCQB' - P
CSQB' L'-H
D1
Fault zone
Hole WT24
CSQB' L'-H
SCQB' L'-H
SCQB' L'-P'
SCQB - E-P
SCQB' E-P'
SCQB' L-P'
SCQB' - P
SCQB P'
SCQB' P
SQ - P
SQ -P'
SQ -P'
542.00
D1
Fault zone
Hole WT25
CEQB
CEQB'
SCQB L
SCQB
CEQB
SCQB
SCQB' - L
SCQB - E
SCQB' L
SCQB - L
SCQB' L
SCQB
CEBQ
93.85
Hole WT25
CEQB
CEQB'
CEQB'
SCQB
CQB'
SCQB
SCQB'
Fault zone

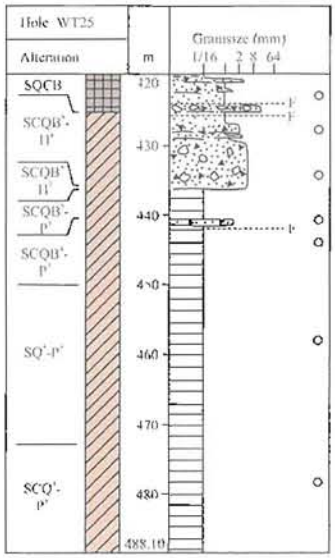
Hole: WT25
Alteration
m
Grainsize (mm)
1/16 2 8 64
SQCB
SCQB'-II'
SCQB'-II'
SCQB'-P'
SCQB'-P'
SQ'-P'
SCQ'-P'
420
430
440
460
470
480
488.10
Fault zone

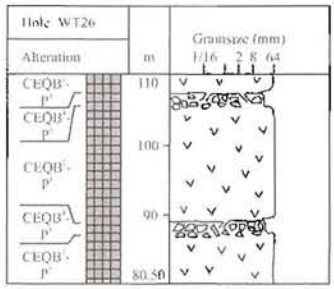
Hole: WT26
Alteration
m
Grainsize (mm)
1/16 2 8 64
CEQB'-P'
CEQB'-P'
CEQB'-P'
CEQB'-P'
CEQB'-P'
110
100
90
80.50

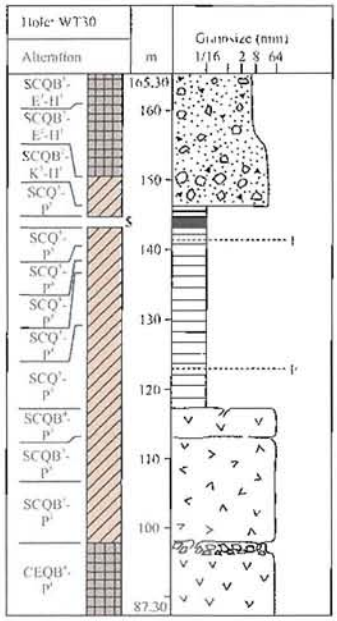
Hole: WT30
Alteration
m
Grainsize (mm)
1/16 2 8 64
SCQB'-E'-H'
SCQB'-E'-H'
SCQB'-K'-H'
SCQ'-P'
SCQ'-P'
SCQ'-P'
SCQ'-P'
SCQ'-P'
SCQB'-P'
SCQB'-P'
SCQB'-P'
CEQB'-P'
165.30
160
150
140
130
120
110
100
87.30

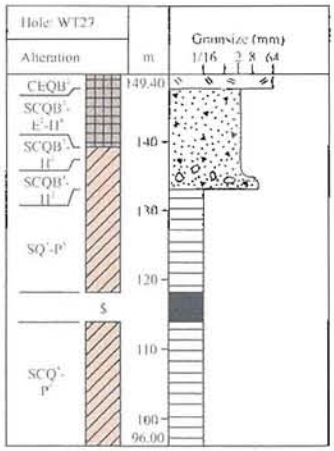
Hole: WT27
Alteration
m
Grainsize (mm)
1/16 2 8 64
CEQB'-
SCQB'-E'-H'
SCQB'-H'
SCQB'-H'
SQ'-P'
SCQ'-P'
149.40
140
130
120
110
100
96.00

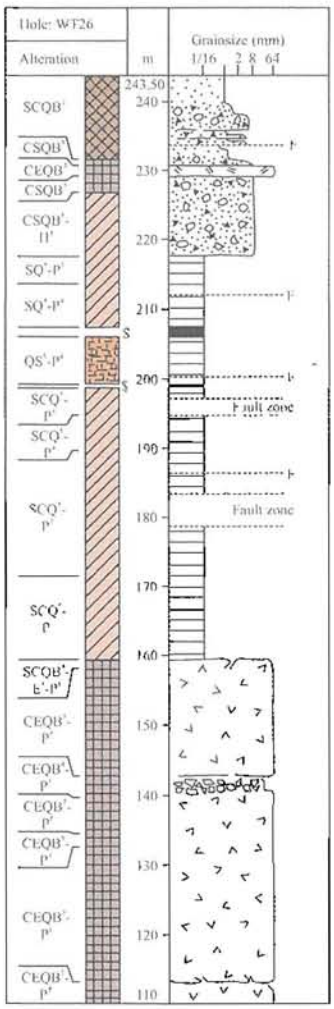
Hole: WT26
Alteration
m
Grainsize (mm)
1/16 2 8 64
SCQB'
CSQB'
CEQB'
CSQB'
CSQB'-H'
SQ'-P'
SQ'-P'
QS'-P'
SCQ'-P'
SCQ'-P'
SCQ'-P'
SCQ'-P'
SCQB'-E'-P'
CEQB'-P'
CEQB'-P'
CEQB'-P'
CEQB'-P'
CEQB'-P'
CEQB'-P'
243.50
240
230
220
210
200
190
180
170
160
150
140
130
120
110
Fault zone
Fault zone

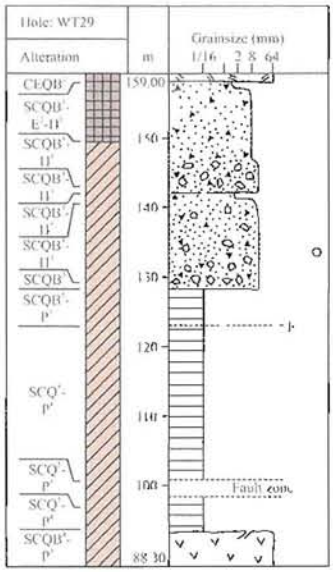
Hole: WT29
Alteration
m
Grainsize (mm)
1/16 2 8 64
CEQB'
SCQB'-E'-H'
SCQB'-H'
SCQB'-H'
SCQB'-H'
SCQB'-H'
SCQB'-P'
SCQ'-P'
SCQ'-P'
SCQ'-P'
SCQB'-P'
159.00
150
140
130
120
110
100
88.30
Fault zone

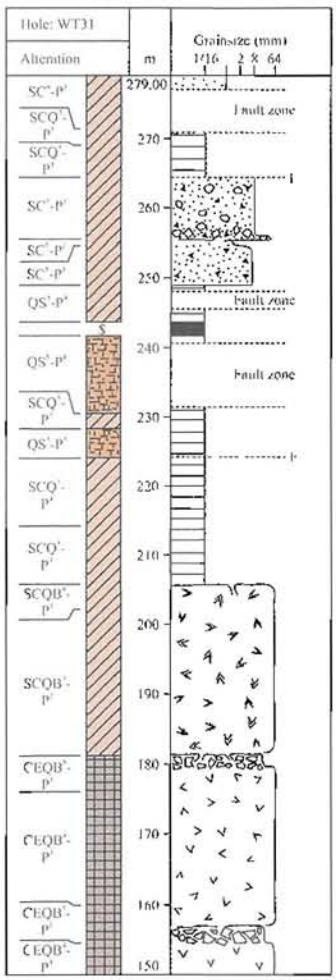
Hole: WT31
Alteration
m
Grainsize (mm)
1/16 2 8 64
SC'-P'
SCQ'-P'
SCQ'-P'
SC'-P'
SC'-P'
SC'-P'
QS'-P'
QS'-P'
SCQ'-P'
QS'-P'
SCQ'-P'
SCQ'-P'
SCQB'-P'
SCQB'-P'
CEQB'-P'
CEQB'-P'
CEQB'-P'
CEQB'-P'
279.00
270
260
250
240
230
220
210
200
190
180
170
160
150
Fault zone
Fault zone
Fault zone

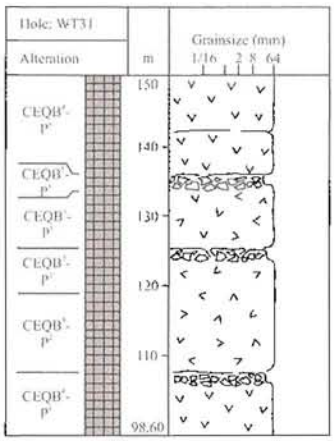
Hole: WT31
Alteration
m
Grainsize (mm)
1/16 2 8 64
150
140
130
120
110
98.60

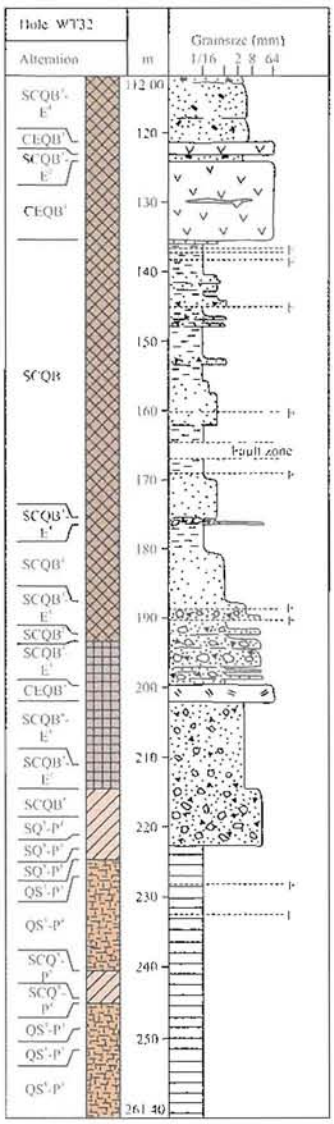
Hole: WT32
Alteration
m
Grainsize (mm)
1/16 2 8 64
112.00
120
130
140
150
160
170
180
190
200
210
220
230
240
250
261.40
Fault zone

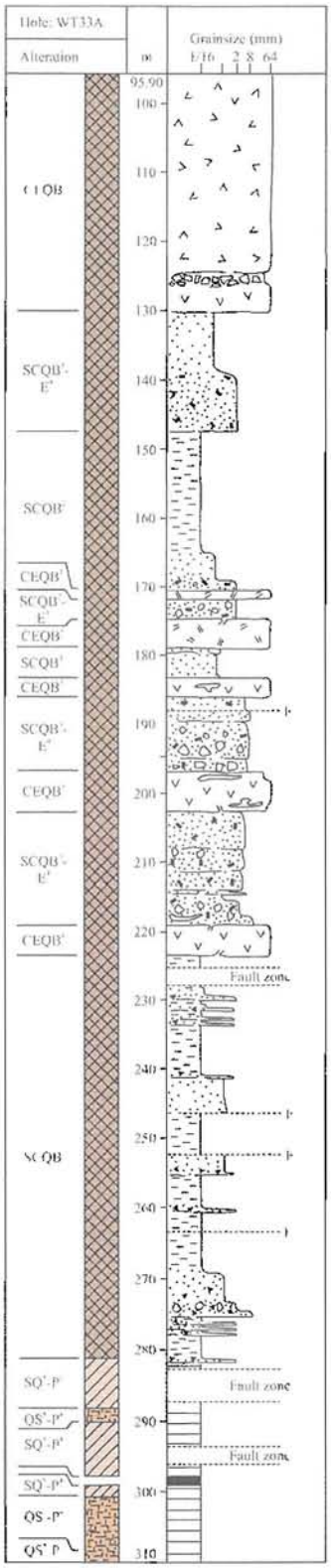
Hole: WT33A
Alteration
m
Grainsize (mm)
1/16 2 8 64
95.90
100
110
120
130
140
150
160
170
180
190
200
210
220
230
240
250
260
270
280
290
300
310
Fault zone
Fault zone
Fault zone

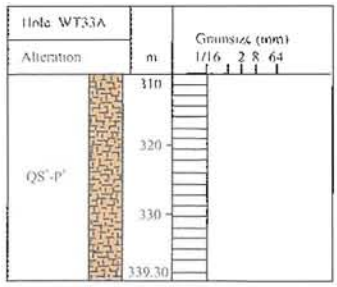
Hole: WT33A
Alteration
m
Grainsize (mm)
1/16 2 8 64
310
320
330
339.30

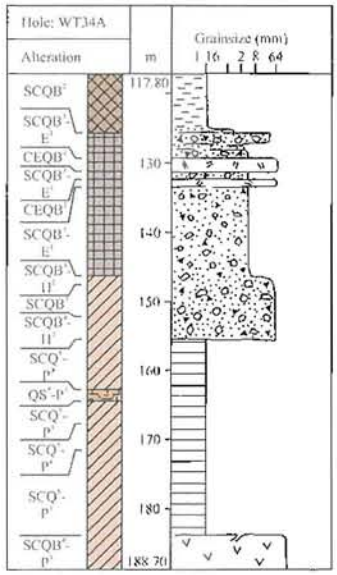
Hole: WT34A
Alteration
m
Grainsize (mm)
1/16 2 8 64
117.80
130
140
150
160
170
180
188.70

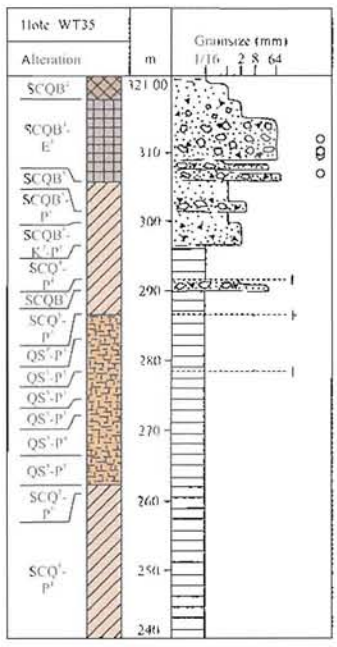
Hole: WT35
Alteration
m
Grainsize (mm)
1/16 2 8 64
321.00
310
300
290
280
270
260
250
240

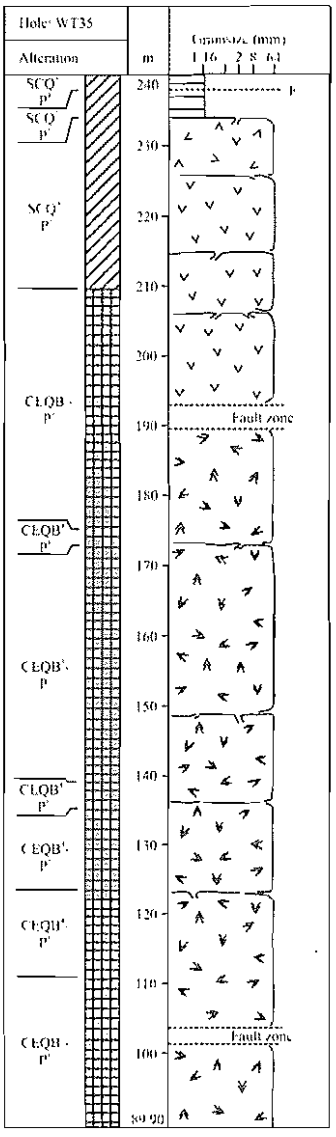
Hole WT35
Alteration
m
Grainsize (mm)
1 16 2 8 64
SCQ' P'
SCQ P'
SCQ' P'
CEQB - P'
CEQB' P'
CEQB' P
CEQB' P'
CEQB' P'
CEQB - P'
240
230
220
210
200
190
180
170
160
150
140
130
120
110
100
90
Fault zone
Fault zone

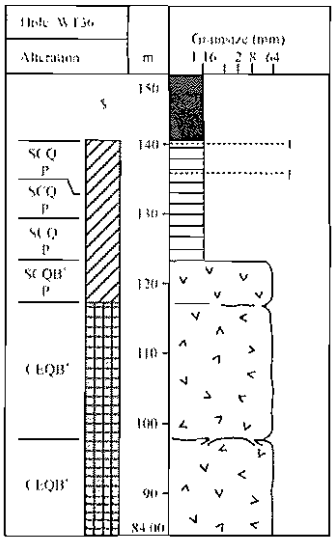
Hole WT36
Alteration
m
Grainsize (mm)
1 16 2 8 64
S
SCQ P
SCQ P
SCQ P
SCQB' P
CEQB'
CEQB'
150
140
130
120
110
100
90
84 80

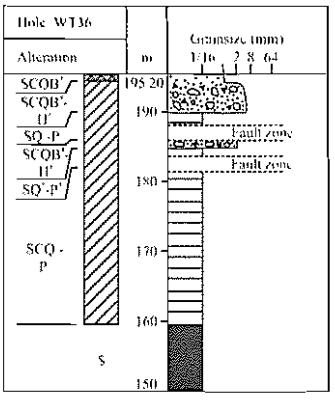
Hole WT36
Alteration
m
Grainsize (mm)
1 16 2 8 64
SCQB' U'
SCQB' U'
SQ -P
SCQB' U'
SQ' P'
SCQ - P
S
195 20
190
180
170
160
150
Fault zone
Fault zone

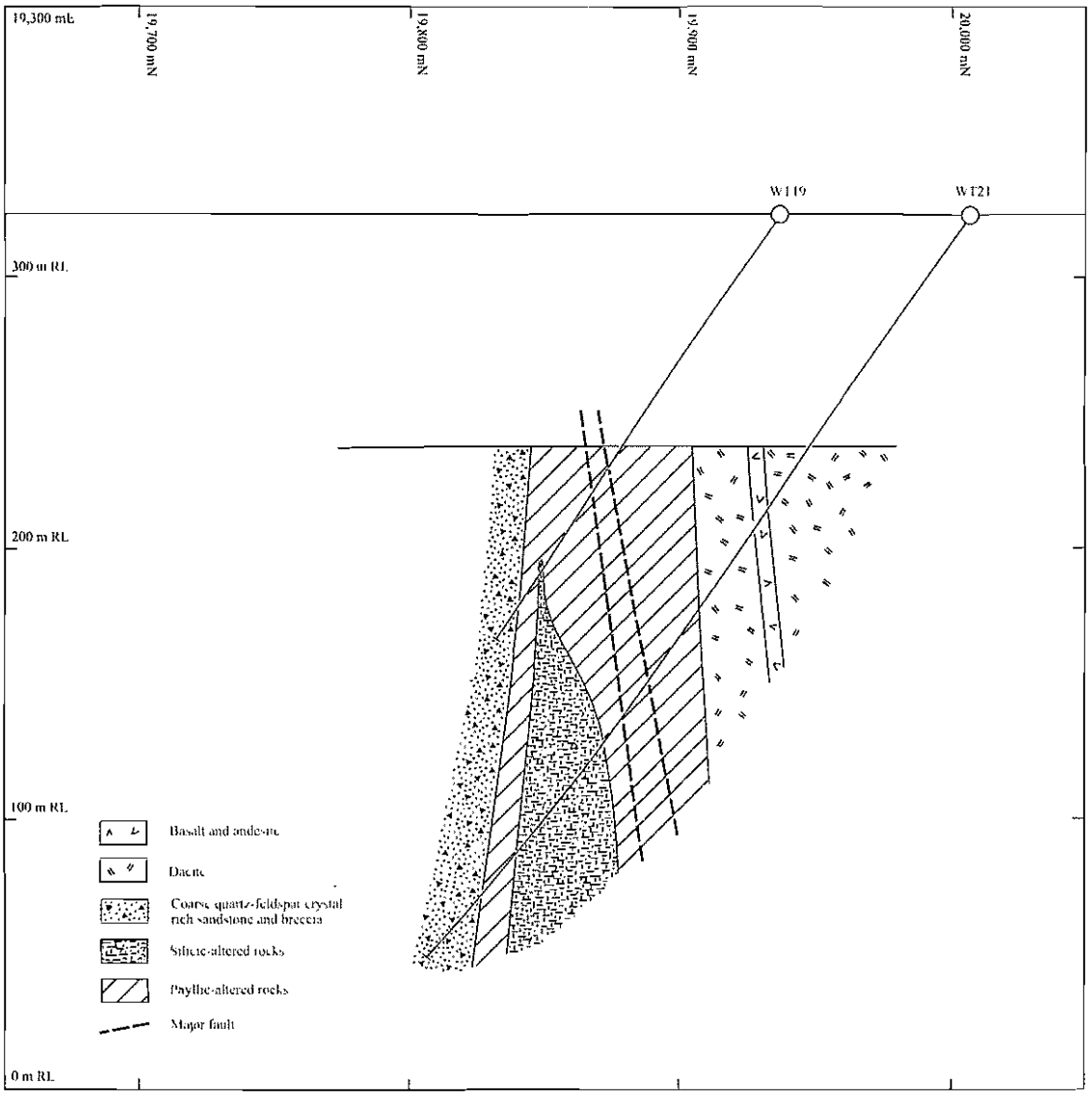
19,300 mE
19,700 mN
19,800 mN
19,900 mN
20,000 mN
WT19
WT21
300 m RL
200 m RL
100 m RL
0 m RL
Basalt and andesite
Dacite
Coarse quartz-feldspar crystal rich sandstone and breccia
Silicic-altered rocks
Pyrite-altered rocks
Major fault

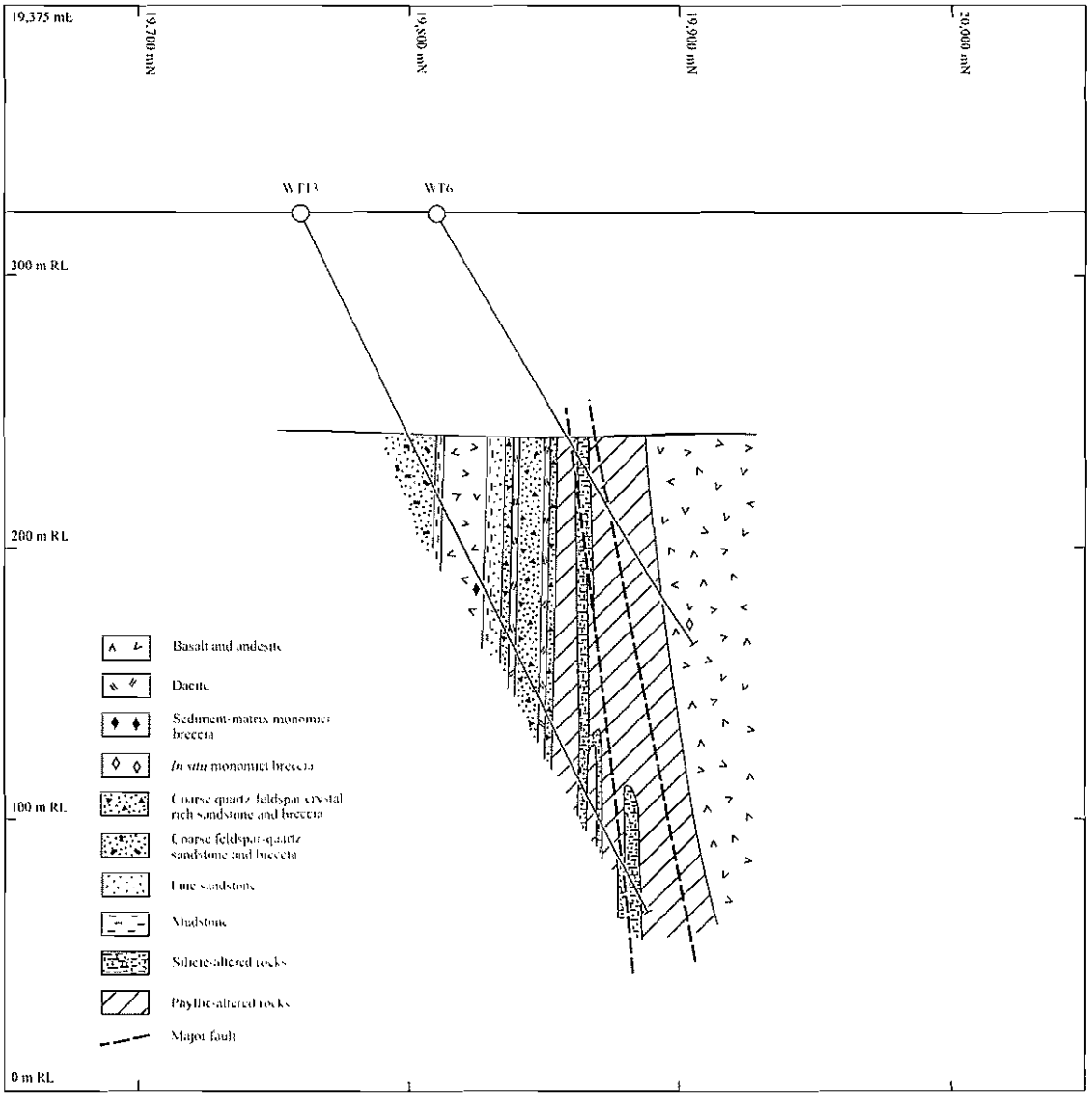
19,375 mE
19,700 mN
19,850 mN
19,900 mN
20,000 mN
WT13
WT6
300 m RL
200 m RL
100 m RL
0 m RL
Basalt and andesite
Dacite
Sediment-matrix monomict breccia
In situ monomict breccia
Coarse quartz feldspar crystal rich sandstone and breccia
Coarse feldspar-quartz sandstone and breccia
Fine sandstone
Mudstone
Silicic-altered rocks
Phyllic-altered rocks
Major fault

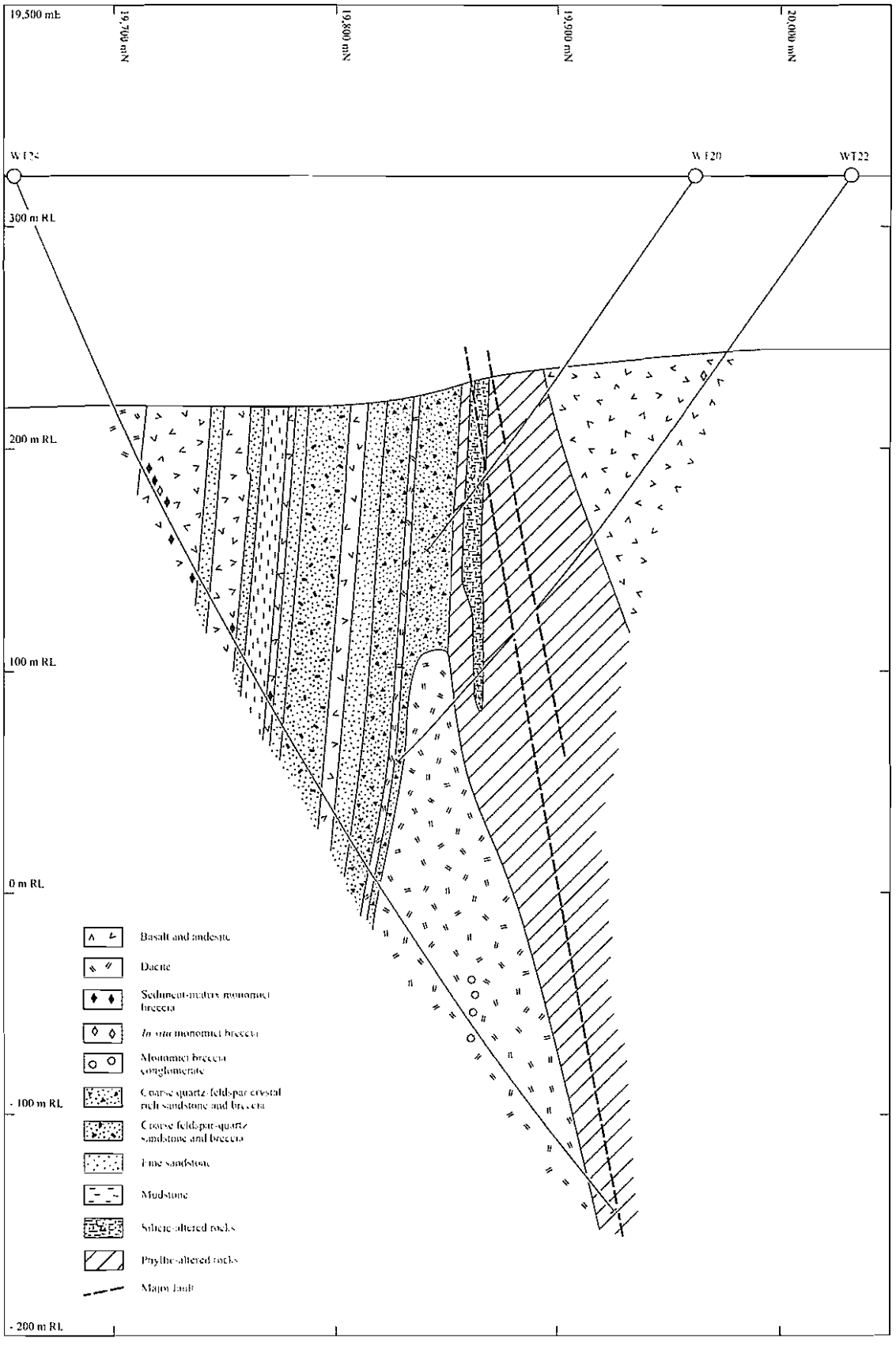
19,500 mE
19,700 mN
19,800 mN
19,900 mN
20,000 mN
WT25
WT20
WT22
300 m RL
200 m RL
100 m RL
0 m RL
- 100 m RL
- 200 m RL
Basalt and andesite
Dacite
Sediment-matrix monomict breccia
In situ monomict breccia
Monomict breccia conglomerate
Coarse quartz-feldspar crystal rich sandstone and breccia
Coarse feldspar-quartz sandstone and breccia
Fine sandstone
Mudstone
Silicic-altered rocks
Phyllic-altered rocks
Major fault

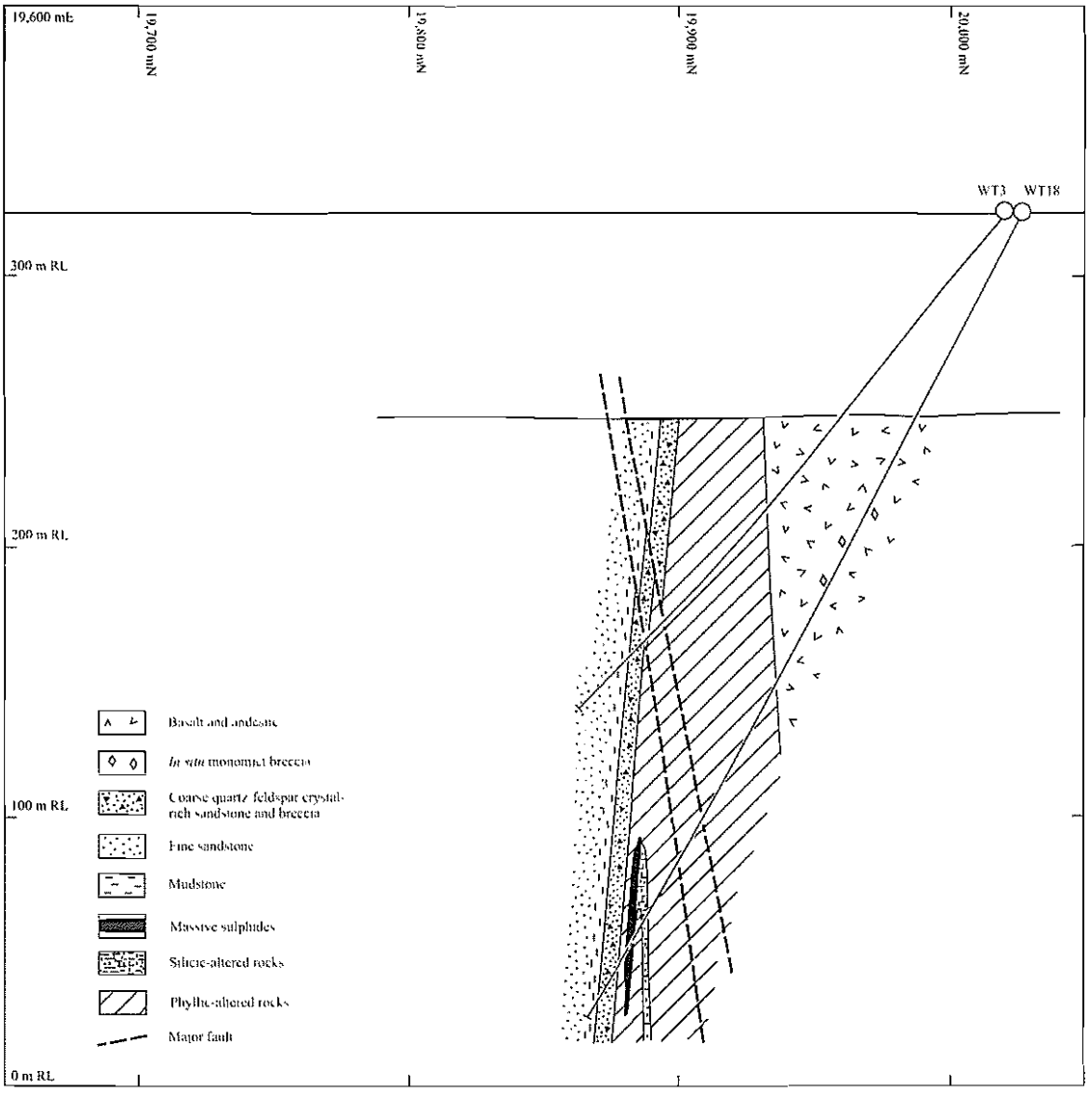
19,600 mE
19,700 mN
19,800 mN
19,900 mN
20,000 mN
WT3
WT18
300 m RL
200 m RL
100 m RL
0 m RL
Basalt and andesite
In situ monomict breccia
Coarse quartz feldspar crystal-rich sandstone and breccia
Fine sandstone
Mudstone
Massive sulphides
Silicic-altered rocks
Phyllic-altered rocks
Major fault

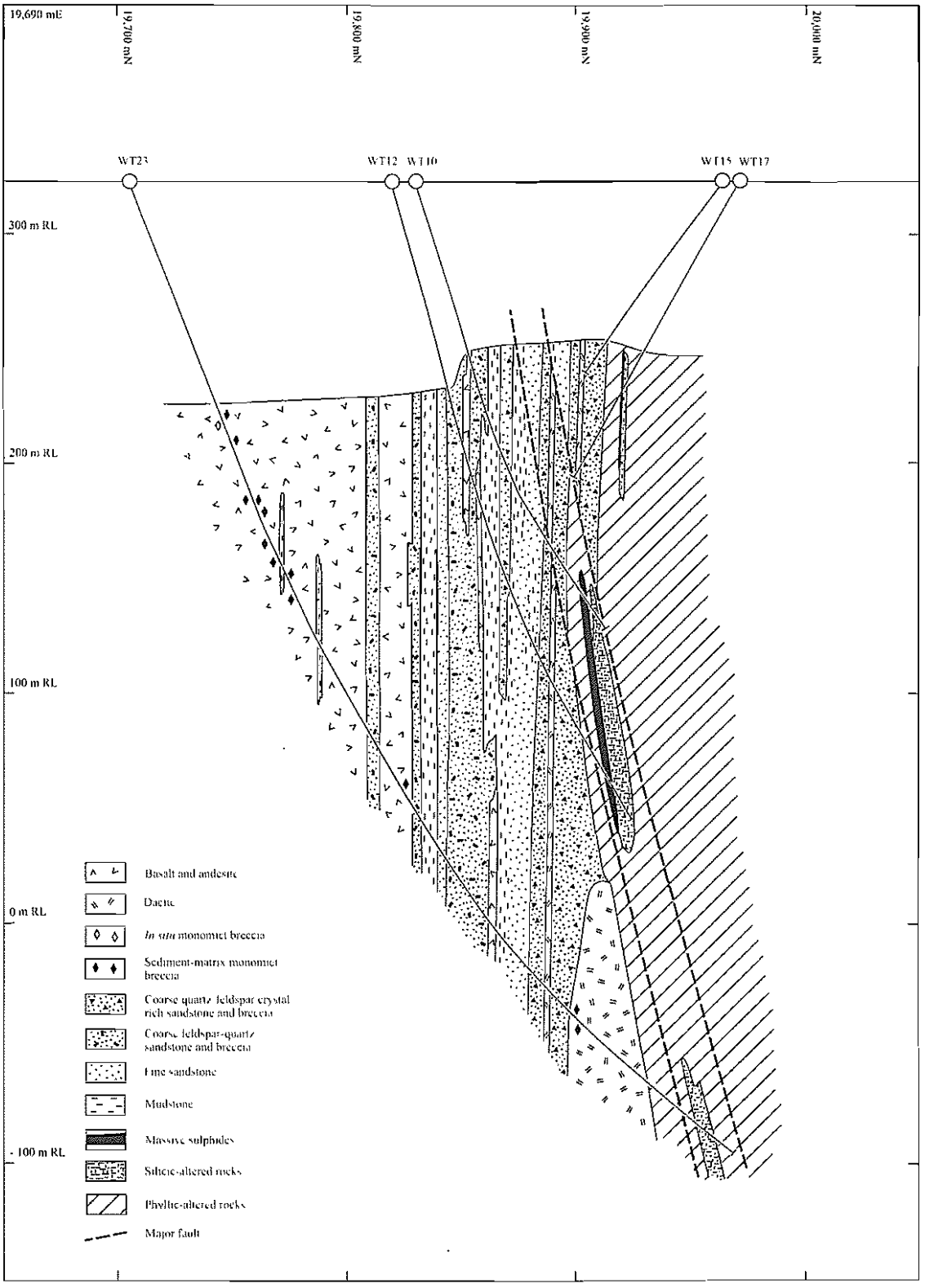
19,690 mE
19,700 mN
19,800 mN
19,900 mN
20,000 mN
WT23
WT12
WT10
WT15
WT17
300 m RL
200 m RL
100 m RL
0 m RL
- 100 m RL
Basalt and andesite
Dacite
In situ monomict breccia
Sediment-matrix monomict breccia
Coarse quartz feldspar crystal rich sandstone and breccia
Coarse feldspar-quartz sandstone and breccia
Fine sandstone
Mudstone
Massive sulphides
Silicic-altered rocks
Phyllic-altered rocks
Major fault

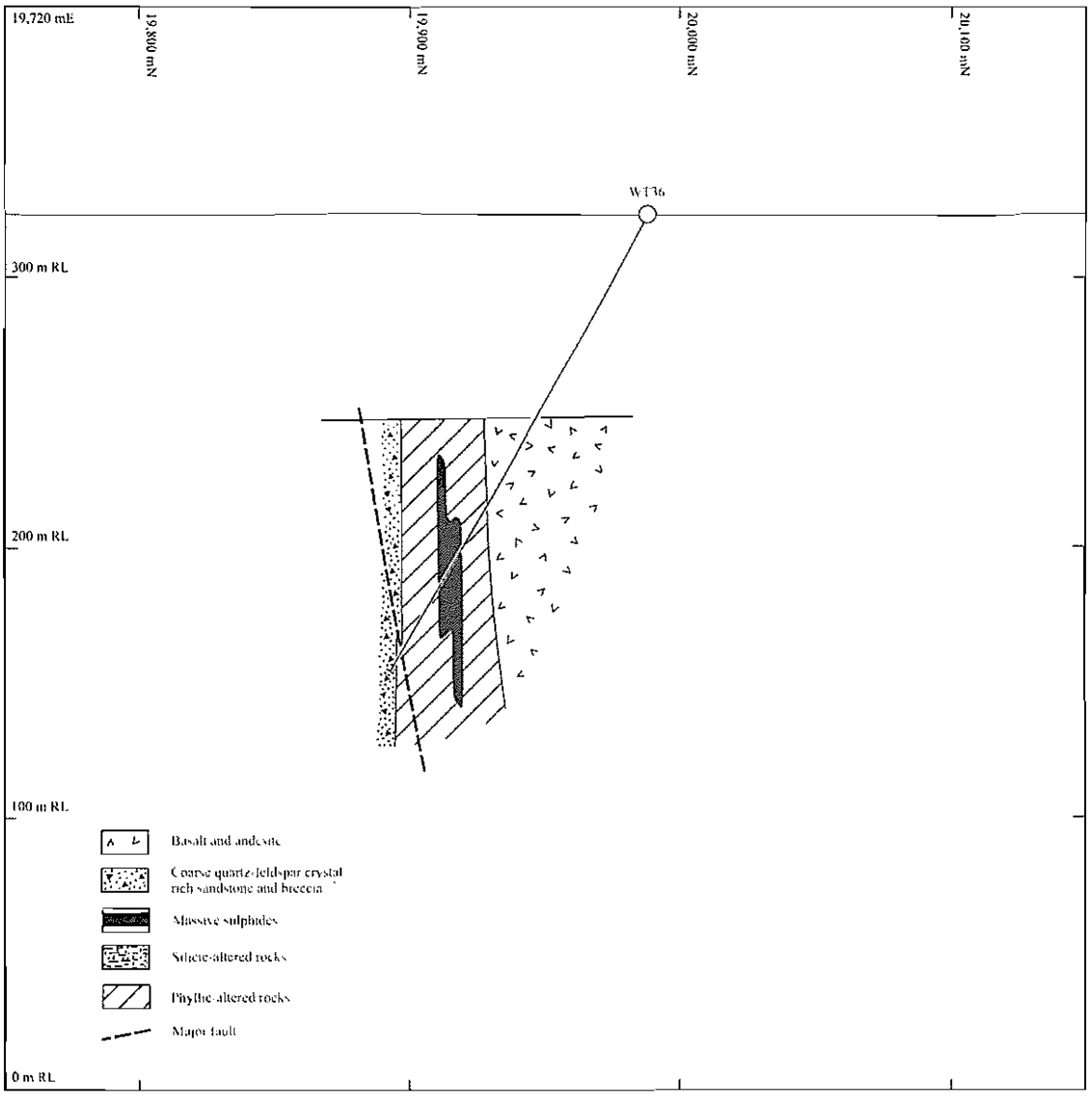
19,720 mE
19,800 mN
19,900 mN
20,000 mN
20,100 mN
WT36
300 m RL
200 m RL
100 m RL
0 m RL
Basalt and andesite
Coarse quartz-feldspar crystal rich sandstone and breccia
Massive sulphides
Silicic-altered rocks
Phyllic-altered rocks
Major fault

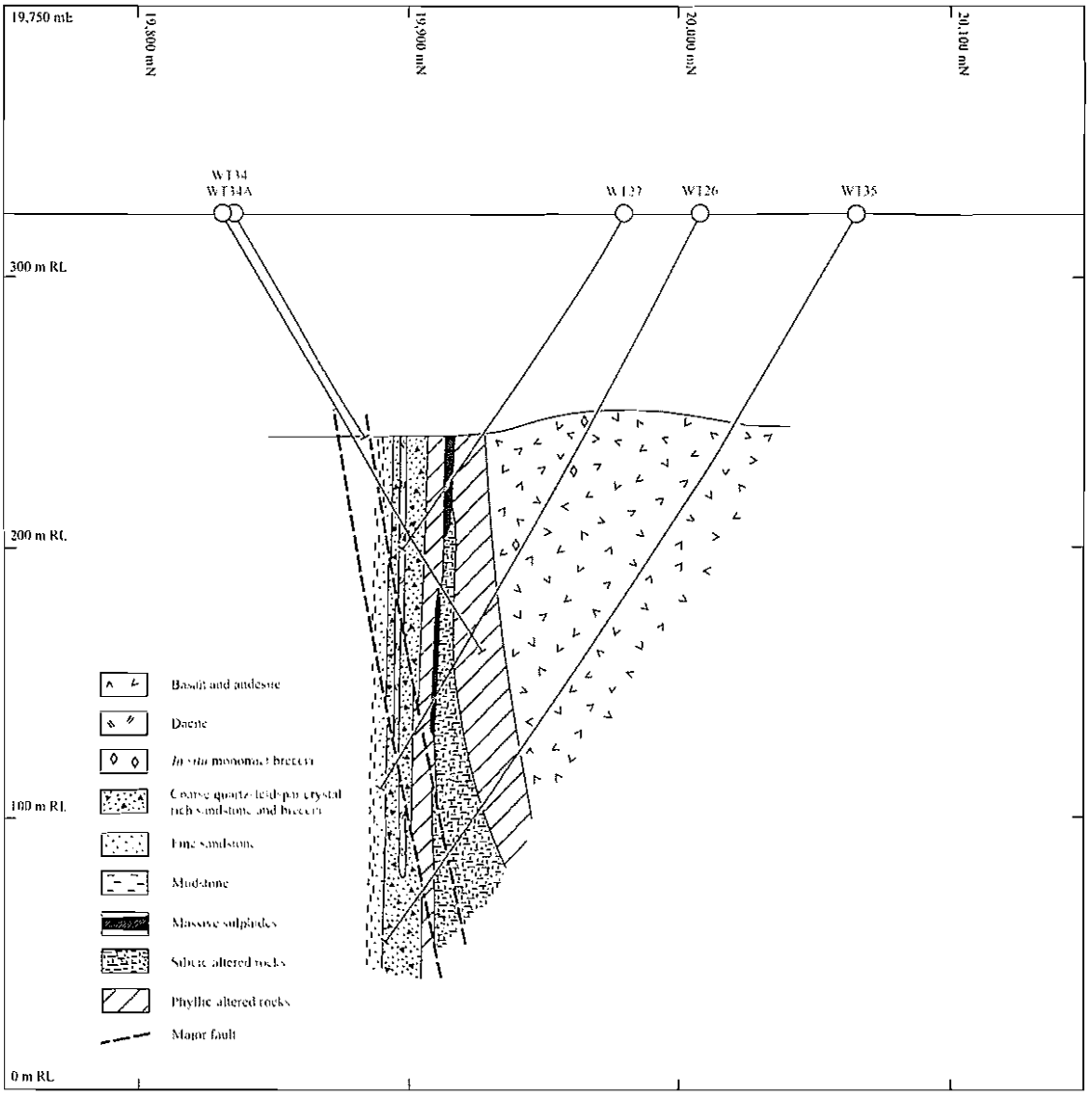
19,750 mE
19,800 mN
19,900 mN
20,000 mN
20,100 mN
WT34
WT34A
WT27
WT26
WT35
300 m RL
200 m RL
100 m RL
0 m RL
Basalt and andesite
Dacite
In situ monomict breccia
Coarse quartz-feldspar crystal rich sandstone and breccia
Fine sandstone
Mudstone
Massive sulphides
Silicic altered rocks
Phyllic altered rocks
Major fault

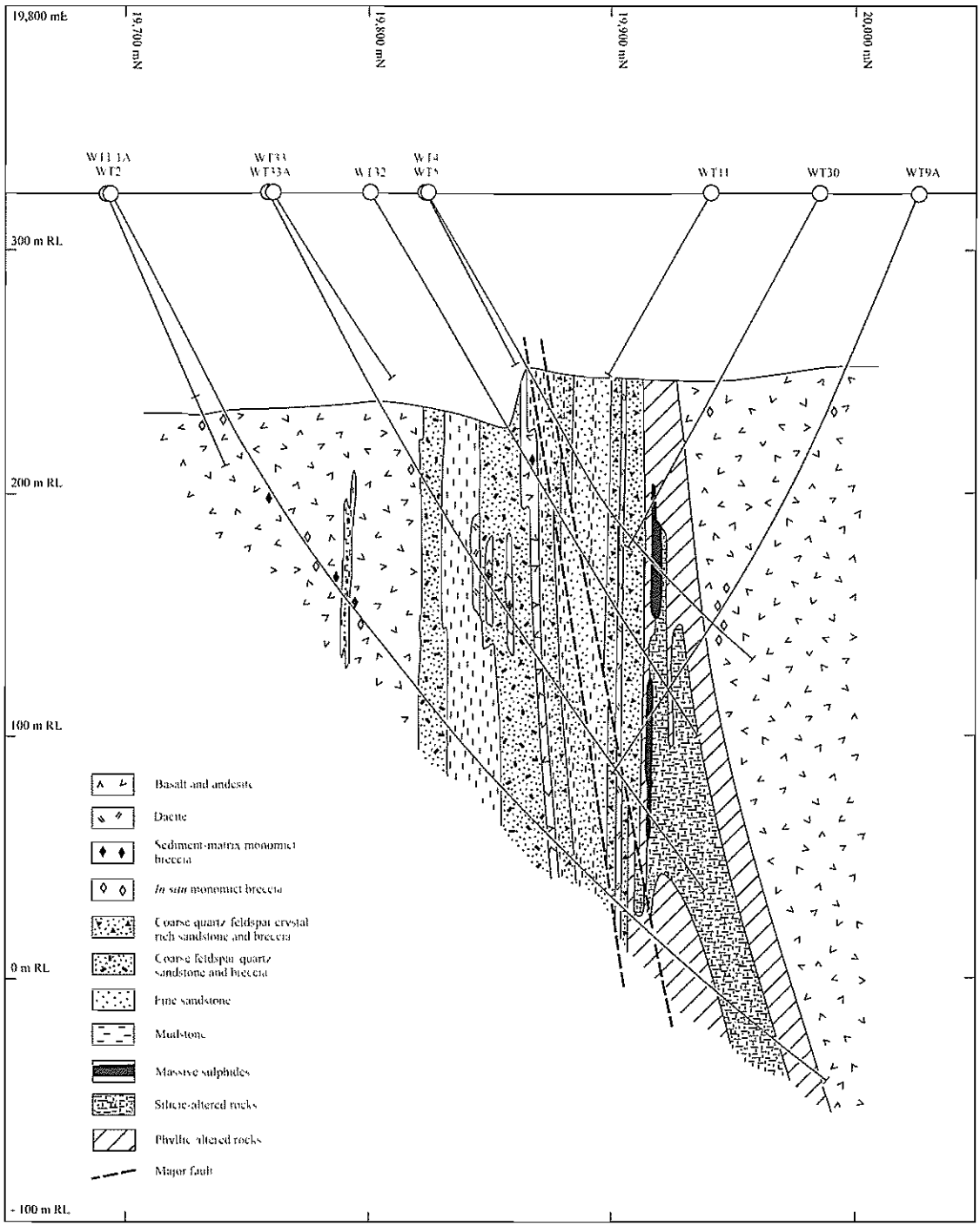
19,800 mE
19,700 mN
19,800 mN
19,900 mN
20,000 mN
WT1 1A
WT2
WT33
WT33A
WT32
WT3
WT5
WT31
WT30
WT9A
300 m RL
200 m RL
100 m RL
0 m RL
- 100 m RL
Basalt and andesite
Dacite
Sediment-matrix monomict breccia
In situ monomict breccia
Coarse quartz feldspar crystal rich sandstone and breccia
Coarse feldspar quartz sandstone and breccia
Fine sandstone
Mudstone
Massive sulphides
Silicic-altered rocks
Phyllic-altered rocks
Major fault

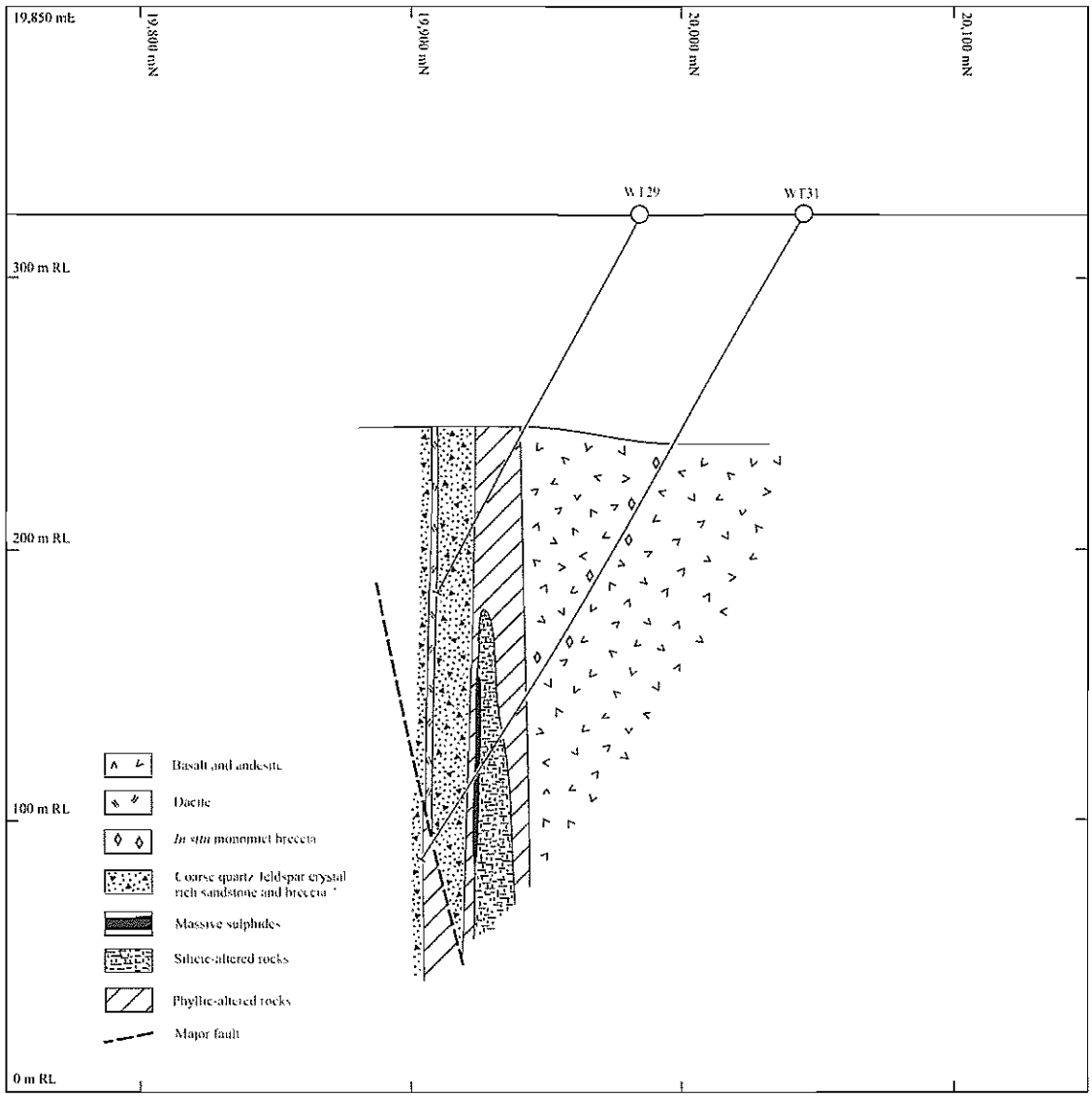
19,850 mE
19,800 mN
19,900 mN
20,000 mN
20,100 mN
WT29
WT31
300 m RL
200 m RL
100 m RL
0 m RL
Basalt and andesite
Dacite
In situ monomict breccia
Coarse quartz feldspar crystal rich sandstone and breccia
Massive sulphides
Silicic-altered rocks
Phyllic-altered rocks
Major fault

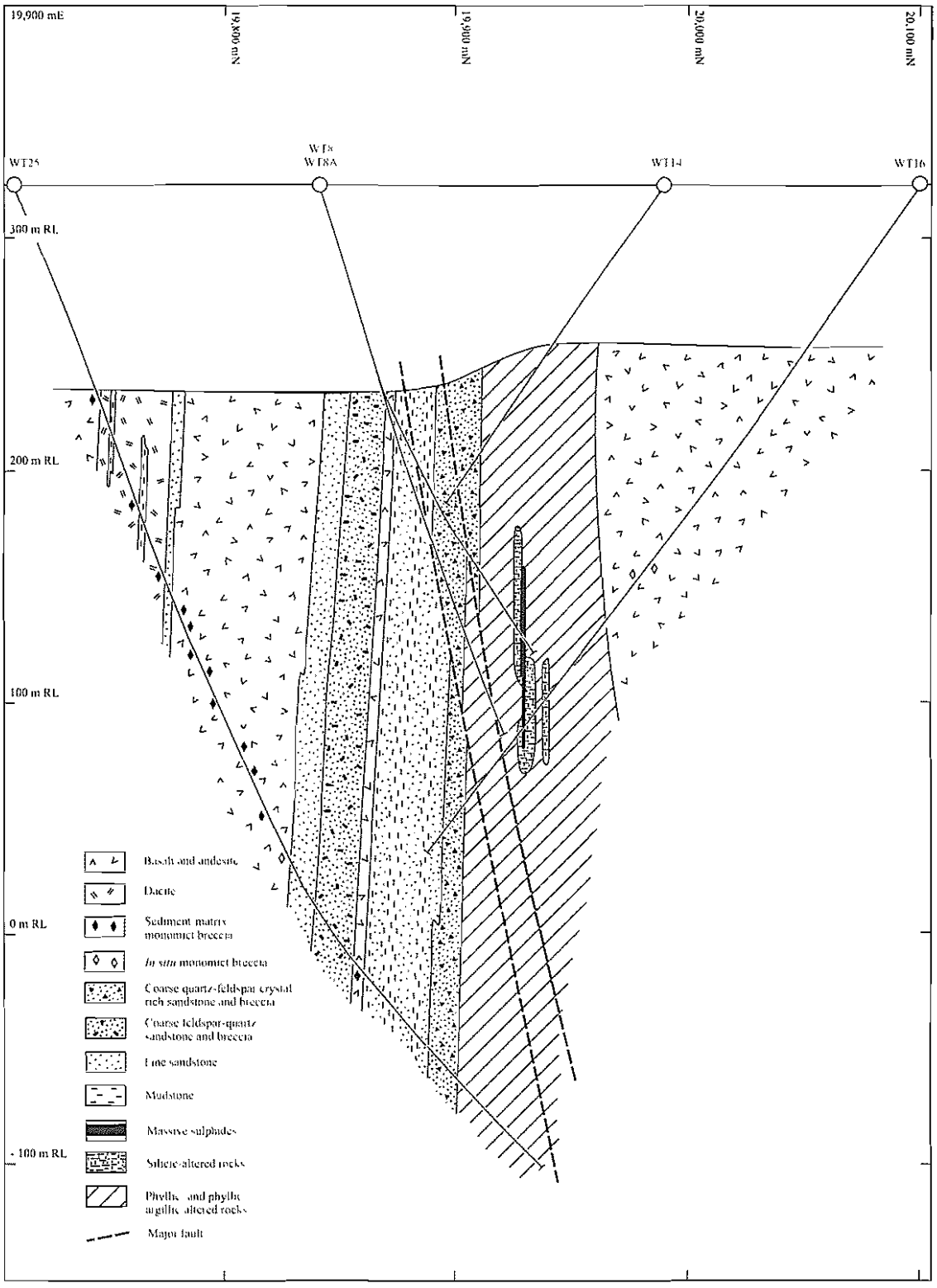
19,900 mE
19,800 mN
19,900 mN
20,000 mN
20,100 mN
WT25
WT8
WT8A
WT14
WT16
300 m RL
200 m RL
100 m RL
0 m RL
- 100 m RL
Basalt and andesite
Dacite
Sediment matrix monomict breccia
In situ monomict breccia
Coarse quartz-feldspar crystal rich sandstone and breccia
Coarse feldspar-quartz sandstone and breccia
Fine sandstone
Mudstone
Massive sulphides
Silicic-altered rocks
Phyllic and phyllic argillic altered rocks
Major fault

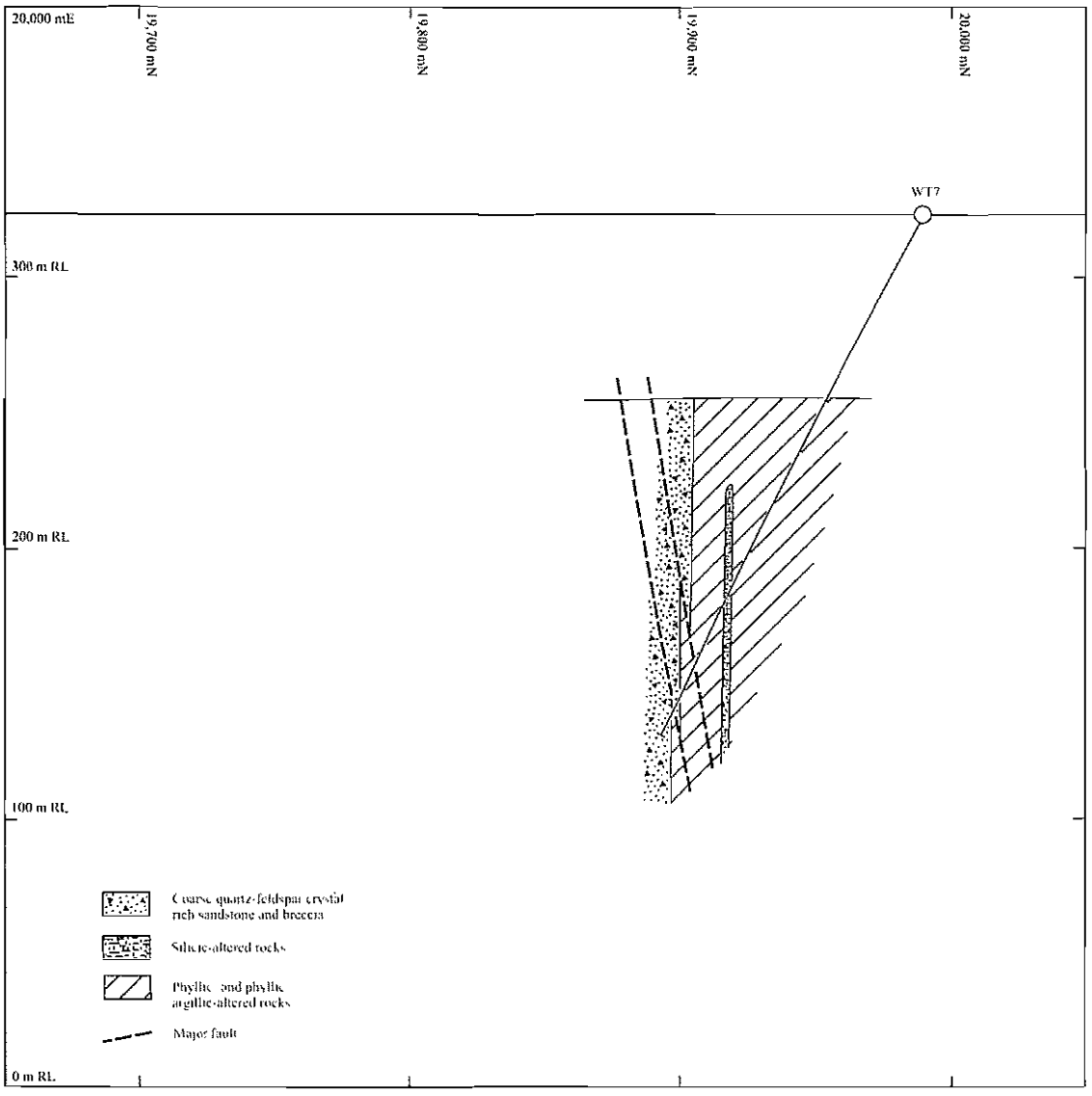
20,000 mE
19,700 mN
19,800 mN
19,900 mN
20,000 mN
WT7
300 m RL
200 m RL
100 m RL
0 m RL
Coarse quartz-feldspar crystal rich sandstone and breccia
Silicic-altered rocks
Phyllic and phyllic argillic-altered rocks
Major fault

Sample (drill hole, meters)	Petrographic description
WT2-103 (WT2, 103.90-104.50)	Basalt. Very weakly px porphyritic. Highly amygdaloidal (qtz+chl+carb and chl+qtz filled). Regional alteration: px phenocrysts entirely replaced, pervasive groundmass alteration resulted in a fine intergrowth of fdsp laths with chl, ep, qtz, and carb. Spotted ep and disseminated py. Qtz and qtz+carb+hem veinlets.
WT2-117 (WT2, 117.50-118.15)	Basalt. Very weakly px porphyritic. Highly amygdaloidal (qtz+chl+carb and chl+qtz filled). Regional alteration: px phenocrysts entirely replaced, pervasive groundmass alteration resulted in a fine intergrowth of fdsp laths with chl, ep, qtz, and carb. Spotted ep and disseminated py. Qtz+ep and qtz+carb+hem veinlets.
WT2-131 (WT2, 131.60-132.20)	Basalt. Very weakly px porphyritic. Highly amygdaloidal (qtz+chl+carb and chl+qtz filled). Regional alteration: px phenocrysts entirely replaced, pervasive groundmass alteration resulted in a fine intergrowth of fdsp laths with chl, ep, qtz, and carb. Disseminated py. Ep+qtz and qtz+carb veinlets.
WT2-150 (WT2, 150.40-151.00)	Basalt. Weakly fdsp porphyritic. Moderately amygdaloidal (qtz+chl+carb and chl+qtz filled). Regional alteration: fdsp phenocrysts are albitised, pervasive groundmass alteration resulted in a fine intergrowth of fdsp laths with ep, chl, qtz, and carb. Spotted ep and disseminated py. Ep+qtz veinlets.
WT2-164 (WT2, 164.00-164.50)	Basalt. Very weakly px porphyritic. Moderately amygdaloidal (qtz+chl+carb and chl+qtz filled). Regional alteration: px phenocrysts entirely replaced, pervasive groundmass alteration resulted in a fine intergrowth of fdsp laths with chl, ep, qtz, and carb. Spotted ep and disseminated py. Ep+qtz veinlets.
WT2-176 (WT2, 176.50-177.10)	Andesite. Very weakly fdsp porphyritic. Sparsely amygdaloidal (qtz+chl+carb and chl+qtz filled). Regional alteration: fdsp phenocrysts are albitised, domains of chl+qtz+carb and white mica+chl+qtz groundmass alteration. Disseminated py. Carb+qtz+ep+qtz veinlets.
WT2-193 (WT2, 192.80-193.20)	Mudstone. Greenish grey and dark greenish grey. Laminated to very thinly bedded. Individual beds: unequal thickness and laterally discontinuous. Detrital qtz and fdsp. Less detrital ap. No diagenetic py. Regional alteration: fdsp grains are albitised, fine grained matrix of qtz and white mica with minor chl and carb. Weakly developed cleavage. Qtz and carb veinlets crosscut foliation.
WT2-210 (WT2, 210.40-211.00)	Basalt. Very weakly px porphyritic. Moderately amygdaloidal (qtz+chl+carb and chl+qtz filled). Regional alteration: px phenocrysts entirely replaced, pervasive groundmass alteration resulted in a fine intergrowth of fdsp laths with ep, chl, qtz, and carb. Spotted ep. Carb+qtz veinlets.
WT2-227 (WT2, 227.60-228.10)	Basalt. Very weakly px porphyritic. Sparsely amygdaloidal (qtz+chl+carb and chl+qtz filled). Regional alteration: px phenocrysts entirely replaced, pervasive groundmass alteration resulted in a fine intergrowth of fdsp laths with chl, ep, qtz, and carb. Carb+qtz and ep+qtz veinlets.
WT2-239 (WT2, 239.80-240.30)	Mudstone. Greenish grey, dark greenish grey, and greenish black. Massive. Rare detrital qtz and rare fdsp. Less detrital ap. Patchy induration of qtz, ep, and carb. Diagenetic py. Regional alteration: fdsp grains are albitised, fine grained matrix of qtz and white mica with minor chl and carb. Weakly to well developed cleavage. Carb veinlets crosscut foliation.
WT2-265 (WT2, 265.50-266.30)	Mudstone. Greenish black. Laminated. Individual beds: unequal thickness and laterally discontinuous. Phyllitic. Detrital qtz and rare fdsp. Less detrital ap. Diagenetic py. Regional alteration: fdsp grains are albitised, fine grained matrix of qtz and white mica with chl and rare carb. Intensely developed cleavage. Carb veinlets crosscut foliation.
WT2-280 (WT2, 280.75-281.45)	Mudstone. Dark greenish grey. Laminated. Individual beds: unequal thickness and laterally continuous. Phyllitic. Detrital qtz and abundant detrital fdsp. Less detrital ap. Diagenetic py. Regional alteration: fdsp grains are albitised, fine grained matrix of qtz and white mica with chl and carb. Intensely developed cleavage. Carb veinlets crosscut foliation.
WT2-294 (WT2, 294.75-295.35)	Mudstone. Dark greenish grey. Laminated to thinly bedded. Individual beds: unequal thickness and laterally continuous, normal graded. Detrital qtz and very rare fdsp. Less detrital ap. Diagenetic py. Regional alteration: fdsp grains are albitised, fine grained matrix of qtz and white mica with rare chl and carb. Carb+qtz and carb veinlets crosscut foliation.
WT2-315 (WT2, 315.90-316.40)	Coarse feldspar-quartz sandstone-breccia. Abundant fdsp (abundance: 40%, size: 1-2 mm) and quartz (abundance: 10%, size: < 1 mm) crystals, rare lithic fragments (abundance: < 1%, size: < 2 mm). Phyllitic matrix. Diagenetic py. Regional alteration: fdsp and lithic fragments are preserved, fdsp is albitised, fine grained matrix of white mica, chl, qtz, and carb. Spotted ep and minor lcx. Carb veinlets.
WT2-323 (WT2, 323.30-323.90)	Andesite. Aphyric. Non amygdaloidal. Regional alteration: pervasive groundmass alteration resulted in a fine intergrowth of fdsp laths with chl, qtz, and carb. Carb+qtz veinlets.
WT2-338 (WT2, 338.05-338.60)	Mudstone. Greenish black. Massive. Phyllitic. Detrital qtz and fdsp. Less detrital ap. Diagenetic py frequently enveloped by carb halos. Small face-centred qtz strain fringes on py. Regional alteration: fdsp grains are albitised, fine grained matrix of qtz, white mica, chl, and minor carb. Very intensely developed cleavage. Carb veinlets crosscut foliation.
WT2-345 (WT2, 345.45-346.35)	Fine sandstone. Greenish grey. Laminated. Individual beds: unequal thickness and laterally continuous, normal graded. Detrital qtz and fdsp. Less detrital ap. No diagenetic py. Regional alteration: fdsp grains are albitised, fine grained matrix of qtz and white mica with rare chl and carb. Carb veinlets crosscut foliation.
WT2-353 (WT2, 353.40-354.10)	Coarse quartz-feldspar crystal-rich sandstone-breccia. Abundant qtz (abundance: 30%, size: 1-4 mm) and fdsp (abundance: 50%, size: 1-3 mm) crystals, rare lithic fragments (abundance: 1%, size: < 2 mm). Phyllitic matrix. Hydrothermal alteration (propylitic): fdsp and lithic fragments partially replaced by white mica, qtz, and carb, fdsp is albitised, fine grained matrix of white mica, chl, qtz, and carb. Patchy and spotted ep, spotted hem, and minor lcx. Weakly developed cleavage. Qtz and qtz+carb veinlets.
WT2-360 (WT2, 360.40-361.50)	Dacite. Moderately fdsp porphyritic. Non amygdaloidal. Hydrothermal alteration (phyllic): fdsp phenocrysts partially replaced by white mica, qtz, and carb, pervasive groundmass alteration resulted in a fine intergrowth of fdsp laths with white mica, chl, qtz, and carb. Poorly developed cleavage. Carb veinlets.

Notes: Ap = apatite, carb = carbonate, chl = chlorite, ep = epidote, fdsp = feldspar, gn = galena, hem = hematite, kln = kaolinite, lcx = lcx, prl = pyrophyllite, py = pyrite, px = pyroxene, qtz = quartz, sp = sphalerite, zrn = zircon.

Sample (drill hole, meters)	Petrographic description
WT2-386 (WT2, 386.00-387.85)	Intensely altered rock. Hydrothermal alteration (silicic): texturally destructive alteration resulted in a fine intergrowth of qtz and white mica. Disseminated py. Intensely developed cleavage.
WT2-402 (WT2, 402.30-403.05)	Intensely altered rock. Hydrothermal alteration (phyllic): texturally destructive alteration resulted in a fine intergrowth of white mica, chl, and qtz. Disseminated py. Very intensely developed cleavage.
WT2-421 (WT2, 421.80-422.70)	Intensely altered rock. Hydrothermal alteration (silicic): texturally destructive alteration resulted in a fine intergrowth of qtz and white mica. Disseminated py. Intensely developed cleavage.
WT2-440 (WT2, 440.00-441.00)	Intensely altered rock. Hydrothermal alteration (silicic): texturally destructive alteration resulted in a fine intergrowth of qtz and white mica. Disseminated py. Intensely developed cleavage.
WT2-461 (WT2, 461.80-462.80)	Intensely altered rock. Hydrothermal alteration (phyllic): texturally destructive alteration resulted in a fine intergrowth of remnant fdsp laths with white mica, chl, and qtz. Disseminated py. Very intensely developed cleavage.
WT5-118 (WT5, 118.60-119.10)	Mudstone. Greenish grey. Laminated. Individual beds: unequal thickness and laterally continuous. Phyllitic. Detrital qtz and fdsp. Less detrital ap. No diagenetic py. Regional alteration: fdsp grains are albitised, fine grained matrix of qtz, white mica, and chl. Very intensely developed cleavage. Carb veinlets crosscut foliation.
WT5-129 (WT5, 129.10-129.40)	Fine sandstone. Dark greenish grey. Massive. Detrital qtz and fdsp. Less detrital ap. No diagenetic py. Regional alteration: fdsp grains are albitised, fine grained matrix of qtz, white mica, and chl with minor carb. Carb veinlets crosscut foliation.
WT5-136 (WT5, 136.00-137.00)	Mudstone. Greenish black. Massive. Detrital qtz and fdsp. Less detrital ap. Diagenetic py. Regional alteration: fdsp grains are albitised, fine grained matrix of qtz, white mica, and chl with rare carb. Poorly developed cleavage. Carb veinlets crosscut foliation.
WT5-148 (WT5, 148.30-148.70)	Fine sandstone. Dark greenish grey. Massive. Rare lithic fragments. Detrital qtz and fdsp. Less detrital ap. Diagenetic py. Hydrothermal alteration (propylitic): fdsp grains are albitised, fine grained matrix of qtz, white mica, and chl with minor carb. Patchy and spotted ep. Carb veinlets crosscut foliation.
WT5-156 (WT5, 156.20-157.00)	Coarse quartz-feldspar crystal-rich sandstone-breccia. Abundant qtz (abundance: 40%, size: 1-2.5 mm) and fdsp (abundance: 40%, size: 1-2.5 mm) crystals, rare lithic fragments (abundance: 1%, size: < 2 mm). Phyllitic matrix. Hydrothermal alteration (propylitic): fdsp and lithic fragments partially replaced by white mica, qtz, and carb, fdsp is albitised, fine grained matrix of white mica, chl, qtz, and carb. Patchy and spotted ep, spotted hem, and minor lcx. Qtz and qtz+carb+chl veinlets.
WT5-158 (WT5, 158.50-158.86)	Dacite (type D2). Moderately fdsp porphyritic. Non amygdaloidal. Hydrothermal alteration (propylitic): fdsp phenocrysts partially replaced by white mica, qtz, and carb, fdsp is albitised, domains of chl+ep+qtz+carb and white mica+chl+qtz groundmass alteration. Qtz veinlets.
WT5-163 (WT5, 163.75-164.30)	Coarse quartz-feldspar crystal-rich sandstone-breccia. Abundant qtz (abundance: 40%, size: 1-4 mm) and fdsp (abundance: 30%, size: 1-3 mm) crystals. Phyllitic matrix. Hydrothermal alteration (propylitic): fdsp is partially replaced by white mica, qtz, and carb, fdsp is albitised, fine grained matrix of white mica, chl, qtz, and carb. Patchy ep, spotted hem, and minor lcx. Hem+carb veinlets.
WT5-171 (WT5, 171.60-172.00)	Coarse quartz-feldspar crystal-rich sandstone-breccia. Abundant qtz (abundance: 30%, size: 1-4 mm) and fdsp (abundance: 30%, size: 1-3 mm) crystals. Phyllitic matrix. Hydrothermal alteration (phyllic): fdsp replaced by white mica, qtz, and carb, fine grained matrix of white mica, chl, qtz, and carb. Spotted hem, minor kln and lcx. Well developed cleavage.
WT5-186 (WT5, 186.60-187.00)	Intensely altered rock. Hydrothermal alteration (phyllic): texturally destructive alteration resulted in a fine intergrowth of white mica, chl, and qtz. Disseminated py. Very intensely developed cleavage.
WT5-213 (WT5, 213.00-213.50)	Andesite. Weakly fdsp porphyritic. Poorly amygdaloidal. Hydrothermal alteration (phyllic): faint phenocrysts, remnant fdsp is albitised, pervasive groundmass alteration resulted in a fine intergrowth of fdsp laths with white mica, chl, qtz, and carb. Disseminated py. Intensely developed cleavage. Veinlets (qtz).
WT5-223 (WT5, 223.70-224.20)	Andesite. Weakly fdsp porphyritic. Moderately to highly amygdaloidal. Hydrothermal alteration (phyllic): faint phenocrysts, pervasive groundmass alteration resulted in a fine intergrowth of white mica, chl, qtz, and carb. Disseminated py. Poorly developed cleavage. Qtz+carb veinlets.
WT5-231 (WT5, 231.30-231.70)	Andesite. Weakly fdsp porphyritic. Moderately to highly amygdaloidal. Hydrothermal alteration (phyllic): faint phenocrysts, pervasive groundmass alteration resulted in a fine intergrowth of white mica, chl, qtz, and carb. Disseminated py and minor ep. Weakly developed cleavage. Qtz+carb veinlets.
WT6-109 (WT6, 109.80-110.80)	Intensely altered rock. Hydrothermal alteration (silicic): texturally destructive alteration resulted in a fine intergrowth of qtz and white mica. Disseminated py. Intensely developed cleavage.
WT6-135 (WT6, 135.30-136.30)	Intensely altered rock. Hydrothermal alteration (phyllic): texturally destructive alteration resulted in a fine intergrowth of white mica, chl, and qtz. Disseminated py and minor carb. Very intensely developed cleavage.
WT6-153 (WT6, 153.35-154.35)	Intensely altered rock. Hydrothermal alteration (phyllic): texturally destructive alteration resulted in a fine intergrowth of remnant fdsp laths with white mica, chl, qtz, and carb. Disseminated py. Very intensely developed cleavage.
WT6-167 (WT6, 167.60-168.60)	Andesite. Very weakly fdsp porphyritic. Poorly amygdaloidal. Hydrothermal alteration (phyllic): faint phenocrysts, remnant fdsp is albitised, pervasive groundmass alteration resulted in a fine intergrowth of fdsp laths with white mica, chl, qtz, and carb. Disseminated py. Weakly developed cleavage.
WT6-180 (WT6, 180.20-181.20)	Andesite. Very weakly fdsp porphyritic. Poorly amygdaloidal. Hydrothermal alteration (phyllic): faint phenocrysts, remnant fdsp is albitised, pervasive groundmass alteration resulted in a fine intergrowth of fdsp laths with white mica, chl, qtz, and carb. Disseminated py. Poorly developed cleavage.
WT7-92 (WT7, 92.50-92.80)	Intensely altered rock. Hydrothermal alteration (phyllic): texturally destructive alteration resulted in a fine intergrowth of remnant fdsp laths with white mica and qtz. Disseminated py. Very intensely developed cleavage.
WT7-108 (WT7, 108.60-109.60)	Intensely altered rock. Hydrothermal alteration (phyllic): texturally destructive alteration resulted in a fine intergrowth of white mica, chl, and qtz. Disseminated py. Very intensely developed cleavage.

Notes: Ap = apatite, carb = carbonate, chl = chlorite, ep = epidote, fdsp = feldspar, gn = galena, hem = hematite, kln = kaolinite, lcx = lcx, prl = pyrophyllite, py = pyrite, px = pyroxene, qtz = quartz, sp = sphalerite, zrn = zircon.

Sample (drill hole, meters)	Petrographic description
WT7-123 (WT7, 123.00-125.40)	Intensely altered rock. Hydrothermal alteration (phyllic): texturally destructive alteration resulted in a fine intergrowth of white mica and qtz. Disseminated py. Very intensely developed cleavage.
WT7-155 (WT7, 155.40-156.90)	Intensely altered rock. Hydrothermal alteration (phyllic): texturally destructive alteration resulted in a fine intergrowth of white mica and qtz. Disseminated py. Very intensely developed cleavage.
WT7-171 (WT7, 171.15-171.65)	Intensely altered rock. Hydrothermal alteration (phyllic-argillic): texturally destructive alteration resulted in a fine intergrowth of white mica and qtz, fracture-controlled kln and prl. Disseminated py. Very intensely developed cleavage.
WT7-200 (WT7, 200.60-201.20)	Coarse quartz-feldspar crystal-rich sandstone-breccia. Abundant qtz (abundance: 40%, size: 1-3 mm) and fdsp (abundance and size obscured by alteration) crystals. Hydrothermal alteration (phyllic): faint fdsp crystals, fine grained matrix of white mica, chl, qtz, and carb. Spotted hem and minor lcx. Very intensely developed cleavage. Carb veinlets.
WT7-205 (WT7, 205.00-205.80)	Mudstone. Dark greenish grey. Massive and laminated intervals. Individual beds in laminated intervals: unequal thickness and laterally continuous. Detrital qtz and fdsp. Less detrital ap. Diagenetic py. Regional alteration: fdsp grains are albitised, fine grained matrix of qtz, chl, and white mica with minor carb. Well developed cleavage. Carb veinlets crosscut foliation.
WT7-208 (WT7, 208.90-209.60)	Fine sandstone. Dark greenish grey. Laminated. Individual beds: unequal thickness and laterally continuous. Detrital qtz and fdsp. Less detrital ap and zrn. Diagenetic py. Regional alteration: fdsp grains are albitised, fine grained matrix of qtz and white mica with rare chl and carb. Intensely developed cleavage. Carb+qtz veinlets crosscut foliation.
WT7-213 (WT7, 213.50-214.60)	Mudstone. Greenish grey. Massive and laminated intervals. Individual beds in laminated intervals: unequal thickness and laterally continuous. Detrital qtz and fdsp. Less detrital ap. Diagenetic py. Regional alteration: fdsp grains are albitised, fine grained matrix of qtz, chl, and white mica with carb. Well developed cleavage. Carb veinlets crosscut foliation.
WT8A-103 (WT8A, 103.00-103.20)	Resedimented dacitic hyaloclastite. Moderately fdsp porphyritic. Non amygdaloidal. Regional alteration: fdsp phenocrysts are albitised, pervasive groundmass alteration resulted in a fine intergrowth of fdsp laths with white mica, chl, qtz, and carb. Minor hem and lcx. Carb veinlets.
WT8A-172 (WT8A, 172.00-172.20)	Resedimented dacitic hyaloclastite. Moderately fdsp porphyritic. Non amygdaloidal. Regional alteration: fdsp phenocrysts are albitised, pervasive groundmass alteration resulted in a fine intergrowth of fdsp laths with chl, qtz, and carb. Minor lcx. Carb veinlets.
WT9A-86 (WT9A, 86.30-86.83)	Andesite. Moderately fdsp porphyritic. Poorly to moderately amygdaloidal. Hydrothermal alteration (propylitic): fdsp phenocrysts largely preserved, fdsp is albitised, domains of chl+ep+qtz+carb and white mica+qtz+py groundmass alteration. Disseminated py. Qtz+carb veinlets.
WT9A-100 (WT9A, 100.25-100.65)	Andesite. Very weakly fdsp porphyritic. Highly amygdaloidal. Hydrothermal alteration (propylitic): fdsp phenocrysts largely preserved, fdsp is albitised, pervasive groundmass alteration resulted in a fine intergrowth of fdsp laths with chl, ep, qtz, and carb. Disseminated py. Qtz+carb veinlets.
WT9A-109 (WT9A, 109.10-109.50)	Andesite. Strongly fdsp porphyritic. Non amygdaloidal. Hydrothermal alteration (propylitic): fdsp phenocrysts largely preserved, fdsp is albitised, domains of chl+ep+qtz+carb and white mica+qtz groundmass alteration. Disseminated py. Qtz+carb veinlets.
WT9A-126 (WT9A, 126.40-126.90)	Andesite. Very weakly fdsp porphyritic. Non amygdaloidal. Hydrothermal alteration (propylitic): fdsp phenocrysts partially replaced by white mica, qtz, and carb, fdsp is albitised, pervasive chl+ep+qtz+carb groundmass alteration. Patchy and spotted ep, disseminated py. Qtz+carb and ep+qtz veinlets.
WT9A-144 (WT9A, 144.00-144.50)	Andesite. Weakly fdsp porphyritic. Poorly amygdaloidal. Hydrothermal alteration (propylitic): fdsp phenocrysts largely preserved, fdsp is albitised, domains of chl+ep+qtz+carb and ep+chl+carb groundmass alteration. Disseminated py. Qtz+carb veinlets.
WT9A-162 (WT9A, 162.80-163.30)	Andesite. Weakly fdsp porphyritic. Poorly to moderately amygdaloidal. Hydrothermal alteration (propylitic): fdsp phenocrysts largely preserved, fdsp is albitised, domains of chl+ep+qtz+carb and ep+chl+carb groundmass alteration. Disseminated py.
WT9A-176 (WT9A, 176.10-176.60)	Andesite. Weakly fdsp porphyritic. Moderately amygdaloidal. Hydrothermal alteration (propylitic): fdsp phenocrysts largely preserved, fdsp is albitised, pervasive groundmass alteration resulted in a fine intergrowth of fdsp laths with chl, ep, qtz, and carb. Patchy ep and disseminated py. Qtz+carb veinlets.
WT9A-186 (WT9A, 186.35-186.90)	Andesite. Very weakly fdsp porphyritic. Moderately amygdaloidal. Hydrothermal alteration (propylitic): fdsp phenocrysts partially replaced by white mica, qtz, and carb, fdsp is albitised, pervasive groundmass alteration resulted in a fine intergrowth of fdsp laths with chl, white mica, qtz, and carb. Spotted ep and disseminated py. Poorly developed cleavage. Qtz+carb veinlets.
WT9A-198 (WT9A, 198.20-199.20)	Andesite. Very strongly fdsp porphyritic. Poorly amygdaloidal. Hydrothermal alteration (phyllic): fdsp phenocrysts entirely replaced by white mica, qtz, and carb, pervasive groundmass alteration resulted in a fine intergrowth of white mica, chl, qtz, and carb. Disseminated py. Intensely developed cleavage. Qtz+carb veinlets.
WT9A-218 (WT9A, 218.50-219.50)	Intensely altered rock. Hydrothermal alteration (silicic): texturally destructive alteration resulted in a fine intergrowth of qtz and white mica. Disseminated py. Intensely developed cleavage.
WT9A-228 (WT9A, 228.20-229.10)	Intensely altered rock. Hydrothermal alteration (silicic): texturally destructive alteration resulted in a fine intergrowth of qtz and white mica. Disseminated py. Intensely developed cleavage.
WT9A-238 (WT9A, 238.60-239.15)	Intensely altered rock. Hydrothermal alteration (phyllic): texturally destructive alteration resulted in a fine intergrowth of white mica, chl, qtz, and carb. Substantial amounts of py, sp, and minor gn. Intensely developed cleavage.

Notes: Ap = apatite, carb = carbonate, chl = chlorite, ep = epidote, fdsp = feldspar, gn = galena, hem = hematite, kln = kaolinite, lcx = lcx, prl = pyrophyllite, py = pyrite, px = pyroxene, qtz = quartz, sp = sphalerite, zrn = zircon.

Sample (drill hole, meters)	Petrographic description
WT9A-254 (WT9A, 254.05-255.00)	Coarse quartz-feldspar crystal-rich sandstone-breccia. Abundant qtz (abundance: 60%, size: 1-4 mm) and fdsp (abundance: 10%, size: 1-3 mm) crystals, rare lithic fragments (abundance: 1%, size: < 3 mm). Phyllitic matrix. Hydrothermal alteration (phyllic): fdsp and lithic fragments replaced by white mica, qtz, and carb, fine grained matrix of white mica, chl, qtz, and carb. Spotted hem, minor kln and lcx. Very intensely developed cleavage.
WT9A-265 (WT9A, 265.70-266.20)	Dacite (type D2). Moderately fdsp porphyritic. Non amygdaloidal. Hydrothermal alteration (phyllic): fdsp phenocrysts largely replaced by white mica, qtz, and carb, fdsp is albitised, pervasive groundmass alteration resulted in a fine intergrowth of fdsp laths with white mica, chl, qtz, and carb. Poorly developed cleavage. Carb veinlets.
WT16-87 (WT16, 87.30-87.80)	Andesite. Strongly fdsp porphyritic. Highly amygdaloidal. Hydrothermal alteration (propylitic): fdsp phenocrysts partially replaced by white mica, qtz, and carb, fdsp is albitised, pervasive groundmass alteration resulted in a fine intergrowth of fdsp laths with chl, ep, qtz, and carb. Patchy and spotted ep, disseminated py.
WT16-112 (WT16, 112.10-112.80)	Andesite. Strongly fdsp porphyritic. Highly amygdaloidal. Hydrothermal alteration (propylitic): fdsp phenocrysts largely preserved, fdsp is albitised, pervasive groundmass alteration resulted in a fine intergrowth of fdsp laths with chl, ep, qtz, and carb, fracture-controlled white mica, qtz, and py. Disseminated py. Qtz and py veinlets.
WT16-125 (WT16, 125.85-126.65)	Intensely altered rock. Hydrothermal alteration (phyllic): texturally destructive alteration resulted in a fine intergrowth of white mica, chl, and qtz. Disseminated py. Very intensely developed cleavage.
WT16-132 (WT16, 132.05-132.65)	Andesite. Strongly fdsp porphyritic. Highly amygdaloidal. Hydrothermal alteration (propylitic): fdsp phenocrysts largely preserved, fdsp is albitised, pervasive groundmass alteration resulted in a fine intergrowth of fdsp laths with chl, ep, qtz, and carb. Patchy and spotted ep, disseminated py. Qtz+carb and py veinlets.
WT16-145 (WT16, 145.00-145.80	Andesite. Strongly fdsp porphyritic. Highly amygdaloidal. Hydrothermal alteration (propylitic): fdsp phenocrysts largely preserved, fdsp is albitised, pervasive groundmass alteration resulted in a fine intergrowth of fdsp laths with chl, ep, qtz, and carb, fracture-controlled white mica. Disseminated py. Qtz+chl veinlets.
WT16-161 (WT16, 161.80-162.70	Andesite. Strongly fdsp porphyritic. Moderately amygdaloidal. Hydrothermal alteration (phyllic): fdsp phenocrysts largely replaced by white mica, qtz, and carb, fdsp is albitised, pervasive groundmass alteration resulted in a fine intergrowth of white mica, chl, and qtz. Disseminated py. Well developed cleavage.
WT16-170 (WT16, 170.70-171.50	Intensely altered rock. Hydrothermal alteration (phyllic): texturally destructive alteration resulted in a fine intergrowth of white mica, chl, and qtz. Disseminated py. Very intensely developed cleavage.
WT16-186 (WT16, 186.85-187.45	Andesite. Strongly fdsp porphyritic. Highly amygdaloidal. Hydrothermal alteration (propylitic): fdsp phenocrysts partially preserved, fdsp is albitised, domains of chl+ep+qtz+carb and white mica+chl+qtz+carb groundmass alteration. Patchy and spotted ep, disseminated py. Qtz and qtz+carb veinlets.
WT16-195 (WT16, 195.15-195.85	Andesite. Strongly fdsp porphyritic. Highly amygdaloidal. Hydrothermal alteration (propylitic): fdsp phenocrysts largely preserved, fdsp is albitised, domains of chl+ep+qtz+carb and white mica+chl+qtz+carb groundmass alteration. Patchy and spotted ep, disseminated py. Py veinlets.
WT16-206 (WT16, 206.70-207.45	Andesite. Very weakly fdsp porphyritic. Highly amygdaloidal. Hydrothermal alteration (propylitic): fdsp phenocrysts partially preserved, fdsp is albitised, pervasive groundmass alteration resulted in a fine intergrowth of fdsp laths with white mica, chl, qtz, and carb. Patchy and spotted ep, disseminated py. Qtz+carb veinlets.
WT16-210 (WT16, 210.90-211.70	Andesite. Moderately fdsp porphyritic. Non amygdaloidal. Hydrothermal alteration (propylitic): fdsp phenocrysts largely preserved, fdsp is albitised, pervasive groundmass alteration resulted in a fine intergrowth of fdsp laths with chl, ep, qtz, and carb. Disseminated py. Qtz and qtz+carb veinlets.
WT16-223 (WT16, 223.30-223.80	Andesite. Strongly fdsp porphyritic. Non amygdaloidal. Hydrothermal alteration (propylitic): fdsp phenocrysts largely preserved, fdsp is albitised, pervasive groundmass alteration resulted in a fine intergrowth of fdsp laths with white mica, chl, qtz, and carb. Patchy and spotted ep, disseminated py. Qtz veinlets.
WT16-245 (WT16, 245.55-246.25	Intensely altered rock. Hydrothermal alteration (phyllic-argillic): texturally destructive alteration resulted in a fine intergrowth of white mica and qtz, fracture-controlled kln and prl. Disseminated py. Very intensely developed cleavage.
WT16-257 (WT16, 257.00-257.90	Intensely altered rock. Hydrothermal alteration (phyllic-argillic): texturally destructive alteration resulted in a fine intergrowth of white mica, chl, and qtz, fracture-controlled kln and prl. Disseminated py. Very intensely developed cleavage.
WT16-276 (WT16, 276.00-276.75)	Intensely altered rock. Hydrothermal alteration (silicic): texturally destructive alteration resulted in a fine intergrowth of qtz and white mica. Disseminated py. Intensely developed cleavage.
WT16-292 (WT16, 292.00-292.75)	Intensely altered rock. Hydrothermal alteration (silicic): texturally destructive alteration resulted in a fine intergrowth of qtz and white mica. Disseminated py. Intensely developed cleavage.
WT16-322 (WT16, 322.00-323.00)	Intensely altered rock. Hydrothermal alteration (phyllic): texturally destructive alteration resulted in a fine intergrowth of white mica and qtz. Disseminated py and minor carb. Very intensely developed cleavage.
WT16-333 (WT16, 333.50-334.40)	Coarse quartz-feldspar crystal-rich sandstone-breccia. Abundant qtz (abundance: 60%, size: 1-3 mm) and fdsp (abundance: 10%, size: 1-2 mm) crystals. Phyllitic matrix. Hydrothermal alteration (propylitic): fdsp crystals largely replaced by white mica, qtz, and carb, some fdsp grains are albitised, fine grained matrix of white mica, chl, qtz, and carb. Minor lcx. Well developed cleavage. Qtz+carb+chl veinlets.
WT16-338 (WT16, 338.20-339.00)	Coarse quartz-feldspar crystal-rich sandstone-breccia. Abundant qtz (abundance: 40%, size: 0.5-3 mm) and fdsp (abundance: 30%, size: 0.5-2 mm) crystals, rare lithic fragments (abundance: 1%, size: 1-3 mm). Phyllitic matrix. Hydrothermal alteration (propylitic): fdsp crystals and lithic fragments largely preserved, fdsp grains are albitised, fine grained matrix of white mica, chl, qtz, and carb. Spotted ep, disseminated py, and minor lcx. Qtz+carb veinlets.

Notes: Ap = apatite, carb = carbonate, chl = chlorite, ep = epidote, fdsp = feldspar, gn = galena, hem = hematite, kln = kaolinite, lcx = lcx, prl = pyrophyllite, py = pyrite, px = pyroxene, qtz = quartz, sp = sphalerite, zrn = zircon.

Sample (drill hole, meters)	Petrographic description
WT16-343 (WT16, 343.10-343.80)	Coarse quartz-feldspar crystal-rich sandstone-breccia. Abundant qtz (abundance: 30%, size: 0.5-4 mm) and fdsp (abundance: 40%, size: 1-2.5 mm) crystals, lithic fragments (abundance: 5%, size: 1 mm to >10 cm). Phyllitic matrix. Hydrothermal alteration (propylitic): fdsp crystals and lithic fragments largely preserved, fdsp grains are albitised, fine grained matrix of white mica, chl, qtz, and carb. Spotted ep, disseminated py, and minor lcx. Qtz+ carb veinlets.
WT16-344 (WT16, 343.10-343.15)	Resedimented dacitic hyaloclastite (dacite D1). Weakly fdsp porphyritic. Non amygdaloidal. Clast size: 10 cm. Clast shape: blocky with subrounded to rounded corners. Hydrothermal alteration (propylitic): fdsp phenocrysts largely preserved, fdsp is albitised, pervasive groundmass alteration resulted in a fine intergrowth of fdsp laths with white mica, chl, qtz, and carb. Disseminated py and minor lcx. Carb and qtz+carb veinlets.
WT16-349 (WT16, 349.50-350.10)	Fine sandstone. Dark greenish grey. Laminated. Individual beds: unequal thickness and laterally discontinuous. Detrital qtz and fdsp. Less detrital ap. Diagenetic py. Regional alteration: fdsp grains are albitised, fine grained matrix of qtz, white mica, and chl with minor carb. Spotted ep. Carb veinlets crosscut foliation.
WT16-355 (WT16, 355.15-355.65)	Fine sandstone. Dark greenish grey, greenish black, and greenish brown. Laminated. Individual beds: unequal thickness and laterally continuous. Detrital qtz and fdsp. Rare large (>1 mm) crystal fragments. Less detrital ap. No diagenetic py. Regional alteration: fdsp grains are albitised, fine grained matrix of qtz, white mica, and chl with carb. Spotted ep. Carb veinlets crosscut foliation.
WT17-114 (WT17, 114.50-115.40)	Coarse quartz-feldspar crystal-rich sandstone-breccia. Abundant qtz (abundance: 40%, size: 2-5 mm) and fdsp (abundance and size obscured by alteration) crystals, lithic fragments (abundance: 5%, size: 1-15 mm). Phyllitic matrix. Hydrothermal alteration (phyllic): fdsp and lithic fragments largely replaced by white mica, qtz, and carb, fine grained matrix of white mica and qtz. Disseminated py. Well developed cleavage. Py veinlets.
WT17-118 (WT17, 118.30-118.80)	Coarse quartz-feldspar crystal-rich sandstone-breccia. Abundant qtz (abundance: 15%, size: 0.5-1 mm) and fdsp (abundance: 15%, size: 0.5-1 mm) crystals, abundant lithic fragments (abundance: 60%, size: 1-10 cm). Phyllitic matrix. Hydrothermal alteration (phyllic): fdsp and lithic fragments largely replaced by white mica, qtz, and carb, fine grained matrix of white mica, chl, and qtz. Minor lcx. Weakly to well developed cleavage.
WT17-122 (WT17, 122.30-123.00)	Coarse quartz-feldspar crystal-rich sandstone-breccia. Abundant qtz (abundance: 25%, size: 0.5-3 mm) and fdsp (abundance: 30%, size: 0.5-3 mm) crystals, abundant lithic fragments (abundance: 10%, size: 0.5-40 mm). Phyllitic matrix. Hydrothermal alteration (phyllic): fdsp and lithic fragments largely replaced by white mica, qtz, and carb, fine grained matrix of white mica, chl, and qtz. Minor lcx. Well developed cleavage.
WT17-127 (WT17, 127.00-127.50)	Coarse quartz-feldspar crystal-rich sandstone-breccia. Abundant qtz (abundance: 40%, size: 0.5-4 mm) and fdsp (abundance: 40%, size: 0.5-3 mm) crystals, lithic fragments (abundance: 5%, size: 2-5 mm). Phyllitic matrix. Hydrothermal alteration (phyllic): fdsp and lithic fragments largely replaced by white mica, qtz, and carb, fine grained matrix of white mica, chl, and qtz. Spotted ep and minor lcx. Poorly developed cleavage.
WT17-132 (WT17, 132.80-133.30)	Coarse quartz-feldspar crystal-rich sandstone-breccia. Abundant qtz (abundance: 40%, size: 1-3.5 mm) and fdsp (abundance: 30%, size: 0.5-3 mm) crystals. Phyllitic matrix. Hydrothermal alteration (phyllic): fdsp crystals largely replaced by white mica, qtz, and carb, fine grained matrix of white mica, chl, and qtz. Patchy and spotted ep, minor lcx. Weakly developed cleavage.
WT17-138 (WT17, 138.00-139.00)	Coarse quartz-feldspar crystal-rich sandstone-breccia. Abundant qtz (abundance: 60%, size: 1-3 mm) and fdsp (abundance: 25%, size: 1-2 mm) crystals, abundant lithic fragments (abundance: 10%, size: < 8 cm). Phyllitic matrix. Hydrothermal alteration (phyllic): fdsp and lithic fragments largely replaced by white mica and qtz, fine grained matrix of white mica, chl, and qtz. Minor lcx. Well developed cleavage.
WT17-146 (WT17, 146.50-147.50)	Coarse quartz-feldspar crystal-rich sandstone-breccia. Abundant qtz (abundance: 30%, size: 0.5-3 mm) and fdsp (abundance: 60%, size: 0.5-2.5 mm) crystals. Phyllitic matrix. Hydrothermal alteration (propylitic): fdsp crystals largely preserved, fdsp is albitised, fine grained matrix of white mica, chl, and qtz. Spotted and patchy ep, minor lcx. Poorly developed cleavage.
WT21-109 (WT21, 109.60-110.00)	Dacite. Very weakly fdsp porphyritic. Non amygdaloidal. Hydrothermal alteration (phyllic): fdsp phenocrysts largely replaced by white mica, qtz, and carb, remnant fdsp is albitised, pervasive groundmass alteration resulted in a fine intergrowth of white mica, chl, qtz, and carb. Vein-like zones of py and disseminated py. Well developed cleavage.
WT21-121 (WT21, 121.00-122.00)	Dacite. Very weakly fdsp porphyritic. Non amygdaloidal. Hydrothermal alteration (phyllic): fdsp phenocrysts largely replaced by white mica, qtz, and carb, remnant fdsp is albitised, pervasive groundmass alteration resulted in a fine intergrowth of white mica, chl, qtz, and carb. Disseminated py. Well developed cleavage. Carb veinlets.
WT21-126 (WT21, 126.60-127.00)	Dacite. Very weakly fdsp porphyritic. Non amygdaloidal. Hydrothermal alteration (phyllic): fdsp phenocrysts largely replaced by white mica, qtz, and carb, remnant fdsp is albitised, pervasive groundmass alteration resulted in a fine intergrowth of white mica, chl, qtz, and carb. Disseminated py. Well developed cleavage. Carb veinlets.
WT21-135 (WT21, 135.15-135.80)	Andesite. Aphyric. Poorly amygdaloidal. Hydrothermal alteration (phyllic): pervasive groundmass alteration resulted in a fine intergrowth of white mica, chl, qtz, and carb. Disseminated py and vein-like zones of py, patchy ep. Well developed cleavage. Qtz+carb veinlets.
WT21-147 (WT21, 147.75-148.05)	Dacite. Moderately fdsp porphyritic. Poorly amygdaloidal. Hydrothermal alteration (propylitic): fdsp phenocrysts largely replaced by white mica, qtz, and carb, fdsp is albitised, pervasive groundmass alteration resulted in a fine intergrowth of fdsp laths with white mica, chl, qtz, and carb. Disseminated py and spotted ep. Poorly developed cleavage.
WT21-159 (WT21, 159.25-159.75)	Dacite. Moderately fdsp porphyritic. Poorly amygdaloidal. Hydrothermal alteration (propylitic): fdsp phenocrysts largely replaced by white mica, qtz, and carb, fdsp is albitised, pervasive groundmass alteration resulted in a fine intergrowth of fdsp laths with white mica, chl, qtz, and carb. Disseminated py and spotted ep. Poorly developed cleavage.

Notes: Ap = apatite, carb = carbonate, chl = chlorite, ep = epidote, fdsp = feldspar, gn = galena, hem = hematite, kln = kaolinite, lcx = lcx, prl = pyrophyllite, py = pyrite, px = pyroxene, qtz = quartz, sp = sphalerite, zrn = zircon.

Sample (drill hole, meters)	Petrographic description
WT21-172 (WT21, 172.00-172.70)	Dacite. Moderately fdsp porphyritic. Poorly amygdaloidal. Hydrothermal alteration (phyllic): fdsp phenocrysts largely replaced by white mica, qtz, and carb, remnant fdsp is albitised, pervasive groundmass alteration resulted in a fine intergrowth of white mica, chl, qtz, and carb. Disseminated py. Poorly developed cleavage.
WT21-185 (WT21, 185.40-186.00)	Intensely altered rock. Hydrothermal alteration (phyllic): texturally destructive alteration resulted in a fine intergrowth of remnant fdsp laths with white mica, chl, qtz, and carb. Disseminated py. Very intensely developed cleavage.
WT21-199 (WT21, 199.10-199.70)	Intensely altered rock. Hydrothermal alteration (phyllic): texturally destructive alteration resulted in a fine intergrowth of remnant fdsp laths with white mica, chl, qtz, and carb. Disseminated py. Very intensely developed cleavage.
WT21-212 (WT21, 212.40-212.80)	Intensely altered rock. Hydrothermal alteration (phyllic): texturally destructive alteration resulted in a fine intergrowth of remnant fdsp laths with white mica, chl, qtz, and carb. Disseminated py. Very intensely developed cleavage.
WT21-223 (WT21, 223.15-223.75)	Intensely altered rock. Hydrothermal alteration (phyllic): texturally destructive alteration resulted in a fine intergrowth of remnant fdsp laths with white mica, chl, qtz, and carb. Disseminated py. Very intensely developed cleavage.
WT21-237 (WT21, 237.85-238.40)	Intensely altered rock. Hydrothermal alteration (phyllic): texturally destructive alteration resulted in a fine intergrowth of white mica, chl, and qtz. Disseminated py. Very intensely developed cleavage.
WT21-249 (WT21, 249.60-250.20)	Intensely altered rock. Hydrothermal alteration (phyllic): texturally destructive alteration resulted in a fine intergrowth of white mica, chl, and qtz. Disseminated py and minor carb. Very intensely developed cleavage.
WT21-261 (WT21, 261.30-262.30)	Intensely altered rock. Hydrothermal alteration (silicic): texturally destructive alteration resulted in a fine intergrowth of qtz and white mica. Disseminated py. Intensely developed cleavage.
WT21-277 (WT21, 277.30-278.00)	Intensely altered rock. Hydrothermal alteration (phyllic): texturally destructive alteration resulted in a fine intergrowth of white mica, chl, and qtz. Disseminated py. Very intensely developed cleavage.
WT21-298 (WT21, 298.50-299.20)	Intensely altered rock. Hydrothermal alteration (phyllic): texturally destructive alteration resulted in a fine intergrowth of white mica, chl, qtz, and carb. Disseminated py. Very intensely developed cleavage.
WT21-306 (WT21, 306.15-306.80)	Intensely altered rock. Hydrothermal alteration (phyllic): texturally destructive alteration resulted in a fine intergrowth of white mica, chl, qtz, and carb. Disseminated py. Very intensely developed cleavage.
WT21-311 (WT21, 311.70-312.30)	Coarse quartz-feldspar crystal-rich sandstone-breccia. Abundant qtz (abundance and size obscured by alteration) and fdsp (abundance and size obscured by alteration) crystals, abundant lithic fragments (abundance: 10%, size: 2-20 mm). Phyllitic matrix. Hydrothermal alteration (propylitic): fdsp and lithic fragments largely replaced by white mica, qtz, and carb, fdsp is albitised, fine grained matrix of white mica, chl, qtz, and carb. Disseminated py. Very intensely developed cleavage.
WT21-314 (WT21, 314.00-314.50)	Coarse quartz-feldspar crystal-rich sandstone-breccia. Abundant qtz (abundance and size obscured by alteration) and fdsp (abundance and size obscured by alteration) crystals, abundant lithic fragments (abundance and size obscured by alteration). Phyllitic matrix. Hydrothermal alteration (propylitic): fdsp and lithic fragments largely replaced by white mica, qtz, and carb, fdsp is albitised, fine grained matrix of white mica, chl, qtz, and carb. Disseminated py and minor lcx. Intensely developed cleavage. Qtz+carb veinlets.
WT21-319 (WT21, 319.60-320.30)	Coarse quartz-feldspar crystal-rich sandstone-breccia. Abundant qtz (abundance: 30%, size: 1-3 mm) and fdsp (abundance: 30%, size: 1-2 mm) crystals, abundant lithic fragments (abundance: 5%, size: 5-10 mm). Phyllitic matrix. Hydrothermal alteration (propylitic): fdsp and lithic fragments partially replaced by white mica, qtz, and carb, fdsp is albitised, fine grained matrix of white mica, chl, qtz, and carb. Minor lcx. Well developed cleavage. Carb veinlets.
WT21-324 (WT21, 324.05-324.95)	Coarse quartz-feldspar crystal-rich sandstone-breccia. Abundant qtz (abundance: 40%, size: 1-3 mm) and fdsp (abundance: 30%, size: 1-2 mm) crystals, lithic fragments (abundance: 5%, size: < 8 mm). Phyllitic matrix. Hydrothermal alteration (phyllic): fdsp and lithic fragments largely replaced by white mica, qtz, and carb, fdsp is albitised, fine grained matrix of white mica, chl, qtz, and carb. Spotted hem and ep, minor lcx. Very intensely developed cleavage. Qtz veinlets.
WT21-328 (WT21, 328.70-329.30)	Coarse quartz-feldspar crystal-rich sandstone-breccia. Abundant qtz (abundance and size obscured by alteration) and feldspar (abundance and size obscured by alteration) crystals. Phyllitic matrix. Hydrothermal alteration (phyllic): feldspar crystals entirely replaced by white mica, qtz, and carb, fine grained matrix of hem, chl, qtz, and carb. Weakly developed cleavage.
WT21-335 (WT21, 335.00-335.50)	Coarse quartz-feldspar crystal-rich sandstone-breccia. Abundant qtz (abundance: 30%, size: 1-3 mm) and fdsp (abundance: 40%, size: 1-3 mm) crystals. Phyllitic matrix. Hydrothermal alteration (phyllic): fdsp crystals entirely replaced by white mica, qtz, and carb, fine grained matrix of white mica, chl, qtz, and carb. Minor lcx. Intensely developed cleavage.
WT22-100 (WT22, 100.30-100.90)	Andesite. Weakly fdsp porphyritic. Poorly amygdaloidal. Hydrothermal alteration (propylitic): fdsp phenocrysts largely replaced by white mica, qtz, and carb, fdsp is albitised, domains of white mica+chl+qtz+carb and chl+ep+qtz+carb groundmass alteration. Disseminated py. Poorly developed cleavage.
WT22-109 (WT22, 109.50-110.50)	Andesite. Weakly fdsp porphyritic. Poorly amygdaloidal. Hydrothermal alteration (propylitic): fdsp phenocrysts largely replaced by white mica, qtz, and carb, fdsp is albitised, domains of white mica+chl+qtz+carb and chl+ep+qtz+carb groundmass alteration. Disseminated py. Poorly developed cleavage.
WT22-122 (WT22, 122.85-123.85)	Andesite. Very weakly fdsp porphyritic. Highly amygdaloidal. Hydrothermal alteration (phyllic): faint phenocrysts, remnant fdsp is albitised, pervasive groundmass alteration resulted in a fine intergrowth of fdsp laths with white mica, chl, qtz, and carb. Disseminated py. Well developed cleavage.
WT22-132 (WT22, 132.70-133.40)	Andesite. Very weakly fdsp porphyritic. Highly amygdaloidal. Hydrothermal alteration (phyllic): faint phenocrysts, remnant fdsp is albitised, domains of white mica+chl+qtz+carb and qtz+white mica+chl+carb groundmass alteration. Disseminated py. Poorly developed cleavage. Py and qtz+carb veinlets.

Notes: Ap = apatite, carb = carbonate, chl = chlorite, ep = epidote, fdsp = feldspar, gn = galena, hem = hematite, kln = kaolinite, lcx = lcx, prl = pyrophyllite, py = pyrite, px = pyroxene, qtz = quartz, sp = sphalerite, zrn = zircon.

Sample (drill hole, meters)	Petrographic description
WT22-148 (WT22, 148.75-150.05)	Andesite. Very weakly fdsp porphyritic. Moderately amygdaloidal. Hydrothermal alteration (phyllic): faint phenocrysts, remnant fdsp is albitised, pervasive groundmass alteration resulted in a fine intergrowth of fdsp laths with white mica, chl, qtz, and carb. Disseminated py. Poorly developed cleavage. Py veinlets.
WT22-163 (WT22, 163.30-164.10)	Andesite. Very weakly fdsp porphyritic. Moderately amygdaloidal. Hydrothermal alteration (phyllic): faint phenocrysts, remnant fdsp is albitised, pervasive groundmass alteration resulted in a fine intergrowth of fdsp laths with white mica, chl, qtz, and carb. Disseminated py. Intensely developed cleavage.
WT22-176 (WT22, 176.40-177.30)	Andesite. Very weakly fdsp porphyritic. Poorly amygdaloidal. Hydrothermal alteration (phyllic): faint phenocrysts, remnant fdsp is albitised, pervasive groundmass alteration resulted in a fine intergrowth of fdsp laths with white mica, chl, qtz, and carb. Disseminated py. Well developed cleavage. Qtz+carb veinlets.
WT22-190 (WT22, 190.80-191.80)	Andesite. Very weakly fdsp porphyritic. Poorly amygdaloidal. Hydrothermal alteration (phyllic): faint phenocrysts, remnant fdsp is albitised, pervasive groundmass alteration resulted in a fine intergrowth of fdsp laths with white mica, chl, qtz, and carb. Disseminated py. Very intensely developed cleavage.
WT22-208 (WT22, 208.45-209.05)	Intensely altered rock. Hydrothermal alteration (phyllic): texturally destructive alteration resulted in a fine intergrowth of white mica, chl, and qtz. Disseminated py. Very intensely developed cleavage.
WT22-222 (WT22, 222.30-223.20)	Intensely altered rock. Hydrothermal alteration (phyllic): texturally destructive alteration resulted in a fine intergrowth of remnant fdsp laths with white mica, chl, qtz, and carb. Disseminated py. Very intensely developed cleavage.
WT22-237 (WT22, 237.70-238.40)	Intensely altered rock. Hydrothermal alteration (phyllic): texturally destructive alteration resulted in a fine intergrowth of white mica, chl, and qtz. Disseminated py. Very intensely developed cleavage.
WT22-244 (WT22, 244.90-245.70)	Intensely altered rock. Qtz crystal fragment may indicate a rhyolitic precursor material. Hydrothermal alteration (phyllic): texturally destructive alteration resulted in a fine intergrowth of white mica, chl, and qtz. Disseminated py. Very intensely developed cleavage.
WT22-256 (WT22, 256.00-257.00)	Intensely altered rock. Hydrothermal alteration (phyllic): texturally destructive alteration resulted in a fine intergrowth of white mica, chl, and qtz. Disseminated py. Very intensely developed cleavage.
WT22-264 (WT22, 264.45-265.45)	Intensely altered rock. Hydrothermal alteration (phyllic): texturally destructive alteration resulted in a fine intergrowth of white mica, chl, and qtz. Disseminated py. Very intensely developed cleavage.
WT22-277 (WT22, 277.70-278.70)	Intensely altered rock. Hydrothermal alteration (silicic): texturally destructive alteration resulted in a fine intergrowth of qtz and white mica. Disseminated py. Intensely developed cleavage.
WT22-286 (WT22, 286.50-287.60)	Dacite (type D1). Weakly fdsp porphyritic. Non amygdaloidal. Hydrothermal alteration (phyllic): faint fdsp phenocrysts, pervasive groundmass alteration resulted in a fine intergrowth of white mica and qtz. Disseminated py. Very intensely developed cleavage.
WT22-295 (WT22, 295.35-296.35)	Dacite (type D1). Weakly fdsp porphyritic. Non amygdaloidal. Hydrothermal alteration (phyllic): faint fdsp phenocrysts, pervasive groundmass alteration resulted in a fine intergrowth of white mica, qtz, and carb. Disseminated py. Very intensely developed cleavage.
WT22-302 (WT22, 302.00-303.80)	Dacite (type D1). Weakly fdsp porphyritic. Non amygdaloidal. Hydrothermal alteration (propylitic): fdsp phenocrysts partially replaced by white mica, qtz, and carb, fdsp is albitised, pervasive groundmass alteration resulted in a fine intergrowth of fdsp laths with white mica, chl, qtz, and carb. Minor lcx. Qtz+carb and carb+py veinlets.
WT22-307 (WT22, 307.90-308.55)	Dacite (type D1). Weakly fdsp porphyritic. Non amygdaloidal. Hydrothermal alteration (propylitic): fdsp phenocrysts partially replaced by white mica, qtz, and carb, fdsp is albitised, pervasive groundmass alteration resulted in a fine intergrowth of fdsp laths with white mica, qtz, and carb. Vein-like zones of py and minor lcx. Qtz+py and carb+py veinlets.
WT22-314 (WT22, 314.40-315.10)	Dacite (type D1). Weakly fdsp porphyritic. Non amygdaloidal. Hydrothermal alteration (propylitic): fdsp phenocrysts largely preserved, fdsp is albitised, pervasive groundmass alteration resulted in a fine intergrowth of fdsp laths with white mica, chl, qtz, and carb. Vein-like zones of hem, patchy and spotted ep, minor lcx. Qtz+carb veinlets.
WT22-322 (WT22, 322.40-323.30)	Dacite (type D1). Weakly fdsp porphyritic. Non amygdaloidal. Hydrothermal alteration (propylitic): fdsp phenocrysts largely preserved, fdsp is albitised, pervasive groundmass alteration resulted in a fine intergrowth of fdsp laths with white mica, chl, qtz, and carb. Diffuse and vein-like zones of hem, minor lcx. Qtz+carb and ep+qtz veinlets.
WT22-328 (WT22, 328.96-329.45)	Dacite (type D1). Weakly fdsp porphyritic. Non amygdaloidal. Hydrothermal alteration (propylitic): fdsp phenocrysts partially replaced by white mica, qtz, and carb, fdsp is albitised, pervasive groundmass alteration resulted in a fine intergrowth of fdsp laths with white mica, chl, qtz, and carb. Disseminated py and minor lcx. Well developed cleavage.
WT22-329 (WT22, 329.40-329.95)	Coarse quartz-feldspar crystal-rich sandstone-breccia. Abundant qtz (abundance: 30%, size: 1-5 mm) and fdsp (abundance: 30%, size: 1-3 mm) crystals. Phyllitic matrix. Hydrothermal alteration (propylitic): fdsp crystals largely preserved, fdsp is albitised, fine grained matrix of white mica, chl, qtz, and carb. Minor lcx. Well developed cleavage. Qtz veinlets.
WT22-332 (WT22, 332.85-333.35)	Mudstone. Dark greenish grey. Laminated. Individual beds: unequal thickness and laterally continuous. Detrital qtz and fdsp. Less detrital ap. Hydrothermal alteration (propylitic): fdsp grains are albitised, fine grained matrix of qtz, white mica, and chl. Bedding-parallel carb aggregates and disseminated carb. Well developed cleavage. Carb veinlets crosscut foliation.
WT23-114 (WT23, 114.90-115.50)	Basalt. Weakly fdsp and px porphyritic. Moderately amygdaloidal (qtz+chl+carb and chl+qtz filled). Regional alteration: fdsp phenocrysts are albitised, px phenocrysts entirely replaced, pervasive groundmass alteration resulted in a fine intergrowth of fdsp laths with chl, ep, qtz, and carb. Spotted ep and disseminated py. Ep and carb+qtz veinlets.

Notes: Ap = apatite, carb = carbonate, chl = chlorite, ep = epidote, fdsp = feldspar, gn = galena, hem = hematite, kln = kaolinite, lcx = lcx, prl = pyrophyllite, py = pyrite, px = pyroxene, qtz = quartz, sp = sphalerite, zrn = zircon.

Sample (drill hole, meters)	Petrographic description
WT23-140 (WT23, 140.45-141.05)	Andesite. Weakly px and fdsp porphyritic. Moderately amygdaloidal (qtz+chl+carb and chl+qtz filled). Regional alteration: px phenocrysts entirely replaced, fdsp phenocrysts are albitised, pervasive groundmass alteration resulted in a fine intergrowth of fdsp laths with chl, ep, qtz, and carb. Spotted ep and disseminated py. Qtz+hem and ep veinlets.
WT23-152 (WT23, 152.60-153.30)	Andesite. Aphyric. Moderately amygdaloidal (qtz+chl+carb and chl+qtz filled). Regional alteration: pervasive groundmass alteration resulted in a fine intergrowth of fdsp laths with chl, ep, qtz, and carb. Qtz+ep veinlets.
WT23-168 (WT23, 168.40-169.10)	Basalt. Very weakly px porphyritic. Moderately amygdaloidal (qtz+chl+carb and chl+qtz filled). Regional alteration: px phenocrysts entirely replaced, pervasive groundmass alteration resulted in a fine intergrowth of fdsp laths with chl, ep, qtz, and carb. Patchy and spotted ep, disseminated py. Ep veinlets.
WT23-182 (WT23, 182.05-182.75)	Basalt. Very weakly px porphyritic. Moderately amygdaloidal (qtz+chl+carb and chl+qtz filled). Regional alteration: px phenocrysts entirely replaced, pervasive groundmass alteration resulted in a fine intergrowth of fdsp laths with chl, ep, qtz, and carb. Spotted ep. Ep and qtz+carb veinlets.
WT23-198 (WT23, 198.40-199.00)	Basalt. Very weakly fdsp and px porphyritic. Sparsely amygdaloidal (qtz+chl+carb and chl+qtz filled). Regional alteration: fdsp phenocrysts are albitised, px phenocrysts entirely replaced, pervasive groundmass alteration resulted in a fine intergrowth of fdsp laths with chl, ep, qtz, and carb. Patchy and spotted ep. Qtz+carb veinlets.
WT23-208 (WT23, 208.85-209.40)	Fine sandstone. Greenish black. Massive. Detrital qtz and fdsp. Less detrital ap. Diagenetic py. Regional alteration: fdsp grains are albitised, fine grained matrix of qtz, white mica, chl, and rare carb. Carb veinlets crosscuts foliation.
WT23-227 (WT23, 227.75-228.45)	Basalt. Very weakly px porphyritic. Highly amygdaloidal (qtz+chl+carb and chl+qtz filled). Regional alteration: px phenocrysts entirely replaced, pervasive groundmass alteration resulted in a fine intergrowth of fdsp laths with chl, ep, qtz, and carb. Qtz and qtz+carb veinlets.
WT23-242 (WT23, 242.50-243.20)	Basalt. Very weakly px porphyritic. Non amygdaloidal. Regional alteration: px phenocrysts entirely replaced, pervasive groundmass alteration resulted in a fine intergrowth of fdsp laths with chl, ep, qtz, and carb. Spotted ep+carb. Qtz+carb veinlets.
WT23-256 (WT23, 256.50-257.20)	Basalt. Very weakly px porphyritic. Sparsely amygdaloidal (qtz+chl+carb and chl+qtz filled). Regional alteration: px phenocrysts entirely replaced, pervasive groundmass alteration resulted in a fine intergrowth of fdsp laths with chl, ep, qtz, and carb. Ep and qtz+carb veinlets.
WT23-261 (WT23, 261.80-262.50)	Mudstone. Dark greenish grey. Massive. Rare detrital qtz and fdsp. Less detrital ap and zrn. Patchy induration of qtz, ep, and carb. No diagenetic py. Regional alteration: fdsp grains are albitised, fine grained matrix of qtz and white mica with minor chl and carb. Poorly developed cleavage. Carb veinlets crosscut foliation.
WT23-282 (WT23, 282.00-282.60)	Basalt. Very weakly px porphyritic. Moderately amygdaloidal (qtz+chl+carb and chl+qtz filled). Regional alteration: px phenocrysts entirely replaced, pervasive groundmass alteration resulted in a fine intergrowth of fdsp laths with chl, ep, qtz, and carb. Patchy and spotted ep. Ep, qtz+carb, and qtz+hem veinlets.
WT23-295 (WT23, 295.15-295.65)	Basalt. Very weakly px porphyritic. Sparsely amygdaloidal (qtz+chl+carb and chl+qtz filled). Regional alteration: px phenocrysts entirely replaced, pervasive groundmass alteration resulted in a fine intergrowth of fdsp laths with chl, ep, qtz, and carb. Ep and qtz+carb veinlets.
WT23-322 (WT23, 322.65-323.25)	Coarse feldspar-quartz sandstone-breccia. Abundant fdsp (abundance: 25%, size: 1-2 mm) and quartz (abundance: < 1 %, size: < 1 mm) crystals. Phyllitic matrix. Diagenetic py. Regional alteration: fdsp crystals preserved, fdsp is albitised, fine grained matrix of white mica, chl, qtz, and carb. Patchy ep. Carb veinlets.
WT23-343 (WT23, 343.45-344.20)	Coarse feldspar-quartz sandstone-breccia. Abundant fdsp (abundance: 35%, size: 1-3 mm) and quartz (abundance: < 2 %, size: 1-2 mm) crystals. Phyllitic matrix. Regional alteration: fdsp crystals preserved, fdsp is albitised, fine grained matrix of white mica, chl, qtz, and carb. Patchy ep and minor lcx. Qtz veinlets.
WT23-368 (WT23, 368.60-369.20)	Fine sandstone. Dark greenish grey. Massive. Detrital qtz and fdsp. Less detrital ap. Patchy induration of qtz and ep. No diagenetic py. Regional alteration: fdsp grains are albitised, fine grained matrix of qtz and white mica with minor chl and carb. Carb veinlets crosscut foliation.
WT23-391 (WT23, 391.40-392.10)	Coarse quartz-feldspar crystal-rich sandstone-breccia. Abundant qtz (abundance: 30%, size: 1-3 mm) and fdsp (abundance: 50%, size: 1-3 mm) crystals, lithic fragments (abundance: 5%, size: < 8 mm). Phyllitic matrix. Hydrothermal alteration (propylitic): fdsp crystals and lithic fragments preserved, fdsp is albitised, fine grained matrix of white mica, chl, qtz, and carb. Patchy ep, spotted hem, and minor lcx. Poorly developed cleavage. Qtz+carb veinlets.
WT23-399 (WT23, 399.50-400.20)	Dacite. Moderately fdsp porphyritic. Non amygdaloidal. Hydrothermal alteration (propylitic): fdsp phenocrysts partially replaced by white mica, qtz, and carb, fdsp is albitised, pervasive groundmass alteration resulted in a fine intergrowth of fdsp laths with white mica, chl, and qtz. Spotted ep. Qtz+carb veinlets.
WT23-406 (WT23, 406.50-407.10)	Coarse quartz-feldspar crystal-rich sandstone-breccia. Abundant qtz (abundance: 35%, size: 2-3 mm) and fdsp (abundance: 35%, size: 2 mm) crystals. Phyllitic matrix. Hydrothermal alteration (phyllic): fdsp crystals entirely replaced by white mica, qtz, and carb, fine grained matrix of white mica, chl, qtz, and carb. Spotted ep and hem, minor lcx. Very intensely developed cleavage.
WT23-411 (WT23, 411.20-412.10)	Coarse quartz-feldspar crystal-rich sandstone-breccia. Abundant qtz (abundance: 30%, size: 1-3 mm) and fdsp (abundance and size obscured by alteration) crystals. Phyllitic matrix. Hydrothermal alteration (propylitic): fdsp crystals largely replaced by white mica, qtz, and carb, fdsp is albitised, fine grained matrix of white mica, chl, qtz, and carb. Minor lcx. Very intensely developed cleavage. Carb veinlets.
WT23-416 (WT23, 416.75-418.05)	Dacite (type D1). Weakly fdsp porphyritic. Non amygdaloidal. Hydrothermal alteration (propylitic): fdsp phenocrysts largely preserved, fdsp is albitised, pervasive groundmass alteration resulted in a fine intergrowth of fdsp laths with white mica, chl, qtz, and carb. Fracture controlled hem, patchy ep, and minor lcx. Qtz+carb and Ep+qtz veinlets.

Notes: Ap = apatite, carb = carbonate, chl = chlorite, ep = epidote, fdsp = feldspar, gn = galena, hem = hematite, kln = kaolinite, lcx = lcx, prl = pyrophyllite, py = pyrite, px = pyroxene, qtz = quartz, sp = sphalerite, zrn = zircon.

Sample (drill hole, meters)	Petrographic description
WT23-422 (WT23, 422.10-422.70)	Dacite (type D1). Weakly fdsp porphyritic. Non amygdaloidal. Hydrothermal alteration (propylitic): fdsp phenocrysts largely preserved, fdsp is albitised, pervasive groundmass alteration resulted in a fine intergrowth of fdsp laths with white mica, chl, qtz, and carb. Diffuse hem zones, patchy ep, fracture controlled mica+chl, and minor lcx. Qtz+carb veinlets.
WT23-430 (WT23, 430.05-430.85)	Dacite (type D1). Weakly fdsp porphyritic. Non amygdaloidal. Hydrothermal alteration (propylitic): fdsp phenocrysts largely preserved, fdsp is albitised, pervasive groundmass alteration resulted in a fine intergrowth of fdsp laths with white mica, chl, qtz, and carb. Diffuse hem zones, patchy ep, and minor lcx. Ep+qtz veinlets.
WT23-436 (WT23, 436.60-437.20)	Dacite (type D1). Weakly fdsp porphyritic. Non amygdaloidal. Hydrothermal alteration (propylitic): fdsp phenocrysts largely preserved, fdsp is albitised, pervasive groundmass alteration resulted in a fine intergrowth of fdsp laths with white mica, chl, qtz, and carb. Vein-like hem zones, patchy ep, and minor lcx. Qtz+carb veinlets.
WT23-443 (WT23, 443.80-444.60)	Dacite (type D1). Weakly fdsp porphyritic. Non amygdaloidal. Hydrothermal alteration (propylitic): fdsp phenocrysts largely preserved, fdsp is albitised, pervasive groundmass alteration resulted in a fine intergrowth of fdsp laths with white mica, chl, qtz, and carb. Patchy ep and minor lcx. Qtz+carb veinlets.
WT23-450 (WT23, 450.80-451.90)	Dacite (type D1). Weakly fdsp porphyritic. Non amygdaloidal. Hydrothermal alteration (propylitic): fdsp phenocrysts largely preserved, fdsp is albitised, pervasive groundmass alteration resulted in a fine intergrowth of fdsp laths with chl, qtz, and carb. Spotted hem, patchy ep, and minor lcx. Ep+carb veinlets.
WT23-455 (WT23, 455.45-456.45)	Dacite (type D1). Weakly fdsp porphyritic. Non amygdaloidal. Hydrothermal alteration (propylitic): fdsp phenocrysts partially replaced by white mica, qtz, and carb, fdsp is albitised, pervasive groundmass alteration resulted in a fine intergrowth of fdsp laths with white mica, chl, qtz, and carb. Minor lcx. Qtz+carb veinlets.
WT23-460 (WT23, 460.20-461.20)	Dacite (type D1). Weakly fdsp porphyritic. Non amygdaloidal. Hydrothermal alteration (phyllic): faint phenocrysts, pervasive groundmass alteration resulted in a fine intergrowth of fdsp laths with white mica, chl, and qtz. Disseminated py. Weakly developed cleavage. Py+carb veinlets.
WT23-477 (WT23, 477.20-478.20)	Intensely altered rock. Hydrothermal alteration (silicic): texturally destructive alteration resulted in a fine intergrowth of qtz and white mica. Disseminated py. Intensely developed cleavage.
WT23-488 (WT23, 488.00-489.00)	Intensely altered rock. Hydrothermal alteration (silicic): texturally destructive alteration resulted in a fine intergrowth of qtz and white mica. Disseminated py. Intensely developed cleavage.
WT23-505 (WT23, 505.50-506.50)	Intensely altered rock. Hydrothermal alteration (phyllic): texturally destructive alteration resulted in a fine intergrowth of white mica, chl, and qtz. Disseminated py. Very intensely developed cleavage.
WT24-115 (WT24, 115.65-116.35)	Dacite. Moderately fdsp porphyritic. Non amygdaloidal. Regional alteration: fdsp phenocrysts are albitised, pervasive groundmass alteration resulted in a fine intergrowth of fdsp laths with white mica, chl, qtz, and carb. Minor lcx. Qtz+carb veinlets.
WT24-137 (WT24, 137.25-137.75)	Dacite. Moderately fdsp porphyritic. Non amygdaloidal. Regional alteration: fdsp phenocrysts are albitised, pervasive groundmass alteration resulted in a fine intergrowth of fdsp laths with chl, qtz, and carb. Disseminated py and minor lcx. Qtz+carb veinlets.
WT24-155 (WT24, 155.70-156.30)	Andesite. Aphyric. Moderately amygdaloidal (qtz+chl+carb and chl+qtz filled). Regional alteration: pervasive groundmass alteration resulted in a fine intergrowth of fdsp laths with chl, ep, qtz, and carb. Ep+qtz and carb veinlets.
WT24-167 (WT24, 167.20-167.80)	Andesite. Aphyric. Highly amygdaloidal (qtz+chl+carb and chl+qtz filled). Regional alteration: pervasive groundmass alteration resulted in a fine intergrowth of fdsp laths with chl, ep, qtz, and carb. Qtz and qtz+carb veinlets.
WT24-182 (WT24, 182.70-183.30)	Basalt. Strongly fdsp porphyritic. Moderately amygdaloidal (chl+qtz filled). Regional alteration: fdsp phenocrysts are albitised, pervasive groundmass alteration resulted in a fine intergrowth of fdsp laths with chl, ep, qtz, and carb. Spotted ep. Qtz+ep and qtz+carb veinlets.
WT24-196 (WT24, 196.80-197.40)	Mudstone. Dark greenish grey. Laminated. Individual beds: unequal thickness and laterally discontinuous. Detrital qtz and rare fdsp. Less detrital ap. Diagenetic py. Regional alteration: fdsp grains are albitised, fine grained matrix of qtz, white mica, chl, and carb. Carb veinlets crosscut foliation.
WT24-219 (WT24, 219.95-220.65)	Basalt. Aphyric. Poorly amygdaloidal (qtz+chl filled). Regional alteration: pervasive groundmass alteration resulted in a fine intergrowth of fdsp laths with chl, ep, qtz, and carb. Qtz+carb veinlets.
WT24-231 (WT24, 231.25-231.70)	Andesite. Aphyric. Non amygdaloidal. Regional alteration: pervasive groundmass alteration resulted in a fine intergrowth of fdsp laths with chl, ep, qtz, and carb. Qtz+carb veinlets.
WT24-239 (WT24, 239.90-240.60)	Andesite. Aphyric. Non amygdaloidal. Regional alteration: pervasive groundmass alteration resulted in a fine intergrowth of fdsp laths with chl, qtz, and carb. Disseminated py. Qtz+carb veinlets.
WT24-266 (WT24, 266.45-267.25)	Fine sandstone. Dark greenish grey. Very thinly to thinly bedded. Individual beds: unequal thickness and laterally continuous, normal graded. Detrital qtz and fdsp. Less detrital ap. Rare lithic fragments. Diagenetic py. Regional alteration: fdsp grains are albitised, fine grained matrix of qtz and white mica with minor chl and carb. Carb veinlets crosscut foliation.
WT24-290 (WT24, 290.85-291.50)	Coarse feldspar-quartz sandstone-breccia. Abundant fdsp (abundance: 35%, size: 1-3 mm) and quartz (abundance: < 5 %, size: 1mm) crystals. Diagenetic py. Phyllitic matrix. Regional alteration: fdsp crystals preserved, fdsp is albitised, fine grained matrix of white mica, chl, qtz, and carb. Spotted ep and minor lcx. Carb veinlets.
WT24-300 (WT24, 300.90-300.95)	Resedimented dacitic hyaloclastite. Very weakly fdsp porphyritic. Non amygdaloidal. Clast size: >15 cm. Clast shape: blocky with subrounded to rounded corners. Regional alteration: fdsp phenocrysts are albitised, pervasive groundmass alteration resulted in a fine intergrowth of fdsp laths with chl, qtz, and carb. Minor lcx. Carb and qtz+carb veinlets.
WT24-318 (WT24, 318.10-318.70)	Basalt. Very weakly fdsp porphyritic. Poorly amygdaloidal (qtz+chl filled). Regional alteration: fdsp phenocrysts are albitised, pervasive groundmass alteration resulted in a fine intergrowth of fdsp laths with chl, ep, qtz, and carb. Streaky ep. Ep and qtz+carb veinlets.

Notes: Ap = apatite, carb = carbonate, chl = chlorite, ep = epidote, fdsp = feldspar, gn = galena, hem = hematite, kln = kaolinite, lcx = lcx, prl = pyrophyllite, py = pyrite, px = pyroxene, qtz = quartz, sp = sphalerite, zrn = zircon.

Sample (drill hole, meters)	Petrographic description
WT24-327 (WT24, 327.30-327.80)	Mudstone. Dark greenish grey. Massive. Abundant detrital qtz and fdsp. Less detrital ap. Diagenetic py. Small face-centred qtz strain fringes on py. Regional alteration: fdsp grains are albitised, fine grained matrix of qtz, white mica, chl, and carb. Intensely developed cleavage. Carb veinlets crosscut foliation.
WT24-351 (WT24, 351.20-351.80)	Fine sandstone. Greenish grey and dark greenish grey. Laminated. Individual beds: unequal thickness and laterally discontinuous. Abundant detrital qtz and fdsp. Less detrital ap. No diagenetic py. Regional alteration: fdsp grains are albitised, fine grained matrix of qtz, white mica, chl, and carb. Carb veinlets crosscut foliation.
WT24-356 (WT24, 356.45-356.90)	Dacite. Moderately fdsp porphyritic. Non amygdaloidal. Hydrothermal alteration (propylitic): fdsp phenocrysts partially replaced by white mica, qtz, and carb, fdsp is albitised, pervasive groundmass alteration resulted in a fine intergrowth of fdsp laths with white mica, chl, qtz, and carb. Spotted ep. Qtz+carb and qtz+carb+hem veinlets.
WT24-370 (WT24, 370.50-371.00)	Dacite (type D1). Weakly fdsp porphyritic. Non amygdaloidal. Hydrothermal alteration (propylitic): fdsp phenocrysts largely preserved, fdsp is albitised, domains of chl+qtz+carb and qtz+hem, patchy ep+qtz+carb groundmass alteration. Spotted hem and minor lcx. Ep+qtz and qtz+carb veinlets.
WT24-383 (WT24, 383.30-384.00)	Dacite (type D1). Weakly fdsp porphyritic. Non amygdaloidal. Hydrothermal alteration (propylitic): fdsp phenocrysts largely preserved, fdsp is albitised, domains of chl+white mica+qtz+carb and qtz+hem, patchy ep+qtz+carb groundmass alteration. Spotted hem and minor lcx. Qtz+carb veinlets.
WT24-393 (WT24, 393.90-394.35)	Dacite. Moderately fdsp porphyritic. Non amygdaloidal. Hydrothermal alteration (propylitic): fdsp phenocrysts partially replaced by white mica, qtz, and carb, fdsp is albitised, pervasive groundmass alteration resulted in a fine intergrowth of fdsp laths with white mica, chl, qtz, and carb. Spotted ep. Qtz+carb veinlets.
WT24-396 (WT24, 396.50-397.10)	Mudstone. Dark greenish grey. Massive. Rare detrital qtz and fdsp. Less detrital ap. No diagenetic py. Regional alteration: fdsp grains are albitised, fine grained matrix of qtz, white mica, and chl with minor carb. Very intensely developed cleavage. Carb veinlets crosscut foliation.
WT24-405 (WT24, 405.65-406.25)	Dacite (type D1). Weakly fdsp porphyritic. Non amygdaloidal. Hydrothermal alteration (propylitic): fdsp phenocrysts largely preserved, fdsp is albitised, domains of chl+white mica+qtz+carb and qtz+hem, patchy ep+qtz+carb groundmass alteration. Spotted hem and minor lcx. Qtz+carb veinlets.
WT24-415 (WT24, 415.45-416.05)	Dacite (type D1). Weakly fdsp porphyritic. Non amygdaloidal. Hydrothermal alteration (propylitic): fdsp phenocrysts largely preserved, fdsp is albitised, domains of chl+white mica+qtz+carb and qtz+hem, patchy ep+qtz+carb groundmass alteration. Spotted hem and minor lcx. Qtz+carb veinlets.
WT24-433 (WT24, 433.90-434.50)	Monomict dacitic breccia-conglomerate (type D1). Weakly fdsp porphyritic. Non amygdaloidal. Clast size: 1 mm to 4 cm. Clast shape: blocky and angular with subrounded to rounded corners. Hydrothermal alteration (propylitic): fdsp phenocrysts largely preserved, fdsp is albitised, pervasive groundmass alteration resulted in a fine intergrowth of fdsp laths with chl, white mica, and qtz. Spotted ep and minor lcx. Qtz+carb veinlets.
WT24-441 (WT24, 441.50-442.20)	Dacite (type D1). Weakly fdsp porphyritic. Non amygdaloidal. Hydrothermal alteration (propylitic): fdsp phenocrysts partially replaced by white mica, qtz, and carb, fdsp is albitised, domains of chl+white mica+qtz+carb and qtz+hem, patchy ep+qtz+carb groundmass alteration. Vein-like hem zones and minor lcx. Qtz+carb veinlets.
WT24-456 (WT24, 456.20-456.90)	Dacite (type D1). Weakly fdsp porphyritic. Non amygdaloidal. Hydrothermal alteration (propylitic): fdsp phenocrysts partially replaced by white mica, qtz, and carb, fdsp is albitised, domains of white mica+chl+qtz+carb and qtz+hem, patchy ep+qtz+carb groundmass alteration. Vein-like hem zones and minor lcx. Qtz+carb veinlets.
WT24-470 (WT24, 470.20-471.90)	Dacite (type D1). Weakly fdsp porphyritic. Non amygdaloidal. Hydrothermal alteration (propylitic): fdsp phenocrysts partially replaced by white mica, qtz, and carb, fdsp is albitised, domains of white mica+chl+qtz+carb, white mica+chl+ep+qtz+carb, and white mica+qtz groundmass alteration. Spotted ep and hem, minor lcx. Qtz+carb veinlets.
WT24-488 (WT24, 488.80-489.45)	Dacite (type D1). Weakly fdsp porphyritic. Non amygdaloidal. Hydrothermal alteration (propylitic): fdsp phenocrysts partially replaced by white mica+qtz+carb, fdsp is albitised, pervasive groundmass alteration resulted in a fine intergrowth of fdsp laths with white mica, chl, qtz, and carb. Patchy ep and disseminated py. Qtz+carb veinlets.
WT24-497 (WT24, 497.50-498.10)	Dacite (type D1). Weakly fdsp porphyritic. Non amygdaloidal. Hydrothermal alteration (propylitic): fdsp phenocrysts partially replaced by white mica, qtz, and carb, fdsp is albitised, pervasive groundmass alteration resulted in a fine intergrowth of fdsp laths with white mica, chl, qtz, and carb. Patchy ep+chl+qtz+carb and disseminated py. Qtz+carb veinlets.
WT24-516 (WT24, 516.40-517.10)	Dacite (type D1). Weakly fdsp porphyritic. Non amygdaloidal. Hydrothermal alteration (phyllic): faint phenocrysts, pervasive groundmass alteration resulted in a fine intergrowth of fdsp laths with white mica, chl, qtz, and carb. Disseminated py. Intensely developed cleavage. Carb veinlets.
WT24-534 (WT24, 534.95-535.85)	Intensely altered rock. Hydrothermal alteration (phyllic): texturally destructive alteration resulted in a fine intergrowth of white mica and qtz. Disseminated py. Intensely developed cleavage.
WT25-97 (WT25, 97.10-97.60)	Basalt. Very weakly fdsp porphyritic. Non amygdaloidal. Regional alteration: fdsp phenocrysts are albitised, pervasive groundmass alteration resulted in a fine intergrowth of fdsp laths with chl, ep, qtz, and carb. Patchy and spotted ep. Carb+qtz veinlets.
WT25-110 (WT25, 110.75-111.30)	Dacite. Aphyric. Non amygdaloidal. Regional alteration: pervasive groundmass alteration resulted in a fine intergrowth of fdsp laths with white mica, chl, qtz, and carb. Spotted ep and minor lcx. Qtz+carb veinlets.
WT25-126 (WT25, 126.50-127.05)	Dacite. Weakly fdsp porphyritic. Poorly amygdaloidal (qtz+chl filled). Regional alteration: fdsp phenocrysts are albitised, pervasive groundmass alteration resulted in a fine intergrowth of fdsp laths with chl, qtz, and carb. Minor lcx. Carb veinlets.
WT25-139 (WT25, 139.35-140.00)	Dacite. Weakly fdsp porphyritic. Non amygdaloidal. Regional alteration: fdsp phenocrysts are albitised, pervasive groundmass alteration resulted in a fine intergrowth of fdsp laths with chl, ep, qtz, and carb. Spotted ep and minor lcx. Qtz+carb+hem veinlets.

Notes: Ap = apatite, carb = carbonate, chl = chlorite, ep = epidote, fdsp = feldspar, gn = galena, hem = hematite, kln = kaolinite, lcx = lcx, prl = pyrophyllite, py = pyrite, px = pyroxene, qtz = quartz, sp = sphalerite, zrn = zircon.

Sample (drill hole, meters)	Petrographic description
WT25-162 (WT25, 162.70-163.30)	Dacite. Moderately fdsp porphyritic. Non amygdaloidal. Regional alteration: fdsp phenocrysts are albitised, pervasive groundmass alteration resulted in a fine intergrowth of fdsp laths with white mica, chl, qtz, and carb. Spotted ep. Qtz veinlets..
WT25-174 (WT25, 174.50-175.00)	Dacite. Moderately fdsp porphyritic. Non amygdaloidal. Regional alteration: fdsp phenocrysts are albitised, pervasive groundmass alteration resulted in a fine intergrowth of fdsp laths with white mica, chl, qtz, and carb. Spotted ep and disseminated py. Qtz+carb veinlets.
WT25-198 (WT25, 198.15-198.70)	Andesite. Very weakly fdsp porphyritic. Non amygdaloidal. Regional alteration: fdsp phenocrysts are albitised, pervasive groundmass alteration resulted in a fine intergrowth of fdsp laths with chl, ep, qtz, and carb. Patchy and spotted ep. Carb+qtz veinlets.
WT25-228 (WT25, 228.70-229.70)	Basalt. Strongly fdsp porphyritic. Highly amygdaloidal (qtz+chl filled). Regional alteration: fdsp phenocrysts are albitised, pervasive groundmass alteration resulted in a fine intergrowth of fdsp laths with chl, ep, qtz, and carb. Spotted ep. Hem+qtz veinlets.
WT25-242 (WT25, 242.35-243.15)	Andesite. Aphyric. Highly amygdaloidal (qtz+carb filled). Regional alteration: pervasive groundmass alteration resulted in a fine intergrowth of fdsp laths with chl, ep, qtz, and carb. Qtz+carb veinlets.
WT25-265 (WT25, 265.45-265.80)	Basalt. Moderately fdsp porphyritic. Moderately amygdaloidal (qtz+carb filled). Regional alteration: fdsp phenocrysts are albitised, pervasive groundmass alteration resulted in a fine intergrowth of fdsp laths with chl, ep, qtz, and carb. Spotted ep. Qtz+carb veinlets.
WT25-280 (WT25, 280.80-281.40)	Basalt. Weakly fdsp porphyritic. Moderately amygdaloidal (qtz+carb filled). Regional alteration: fdsp phenocrysts are albitised, pervasive groundmass alteration resulted in a fine intergrowth of fdsp laths with chl, ep, qtz, and carb. Patchy and spotted ep. Qtz and qtz+carb veinlets.
WT25-296 (WT25, 296.65-296.90)	Basalt. Very weakly fdsp porphyritic. Highly amygdaloidal (qtz+carb filled). Regional alteration: fdsp phenocrysts are albitised, pervasive groundmass alteration resulted in a fine intergrowth of fdsp laths with chl, ep, qtz, and carb. Spotted ep. Qtz+ep and qtz+hem veinlets.
WT25-318 (WT25, 318.40-319.10)	Fine sandstone. Dark greenish grey. Massive. Abundant detrital qtz and rare fdsp. Less detrital ap. Diagenetic py. Regional alteration: fdsp grains are albitised, fine grained matrix of qtz, white mica, chl, and carb.
WT25-328 (WT25, 328.00-328.60)	Mudstone. Dark greenish grey. Massive. Abundant detrital qtz and rare fdsp. Less detrital ap. No diagenetic py. Regional alteration: fdsp grains are albitised, fine grained matrix of qtz and white mica with minor chl and carb.
WT25-339 (WT25, 339.85-340.45)	Coarse feldspar-quartz sandstone-breccia. Abundant fdsp (abundance: 70%, size: 1-2 mm) and quartz (abundance: < 5 %, size: < 2 mm) crystals, lithic fragments (abundance: < 5%, size: 1-2 mm). Diagenetic py. Phyllitic matrix. Regional alteration: fdsp crystals and lithic fragments preserved, fdsp is albitised, fine grained matrix of white mica, chl, qtz, and carb. Minor lcx. Carb veinlets.
WT25-357 (WT25, 357.30-357.90)	Fine sandstone. Dark greenish grey. Laminated to very thinly bedded. Individual beds: unequal thickness and laterally continuous. Abundant detrital qtz and fdsp. Less detrital ap. No diagenetic py. Regional alteration: fdsp grains are albitised, fine grained matrix of qtz, white mica, chl, and carb. Carb+qtz veinlets.
WT25-372 (WT25, 372.30-373.00)	Andesite. Aphyric. Non amygdaloidal. Regional alteration: pervasive groundmass alteration resulted in a fine intergrowth of fdsp laths with chl, qtz, and carb. Disseminated py. Qtz+carb veinlets.
WT25-386 (WT25, 386.60-387.25)	Mudstone. Greenish black. Massive. Phyllitic. Detrital qtz and abundant fdsp. Less detrital ap. Diagenetic py frequently enveloped by carb halos. Regional alteration: fdsp grains are albitised, fine grained matrix of qtz, white mica, chl, and carb. Well developed cleavage. Carb veinlets crosscut foliation.
WT25-401 (WT25, 401.95-402.55)	Dacite. Aphyric. Non amygdaloidal. Regional alteration: pervasive groundmass alteration resulted in a fine intergrowth of fdsp laths with white mica, chl, qtz, and carb. Carb and carb+qtz veinlets.
WT25-408 (WT25, 408.80-409.50)	Mudstone. Dark greenish grey. Massive. Abundant detrital qtz and fdsp. Less detrital ap. No diagenetic py. Regional alteration: fdsp grains are albitised, fine grained matrix of qtz, white mica, chl, and carb. Intensely developed cleavage. Carb veinlets crosscut foliation.
WT25-417 (WT25, 417.90-417.95)	Resedimented dacitic hyaloclastite (type D1). Weakly fdsp porphyritic. Non amygdaloidal. Clast size: 4 cm. Clast shape: blocky with subrounded to rounded corners. Hydrothermal alteration (propylitic): fdsp phenocrysts are albitised, pervasive groundmass alteration resulted in a fine intergrowth of fdsp laths with qtz and carb. Spotted hem and minor lcx. Carb and qtz+carb veinlets.
WT25-418 (WT25, 418.20-418.70)	Coarse quartz-feldspar crystal-rich sandstone-breccia. Abundant qtz (abundance: 25%, size: 2-3 mm) and fdsp (abundance: 15%, size: 3 mm) crystals, abundant lithic fragments (abundance: 40%, size: < 8 cm). Phyllitic matrix. Hydrothermal alteration (propylitic): fdsp crystals and lithic fragments preserved, fdsp is albitised, fine grained matrix of white mica, chl, qtz, and carb. Minor lcx. Qtz+carb veinlets.
WT25-423 (WT25, 423.75-424.95)	Coarse quartz-feldspar crystal-rich sandstone-breccia. Abundant qtz (abundance: 30%, size: 1-3 mm) and fdsp (abundance: 50%, size: 1-2 mm) crystals, lithic fragments (abundance: 5%, size: 1-6 mm). Phyllitic matrix. Hydrothermal alteration (propylitic): fdsp crystals and lithic fragments largely preserved, fdsp is albitised, fine grained matrix of white mica, chl, qtz, and carb. Minor ep and lcx. Qtz+carb veinlets.
WT25-428 (WT25, 428.65-428.95)	Coarse quartz-feldspar crystal-rich sandstone-breccia. Abundant qtz (abundance: 30%, size: 2-3 mm) and fdsp (abundance and size obscured by alteration) crystals. Phyllitic matrix. Hydrothermal alteration (phyllic): fdsp crystals entirely replaced by white mica, qtz, and carb, fine grained matrix of white mica, chl, qtz, and carb. Spotted hem and minor lcx. Intensely developed cleavage. Qtz+carb veinlets.
WT25-434 (WT25, 434.45-435.45)	Coarse quartz-feldspar crystal-rich sandstone-breccia. Abundant qtz (abundance: 50%, size: 2-3 mm) and fdsp (abundance and size obscured by alteration) crystals. Phyllitic matrix. Hydrothermal alteration (phyllic): fdsp crystals entirely replaced by white mica, qtz, and carb, fine grained matrix of white mica, chl, qtz, and carb. Spotted hem and minor lcx. Intensely to very intensely developed cleavage. Qtz+ep veinlets.
WT25-441 (WT25, 441.00-442.00)	Intensely altered rock. Hydrothermal alteration (phyllic): texturally destructive alteration resulted in a fine intergrowth of remnant fdsp laths with white mica, chl, qtz, and carb. Disseminated py. Very intensely developed cleavage.

Notes: Ap = apatite, carb = carbonate, chl = chlorite, ep = epidote, fdsp = feldspar, gn = galena, hem = hematite, kln = kaolinite, lcx = lcx, prl = pyrophyllite, py = pyrite, px = pyroxene, qtz = quartz, sp = sphalerite, zrn = zircon.

Sample (drill hole, meters)	Petrographic description
WT25-444 (WT25, 444.85-445.95)	Intensely altered rock. Hydrothermal alteration (phyllic): texturally destructive alteration resulted in a fine intergrowth of white mica, chl, qtz, and carb. Disseminated py. Very intensely developed cleavage.
WT25-458 (WT25, 458.80-459.90)	Intensely altered rock. Hydrothermal alteration (phyllic): texturally destructive alteration resulted in a fine intergrowth of white mica and qtz. Disseminated py. Intensely developed cleavage.
WT25-478 (WT25, 478.40-479.40)	Intensely altered rock. Hydrothermal alteration (phyllic): texturally destructive alteration resulted in a fine intergrowth of white mica, chl, and qtz. Disseminated py. Very intensely developed cleavage.
WT29-133 (WT29, 133.10-133.15)	Resedimented dacitic hyaloclastite. Moderately fdsp and very weakly quartz porphyritic. Non amygdaloidal. Clast size: 5 cm. Clast shape: blocky with rounded corners. Hydrothermal alteration (phyllic): fdsp phenocrysts are replaced by white mica, qtz, and carb, pervasive groundmass alteration resulted in a fine intergrowth of fdsp laths with qtz and chl. Minor lcx. Carb and qtz+chl veinlets.
WT35-306 (WT35, 306.20-306.30)	Resedimented dacitic hyaloclastite. Weakly fdsp and very weakly quartz porphyritic. Non amygdaloidal. Clast size: >15 cm. Clast shape: blocky with rounded corners. Hydrothermal alteration (propylitic): fdsp phenocrysts largely preserved, fdsp is albitised, domains of qtz+chl and qtz groundmass alteration. Minor lcx. Qtz+chl veinlets.
WT35-309 (WT35, 309.00-309.10)	Resedimented dacitic hyaloclastite (type D1). Weakly fdsp porphyritic. Non amygdaloidal. Clast size: >15 cm. Clast shape: blocky with subrounded to rounded corners. Hydrothermal alteration (propylitic): fdsp phenocrysts largely preserved, fdsp is albitised, pervasive groundmass alteration resulted in a fine intergrowth of fdsp laths with qtz and hem. Minor lcx. Carb and qtz+carb veinlets.
WT35-310 (WT35, 310.20-310.25)	Resedimented dacitic hyaloclastite. Moderately fdsp and strongly quartz porphyritic. Non amygdaloidal. Clast size: 3 cm. Clast shape: blocky with planar to curviplanar margins, rounded corners. Hydrothermal alteration (propylitic): fdsp phenocrysts largely preserved, fdsp is albitised, pervasive groundmass alteration resulted in a fine intergrowth of fdsp laths with qtz and chl. Spotted hem and minor lcx.
WT35-312 (WT35, 312.00-312.05)	Resedimented dacitic hyaloclastite. Moderately fdsp porphyritic. Non amygdaloidal. Clast size: 4.5 cm. Clast shape: blocky with subrounded to rounded corners. Hydrothermal alteration (phyllic): fdsp phenocrysts largely preserved, fdsp is albitised, pervasive groundmass alteration resulted in a fine intergrowth of fdsp laths with qtz and hem. Minor lcx.

Notes: Ap = apatite, carb = carbonate, chl = chlorite, ep = epidote, fdsp = feldspar, gn = galena, hem = hematite, kln = kaolinite, lcx = lcx, prl = pyrophyllite, py = pyrite, px = pyroxene, qtz = quartz, sp = sphalerite, zrn = zircon.

	Detection limits	WT2-103	WT2-117	WT2-131	WT2-150	WT2-164	WT2-176	WT2-193	WT2-210	WT2-227	WT2-239	WT2-265	WT2-280	WT2-294	WT2-315	WT2-323	WT2-338	WT2-345
Major elements (weight %; XRF and Leco):																		
SiO_2	0.01	57.32	50.04	47.69	50.11	47.12	59.06	78.62	51.29	50.98	74.05	62.86	65.01	74.59	67.61	57.32	60.41	70.14
TiO_2	0.01	0.74	0.83	0.92	0.55	0.78	0.64	0.21	0.70	0.72	0.29	0.77	0.69	0.35	0.56	1.09	0.75	0.43
Al_2O_3	0.01	15.23	16.91	17.31	18.72	18.69	15.77	9.88	15.58	15.73	10.96	17.00	15.75	11.76	14.72	15.43	17.66	12.96
Fe_2O_3	0.01	9.55	12.83	14.12	8.52	12.87	8.92	1.58	10.99	10.98	2.33	7.19	5.90	1.60	4.55	8.62	6.82	3.30
MnO	0.01	0.12	0.13	0.18	0.08	0.12	0.10	0.02	0.14	0.16	0.03	0.05	0.07	0.03	0.05	0.16	0.05	0.07
MgO	0.01	3.60	4.96	4.73	3.50	6.61	3.96	0.68	4.27	4.27	1.12	2.81	2.61	1.05	2.20	3.24	2.74	1.37
CaO	0.01	6.82	7.38	7.83	10.93	5.77	2.03	2.16	9.38	8.15	4.04	0.27	0.95	2.21	1.87	3.23	1.13	2.67
Na_2O	0.03	3.16	2.76	1.81	2.50	3.87	4.44	0.75	2.19	2.60	<0.03	<0.03	1.44	0.11	1.47	5.67	1.24	1.39
K_2O	0.01	0.09	0.07	0.10	0.13	0.03	0.66	2.90	0.13	0.09	3.08	4.56	4.10	4.15	2.90	0.06	4.01	3.06
P_2O_5	0.01	0.13	0.14	0.15	0.09	0.12	0.10	0.04	0.10	0.10	0.06	0.14	0.13	0.06	0.09	0.28	0.18	0.13
LOI	0.01	3.33	3.83	4.93	4.64	4.05	4.12	3.15	5.50	6.00	3.99	4.02	3.08	3.48	3.98	4.61	4.23	4.03
Total	-	100.09	99.88	99.77	99.77	100.03	99.80	99.99	100.27	99.78	99.95	99.67	99.73	99.39	100.00	99.71	99.22	99.55
C	0.005	0.25	0.18	0.26	0.57	0.08	0.34	0.49	0.75	0.68	0.68	0.06	0.11	0.51	0.42	0.61	0.25	0.57
S	0.01	0.02	0.02	0.02	0.01	0.01	0.05	<0.01	0.02	0.02	0.02	0.09	0.04	0.02	0.03	0.11	0.47	0.08
Trace elements (ppm; XRF):																		
Sc	2	31	33	36	27	35	39	6	35	42	7	18	15	9	13	34	20	12
V	1.5	288	325	351	254	339	311	21	339	338	23	112	89	10	50	210	139	37
Cr	1	5	6	5	11	15	17	7	13	14	7	102	78	3	4	4	115	32
Ni	1	3	6	5	6	5	6	6	7	6	3	35	29	2	1	3	36	14
Cu	2	115	134	51	103	100	87	2	93	124	14	37	32	12	21	50	63	13
Zn	1	69	96	132	65	100	75	17	70	78	24	102	89	24	56	206	116	68
As	3	4	<3	9	7	6	<3	<3	<3	<3	<3	33	16	<3	<3	<3	67	<3
Rb	1	1	<1	2	3	<1	20	71	3	3	99	169	151	162	96	2	160	123
Sr	1	429	254	572	310	357	178	37	556	281	179	42	70	48	101	165	71	126
Y	1	13	14	16	11	12	11	14	10	11	19	33	33	34	30	19	33	32
Zr	1	45	51	57	30	40	48	131	34	35	192	155	175	234	228	81	151	242
Nb	1	3	3	3	<1	2	4	8	2	2	11	18	17	15	16	7	16	13
Ba	4	322	56	44	63	47	150	645	40	42	516	523	703	1204	781	56	1122	1076
La	2	8	9	11	9	7	11	15	8	10	24	45	46	20	23	17	33	28
Ce	4	19	18	24	13	16	22	37	16	15	54	87	99	52	52	34	71	66
Nd	2	10	8	11	9	8	10	16	8	10	20	39	42	23	24	18	27	28
Pb	1.5	3	4	6	2	<1.5	3	14	3	3	9	19	18	7	14	4	23	4
Bi	2	<2	<2	<2	<2	<2	<2	<2	3	<2	<2	<2	<2	<2	<2	<2	<2	<2
Th	1.5	3	3	3	2	<1.5	4	11	<1.5	2	15	18	18	12	11	4	17	16
Trace elements (ppm; ICP-MS):																		
Cd	0.1	0.3	0.3	0.3	0.2	0.2	0.2	0.3	0.3	0.2	0.2	0.2	0.2	0.2	0.2	<0.1	0.9	0.2
Cs	0.05	0.2	0.4	0.4	0.2	0.1	0.6	2.1	0.4	0.3	1.9	5.3	4.6	4.9	4.4	0.1	4.4	3.2
Tl	0.5	<0.5	<0.5	<0.5	<0.5	<0.5	<0.5	<0.5	<0.5	<0.5	0.6	1.0	0.9	0.9	0.6	<0.5	1.0	0.8
Bi	0.1	<0.1	<0.1	<0.1	<0.1	<0.1	0.1	0.5	0.7	0.3	0.5	0.8	0.7	0.4	0.4	0.2	0.5	0.2
Th	0.05	2.8	-	-	1.8	-	3.3	-	-	2.2	-	-	17.8	11.8	11.4	-	18.6	-
U	0.05	0.6	0.8	0.9	0.5	0.7	0.8	2.2	0.5	0.5	3.2	3.8	3.7	3.2	3.2	1.3	3.9	3.0

	WT2-353	WT2-360	WT2-386	WT2-402	WT2-421	WT2-440	WT2-461	WT5-118	WT5-129	WT5-136	WT5-148	WT5-156	WT5-158	WT5-163	WT5-171	WT5-186	WT5-213
Major elements (weight %; XRF and Leco):																	
SiO_2	63.83	62.04	63.38	63.33	61.75	60.90	56.45	62.34	62.54	66.39	69.71	67.49	64.93	71.71	67.47	57.38	52.88
TiO_2	0.41	0.20	0.79	0.65	0.47	0.54	1.22	0.72	0.52	0.54	0.37	0.37	0.20	0.31	0.35	1.00	1.10
Al_2O_3	15.15	17.35	14.89	15.78	7.46	7.47	18.55	17.48	15.87	15.54	14.57	15.74	16.95	12.92	14.54	19.76	15.43
Fe_2O_3	3.75	3.67	8.99	8.27	17.46	17.44	8.15	7.30	4.25	5.17	3.00	3.84	3.96	2.68	2.67	7.20	8.85
MnO	0.18	0.14	<0.01	<0.01	0.01	<0.01	0.03	0.04	0.12	0.06	0.05	0.10	0.15	0.06	0.07	<0.01	0.10
MgO	1.20	1.29	0.28	0.57	0.24	0.24	2.00	3.09	1.43	2.38	0.97	1.12	1.07	1.19	2.39	0.98	1.46
CaO	4.93	4.72	0.20	0.24	0.22	0.22	1.53	0.17	3.85	0.93	3.11	3.26	4.99	5.07	3.72	0.34	6.30
Na_2O	2.99	1.61	0.58	0.41	0.81	0.38	0.89	0.69	3.16	1.29	3.34	5.10	3.73	1.30	1.29	0.64	1.89
K_2O	1.98	2.00	3.68	4.09	2.10	2.02	2.61	3.95	2.93	3.60	1.67	0.73	1.03	0.99	1.21	4.55	0.54
P_2O_5	0.08	0.18	0.14	0.18	0.17	0.15	0.28	0.13	0.23	0.10	0.07	0.09	0.18	0.05	0.06	0.23	0.29
LOI	5.38	6.51	6.67	6.50	9.73	10.42	7.66	4.10	4.86	3.39	2.56	2.44	2.56	3.71	6.18	6.96	10.43
Total	99.88	99.71	99.60	100.02	100.42	99.78	99.37	100.01	99.76	99.39	99.42	100.28	99.75	99.99	99.95	99.04	99.27
C	0.97	1.01	0.03	0.05	0.03	0.03	0.03	0.05	0.78	0.26	0.25	0.26	0.35	0.84	0.83	0.01	0.94
S	<0.01	<0.01	7.16	6.53	13.70	13.68	6.19	<0.01	0.01	0.03	<0.01	<0.01	<0.01	0.02	<0.01	5.74	6.10
Trace elements (ppm; XRF):																	
Sc	14	4	29	29	9	8	41	18	9	14	10	11	4	10	11	16	31
V	49	9	200	170	49	51	269	106	31	72	30	40	8	25	28	106	218
Cr	5	2	5	6	4	5	6	96	2	65	12	5	2	3	3	5	7
Ni	3	<1	4	3	5	6	4	38	<1	27	5	2	<1	2	2	5	4
Cu	2	4	294	28	551	352	40	30	4	22	4	3	3	2	2	115	44
Zn	57	121	483	604	4100	15	69	155	61	86	44	70	53	27	89	956	110
As	<3	<3	14	13	19	28	7	<3	<3	9	6	7	8	10	7	22	13
Rb	70	56	66	79	37	36	53	154	117	138	58	23	34	30	33	86	9
Sr	480	432	59	48	25	31	271	40	336	92	697	820	707	712	380	130	1265
Y	15	11	14	19	8	4	17	33	25	31	35	9	11	19	19	4	23
Zr	90	92	103	90	64	72	110	144	195	152	228	53	87	133	137	115	86
Nb	6	5	6	5	3	4	6	16	13	15	13	3	5	7	7	7	5
Ba	485	852	826	630	211	203	687	946	594	887	442	224	362	394	1437	1434	1080
La	13	19	9	11	9	6	4	44	34	36	38	9	19	15	22	26	7
Ce	29	46	26	29	17	12	10	93	73	70	84	22	50	33	25	60	20
Nd	12	17	12	16	8	5	7	39	31	30	37	10	20	14	9	26	12
Pb	10	15	18	28	89	14	21	6	9	24	8	18	18	17	8	39	14
Bi	<2	<2	<2	<2	3	3	<2	<2	<2	<2	<2	<2	<2	<2	<2	2	<2
Th	5	10	3	2	<1.5	<1.5	<1.5	19	16	19	15	3	10	7	8	2	2
Trace elements (ppm; ICP-MS):																	
Cd	0.1	0.1	1.9	1.9	11.3	0.2	0.1	0.2	-	0.1	0.2	<0.1	0.3	0.1	0.1	3.3	0.2
Cs	1.5	1.3	1.3	1.3	0.8	0.6	0.8	5.0	-	4.0	1.2	0.5	0.5	0.8	0.9	1.4	0.2
Tl	0.8	1.4	3.8	2.5	0.7	<0.5	1.2	1.0	-	0.9	0.7	0.5	0.6	1.0	2.4	6.1	0.9
Bi	0.2	0.2	0.7	0.7	3.9	3.8	0.4	2.2	-	2.1	0.9	0.5	0.4	0.5	0.3	1.8	0.3
Th	4.9	-	-	2.4	0.8	0.8	2.2	-	-	-	-	-	-	-	-	-	-
U	0.8	1.5	1.3	0.6	0.3	0.2	1.3	3.3	-	4.1	3.3	0.7	1.6	1.0	1.1	0.7	0.5

	WT5-223	WT5-231	WT6-109	WT6-135	WT6-153	WT6-167	WT6-180	WT7-92	WT7-108	WT7-123	WT7-155	WT7-171	WT7-200	WT7-205	WT7-208	WT7-213	WT8A-103
Major elements (weight %; XRF and Leco):																	
SiO_2	47.94	50.43	66.45	58.45	61.72	63.62	59.03	64.80	51.80	56.50	59.04	60.07	69.83	69.66	71.57	66.36	70.07
TiO_2	0.73	0.80	0.48	0.61	0.77	0.74	0.91	0.88	1.10	1.16	0.65	1.02	0.29	0.45	0.45	0.52	0.20
Al_2O_3	18.62	19.40	14.21	15.46	13.83	13.59	15.41	13.34	17.10	17.35	16.61	12.09	11.87	12.45	13.46	15.80	13.95
Fe_2O_3	8.67	7.74	7.41	7.93	6.67	6.74	7.92	8.77	11.84	10.17	9.94	12.46	2.45	4.66	3.32	3.79	1.24
MnO	0.28	0.27	0.01	0.05	0.10	0.13	0.13	<0.01	0.10	<0.01	<0.01	<0.01	0.17	0.10	0.05	0.09	0.06
MgO	2.44	2.28	0.36	2.12	2.61	1.75	3.32	0.12	4.56	0.16	0.19	0.13	1.55	1.68	1.11	1.57	0.47
CaO	9.28	7.23	0.03	2.12	2.35	1.80	1.01	0.55	1.23	0.62	0.14	0.53	4.64	2.62	1.49	2.27	3.69
Na_2O	1.77	2.13	0.39	0.46	1.33	5.24	3.60	1.90	1.10	2.19	1.14	0.98	0.62	1.45	2.24	1.42	6.97
K_2O	0.50	0.73	3.82	3.32	2.17	0.65	1.56	0.62	0.77	1.46	3.04	1.70	1.78	2.30	2.93	3.80	0.19
P_2O_5	0.12	0.15	0.08	0.16	0.24	0.23	0.27	0.19	0.28	0.31	0.02	0.25	0.05	0.09	0.12	0.08	0.04
LOI	9.32	7.95	6.61	8.87	8.44	5.73	6.44	8.58	9.38	9.42	8.33	9.82	6.28	4.14	3.28	4.35	3.22
Total	99.67	99.11	99.85	99.55	100.23	100.22	99.60	99.75	99.26	99.34	99.10	99.05	99.53	99.60	100.02	100.05	100.10
C	1.34	1.30	0.02	0.28	0.30	0.25	0.06	0.04	0.04	0.04	0.05	0.05	1.02	0.57	0.33	0.49	0.77
S	0.44	0.91	5.88	6.23	5.03	4.74	5.27	6.91	6.14	7.92	7.80	9.83	0.01	0.12	0.10	0.03	0.12
Trace elements (ppm; XRF):																	
Sc	32	32	30	27	32	30	34	28	43	33	43	26	10	12	12	13	8
V	285	294	182	137	122	111	143	186	279	244	271	127	25	59	44	22	13
Cr	15	16	4	4	4	2	3	7	18	7	28	2	3	42	27	3	1
Ni	11	11	4	3	3	1	1	5	8	5	8	2	<1	19	12	2	3
Cu	79	75	51	36	22	42	55	57	115	80	104	37	16	39	15	35	46
Zn	162	150	969	604	250	444	316	23	569	41	20	4	131	94	58	56	16
As	6	6	19	10	18	20	25	14	14	21	30	48	<3	3	<3	<3	4
Rb	9	16	83	72	43	12	32	10	17	26	59	31	48	82	123	135	6
Sr	434	464	43	63	75	130	111	417	332	450	257	178	242	148	109	128	267
Y	14	19	14	23	17	20	22	15	23	18	27	12	18	22	30	36	13
Zr	70	77	78	113	98	97	116	73	100	97	84	138	109	126	240	253	94
Nb	4	5	4	7	6	5	6	4	6	5	5	7	6	11	13	16	4
Ba	327	499	817	843	432	153	465	399	1180	991	2100	1215	2100	902	786	1289	136
La	8	10	8	17	5	24	9	5	19	8	11	12	17	22	29	25	9
Ce	18	21	21	38	21	47	26	8	21	17	23	29	32	50	62	60	21
Nd	10	12	9	16	10	19	12	4	11	7	5	12	10	20	26	23	11
Pb	8	15	183	570	124	98	19	33	51	60	29	22	7	8	13	3	3
Bi	<2	<2	8	<2	<2	<2	<2	<2	<2	<2	<2	<2	<2	<2	<2	<2	<2
Th	<1.5	3	7	7	4	3	4	2	<1.5	2	2	3	5	11	15	13	5
Trace elements (ppm; ICP-MS):																	
Cd	0.1	0.1	-	-	-	-	-	0.1	0.1	0.1	0.1	0.1	<0.1	0.1	0.1	0.3	-
Cs	0.2	0.2	-	-	-	-	-	0.7	0.4	0.6	1.0	0.7	1.2	1.8	3.6	3.0	-
Tl	0.6	0.8	-	-	-	-	-	0.6	1.0	1.4	2.7	1.6	1.9	0.6	0.7	0.9	-
Bi	0.2	0.1	-	-	-	-	-	0.3	0.2	1.0	0.4	0.5	0.1	1.2	0.3	0.2	-
Th	-	-	-	-	-	-	-	-	-	-	-	-	-	-	-	-	-
U	0.6	0.6	-	-	-	-	-	0.5	0.8	0.6	0.6	0.8	1.1	2.2	3.0	3.0	-

	WT8A-172	WT9A-86	WT9A-100	WT9A-109	WT9A-126	WT9A-144	WT9A-162	WT9A-176	WT9A-186	WT9A-198	WT9A-218	WT9A-228	WT9A-238	WT9A-254	WT9A-265	WT16-87	WT16-112
Major elements (weight %; XRF and Leco):																	
SiO_2	75.44	46.83	56.89	50.52	56.89	48.78	53.87	48.97	49.96	51.96	80.45	82.06	31.40	64.06	62.44	55.56	56.04
TiO_2	0.20	0.90	1.16	1.17	1.15	1.21	1.30	1.20	1.30	1.03	0.41	0.54	0.41	0.37	0.21	0.72	0.66
Al_2O_3	12.92	19.71	14.96	18.95	14.89	17.55	16.25	15.73	17.59	13.76	7.31	9.68	15.91	15.63	17.53	17.79	16.99
Fe_2O_3	0.88	10.82	9.91	11.91	9.47	10.26	10.11	11.71	10.30	10.73	5.15	2.29	6.55	2.95	3.87	9.26	9.56
MnO	0.04	0.13	0.17	0.22	0.18	0.18	0.17	0.18	0.24	0.13	<0.01	<0.01	0.29	0.10	0.13	0.12	0.08
MgO	0.28	1.84	3.60	4.27	3.36	2.65	3.68	4.36	2.66	3.27	0.11	0.12	13.53	2.64	1.33	3.69	2.71
CaO	1.99	9.37	5.51	2.81	6.47	11.97	7.38	7.01	6.58	6.43	0.11	0.19	3.51	4.24	4.07	6.30	4.42
Na_2O	6.98	0.78	3.23	4.89	3.46	2.72	3.34	3.85	3.59	1.41	0.32	0.58	0.77	1.06	1.86	2.80	4.98
K_2O	0.02	1.98	0.02	0.56	0.02	0.02	0.10	0.02	0.25	0.37	1.73	2.42	1.49	1.49	1.93	0.15	0.14
P_2O_5	0.03	0.15	0.28	0.32	0.29	0.22	0.33	0.29	0.32	0.28	0.09	0.14	0.06	0.06	0.19	0.11	0.14
LOI	1.78	6.95	3.89	3.98	3.61	4.02	4.31	5.98	6.25	9.67	4.06	2.70	15.58	6.53	6.13	3.51	4.87
Total	100.55	99.46	99.62	99.60	99.79	99.58	100.84	99.30	99.04	99.04	99.74	100.72	89.50	99.13	99.69	100.01	100.59
C	0.41	0.67	0.27	0.14	0.40	0.46	0.38	0.89	1.11	1.08	0.02	0.03	1.29	0.97	0.85	0.02	0.34
S	<0.01	3.26	0.24	0.30	0.05	0.02	0.17	1.09	0.46	6.44	4.16	1.84	8.47	0.05	<0.01	0.01	2.39
Trace elements (ppm; XRF):																	
Sc	4	40	28	33	27	29	29	27	33	30	8	7	15	14	5	29	29
V	11	364	207	241	234	286	228	205	274	223	46	45	169	52	7	253	257
Cr	1	18	9	3	9	9	9	7	11	8	2	4	14	3	2	16	15
Ni	2	13	5	5	5	5	6	5	6	5	3	1	49	2	<1	13	11
Cu	13	91	55	89	57	56	56	52	67	53	141	26	4400	8	3	79	76
Zn	14	151	100	216	96	76	118	242	214	240	433	8	73200	222	92	90	72
As	<3	14	10	9	4	6	11	17	4	11	32	4	1135	<3	<3	6	5
Rb	<1	48	<1	11	<1	<1	1	7	5	7	30	42	32	45	55	3	3
Sr	232	302	410	162	141	604	436	452	343	464	36	38	252	1317	457	325	288
Y	15	17	25	30	26	26	28	22	27	21	3	4	-	22	11	13	15
Zr	98	89	89	110	87	90	99	79	101	80	50	70	141	136	94	69	64
Nb	6	5	6	7	5	5	6	4	6	4	3	5	6	7	5	4	3
Ba	25	520	59	558	48	350	134	458	274	491	204	247	5600	2100	938	146	118
La	18	9	7	8	8	13	11	5	10	6	4	6	6	18	21	9	9
Ce	37	21	20	23	24	26	25	15	27	16	8	15	59	48	47	17	18
Nd	15	12	14	13	11	14	16	10	17	8	5	6	6	19	20	10	10
Pb	5	19	4	8	4	7	8	14	10	15	13	7	6600	7	14	7	9
Bi	<2	<2	3	<2	<2	<2	<2	<2	<2	<2	<2	<2	<2	<2	<2	<2	<2
Th	6	4	<1.5	3	2	2	2	2	2	<1.5	<1.5	<1.5	-	7	10	3	3
Trace elements (ppm; ICP-MS):																	
Cd	-	0.2	0.4	0.4	0.2	0.6	0.2	0.3	0.3	0.2	2.1	<0.1	211	1.4	0.4	0.2	<0.1
Cs	-	1.0	0.2	0.5	0.2	0.1	0.2	0.1	0.3	0.3	1.0	1.0	0.7	1.2	1.8	0.1	0.2
Tl	-	1.3	0.6	0.9	<0.5	<0.5	<0.5	1.4	<0.5	0.5	1.0	2.0	4.3	2.6	1.3	<0.5	<0.5
Bi	-	0.1	1.3	0.9	<0.1	<0.1	<0.1	<0.1	<0.1	<0.1	0.8	1.6	0.4	0.1	0.1	0.1	0.1
Th	-	-	-	-	2.3	-	2.3	-	-	1.7	-	1.3	-	7.1	-	-	2.2
U	-	0.8	1.0	1.7	0.8	0.7	1.0	1.2	0.6	0.5	0.4	0.3	9.4	1.0	1.5	0.5	0.5

	WT16-125	WT16-132	WT16-145	WT16-161	WT16-170	WT16-186	WT16-195	WT16-206	WT16-210	WT16-223	WT16-245	WT16-257	WT16-276	WT16-292	WT16-322	WT16-333	WT16-338
Major elements (weight %; XRF and Leco):																	
SiO_2	55.72	53.84	56.01	51.18	56.52	55.85	54.10	48.71	58.22	57.91	69.28	60.55	72.58	72.36	74.22	67.37	71.21
TiO_2	0.72	0.72	0.58	0.62	0.73	0.66	0.72	0.76	1.01	0.73	0.75	1.15	0.71	0.57	0.65	0.39	0.33
Al_2O_3	18.08	18.17	16.09	16.39	17.21	17.36	18.22	18.78	17.16	15.84	13.50	21.42	13.47	10.83	11.46	15.17	13.48
Fe_2O_3	9.87	9.51	9.50	10.82	11.13	8.24	9.15	10.40	7.01	7.65	6.79	4.84	4.52	7.06	4.87	3.60	3.58
MnO	0.02	0.09	0.11	0.12	0.01	0.10	0.11	0.13	0.09	0.11	<0.01	<0.01	<0.01	<0.01	<0.01	0.09	0.06
MgO	1.26	3.27	3.83	5.47	0.59	3.22	3.21	4.09	1.10	3.12	0.06	0.18	0.18	0.10	0.10	1.39	1.19
CaO	1.35	3.68	3.39	2.20	0.34	5.80	6.88	7.82	4.69	4.37	0.46	0.38	0.23	0.19	0.27	3.19	1.80
Na_2O	1.62	5.64	4.00	2.38	1.85	2.93	2.96	2.36	6.88	4.48	0.70	0.88	0.51	0.47	1.03	1.47	4.58
K_2O	2.71	0.16	0.31	0.81	2.34	0.41	0.49	0.58	0.02	0.13	0.32	3.28	3.27	2.62	1.66	1.93	0.72
P_2O_5	0.17	0.16	0.12	0.14	0.14	0.12	0.13	0.09	0.27	0.18	0.12	0.22	0.16	0.12	0.10	0.08	0.07
LOI	7.97	4.96	5.79	8.99	8.59	5.28	3.83	5.92	3.07	5.43	7.65	6.44	4.29	5.67	5.47	5.13	2.84
Total	99.49	100.20	99.73	99.12	99.45	99.97	99.80	99.64	99.52	99.95	99.63	99.34	99.92	99.99	99.83	99.81	99.86
C	0.12	0.38	0.47	0.28	0.02	0.60	0.18	0.68	0.44	0.77	0.03	0.04	0.03	0.05	0.04	0.67	0.36
S	6.45	1.35	2.35	5.80	8.44	0.10	0.56	0.09	0.05	0.94	5.42	3.74	3.62	5.60	3.69	0.10	<0.01
Trace elements (ppm; XRF):																	
Sc	34	31	26	32	47	29	28	30	30	27	12	32	9	11	21	11	10
V	291	281	220	278	311	290	268	255	188	215	178	187	82	74	82	53	46
Cr	14	14	26	34	64	14	17	18	2	9	2	3	5	3	4	6	5
Ni	7	9	11	12	15	11	14	14	2	6	2	2	3	3	1	2	2
Cu	33	133	114	101	45	69	118	115	78	61	26	19	32	47	31	3	4
Zn	32	84	117	356	29	109	86	94	116	112	4	9	4	4	25	71	54
As	6	<3	9	7	7	4	5	8	4	3	6	8	7	15	18	4	<3
Rb	56	3	7	17	47	9	11	12	<1	3	6	60	58	43	32	59	22
Sr	173	154	116	167	206	349	594	687	342	259	188	183	73	44	203	430	262
Y	19	17	15	15	19	14	15	14	25	17	3	17	3	5	11	13	11
Zr	75	76	54	59	72	65	71	73	98	72	95	169	89	69	88	79	63
Nb	5	5	3	3	5	4	4	4	6	5	5	10	5	4	5	6	4
Ba	622	58	102	228	384	248	170	236	31	43	268	837	562	369	923	778	196
La	9	10	6	6	8	7	7	8	12	8	12	21	5	4	10	10	10
Ce	22	23	18	18	22	18	19	18	25	19	27	48	13	15	26	31	22
Nd	12	12	11	11	11	9	10	10	17	10	12	26	4	7	9	10	10
Pb	9	8	8	15	15	8	8	7	4	12	10	8	13	9	36	11	6
Bi	<2	<2	<2	<2	<2	<2	<2	<2	<2	<2	<2	<2	<2	<2	<2	<2	<2
Th	3	4	<1.5	2	3	2	1	3	2	3	3	4	<1.5	<1.5	2	4	3
Trace elements (ppm; ICP-MS):																	
Cd	<0.1	-	<0.1	<0.1	<0.1	0.1	0.1	0.3	0.3	0.3	0.2	0.3	0.2	0.2	0.3	0.3	0.2
Cs	1.7	-	0.3	0.5	1.2	0.4	0.3	0.6	0.2	0.2	0.4	1.2	1.2	1.0	1.0	2.1	1.1
Tl	0.6	-	<0.5	<0.5	0.6	<0.5	<0.5	<0.5	<0.5	<0.5	<0.5	1.6	1.9	1.1	0.9	0.8	<0.5
Bi	0.2	-	<0.1	<0.1	0.5	<0.1	<0.1	0.2	0.1	<0.1	0.6	0.5	0.4	0.4	0.2	0.2	0.1
Th	-	2.5	1.7	-	2.2	-	-	-	-	2.1	2.6	-	1.0	1.4	2.0	4.9	-
U	0.5	0.6	0.5	0.4	0.5	0.6	0.6	0.7	0.5	0.6	0.6	1.1	0.3	0.3	0.5	0.6	0.6

	WT16-343	WT16-344	WT16-349	WT16-355	WT17-114	WT17-118	WT17-122	WT17-127	WT17-132	WT17-138	WT17-146	WT21-109	WT21-121	WT21-126	WT21-135	WT21-147	WT21-159
Major elements (weight %; XRF and Leco):																	
SiO_2	67.63	59.98	70.11	71.91	54.28	71.35	68.34	73.69	74.17	72.78	71.13	68.20	68.88	68.54	52.47	63.64	59.79
TiO_2	0.35	0.57	0.45	0.43	0.35	0.44	0.40	0.33	0.33	0.34	0.45	0.41	0.42	0.42	0.87	0.58	0.60
Al_2O_3	13.96	19.67	14.84	13.68	15.66	13.15	16.87	14.53	13.61	15.02	15.29	13.46	12.84	12.86	16.62	13.39	15.51
Fe_2O_3	3.55	3.77	3.09	3.50	11.83	5.30	3.07	2.44	3.19	3.24	3.48	4.50	4.55	4.68	9.87	6.45	7.11
MnO	0.15	0.08	0.06	0.05	0.01	0.07	0.05	0.03	0.05	0.04	0.06	0.07	0.06	0.06	0.24	0.11	0.13
MgO	1.07	1.26	1.55	1.38	0.67	3.11	3.56	1.41	1.72	1.53	1.15	2.25	2.74	2.84	5.30	3.61	4.29
CaO	3.39	2.07	1.05	1.25	0.06	0.18	0.42	2.14	1.37	0.19	1.75	2.20	1.53	1.45	6.79	2.25	2.11
Na_2O	4.38	9.04	2.09	1.63	0.78	0.73	1.32	1.09	0.93	1.08	1.89	2.62	2.07	2.76	0.60	3.70	3.43
K_2O	1.32	0.49	3.19	3.12	3.23	1.76	1.50	1.44	1.45	2.07	2.03	0.95	1.47	0.87	0.81	0.36	0.56
P_2O_5	0.07	0.17	0.09	0.12	0.07	0.10	0.07	0.06	0.06	0.09	0.09	0.12	0.12	0.12	0.24	0.13	0.12
LOI	4.03	2.91	3.08	3.02	8.99	3.23	3.74	2.68	2.80	3.11	2.79	4.77	4.81	4.67	6.69	5.25	5.80
Total	99.90	100.01	99.60	100.09	95.93	99.42	99.34	99.84	99.68	99.49	100.11	99.55	99.49	99.27	100.50	99.47	99.45
C	0.71	0.35	0.22	0.28	0.04	0.03	0.04	0.03	0.02	0.04	0.06	0.45	0.27	0.25	0.75	0.27	0.09
S	0.02	0.12	0.02	<0.01	9.89	0.07	<0.01	<0.01	<0.01	0.01	0.01	2.73	2.77	2.76	0.97	3.51	3.80
Trace elements (ppm; XRF):																	
Sc	11	16	11	12	14	16	12	10	9	11	10	15	13	14	22	19	27
V	47	35	49	37	102	72	28	27	29	29	45	31	32	30	247	101	203
Cr	5	2	45	33	5	8	3	3	4	3	10	2	2	2	3	4	4
Ni	2	5	12	13	89	8	4	<1	1	1	4	<1	<1	<1	6	1	3
Cu	7	55	21	18	1500	690	8	7	4	9	19	6	9	35	80	16	48
Zn	97	123	71	73	11200	923	795	197	361	305	672	131	83	202	314	162	414
As	<3	<3	3	<3	364	15	4	9	7	6	4	8	5	5	22	18	20
Rb	47	17	123	121	77	47	43	46	46	67	69	19	30	18	17	7	11
Sr	352	632	116	84	220	107	315	356	406	238	582	287	163	212	333	115	248
Y	12	22	33	34	-	18	31	22	19	21	25	18	16	15	19	22	18
Zr	69	124	176	246	149	109	151	146	124	137	176	119	121	120	89	109	97
Nb	4	7	15	14	7	7	8	7	7	8	10	7	7	7	5	6	6
Ba	309	168	626	752	11900	5500	2800	1702	794	668	506	392	684	475	190	86	164
La	11	2	36	27	6	33	20	14	15	14	30	10	14	8	17	13	12
Ce	27	16	74	64	55	82	49	27	32	34	59	22	31	24	33	26	25
Nd	12	8	29	27	<2	25	20	11	15	15	24	11	12	13	17	13	12
Pb	6	10	5	3	4900	304	12	14	11	8	15	7	11	13	10	15	30
Bi	<2	<2	<2	<2	<2	<2	<2	<2	<2	<2	<2	<2	<2	<2	<2	<2	<2
Th	4	6	17	16	-	5	6	7	6	8	11	6	5	5	9	6	4
Trace elements (ppm; ICP-MS):																	
Cd	0.4	-	0.3	0.4	28.3	0.6	0.7	0.5	0.5	0.3	0.4	0.3	0.3	0.3	0.3	0.3	0.7
Cs	1.5	-	4.7	4.1	1.9	1.2	1.4	1.3	1.6	2.4	1.7	0.7	1.2	0.7	0.7	0.3	2.3
Tl	<0.5	-	0.6	0.5	50.4	4.7	2.9	2.4	1.6	1.9	1.6	0.5	1.0	<0.5	<0.5	<0.5	<0.5
Bi	0.2	-	0.4	0.1	0.7	1.2	<0.1	0.2	0.4	0.1	0.3	0.1	0.4	0.1	0.3	0.7	<0.1
Th	3.9	-	-	-	-	-	-	-	-	-	-	-	-	-	-	-	-
U	0.7	-	3.7	3.9	19.7	2.5	0.9	1.5	1.1	1.4	1.8	1.4	1.2	1.6	1.8	1.9	1.0

	WT21-172	WT21-185	WT21-199	WT21-212	WT21-223	WT21-237	WT21-249	WT21-261	WT21-277	WT21-298	WT21-306	WT21-311	WT21-314	WT21-319	WT21-324	WT21-328	WT21-335
Major elements (weight %; XRF and Leco):																	
SiO_2	60.26	63.73	52.99	56.10	61.66	73.96	72.10	71.34	75.31	57.01	23.63	61.16	57.60	60.76	59.42	54.07	65.54
TiO_2	0.52	0.51	1.01	0.68	0.56	0.56	0.35	0.45	0.43	0.61	0.40	0.68	1.07	0.43	0.42	0.16	0.42
Al_2O_3	14.13	13.00	18.55	13.68	13.65	14.48	9.66	11.69	11.19	16.01	10.64	18.37	22.07	18.35	18.12	5.69	16.64
Fe_2O_3	8.46	6.07	8.83	8.94	6.28	2.41	5.51	6.13	4.41	7.02	27.39	4.73	4.38	4.84	4.78	34.98	3.63
MnO	0.11	0.15	0.13	0.18	0.20	0.01	0.07	0.01	0.01	0.09	0.03	0.02	0.05	0.19	0.27	0.09	0.07
MgO	2.61	3.06	3.22	2.96	3.35	0.78	1.18	0.65	0.77	3.52	0.96	1.68	2.90	2.75	2.93	1.33	2.60
CaO	2.23	2.64	1.86	3.65	2.85	0.16	1.96	0.17	0.13	3.07	1.21	1.44	0.84	2.25	2.89	0.56	1.96
Na_2O	4.06	2.96	1.80	2.43	1.34	0.64	0.25	0.20	0.28	0.79	0.67	2.88	2.55	1.92	1.09	0.49	0.55
K_2O	0.56	0.94	2.85	1.35	1.80	3.73	2.54	3.50	3.08	2.96	2.03	2.21	2.65	2.70	2.95	0.73	3.22
P_2O_5	0.11	0.11	0.30	0.19	0.15	0.13	0.09	0.09	0.11	0.12	0.04	0.13	0.25	0.07	0.07	0.07	0.07
LOI	6.83	6.13	7.84	8.95	7.72	3.48	5.45	5.05	3.99	7.89	20.21	5.71	4.62	5.30	6.59	2.08	4.84
Total	99.88	99.30	99.38	99.11	99.56	100.34	99.16	99.28	99.71	99.09	87.21	99.01	98.98	99.56	99.53	100.25	99.54
C	0.29	0.47	0.24	0.62	0.55	0.03	0.39	0.02	0.02	0.58	0.17	0.19	0.10	0.50	0.86	0.13	0.44
S	5.77	3.58	6.11	6.58	4.38	1.88	4.41	4.96	3.50	5.50	25.15	3.31	0.96	<0.01	<0.01	<0.01	<0.01
Trace elements (ppm; XRF):																	
Sc	29	23	43	32	25	12	16	18	15	27	30	29	29	17	15	5	12
V	185	151	194	153	144	75	81	96	63	131	114	159	58	38	43	40	32
Cr	4	15	4	3	7	4	3	3	2	4	6	4	5	5	4	6	4
Ni	3	3	2	2	3	<1	<1	1	3	1	6	3	2	2	3	1	2
Cu	31	17	24	40	88	11	194	139	108	72	6800	68	19	4	5	11	2
Zn	198	211	206	170	595	34	1517	2100	880	1015	60400	194	253	188	119	189	147
As	10	9	87	35	50	11	24	45	56	48	1696	122	7	6	4	11	<3
Rb	12	21	65	30	39	77	58	84	71	67	56	51	65	83	92	23	98
Sr	207	101	120	85	81	44	37	24	22	129	301	380	370	197	183	28	146
Y	16	15	28	20	15	12	11	13	13	21	-	18	29	26	24	10	22
Zr	86	91	132	92	85	111	71	87	92	126	89	139	192	178	175	64	171
Nb	4	5	7	5	5	7	5	5	5	7	3	9	20	10	10	3	9
Ba	118	164	841	214	306	2400	680	1077	1140	1967	8600	4800	3300	2100	1936	816	1568
La	13	8	13	10	2	5	8	7	6	11	6	14	14	22	14	7	17
Ce	26	17	32	20	13	19	14	18	19	31	82	43	42	49	35	19	33
Nd	15	9	18	13	6	3	6	6	8	12	9	11	15	21	13	4	11
Pb	50	20	21	57	80	7	11	242	95	143	6600	97	21	8	11	23	8
Bi	<2	<2	<2	<2	<2	<2	<2	<2	3	<2	-	<2	<2	<2	<2	3	<2
Th	4	5	3	2	3	3	3	4	3	5	-	5	8	8	8	4	9
Trace elements (ppm; ICP-MS):																	
Cd	0.3	0.3	0.3	0.2	1.3	0.1	4.1	4.8	2.4	2.5	151	0.3	-	-	0.2	<0.1	0.3
Cs	0.4	0.6	1.3	0.4	0.5	1.0	0.9	1.0	0.9	0.8	0.8	0.6	-	-	2.2	0.5	1.9
Tl	<0.5	<0.5	1.3	1.0	1.0	1.2	1.0	2.1	5.8	6.0	9.8	8.1	-	-	5.2	1.1	2.5
Bi	0.3	0.2	<0.1	0.2	0.2	0.4	0.4	0.4	1.8	0.3	907	0.3	-	-	1.3	1.1	0.5
Th	-	-	-	-	-	-	-	-	-	-	-	-	-	-	-	-	-
U	1.0	1.0	1.4	0.9	0.7	0.8	0.7	0.8	3.3	1.4	1.5	4.8	-	-	0.3	0.4	1.1

	WT22-100	WT22-109	WT22-122	WT22-132	WT22-148	WT22-163	WT22-176	WT22-190	WT22-208	WT22-222	WT22-237	WT22-244	WT22-256	WT22-264	WT22-277	WT22-286	WT22-295
Major elements (weight %; XRF and Leco):																	
SiO_2	59.03	61.55	51.61	55.34	55.07	50.49	49.75	58.58	59.43	61.60	59.94	68.67	55.43	64.81	70.25	37.00	55.77
TiO_2	0.85	0.69	1.14	1.00	1.08	1.09	1.41	1.31	0.71	0.53	0.57	0.45	0.67	0.50	0.49	1.02	0.69
Al_2O_3	15.23	12.31	15.89	14.85	15.97	14.35	16.25	16.42	14.88	14.86	15.54	12.11	17.25	13.70	13.14	24.57	17.09
Fe_2O_3	7.55	5.93	11.08	9.27	9.89	12.92	11.89	7.31	8.79	6.60	7.91	7.86	8.68	8.48	6.50	15.26	6.11
MnO	0.15	0.16	0.16	0.09	0.04	0.17	0.15	0.05	0.11	0.10	0.10	0.01	0.08	0.03	<0.01	0.01	0.04
MgO	2.04	1.19	4.14	1.83	0.88	5.50	4.88	0.74	4.32	4.05	4.38	0.67	2.33	0.98	0.17	0.79	1.55
CaO	7.07	6.41	1.75	2.92	2.40	1.55	1.39	1.83	0.39	1.14	0.19	0.09	0.49	0.16	0.11	0.32	2.71
Na_2O	2.68	2.74	2.78	3.86	5.07	2.74	2.93	3.85	1.23	1.40	0.51	0.36	0.39	0.30	0.50	1.04	1.13
K_2O	0.26	1.08	1.86	1.70	1.37	0.77	1.15	2.07	1.39	2.19	3.05	3.16	4.42	3.78	3.30	5.98	3.31
P_2O_5	0.25	0.21	0.27	0.25	0.27	0.27	0.36	0.25	0.16	0.13	0.10	0.06	0.11	0.12	0.08	0.03	0.11
LOI	4.89	7.33	8.75	8.00	7.03	9.21	9.19	6.79	8.08	6.51	7.27	6.44	9.19	7.02	5.38	13.07	7.54
Total	100.00	99.60	99.43	99.11	99.07	99.06	99.35	99.20	99.49	99.11	99.56	99.88	99.04	99.88	99.92	99.09	96.05
C	0.52	1.00	0.08	0.31	0.18	0.20	0.12	0.20	0.03	0.20	0.03	0.02	0.06	0.02	0.02	0.04	0.85
S	1.27	3.49	7.47	6.88	7.65	7.87	7.61	5.67	6.02	4.65	5.54	6.13	6.33	6.73	5.14	11.68	4.72
Trace elements (ppm; XRF):																	
Sc	26	20	36	33	35	37	42	41	32	24	32	27	37	29	20	37	22
V	119	93	240	196	234	230	288	288	222	110	205	165	232	192	139	144	86
Cr	3	2	8	6	7	7	10	10	18	5	4	4	4	3	30	3	1
Ni	2	<1	4	4	3	5	4	5	6	1	2	3	4	4	8	3	3
Cu	37	27	56	32	73	43	286	27	67	24	41	173	53	188	49	418	22
Zn	133	205	313	420	2200	470	317	54	576	753	347	474	441	1485	70	1900	265
As	26	18	67	30	66	30	24	46	32	15	22	48	27	22	40	377	53
Rb	5	23	40	38	29	16	25	45	29	47	69	70	106	90	61	133	78
Sr	292	166	86	98	178	106	128	138	158	75	46	34	47	32	43	234	961
Y	24	21	26	27	26	23	27	39	19	17	17	13	21	16	7	18	16
Zr	107	89	96	86	91	93	114	103	77	117	97	66	114	78	71	223	148
Nb	7	5	5	5	5	5	7	6	5	8	5	4	6	4	4	12	9
Ba	124	463	699	551	661	377	290	563	701	521	820	520	834	631	672	10400	18400
La	11	9	8	9	12	15	11	16	7	9	9	7	12	8	5	13	-
Ce	24	21	21	15	31	30	27	36	16	23	22	22	28	22	17	53	-
Nd	16	14	11	11	18	19	14	20	8	10	10	8	14	9	9	4	-
Pb	12	17	75	171	95	23	21	74	186	145	149	142	95	28	25	846	71
Bi	<2	<2	<2	<2	<2	<2	<2	<2	<2	<2	<2	<2	<2	<2	<2	<2	<2
Th	3	<1.5	2	2	2	2	3	2	2	6	4	3	5	4	<1.5	6	<1.5
Trace elements (ppm; ICP-MS):																	
Cd	0.3	0.2	0.1	0.7	4.6	0.2	0.1	<0.1	1.0	1.3	0.3	-	1.2	-	0.2	5.0	0.7
Cs	0.1	0.5	0.7	0.6	0.3	0.3	0.4	0.5	0.5	0.6	0.8	-	1.1	-	0.7	1.7	0.9
Tl	<0.5	1.8	2.1	1.9	1.9	0.6	0.6	1.7	1.2	1.4	1.1	-	1.7	-	3.3	45.8	16.5
Bi	0.3	0.2	0.3	0.2	0.2	0.3	0.2	0.1	0.1	0.1	0.1	-	0.3	-	1.3	0.3	0.2
Th	-	2.3	2.3	-	-	2.4	-	2.2	2.3	5.3	3.6	-	4.4	-	1.8	-	-
U	0.8	0.7	0.6	0.5	0.4	0.5	0.7	1.0	0.5	1.1	0.7	-	0.9	-	0.4	2.8	4.8

	WT22-302	WT22-307	WT22-314	WT22-322	WT22-328	WT22-329	WT22-332	WT23-114	WT23-140	WT23-152	WT23-168	WT23-182	WT23-198	WT23-208	WT23-227	WT23-242	WT23-256
Major elements (weight %; XRF and Leco):																	
SiO_2	64.69	68.66	64.04	64.81	63.51	55.86	65.37	57.47	55.84	49.56	47.12	46.98	46.62	74.99	45.96	49.63	48.32
TiO_2	0.61	0.52	0.54	0.63	0.68	0.69	0.67	0.76	0.84	1.03	0.66	0.75	0.72	0.46	0.65	0.73	0.88
Al_2O_3	16.40	13.03	14.59	14.76	17.35	23.42	16.51	14.98	16.99	15.71	20.96	17.90	17.50	10.31	17.18	16.05	18.06
Fe_2O_3	4.72	3.84	6.14	6.30	6.34	5.05	5.18	9.31	9.56	13.73	10.29	13.22	13.00	3.84	10.31	11.92	12.49
MnO	0.07	0.02	0.10	0.08	0.06	0.06	0.07	0.11	0.11	0.12	0.09	0.12	0.12	0.04	0.14	0.15	0.18
MgO	1.67	0.28	1.45	1.40	1.56	1.56	2.59	3.65	3.12	5.86	4.62	6.50	6.82	2.07	2.46	4.90	4.96
CaO	2.08	2.67	3.26	2.43	0.95	0.74	0.86	5.75	7.03	7.62	8.05	7.14	7.62	1.71	18.68	8.90	5.23
Na_2O	5.33	5.48	4.80	5.95	3.44	1.81	1.18	4.54	3.60	2.87	4.02	3.05	1.96	1.96	0.05	1.87	4.28
K_2O	0.94	0.68	0.62	0.35	2.36	5.22	3.23	0.15	0.29	0.04	0.32	0.08	0.52	1.94	0.02	0.02	0.30
P_2O_5	0.15	0.15	0.13	0.16	0.17	0.13	0.15	0.14	0.15	0.22	0.10	0.13	0.07	0.12	0.08	0.13	0.14
LOI	3.34	4.47	4.02	3.13	3.40	5.00	3.84	2.87	2.54	3.38	3.71	4.20	4.82	2.32	4.44	5.40	4.91
Total	100.00	99.80	99.69	100.00	99.82	99.54	99.65	99.73	100.07	100.14	99.94	100.07	99.77	99.76	99.97	99.70	99.75
C	0.38	0.46	0.64	0.45	0.17	0.47	0.28	0.21	0.06	0.06	0.12	0.18	0.26	0.22	0.60	0.54	0.43
S	0.01	2.74	<0.01	<0.01	0.30	0.01	0.06	0.07	0.02	0.02	0.02	0.01	0.02	0.01	0.01	0.02	0.01
Trace elements (ppm; XRF):																	
Sc	21	18	19	21	24	21	15	37	32	44	28	39	38	9	38	45	48
V	85	47	73	64	66	87	84	304	335	311	258	325	323	85	419	344	404
Cr	3	4	4	3	3	9	77	4	5	3	12	14	15	56	11	14	16
Ni	2	2	1	2	3	9	30	5	5	4	8	5	4	20	7	6	8
Cu	22	15	2	3	65	12	14	331	149	191	113	77	99	22	45	116	101
Zn	218	186	188	109	103	101	188	75	89	102	87	96	82	47	44	80	92
As	8	10	4	5	7	4	<3	8	7	5	11	<3	5	9	20	<3	<3
Rb	26	17	19	12	79	179	115	2	4	<1	8	1	12	50	<1	<1	9
Sr	241	207	221	194	144	184	81	277	613	134	461	468	485	112	729	267	240
Y	27	20	18	22	25	23	35	13	13	20	9	11	10	23	9	10	11
Zr	128	110	119	127	142	190	213	45	52	70	37	39	37	151	31	37	45
Nb	8	6	7	8	8	11	17	3	3	4	2	2	2	11	2	2	3
Ba	1085	380	349	113	824	1903	856	122	234	13	132	62	224	537	10	34	113
La	24	14	19	18	16	17	36	6	11	12	6	6	7	26	6	9	8
Ce	48	32	39	36	43	44	80	20	23	33	14	14	16	59	13	20	19
Nd	20	16	19	18	20	19	34	9	11	14	7	3	5	26	7	9	7
Pb	9	29	11	8	7	5	5	3	3	4	4	2	5	20	7	4	3
Bi	<2	<2	<2	<2	<2	<2	<2	<2	<2	<2	<2	<2	<2	<2	<2	<2	<2
Th	5	4	6	7	6	9	20	3	3	5	2	2	3	13	<1.5	2	2
Trace elements (ppm; ICP-MS):																	
Cd	0.1	1.2	0.2	0.2	-	0.2	0.3	0.4	0.2	-	0.2	-	0.2	0.3	0.2	-	-
Cs	0.8	0.3	0.4	0.3	-	4.4	2.8	0.1	0.1	-	0.2	-	0.3	1.2	<0.05	-	-
Tl	2.3	0.8	0.6	<0.5	-	2.8	1.4	<0.5	<0.5	-	<0.5	-	<0.5	<0.5	<0.5	-	-
Bi	0.2	0.6	0.2	0.2	-	0.1	0.2	0.1	0.1	-	<0.1	-	0.1	0.3	0.1	-	-
Th	-	5.4	-	-	-	10.9	21.1	-	-	-	-	-	-	-	-	-	-
U	1.3	5.0	0.4	0.2	-	0.7	3.7	0.7	0.7	-	0.7	-	0.6	2.2	0.4	0.4	-

	WT23-261	WT23-282	WT23-295	WT23-322	WT23-343	WT23-368	WT23-391	WT23-399	WT23-406	WT23-411	WT23-416	WT23-422	WT23-430	WT23-436	WT23-443	WT23-450	WT23-455
Major elements (weight %; XRF and Leco):																	
SiO_2	67.24	49.88	50.03	71.38	70.77	72.53	71.40	64.67	67.35	64.17	62.86	56.92	62.28	67.23	64.38	63.69	67.69
TiO_2	0.33	0.76	0.77	0.52	0.50	0.38	0.31	0.20	0.34	0.40	0.60	0.79	0.69	0.59	0.65	0.65	0.69
Al_2O_3	13.74	16.23	16.43	13.12	12.75	12.90	12.47	16.62	14.41	16.32	15.34	18.47	17.05	14.00	16.31	16.21	15.70
Fe_2O_3	2.94	11.52	12.20	3.71	4.66	2.81	3.14	3.80	3.15	3.26	6.39	8.93	6.48	6.46	3.77	4.73	3.71
MnO	0.04	0.17	0.20	0.07	0.08	0.05	0.07	0.14	0.08	0.30	0.09	0.06	0.04	0.04	0.05	0.04	0.04
MgO	1.12	3.89	4.32	1.67	1.78	1.64	1.00	1.29	2.31	3.10	1.30	2.88	2.08	0.95	1.04	1.26	1.39
CaO	6.20	9.49	6.69	2.14	2.81	1.66	3.87	4.89	3.91	3.11	3.33	2.02	2.59	2.69	3.39	3.42	1.96
Na_2O	0.33	2.53	3.43	2.07	3.33	1.25	3.16	2.77	1.48	1.23	5.86	6.10	4.54	5.37	6.68	6.70	5.14
K_2O	3.23	0.09	0.20	2.54	0.89	3.16	0.98	1.23	1.27	1.82	0.56	0.83	1.49	0.23	0.16	0.13	0.37
P_2O_5	0.07	0.14	0.11	0.09	0.08	0.12	0.06	0.17	0.06	0.07	0.12	0.09	0.10	0.15	0.20	0.17	0.17
LOI	4.33	5.03	5.54	2.47	2.01	3.12	3.24	3.59	4.73	5.89	3.58	2.79	2.87	2.05	3.49	3.14	3.36
Total	99.57	99.73	99.92	99.78	99.66	99.62	99.70	99.37	99.09	99.67	100.03	99.88	100.21	99.76	100.12	100.14	100.22
C	0.69	0.59	0.63	0.19	0.10	0.35	0.51	0.48	0.78	0.71	0.60	0.21	0.21	0.28	0.58	0.48	0.37
S	0.01	0.02	0.02	0.02	0.01	<0.01	0.02	<0.01	<0.01	<0.01	0.01	<0.01	0.01	<0.01	0.01	0.01	0.21
Trace elements (ppm; XRF):																	
Sc	8	37	40	10	11	11	8	4	10	14	20	27	24	20	21	22	23
V	38	360	363	35	45	35	40	7	28	28	90	102	90	86	83	71	102
Cr	9	15	14	4	4	30	4	2	3	3	4	4	4	3	2	3	2
Ni	2	7	6	2	2	10	1	<1	1	2	3	4	3	1	2	2	2
Cu	7	101	120	28	30	13	3	3	4	7	14	4	5	3	2	3	15
Zn	22	83	88	53	59	54	31	49	63	110	132	178	102	49	45	61	78
As	<3	7	4	4	4	7	4	6	4	4	5	5	10	10	<3	7	3
Rb	102	2	7	96	31	123	35	39	41	56	17	24	44	6	4	3	8
Sr	387	439	363	218	356	84	541	523	261	270	290	446	411	292	263	323	336
Y	20	11	12	33	30	29	12	11	19	22	17	21	25	22	26	26	24
Zr	198	39	36	226	187	242	61	87	137	147	123	158	142	128	136	135	141
Nb	11	3	2	15	14	12	4	6	7	7	8	9	8	8	8	8	8
Ba	690	59	100	1255	399	1076	1073	567	480	1220	246	292	461	69	88	79	339
La	25	9	8	25	23	23	9	23	15	18	20	21	17	15	15	17	15
Ce	58	20	17	56	46	56	23	46	35	40	44	42	43	36	38	44	36
Nd	25	7	8	22	22	22	9	21	15	17	23	21	21	18	19	21	19
Pb	11	3	4	22	17	29	6	16	7	8	14	16	10	8	7	5	7
Bi	<2	<2	<2	<2	<2	<2	<2	2	<2	<2	<2	<2	<2	<2	<2	<2	<2
Th	17	2	2	11	9	15	3	9	8	6	6	8	5	5	6	7	6
Trace elements (ppm; ICP-MS):																	
Cd	0.3	-	0.2	0.6	0.3	0.4	0.2	0.2	0.3	0.4	0.3	0.3	0.3	0.2	0.3	0.3	0.3
Cs	2.6	-	1.2	3.2	1.1	4.6	0.9	1.0	3.3	2.9	0.8	1.4	1.6	0.6	0.6	0.3	0.6
Tl	<0.5	-	<0.5	<0.5	<0.5	<0.5	<0.5	<0.5	0.9	1.4	0.7	0.8	1.3	<0.5	<0.5	<0.5	<0.5
Bi	0.3	-	<0.1	0.3	0.3	0.3	0.1	0.2	0.5	0.5	0.5	0.5	0.4	0.3	0.3	0.3	0.3
Th	-	-	-	-	-	-	-	-	-	-	-	-	-	-	-	6.9	-
U	2.8	0.5	0.5	2.7	2.4	3.0	0.6	1.3	1.3	1.0	0.3	0.5	0.8	0.5	1.8	0.5	2.6

	WT23-460	WT23-477	WT23-488	WT23-505	WT24-115	WT24-137	WT24-155	WT24-167	WT24-182	WT24-196	WT24-219	WT24-231	WT24-239	WT24-266	WT24-290	WT24-300	WT24-318
Major elements (weight %; XRF and Leco):																	
SiO_2	57.70	61.61	68.36	54.15	70.86	68.07	52.26	52.45	47.21	63.08	50.25	59.74	58.38	76.05	69.67	68.43	50.39
TiO_2	0.52	0.90	0.68	0.56	0.37	0.37	0.92	0.88	0.62	0.44	0.85	1.08	1.11	0.32	0.53	0.32	0.81
Al_2O_3	14.00	15.38	12.34	12.80	13.88	16.09	16.29	16.20	20.19	13.09	18.51	15.12	16.00	11.36	13.60	15.19	18.25
Fe_2O_3	12.09	7.45	8.18	15.81	4.23	3.64	12.17	13.22	10.19	3.66	11.89	8.87	10.18	2.18	4.59	4.23	10.19
MnO	0.05	0.02	<0.01	0.07	0.06	0.06	0.14	0.15	0.09	0.04	0.18	0.14	0.15	0.02	0.05	0.05	0.15
MgO	2.87	0.66	0.14	2.08	1.50	1.14	5.02	5.36	4.91	1.70	5.31	2.22	3.03	1.63	2.12	2.21	4.63
CaO	0.75	1.06	0.12	0.13	0.96	0.92	5.21	4.07	7.00	6.29	3.22	3.55	2.27	1.68	3.14	0.90	7.15
Na_2O	1.30	0.52	0.39	0.27	3.96	8.25	4.88	4.32	4.45	0.17	4.94	5.71	5.77	0.68	1.30	6.49	3.10
K_2O	0.96	3.56	3.30	3.18	1.74	0.05	0.07	0.07	0.37	3.88	0.49	0.14	0.04	2.80	1.88	0.11	0.18
P_2O_5	0.05	0.26	0.12	0.11	0.08	0.08	0.20	0.15	0.12	0.06	0.12	0.33	0.32	0.05	0.11	0.04	0.14
LOI	8.86	8.06	6.16	10.78	2.26	1.46	2.99	3.18	4.95	6.94	4.17	3.26	2.96	3.18	3.30	1.91	4.94
Total	99.15	99.48	99.79	99.94	99.90	100.13	100.15	100.05	100.10	99.35	99.93	100.16	100.21	99.95	100.29	99.88	99.93
C	0.06	0.04	0.04	0.04	0.20	0.16	0.15	0.06	0.44	1.32	0.20	0.37	0.15	0.61	0.30	0.09	0.47
S	9.09	6.08	6.18	11.71	<0.01	<0.01	0.03	0.02	0.03	0.25	0.03	0.01	0.12	0.03	0.01	0.02	0.01
Trace elements (ppm; XRF):																	
Sc	29	32	22	31	12	12	45	42	30	13	43	30	30	9	11	9	31
V	162	119	168	239	9	8	351	319	271	58	394	171	162	10	59	30	296
Cr	5	1	5	10	2	1	4	5	11	8	16	2	2	2	4	2	17
Ni	11	2	2	3	<1	1	5	4	8	4	7	2	2	1	2	4	14
Cu	361	60	31	172	21	3	146	124	109	32	88	95	106	18	24	61	75
Zn	228	703	5	112	69	65	91	105	82	30	100	93	111	36	53	52	75
As	37	27	16	30	<3	4	11	9	1	15	11	5	15	<3	<3	<3	<3
Rb	22	75	60	67	47	<1	<1	<1	8	88	8	3	<1	98	64	3	6
Sr	418	241	26	29	272	140	206	253	616	96	223	122	108	66	298	376	1028
Y	16	25	13	14	24	22	17	15	10	27	14	24	25	31	26	16	12
Zr	106	118	86	78	129	135	63	57	36	230	42	101	103	210	162	153	39
Nb	6	7	5	4	9	9	4	4	2	14	3	9	10	14	12	6	3
Ba	1069	854	281	455	469	26	57	55	146	633	193	57	43	744	664	64	85
La	23	11	9	13	22	20	8	7	6	25	9	22	25	23	20	10	9
Ce	49	27	21	23	43	41	23	17	15	55	17	47	49	54	45	28	20
Nd	21	16	14	12	20	20	10	9	6	24	10	21	25	23	20	12	9
Pb	258	115	11	23	4	3	3	<1.5	4	11	2	6	3	6	12	4	4
Bi	<2	<2	4	5	<2	<2	<2	<2	<2	<2	<2	<2	<2	<2	<2	<2	<2
Th	5	3	2	3	8	9	5	5	2	14	3	6	7	10	7	9	2
Trace elements (ppm; ICP-MS):																	
Cd	0.6	3.1	0.2	0.2	0.3	0.2	-	0.2	-	0.5	0.3	-	0.3	0.3	0.4	-	0.2
Cs	0.7	2.2	1.4	1.4	1.3	<0.05	-	0.1	-	2.9	0.4	-	0.2	6.1	5.2	-	0.7
Tl	1.2	1.7	0.7	0.6	<0.5	<0.5	-	<0.5	-	0.5	<0.5	-	<0.5	0.6	<0.5	-	<0.5
Bi	1.1	0.4	3.2	5.6	0.5	0.2	-	0.2	-	0.4	0.2	-	0.2	2.1	0.6	-	0.3
Th	-	2.8	2.2	-	-	-	-	-	-	-	-	-	-	-	-	-	-
U	7.7	0.8	0.6	0.7	1.7	1.6	-	1.0	-	3.6	0.7	-	1.7	2.8	2.5	-	0.7

	WT24-327	WT24-351	WT24-356	WT24-370	WT24-383	WT24-393	WT24-396	WT24-405	WT24-415	WT24-433	WT24-441	WT24-456	WT24-470	WT24-488	WT24-497	WT24-516	WT24-534
Major elements (weight %; XRF and Leco):																	
SiO_2	64.81	74.58	64.52	66.04	67.46	63.81	71.17	64.67	62.64	67.36	67.72	61.31	65.56	61.46	69.99	63.46	62.01
TiO_2	0.61	0.37	0.20	0.65	0.63	0.20	0.38	0.63	0.72	0.62	0.62	0.88	0.64	0.66	0.52	0.63	0.89
Al_2O_3	15.55	11.14	16.63	14.86	14.20	16.70	14.26	15.38	15.84	14.55	14.63	17.50	15.04	17.90	12.72	15.53	15.80
Fe_2O_3	5.76	2.57	3.74	5.16	5.64	3.84	3.51	5.59	7.08	5.93	4.63	6.51	5.34	3.13	3.08	3.72	7.99
MnO	0.06	0.06	0.18	0.05	0.04	0.14	0.06	0.05	0.07	0.05	0.06	0.05	0.05	0.03	0.05	0.05	<0.01
MgO	2.84	1.45	1.07	1.26	1.28	1.21	2.10	1.34	2.18	1.77	1.37	2.67	2.56	0.96	0.85	1.35	0.25
CaO	1.95	2.29	4.56	3.13	2.39	4.46	0.88	2.94	2.64	1.71	5.43	2.34	2.06	6.62	3.94	4.18	0.28
Na_2O	1.00	1.30	3.70	6.49	5.17	3.61	0.50	6.78	6.01	4.66	4.19	4.43	4.56	2.68	4.77	1.67	0.87
K_2O	3.13	2.48	1.63	0.04	0.59	1.82	3.26	0.27	0.19	0.46	0.16	1.32	0.72	0.76	0.33	1.72	3.87
P_2O_5	0.12	0.12	0.18	0.15	0.16	0.19	0.09	0.16	0.18	0.18	0.15	0.20	0.15	0.17	0.18	0.16	0.20
LOI	4.19	3.38	3.28	1.83	2.52	4.01	3.54	2.68	2.52	2.39	1.55	2.94	2.65	4.71	3.60	6.65	7.25
Total	100.02	99.74	99.69	99.66	100.08	99.99	99.75	100.49	100.07	99.68	100.51	100.15	99.33	99.08	100.03	99.12	99.41
C	0.40	0.47	0.44	0.24	0.27	0.57	0.18	0.37	0.20	0.14	0.07	0.10	0.17	0.48	0.48	0.72	0.02
S	0.08	0.07	<0.01	<0.01	<0.01	<0.01	<0.01	<0.01	<0.01	0.13	<0.01	<0.01	<0.01	1.20	0.72	2.51	5.15
Trace elements (ppm; XRF):																	
Sc	15	9	5	21	21	4	11	22	22	22	18	28	20	20	18	23	36
V	89	29	8	81	70	8	38	82	76	142	69	116	83	65	69	83	206
Cr	76	28	2	3	3	1	27	2	3	2	2	2	3	2	2	2	4
Ni	32	11	<1	2	3	<1	12	2	2	1	2	3	2	<1	3	1	4
Cu	19	3	4	3	2	3	4	3	2	8	3	3	3	12	31	10	20
Zn	95	45	54	63	78	56	81	61	107	126	52	92	141	77	62	69	15
As	20	<3	4	12	5	3	<3	5	7	<3	13	5	6	12	8	13	16
Rb	117	97	58	2	17	63	116	9	6	12	4	35	18	16	8	36	73
Sr	103	76	463	384	255	386	70	243	197	180	476	235	208	324	171	429	65
Y	31	27	11	26	21	12	31	21	29	22	26	30	27	30	28	24	25
Zr	155	222	87	137	132	87	184	133	145	133	124	186	134	135	110	132	108
Nb	15	11	5	8	8	5	12	8	8	8	8	10	8	8	6	8	6
Ba	659	672	607	42	324	564	942	64	74	319	52	340	185	142	70	1128	422
La	31	27	18	18	16	23	34	17	20	20	15	16	16	25	17	14	14
Ce	66	63	42	37	38	45	71	41	41	36	34	38	36	46	39	34	35
Nd	30	26	20	18	18	21	27	18	21	17	19	18	19	22	22	16	18
Pb	24	3	10	9	6	9	6	7	6	8	10	7	5	11	32	11	23
Bi	<2	<2	<2	<2	<2	<2	<2	<2	<2	<2	<2	<2	<2	<2	<2	<2	<2
Th	17	14	9	8	6	10	17	6	7	7	6	9	7	8	5	6	4
Trace elements (ppm; ICP-MS):																	
Cd	0.3	0.3	0.2	0.2	-	0.2	0.3	-	0.2	-	0.2	-	0.2	0.6	0.3	0.3	0.2
Cs	4.4	4.9	1.9	0.1	-	3.4	6.2	-	0.3	-	0.1	-	0.6	0.6	0.3	0.6	1.7
Tl	0.7	0.6	<0.5	<0.5	-	0.5	1.0	-	<0.5	-	<0.5	-	<0.5	<0.5	<0.5	1.5	0.9
Bi	0.7	0.3	0.3	0.3	-	0.2	0.2	-	0.2	-	0.2	-	0.2	0.2	0.3	0.2	0.4
Th	-	-	-	-	-	-	-	-	-	-	-	-	-	-	-	-	-
U	3.6	3.4	1.8	0.7	-	1.8	3.3	-	1.1	-	1.5	-	2.2	7.5	4.2	1.4	1.4

	WT25-97	WT25-110	WT25-126	WT25-139	WT25-162	WT25-174	WT25-198	WT25-228	WT25-242	WT25-265	WT25-280	WT25-296	WT25-318	WT25-328	WT25-339	WT25-357	WT25-372
Major elements (weight %; XRF and Leco):																	
SiO_2	48.58	63.87	66.81	63.19	70.63	62.85	57.19	51.14	52.71	46.70	50.91	54.21	70.65	72.03	59.04	73.26	55.64
TiO_2	0.94	0.54	0.66	0.65	0.36	0.31	0.83	0.52	0.60	0.65	0.77	0.65	0.41	0.34	0.47	0.41	1.04
Al_2O_3	17.05	16.04	14.28	14.45	12.86	17.19	15.80	16.90	18.55	20.98	16.47	16.12	11.80	13.17	14.88	11.44	15.05
Fe_2O_3	13.41	4.31	4.87	7.04	3.76	4.66	10.42	8.74	8.17	9.29	11.81	10.04	3.54	2.45	6.62	2.75	9.99
MnO	0.18	0.10	0.11	0.09	0.09	0.15	0.11	0.08	0.08	0.09	0.14	0.10	0.06	0.03	0.09	0.05	0.20
MgO	5.68	1.43	0.85	2.10	1.13	0.98	4.18	4.18	3.49	4.54	4.94	4.60	1.88	1.28	3.09	1.28	2.28
CaO	5.77	3.44	2.60	3.60	4.12	6.67	3.19	9.52	8.52	9.76	8.67	7.19	3.04	2.07	4.22	2.66	4.51
Na_2O	3.32	3.85	6.42	4.97	1.41	3.32	4.35	2.29	2.88	3.00	2.90	2.85	0.18	0.07	3.16	0.21	5.50
K_2O	0.05	2.26	0.50	0.64	2.36	1.29	0.03	0.28	0.55	0.32	0.07	0.14	3.26	4.11	1.57	3.28	0.08
P_2O_5	0.14	0.24	0.18	0.18	0.08	0.27	0.17	0.08	0.13	0.10	0.14	0.10	0.10	0.06	0.11	0.07	0.31
LOI	4.71	3.83	2.77	3.20	2.71	2.34	3.61	5.73	4.44	4.28	3.42	3.37	4.66	3.64	6.55	3.96	5.35
Total	99.83	99.91	100.05	100.11	99.51	100.03	99.88	99.46	100.12	99.71	100.24	99.37	99.58	99.25	99.80	99.37	99.95
C	0.29	0.45	0.48	0.37	0.30	0.15	0.17	0.79	0.44	0.24	0.21	0.17	0.65	0.43	0.89	0.59	0.87
S	0.02	0.02	<0.01	<0.01	<0.01	0.01	0.02	0.01	0.02	0.02	0.01	0.01	0.03	0.01	0.20	<0.01	0.01
Trace elements (ppm; XRF):																	
Sc	40	10	22	22	11	4	37	24	30	27	41	40	13	8	26	10	32
V	338	35	72	98	10	23	287	209	237	264	350	294	66	26	179	29	162
Cr	5	2	3	2	2	1	6	9	9	10	14	14	16	10	44	2	3
Ni	6	1	<1	1	<1	1	6	6	6	6	7	4	6	3	10	1	<1
Cu	131	2	8	14	5	4	112	84	80	130	123	96	16	6	35	16	95
Zn	116	57	70	75	54	52	85	61	62	70	84	73	47	35	61	52	122
As	<3	4	3	<3	5	<3	11	<3	4	5	<3	3	<3	<3	15	<3	<3
Rb	<1	84	8	11	71	42	<1	8	15	9	<1	3	117	142	59	121	3
Sr	518	220	92	152	237	605	241	412	392	605	392	398	68	52	154	72	281
Y	14	24	19	19	23	16	15	10	10	10	11	10	20	23	15	26	22
Zr	59	194	97	97	128	108	59	29	41	35	38	34	136	217	99	186	95
Nb	4	14	7	6	8	6	4	1	2	2	2	2	10	14	7	12	10
Ba	69	402	104	146	439	367	85	95	135	152	67	98	456	1015	144	927	76
La	8	26	17	16	16	26	12	6	7	5	8	7	21	32	18	20	23
Ce	17	57	38	36	40	56	28	17	16	12	11	16	48	69	39	45	44
Nd	8	25	20	16	18	25	16	8	8	8	6	7	20	23	16	19	21
Pb	4	5	2	3	3	13	3	2	3	6	4	2	5	3	15	21	5
Bi	<2	<2	<2	<2	<2	<2	<2	<2	<2	<2	<2	<2	<2	<2	<2	<2	<2
Th	4	16	6	7	7	12	3	2	3	2	3	2	9	19	7	9	6
Trace elements (ppm; ICP-MS):																	
Cd	0.2	0.4	0.2	-	0.1	-	0.3	<0.1	-	0.1	-	<0.1	-	0.2	-	0.2	0.2
Cs	<0.05	3.1	0.5	-	1.2	-	<0.05	1.0	-	0.5	-	0.1	-	4.2	-	3.8	0.1
Tl	<0.5	<0.5	<0.5	-	<0.5	-	<0.5	<0.5	-	<0.5	-	<0.5	-	0.7	-	0.6	<0.5
Bi	0.2	0.1	0.1	-	0.3	-	0.1	0.1	-	0.1	-	0.3	-	0.6	-	0.3	<0.1
Th	-	-	-	-	8.1	-	-	-	-	-	2.2	-	-	-	7.2	-	5.7
U	0.9	2.4	1.2	1.3	1.7	-	0.8	0.6	-	0.5	0.4	0.5	-	3.9	1.3	2.2	1.4

	WT25-386	WT25-401	WT25-408	WT25-417	WT25-418	WT25-423	WT25-428	WT25-434	WT25-441	WT25-444	WT25-458	WT25-478	WT29-133	WT35-306	WT35-309	WT35-310	WT35-312
Major elements (weight %; XRF and Leco):																	
SiO_2	60.32	62.59	66.07	64.05	64.48	59.91	64.23	69.31	61.44	59.66	63.42	57.71	67.46	69.22	63.49	83.77	54.26
TiO_2	0.78	0.52	0.64	0.58	0.37	0.50	0.39	0.32	0.83	0.73	0.75	0.79	0.19	0.25	0.63	0.21	0.65
Al_2O_3	17.10	15.94	15.69	18.20	13.92	20.15	15.72	13.42	14.67	13.65	16.07	16.99	9.76	15.99	18.51	7.07	20.68
Fe_2O_3	7.30	4.25	5.35	1.81	4.33	4.61	3.32	2.96	8.78	8.56	7.50	10.37	0.94	3.49	2.66	1.65	5.65
MnO	0.05	0.10	0.06	0.04	0.21	0.08	0.06	0.05	0.03	0.07	<0.01	0.03	0.13	0.05	0.08	0.07	0.18
MgO	2.73	1.45	2.31	0.06	0.95	1.56	1.89	1.71	1.12	1.04	0.17	1.58	0.69	0.97	0.14	0.56	0.66
CaO	1.05	3.72	0.95	2.15	4.56	2.09	4.16	3.93	1.43	2.92	0.28	0.43	9.47	1.15	1.85	1.22	4.13
Na_2O	1.38	2.57	1.79	10.82	5.31	4.25	1.15	1.01	1.78	1.54	1.20	0.62	0.75	7.16	10.84	3.55	6.31
K_2O	3.97	3.55	3.36	0.02	0.65	2.48	2.63	1.63	1.04	1.46	2.94	3.95	0.96	0.33	0.02	0.01	2.44
P_2O_5	0.15	0.25	0.14	0.21	0.08	0.08	0.06	0.05	0.25	0.17	0.14	0.20	0.07	0.03	0.15	0.04	0.25
LOI	4.20	4.90	3.17	1.86	4.86	4.22	6.06	5.62	7.63	9.38	6.64	7.50	9.25	1.73	1.43	1.71	4.84
Total	99.03	99.84	99.53	99.80	99.72	99.93	99.67	100.01	99.00	99.18	99.11	100.17	99.67	100.37	99.80	99.86	100.05
C	0.23	0.75	0.19	0.41	0.96	0.44	0.89	0.85	0.16	0.49	0.04	0.02	1.95	0.21	0.36	0.30	0.83
S	0.54	0.07	<0.01	0.13	0.03	0.06	0.01	0.01	6.14	6.35	5.89	7.46	0.01	<0.01	<0.01	<0.01	<0.01
Trace elements (ppm; XRF):																	
Sc	18	10	16	11	14	15	12	11	34	31	34	35	14	6	12	4	23
V	116	34	76	15	52	52	32	31	205	186	208	232	19	14	16	8	71
Cr	110	1	70	1	8	5	3	3	5	4	4	19	1	1	3	3	4
Ni	40	<1	29	<1	4	2	2	2	4	2	3	5	<1	3	1	1	2
Cu	39	4	14	2	3	69	2	2	107	86	42	67	3	3	2	<1	4
Zn	101	58	118	2	49	140	61	93	1735	618	3	576	31	59	6	40	18
As	24	<3	<3	9	<3	<3	<3	<3	12	11	29	18	<3	<3	5	<3	5
Rb	168	143	139	<1	24	77	79	44	26	35	54	81	27	11	<1	<1	92
Sr	81	209	88	275	459	305	314	311	2451	359	133	93	319	415	222	81	748
Y	30	24	33	21	14	22	22	18	21	21	25	17	15	12	16	9	18
Zr	146	203	206	122	88	148	167	125	99	91	95	96	103	128	132	110	135
Nb	18	14	16	7	6	8	9	7	6	5	5	6	5	6	8	6	8
Ba	970	720	887	38	232	1123	1604	1405	1047	1372	310	1025	2183	274	22	5	805
La	35	28	29	9	16	15	17	13	8	8	12	8	23	13	6	<2	4
Ce	71	67	59	22	30	37	39	29	23	23	23	16	62	28	16	9	25
Nd	28	30	28	10	12	14	15	12	11	11	12	10	30	10	7	4	11
Pb	19	5	40	8	7	10	5	3	29	30	13	68	6	11	10	5	11
Bi	<2	<2	<2	<2	<2	<2	<2	<2	<2	<2	<2	<2	<2	<2	<2	<2	<2
Th	20	16	18	6	4	8	8	7	2	2	<1.5	<1.5	4	7	8	8	5
Trace elements (ppm; ICP-MS):																	
Cd	0.1	-	0.2	-	0.2	0.3	0.3	0.2	8.5	3.5	0.2	2.4	-	-	-	-	-
Cs	4.5	-	3.6	-	0.6	1.8	2.2	1.1	0.6	0.8	1.2	1.7	-	-	-	-	-
Tl	0.7	-	0.8	-	<0.5	0.7	1.3	1.1	0.8	0.8	0.6	0.9	-	-	-	-	-
Bi	0.8	-	0.4	-	0.2	0.1	<0.1	<0.1	0.2	0.2	0.3	0.2	-	-	-	-	-
Th	-	-	18.4	-	-	-	-	6.7	-	-	-	2.3	-	-	-	-	-
U	3.7	-	3.9	-	0.6	1.1	0.7	0.9	0.6	0.6	0.5	0.6	-	-	-	-	-

	Detection limit	WT2-103	WT2-176	WT2-227	WT9A-126	WT9A-162	WT16-132	WT23-140	WT25-280	WT25-372
Trace elements (ppm; ICP-MS):										
La	0.02	11.09	11.86	8.99	12.21	13.53	10.80	11.02	9.48	24.13
Ce	0.02	20.99	21.82	16.90	25.78	29.18	24.24	23.39	17.94	51.39
Pr	0.02	2.84	2.83	2.30	3.76	4.42	3.45	2.76	2.38	6.02
Nd	0.02	11.22	11.12	9.37	15.83	18.90	13.86	11.53	9.28	23.30
Sm	0.02	2.67	2.68	2.31	4.38	5.06	3.15	2.78	2.19	5.00
Eu	0.02	0.96	0.80	0.81	1.29	1.49	1.11	0.89	0.75	1.57
Gd	0.02	2.50	2.29	1.80	4.28	5.01	3.02	2.53	2.27	4.51
Tb	0.02	0.39	0.38	0.34	0.76	0.85	0.52	0.40	0.33	0.71
Dy	0.02	2.32	2.34	2.09	4.56	5.28	3.01	2.17	2.06	3.99
Ho	0.02	0.51	0.43	0.39	0.94	1.04	0.59	0.46	0.42	0.85
Er	0.02	1.28	1.27	1.18	2.66	3.01	1.80	1.24	1.23	2.22
Tm	0.02	0.19	0.18	0.16	0.35	0.38	0.25	0.18	0.18	0.34
Yb	0.02	1.09	1.11	1.07	2.19	2.41	1.56	1.24	1.06	2.23
Lu	0.02	0.17	0.16	0.15	0.29	0.29	0.23	0.18	0.14	0.33

	WT2-103	WT2-117	WT2-131	WT2-150	WT2-164	WT2-176	WT2-193	WT2-210	WT2-227	WT2-239	WT2-265	WT2-280	WT2-294	WT2-315	WT2-323	WT2-338	WT2-345
Major minerals (weight %; XRD):																	
Alb	26.2±1.1	21.5±1.1	16.2±1.0	22.0±1.0	35.2±1.0	39.6±1.0	5.8±0.8	17.3±0.9	20.9±0.9	0.9±0.5	-	11.8±0.7	-	11.6±0.8	52.1±1.0	10.1±0.6	11.5±0.8
Ank	-	-	-	-	-	-	-	-	-	-	-	-	-	-	-	-	-
Ap	-	-	-	-	-	-	-	-	-	-	-	-	-	-	0.5±0.2	-	-
Cal	1.7±0.2	1.3±0.2	1.6±0.2	4.2±0.4	0.5±0.2	2.8±0.4	3.2±0.3	5.3±0.5	5.5±0.4	4.4±0.3	-	0.7±0.2	3.5±0.3	2.8±0.3	5.3±0.4	1.5±0.3	4.2±0.3
Chl	25.5±2.2	35.1±2.0	39.4±2.3	26.0±1.9	34.6±1.1	25.9±1.1	2.2±0.4	25.9±1.0	37.3±1.9	3.1±0.5	9.9±1.6	12.5±0.7	1.6±0.5	10.8±0.6	21.7±0.8	13.8±0.7	5.2±0.5
Dol	-	-	-	-	-	-	-	-	-	-	-	-	-	-	-	-	-
Ep	18.4±1.0	21.1±1.1	23.4±1.2	31.1±1.1	16.2±0.8	-	-	27.1±0.8	16.4±0.8	5.4±0.5	-	-	-	-	-	-	-
Gn	-	-	-	-	-	-	-	-	-	-	-	-	-	-	-	-	-
Hem	-	-	-	-	-	-	-	-	-	-	-	-	-	-	-	-	-
Hbl	3.6±0.6	4.2±0.7	-	-	6.6±0.6	-	-	-	-	-	-	-	-	-	-	-	-
Im	-	-	-	-	-	-	-	-	-	-	-	-	-	-	-	-	-
Kln	-	-	-	-	-	-	-	-	-	-	-	-	-	-	-	-	-
Ms	-	-	-	-	-	-	-	-	-	-	-	-	-	-	-	-	-
Or	-	-	-	-	-	-	-	-	-	-	-	3.2±0.7	-	-	-	-	-
Pg	-	-	-	-	-	-	-	-	-	-	-	-	-	-	-	-	-
Phn	-	-	-	-	-	7.4±1.3	24.8±0.8	-	-	27.7±0.7	48.5±1.4	34.9±1.1	37.0±0.8	29.1±0.9	-	40.3±0.9	30.9±0.8
Py	-	-	-	-	-	-	-	-	-	-	-	-	-	-	-	0.8±0.2	-
Prl	-	-	-	-	-	-	-	-	-	-	-	-	-	-	-	-	-
Qtz	22.1±0.9	14.4±0.6	16.4±0.8	15.0±0.5	4.8±0.3	24.3±0.7	64.0±0.9	22.3±0.6	17.7±0.7	58.5±0.8	41.6±1.1	36.9±0.8	57.9±0.7	45.7±0.8	18.9±0.5	32.6±0.7	48.2±0.8
Rt	-	-	-	-	-	-	-	-	-	-	-	-	-	-	-	0.9±0.2	-
Sd	-	-	-	-	-	-	-	-	-	-	-	-	-	-	-	-	-
Sp	-	-	-	-	-	-	-	-	-	-	-	-	-	-	-	-	-
Ttn	2.5±0.5	2.4±0.5	3.0±0.6	1.7±0.5	2.1±0.4	-	-	2.1±0.4	2.2±0.5	-	-	-	-	-	1.5±0.4	-	-
Errors of measurements (in %; XRD):																	
R_{wp}	7.05	6.77	6.14	6.80	7.04	7.29	7.89	6.55	6.02	7.77	8.79	8.40	8.80	7.59	7.99	8.01	7.80
R_{exp}	5.15	5.02	4.73	4.00	3.81	3.93	4.72	4.17	3.96	4.80	3.92	4.08	4.53	4.37	3.97	4.05	4.61

Notes: Alb = albite, ank = ankerite, ap = apatite, cal = calcite, chl = chlorite, dol = dolomite, ep = epidote, gn = galena, hem = hematite, hbl = hornblende, im = intermediate Na/K mica, kln = kaolinite, ms = muscovite, or = orthoclase, pg = paragonite, phn = phengite, py = pyrite, prl = pyrophyllite, qtz = quartz, rt = rutile, sd = siderite, sp = sphalerite, ttn = titanite, - = not detected.

	WT2-353	WT2-360	WT2-386	WT2-402	WT2-421	WT2-440	WT2-461	WT5-118	WT5-129	WT5-136	WT5-148	WT5-156	WT5-158	WT5-163	WT5-171	WT5-186	WT5-213
Major minerals (weight %; XRD):																	
Alb	23.2±0.9	1.0±0.6	-	-	-	-	8.8±1.5	5.1±0.5	26.8±0.9	10.2±0.5	27.6±0.8	43.3±0.9	30.2±0.9	5.4±0.6	-	-	5.7±2.6
Ank	-	-	-	-	-	-	-	-	-	-	-	-	-	-	0.8±0.3	-	-
Ap	-	-	-	-	-	-	-	-	-	-	-	-	-	-	-	-	-
Cal	7.3±0.4	7.8±0.4	-	-	-	-	-	-	5.7±0.4	1.2±0.2	1.7±0.2	1.6±0.3	1.5±0.3	3.9±0.3	5.3±0.4	-	8.5±0.6
Chl	6.7±0.5	7.6±0.5	-	2.0±0.7	-	-	2.8±0.8	15.1±0.7	6.5±0.6	11.1±0.6	4.2±0.5	6.0±0.7	5.9±0.6	4.2±0.5	7.3±0.8	3.3±0.8	5.5±0.7
Dol	-	-	-	-	-	-	-	-	-	-	-	-	-	-	-	-	-
Ep	3.0±0.6	-	-	-	-	-	-	-	-	-	8.7±0.5	10.5±0.7	15.4±0.7	13.9±0.6	-	-	-
Gn	-	-	-	-	-	-	-	-	-	-	-	-	-	-	-	-	-
Hem	-	-	-	-	-	-	-	-	-	-	-	-	-	-	1.0±0.3	-	-
Hbl	-	-	-	-	-	-	-	-	-	-	-	-	-	-	-	-	-
Im	-	7.1±0.8	-	-	-	-	-	-	-	-	-	-	-	-	5.0±0.6	-	3.7±1.3
Kln	-	-	-	-	-	-	-	-	-	-	-	-	-	-	1.0±0.6	-	-
Ms	24.1±0.9	17.7±1.3	41.9±1.0	40.0±1.0	19.2±1.1	18.3±1.3	36.0±1.6	-	-	-	-	7.6±0.7	14.3±1.1	7.6±0.6	9.5±1.9	52.3±1.1	1.4±0.9
Or	-	-	-	-	-	-	-	-	-	-	-	-	-	-	-	-	-
Pg	-	17.8±0.7	-	-	-	-	-	-	-	-	-	-	-	11.6±0.5	18.1±1.4	-	26.1±1.3
Phn	-	-	-	-	-	-	-	40.9±1.0	29.3±1.0	35.5±0.8	16.5±0.8	-	-	-	-	-	-
Py	-	-	10.3±0.4	11.6±0.3	25.1±0.5	24.7±0.5	10.9±0.4	-	-	-	-	-	-	-	-	9.9±0.4	10.5±0.5
Prl	-	-	-	-	-	-	-	-	-	-	-	-	-	-	-	-	-
Qtz	34.9±0.8	40.3±0.8	46.8±0.9	45.5±0.8	55.3±0.8	56.6±1.0	39.6±1.2	37.9±0.8	31.2±0.7	42.0±0.7	40.9±0.7	31.0±0.7	32.7±0.7	53.4±0.8	51.4±1.3	33.0±0.8	38.1±1.3
Rt	0.8±0.3	0.7±0.3	1.0±0.3	0.9±0.3	0.4±0.2	0.4±0.2	1.9±0.4	1.0±0.3	0.5±0.2	-	0.4±0.2	-	-	-	0.6±0.2	1.5±0.4	0.5±0.4
Sd	-	-	-	-	-	-	-	-	-	-	-	-	-	-	-	-	-
Sp	-	-	-	-	-	-	-	-	-	-	-	-	-	-	-	-	-
Ttn	-	-	-	-	-	-	-	-	-	-	-	-	-	-	-	-	-
Errors of measurements (in %; XRD):																	
R_{wp}	7.40	7.84	9.43	8.80	8.66	8.71	9.44	7.76	7.43	8.00	6.81	7.03	7.00	8.22	8.64	9.75	7.57
R_{exp}	4.28	4.30	5.67	5.48	5.18	5.49	5.75	3.99	4.28	4.31	4.37	4.36	4.04	4.53	5.44	5.96	5.45

Notes: Alb = albite, ank = ankerite, ap = apatite, cal = calcite, chl = chlorite, dol = dolomite, ep = epidote, gn = galena, hem = hematite, hbl = hornblende, im = intermediate Na/K mica, kln = kaolinite, ms = muscovite, or = orthoclase, pg = paragonite, phn = phengite, py = pyrite, prl = pyrophyllite, qtz = quartz, rt = rutile, sd = siderite, sp = sphalerite, ttn = titanite, - = not detected.

	WT5-223	WT5-231	WT6-109	WT6-135	WT6-153	WT6-167	WT6-180	WT7-92	WT7-108	WT7-123	WT7-155	WT7-171	WT7-200	WT7-205	WT7-208	WT7-213	WT8A-103
Major minerals (weight %; XRD):																	
Alb	-	-	-	-	5.5±0.5	42.9±0.9	28.2±0.8	5.0±1.2	-	-	-	-	-	11.0±0.8	16.1±0.8	9.7±1.1	60.4±0.9
Ank	-	-	-	-	-	-	-	-	-	-	-	-	-	-	-	-	-
Ap	-	-	-	-	-	-	-	-	-	-	-	-	-	-	-	-	-
Cal	14.5±0.8	9.5±0.6	-	3.1±0.3	3.6±0.3	1.9±0.2	0.6±0.2	0.5±0.2	-	0.4±0.3	-	-	7.6±0.5	4.3±0.3	2.0±0.3	3.5±0.3	6.1±0.4
Chl	21.1±1.0	15.5±0.7	-	4.9±0.6	6.9±0.5	5.5±0.6	11.1±0.7	-	20.3±0.8	-	-	-	3.7±0.8	9.6±0.5	3.1±0.5	6.4±0.9	2.7±0.7
Dol	-	-	-	-	-	-	-	-	-	-	-	-	-	-	-	-	-
Ep	-	2.8±0.8	-	-	-	-	-	-	-	-	-	-	-	-	-	-	-
Gn	-	-	-	-	-	-	-	-	-	-	-	-	-	-	-	-	-
Hem	-	-	-	-	-	-	-	-	-	-	-	-	-	-	-	-	0.2±0.1
Hbl	-	-	-	-	-	-	-	-	-	-	-	-	-	-	-	-	-
Im	13.0±1.4	8.0±2.9	-	-	-	-	-	7.3±1.2	6.8±1.1	7.0±2.5	9.9±1.1	8.2±2.1	-	-	-	-	-
Kln	-	-	-	-	-	-	-	-	-	-	-	1.0±0.6	-	-	-	-	-
Ms	1.8±1.5	4.2±2.4	39.2±0.7	38.8±1.0	25.3±1.0	9.7±1.2	20.5±1.0	5.4±2.4	6.4±1.0	26.8±3.0	27.6±1.6	15.4±2.4	28.4±1.6	-	-	-	-
Or	-	-	-	-	-	-	-	-	-	-	-	-	-	-	-	-	-
Pg	15.8±1.4	27.4±2.6	-	-	4.0±0.5	-	-	22.2±1.2	13.3±0.9	14.0±2.3	5.5±0.9	4.4±1.1	-	-	-	-	-
Phn	-	-	-	-	-	-	-	-	-	-	-	-	-	24.1±0.8	31.5±0.9	36.7±1.2	2.5±0.6
Py	1.0±0.4	1.6±0.2	11.3±0.3	10.4±0.3	9.5±0.2	8.9±0.3	9.5±0.3	10.8±0.4	12.3±0.4	12.9±0.4	13.8±0.4	18.1±0.5	-	-	-	-	-
Prl	-	-	-	-	-	-	-	-	-	-	-	3.6±0.8	-	-	-	-	-
Qtz	32.2±1.0	31.0±0.9	48.9±0.7	41.6±0.8	44.3±0.8	30.6±0.7	30.1±0.7	47.5±1.3	38.9±0.8	37.4±0.9	41.8±0.7	47.8±1.0	60.3±1.4	50.5±0.8	46.7±0.8	43.4±1.1	28.1±0.6
Rt	0.6±0.5	-	0.6±0.2	1.2±0.3	0.9±0.2	0.5±0.2	-	1.3±0.3	2.0±0.4	1.5±0.3	1.4±0.3	1.5±0.4	-	0.5±0.2	0.6±0.3	0.3±0.2	-
Sd	-	-	-	-	-	-	-	-	-	-	-	-	-	-	-	-	-
Sp	-	-	-	-	-	-	-	-	-	-	-	-	-	-	-	-	-
Ttn	-	-	-	-	-	-	-	-	-	-	-	-	-	-	-	-	-
Errors of measurements (in %; XRD):																	
R_{wp}	10.00	7.77	7.90	7.95	6.56	7.53	6.97	7.39	7.84	7.65	7.89	7.58	10.11	7.47	7.42	8.56	8.71
R_{exp}	5.29	5.23	4.51	4.27	4.43	4.12	4.28	5.35	5.09	5.31	5.38	5.29	5.34	4.29	4.31	5.70	4.92

Notes: Alb = albite, ank = ankerite, ap = apatite, cal = calcite, chl = chlorite, dol = dolomite, ep = epidote, gn = galena, hem = hematite, hbl = hornblende, im = intermediate Na/K mica, kln = kaolinite, ms = muscovite, or = orthoclase, pg = paragonite, phn = phengite, py = pyrite, prl = pyrophyllite, qtz = quartz, rt = rutile, sd = siderite, sp = sphalerite, ttn = titanite, - = not detected.

	WT8A-172	WT9A-86	WT9A-100	WT9A-109	WT9A-126	WT9A-144	WT9A-162	WT9A-176	WT9A-186	WT9A-198	WT9A-218	WT9A-228	WT9A-238	WT9A-254	WT9A-265	WT16-87	WT16-112
Major minerals (weight %; XRD):																	
Alb	59.3±0.8	2.6±0.6	27.4±0.8	41.0±1.4	29.3±0.9	23.9±0.9	24.1±0.9	29.6±1.0	24.2±1.0	-	-	-	-	-	2.1±0.5	26.8±1.1	42.7±1.0
Ank	-	-	-	-	-	-	-	-	-	-	-	-	-	1.9±0.4	-	-	-
Ap	-	-	0.4±0.2	-	-	-	-	-	-	0.8±0.3	-	-	-	-	-	-	-
Cal	3.1±0.3	4.8±0.4	2.2±0.3	1.8±0.4	3.2±0.3	3.9±0.4	3.1±0.3	6.7±0.5	8.8±0.5	7.8±0.5	-	-	2.5±0.4	4.6±0.4	6.8±0.5	-	2.8±0.4
Chl	2.2±0.6	13.1±0.8	26.4±0.9	29.5±1.3	23.3±0.9	16.5±0.9	30.2±1.6	36.2±1.6	22.9±0.8	12.3±0.6	-	-	33.1±1.2	9.0±0.6	8.3±0.6	22.0±0.9	17.1±0.8
Dol	-	-	-	-	-	-	-	-	-	-	-	-	9.8±0.7	-	-	-	-
Ep	-	24.9±0.7	14.4±0.6	3.8±0.8	16.2±0.7	37.8±0.8	18.4±0.8	6.3±0.7	5.1±0.8	-	-	-	-	-	-	26.1±0.8	10.5±0.8
Gn	-	-	-	-	-	-	-	-	-	-	-	-	0.8±0.1	-	-	-	-
Hem	-	-	-	-	-	-	-	-	-	-	-	-	-	-	-	-	-
Hbl	-	-	-	-	-	-	-	-	-	-	-	-	-	-	-	-	-
Im	-	-	-	-	-	-	-	-	2.8±0.8	2.2±0.9	-	-	-	6.4±0.7	9.0±0.8	-	-
Kln	-	-	-	-	-	-	-	-	-	-	-	-	-	0.8±0.5	-	-	-
Ms	-	25.6±1.1	-	11.7±1.9	-	-	-	-	1.7±0.5	1.5±0.7	18.9±0.8	25.8±0.8	23.5±1.6	13.7±1.2	14.3±0.8	-	-
Or	-	-	-	-	-	-	-	-	-	-	-	-	-	-	-	-	-
Pg	-	-	-	-	-	-	-	-	12.3±1.5	27.0±0.9	-	-	-	15.6±0.6	15.1±0.8	-	3.2±0.6
Phn	-	-	-	-	-	-	-	-	-	-	-	-	-	-	-	-	-
Py	-	6.3±0.3	0.2±0.1	0.5±0.1	-	-	-	1.7±0.2	0.8±0.2	10.3±0.3	7.0±0.2	3.1±0.2	7.1±0.6	-	-	-	4.2±0.2
Prl	-	-	-	-	-	-	-	-	-	-	-	-	-	-	-	-	-
Qtz	35.5±0.6	21.7±0.5	25.7±0.6	9.5±0.5	24.6±0.5	14.4±0.4	21.0±0.7	16.4±0.6	20.4±0.6	37.5±0.9	73.5±0.7	70.3±0.7	12.1±0.6	47.2±0.9	44.4±0.7	25.1±0.7	19.5±0.6
Rt	-	1.0±0.2	-	-	-	-	-	-	1.0±0.2	0.6±0.3	0.6±0.2	0.8±0.2	0.5±0.3	0.8±0.2	-	-	-
Sd	-	-	-	-	-	-	-	-	-	-	-	-	-	-	-	-	-
Sp	-	-	-	-	-	-	-	-	-	-	-	-	10.6±0.5	-	-	-	-
Ttn	-	-	3.3±0.4	2.2±0.6	3.4±0.5	3.5±0.5	3.2±0.5	3.1±0.5	-	-	-	-	-	-	-	-	-
Errors of measurements (in %; XRD):																	
R_{wp}	8.66	6.51	5.86	8.41	6.42	6.47	6.32	6.56	6.99	6.59	7.28	8.40	9.35	7.61	7.74	7.54	7.18
R_{exp}	4.91	4.15	4.02	3.70	4.05	4.18	4.08	3.76	3.88	4.12	4.37	4.32	4.12	4.15	4.27	4.06	4.12

Notes: Alb = albite, ank = ankerite, ap = apatite, cal = calcite, chl = chlorite, dol = dolomite, ep = epidote, gn = galena, hem = hematite, hbl = hornblende, im = intermediate Na/K mica, kln = kaolinite, ms = muscovite, or = orthoclase, pg = paragonite, phn = phengite, py = pyrite, prl = pyrophyllite, qtz = quartz, rt = rutile, sd = siderite, sp = sphalerite, ttn = titanite, - = not detected.

	WT16-125	WT16-132	WT16-145	WT16-161	WT16-170	WT16-186	WT16-195	WT16-206	WT16-210	WT16-223	WT16-245	WT16-257	WT16-276	WT16-292	WT16-322	WT16-333	WT16-338
Major minerals (weight %; XRD):																	
Alb	-	50.3±1.1	30.7±1.0	14.0±1.1	-	20.8±1.0	24.2±1.0	19.8±1.1	61.9±1.0	35.2±1.0	-	-	-	-	-	4.0±0.7	37.5±1.1
Ank	-	-	-	-	-	-	-	-	-	-	-	-	-	-	-	-	-
Ap	-	-	-	-	-	-	-	-	-	-	-	-	-	-	-	-	-
Cal	1.5±0.3	3.5±0.5	4.1±0.4	2.9±0.3	-	5.1±0.4	1.3±0.3	5.2±0.5	3.7±0.4	6.5±0.5	-	-	-	-	0.4±0.3	4.7±0.5	2.2±0.3
Chl	4.8±0.7	21.7±0.9	21.3±0.8	22.2±0.8	2.2±0.8	20.4±0.8	16.8±0.9	22.9±1.1	12.5±0.8	19.9±0.8	-	-	-	-	-	7.4±0.6	8.2±0.8
Dol	-	-	-	-	-	-	-	-	-	-	-	-	-	-	-	-	-
Ep	-	7.0±0.8	4.5±0.6	-	-	14.0±0.7	23.4±0.9	18.8±0.9	9.7±0.8	2.6±0.7	-	-	-	-	-	-	0.9±0.8
Gn	-	-	-	-	-	-	-	-	-	-	-	-	-	-	-	-	-
Hem	-	-	-	-	-	-	-	-	-	-	-	-	-	-	-	-	-
Hbl	-	-	-	-	-	-	-	-	-	-	-	-	-	-	-	-	-
Im	7.7±2.3	-	-	-	11.3±2.2	-	-	-	-	-	8.3±1.2	8.8±1.3	-	-	7.3±1.3	5.6±0.9	-
Kln	-	-	-	-	-	-	-	-	-	-	4.7±0.9	3.0±0.8	-	-	-	-	-
Ms	23.9±2.0	-	4.0±0.7	9.3±0.8	19.4±2.1	5.6±0.7	12.7±2.0	15.9±2.4	-	-	16.7±3.9	38.2±2.0	36.2±1.0	28.4±1.1	12.7±1.1	17.6±1.5	8.5±1.2
Or	-	-	-	-	-	-	-	-	-	-	-	-	-	-	-	-	-
Pg	12.5±1.6	-	4.5±0.6	10.3±0.7	14.3±2.5	5.7±0.6	-	-	-	5.3±0.7	-	4.1±0.8	-	-	6.7±1.1	11.4±0.6	-
Phn	-	-	-	-	-	-	-	-	-	-	-	-	-	-	-	-	-
Py	11.6±0.5	2.5±0.2	3.9±0.2	10.6±0.3	14.0±0.5	-	0.8±0.2	-	-	1.9±0.2	9.0±0.6	7.2±0.4	6.0±0.3	9.7±0.4	7.5±0.4	-	-
Prl	-	-	-	-	-	-	-	-	-	-	11.7±1.6	5.1±1.0	-	-	-	-	-
Qtz	37.1±1.0	15.0±0.6	27.0±0.7	30.7±0.8	37.4±1.0	27.7±0.7	20.8±0.7	17.4±0.7	12.2±0.5	28.1±0.7	48.3±2.2	31.4±1.0	56.8±1.0	61.3±1.0	64.2±1.0	48.5±1.0	42.1±1.0
Rt	0.9±0.3	-	-	-	1.4±0.3	0.7±0.2	-	-	-	0.5±0.3	1.3±0.5	2.2±0.5	1.0±0.3	0.6±0.3	1.2±0.3	0.8±0.2	0.6±0.3
Sd	-	-	-	-	-	-	-	-	-	-	-	-	-	-	-	-	-
Sp	-	-	-	-	-	-	-	-	-	-	-	-	-	-	-	-	-
Ttn	-	-	-	-	-	-	-	-	-	-	-	-	-	-	-	-	-
Errors of measurements (in %; XRD):																	
R_{wp}	9.13	7.80	7.50	7.32	9.66	6.87	7.00	7.07	8.15	7.60	11.70	11.36	11.72	11.84	11.28	7.84	8.24
R_{exp}	4.82	4.05	3.95	3.99	4.67	4.06	4.13	4.08	4.21	4.08	4.93	4.71	5.53	5.15	4.84	5.33	5.40

Notes: Alb = albite, ank = ankerite, ap = apatite, cal = calcite, chl = chlorite, dol = dolomite, ep = epidote, gn = galena, hem = hematite, hbl = hornblende, im = intermediate Na/K mica, kln = kaolinite, ms = muscovite, or = orthoclase, pg = paragonite, phn = phengite, py = pyrite, prl = pyrophyllite, qtz = quartz, rt = rutile, sd = siderite, sp = sphalerite, ttn = titanite, - = not detected.

	WT16-343	WT16-344	WT16-349	WT16-355	WT17-114	WT17-118	WT17-122	WT17-127	WT17-132	WT17-138	WT17-146	WT21-109	WT21-121	WT21-126	WT21-135	WT21-147	WT21-159
Major minerals (weight %; XRD):																	
Alb	36.1±1.0	80.3±1.1	17.6±1.1	12.0±1.0	-	-	-	-	-	-	12.9±0.8	16.9±1.2	12.7±0.9	19.0±1.1	-	28.4±1.0	26.0±1.0
Ank	-	-	-	-	-	-	-	-	-	-	-	-	-	-	-	-	-
Ap	-	-	-	-	-	-	-	-	-	-	-	-	-	-	-	-	-
Cal	5.2±0.3	2.3±0.3	1.7±0.3	1.6±0.3	-	-	-	-	-	-	-	2.7±0.4	2.0±0.2	1.8±0.4	6.8±0.4	2.0±0.3	0.6±0.3
Chl	7.0±0.7	9.2±0.8	4.9±0.8	6.4±0.7	-	13.5±0.6	14.9±0.8	5.3±0.6	7.9±0.5	7.4±0.5	6.6±0.5	8.2±0.8	8.4±0.6	9.9±0.8	27.7±0.8	12.8±0.7	15.2±0.8
Dol	-	-	-	-	-	-	-	-	-	-	-	-	-	-	-	-	-
Ep	1.5±0.6	-	1.1±0.9	1.4±0.8	-	-	-	9.5±0.5	6.4±0.5	-	6.9±0.5	-	-	-	13.0±0.8	0.8±0.5	3.0±0.7
Gn	-	-	-	-	-	-	-	-	-	-	-	-	-	-	-	-	-
Hem	-	-	-	-	-	-	-	-	-	-	-	-	-	-	-	-	-
Hbl	-	-	-	-	-	-	-	-	-	-	-	-	-	-	-	-	-
Im	-	-	-	-	-	-	5.1±1.7	4.0±0.4	3.3±0.4	-	-	-	1.8±0.4	1.8±0.8	-	-	-
Kln	-	-	-	-	-	-	-	-	-	1.0±0.6	1.3±0.5	-	-	-	-	-	-
Ms	-	-	-	-	42.8±0.9	25.8±0.9	11.6±0.8	10.6±0.6	12.1±0.6	20.1±1.1	25.9±0.9	9.3±0.8	13.0±1.0	4.9±0.5	9.6±0.8	8.4±2.0	6.6±0.8
Or	-	-	-	-	-	-	-	-	-	-	-	-	-	-	-	-	-
Pg	-	-	-	-	-	-	15.6±0.6	11.4±0.5	9.0±0.5	15.3±0.6	-	7.4±0.7	7.8±0.5	7.0±0.6	5.6±0.7	2.9±0.7	5.1±0.7
Phn	14.0±1.2	4.5±0.8	33.0±1.2	29.1±1.1	-	-	-	-	-	-	-	-	-	-	-	-	-
Py	-	0.2±0.1	-	-	18.3±0.5	-	-	-	-	-	-	4.8±0.3	4.7±0.2	4.6±0.3	1.4±0.2	6.2±0.3	7.5±0.3
Prl	-	-	-	-	-	-	-	-	-	-	-	-	-	-	-	-	-
Qtz	36.2±0.9	2.7±0.3	41.2±1.2	49.5±1.1	37.2±0.7	60.1±0.8	52.0±0.8	58.4±0.8	60.7±0.7	55.5±0.9	45.6±0.8	50.3±1.1	49.6±0.9	51.0±1.1	35.0±0.8	38.5±1.0	35.4±0.8
Rt	-	0.8±0.4	0.5±0.3	-	-	0.6±0.2	0.8±0.2	0.8±0.2	0.6±0.2	0.7±0.2	0.8±0.2	0.4±0.3	-	-	0.9±0.3	-	0.6±0.2
Sd	-	-	-	-	-	-	-	-	-	-	-	-	-	-	-	-	-
Sp	-	-	-	-	1.7±0.2	-	-	-	-	-	-	-	-	-	-	-	-
Ttn	-	-	-	-	-	-	-	-	-	-	-	-	-	-	-	-	-
Errors of measurements (in %; XRD):																	
R_{wp}	8.17	8.36	9.67	8.84	8.12	7.29	9.86	8.13	7.92	8.27	6.88	9.16	7.23	8.94	8.14	7.35	6.97
R_{exp}	5.54	3.99	5.24	5.59	4.33	4.20	4.37	4.63	4.59	4.11	4.12	5.90	4.53	5.87	3.98	3.97	4.15

Notes: Alb = albite, ank = ankerite, ap = apatite, cal = calcite, chl = chlorite, dol = dolomite, ep = epidote, gn = galena, hem = hematite, hbl = hornblende, im = intermediate Na/K mica, kln = kaolinite, ms = muscovite, or = orthoclase, pg = paragonite, phn = phengite, py = pyrite, prl = pyrophyllite, qtz = quartz, rt = rutile, sd = siderite, sp = sphalerite, ttn = titanite, - = not detected.

	WT21-172	WT21-185	WT21-199	WT21-212	WT21-223	WT21-237	WT21-249	WT21-261	WT21-277	WT21-298	WT21-306	WT21-311	WT21-314	WT21-319	WT21-324	WT21-328	WT21-335
Major minerals (weight %; XRD):																	
Alb	28.7±0.9	20.4±1.1	5.3±0.6	14.1±1.3	1.8±0.7	-	-	-	-	-	-	14.4±0.9	9.5±0.7	8.9±0.8	1.1±0.5	-	-
Ank	-	-	-	-	-	-	-	-	-	-	-	-	-	-	4.0±0.5	-	-
Ap	-	-	-	-	-	-	-	-	-	-	-	-	-	-	-	-	-
Cal	2.4±0.3	4.0±0.4	2.5±0.2	5.5±0.4	4.8±0.4	-	3.1±0.4	-	-	4.4±0.4	5.0±0.5	1.5±0.3	0.4±0.2	3.8±0.3	2.7±0.3	0.7±0.2	3.2±0.3
Chl	9.0±0.6	10.8±0.8	10.1±0.6	10.1±0.9	10.3±0.9	2.9±1.0	2.5±0.8	-	2.6±0.7	9.4±0.6	2.6±1.0	4.1±0.6	11.1±0.6	12.2±0.7	10.1±0.6	7.5±0.6	9.5±0.6
Dol	-	-	-	-	-	-	-	-	-	-	-	-	-	-	-	-	-
Ep	-	-	-	-	-	-	-	-	-	-	-	-	-	-	1.1±0.5	-	-
Gn	-	-	-	-	-	-	-	-	-	-	0.4±0.1	-	-	-	-	-	-
Hem	-	-	-	-	-	-	-	-	-	-	-	-	-	-	0.4±0.3	36.4±0.5	-
Hbl	-	-	-	-	-	-	-	-	-	-	-	-	-	-	-	-	-
Im	-	-	3.8±0.6	-	-	-	-	-	-	-	-	4.1±1.3	5.3±0.7	-	1.7±0.6	-	-
Kln	-	-	-	-	-	-	-	-	-	-	-	-	-	-	2.2±0.7	-	-
Ms	11.0±2.0	9.3±0.8	27.1±1.0	12.6±0.8	18.5±0.9	37.9±1.2	26.0±1.2	33.2±1.0	30.2±1.1	35.9±0.9	28.7±1.7	24.9±1.2	25.6±1.2	31.3±1.1	27.9±1.0	6.4±0.6	39.4±0.9
Or	-	-	-	-	-	-	-	-	-	-	-	-	-	-	-	-	-
Pg	6.5±1.4	4.2±0.6	10.5±0.6	6.6±0.7	3.9±0.8	-	-	-	-	-	-	9.1±0.6	16.7±0.7	7.1±0.5	12.2±0.5	-	-
Phn	-	-	-	-	-	-	-	-	-	-	-	-	-	-	-	-	-
Py	9.9±0.3	6.3±0.3	10.6±0.3	12.5±0.4	8.2±0.3	3.4±0.3	7.2±0.3	8.9±0.3	6.5±0.3	9.6±0.3	46.5±1.3	5.6±0.2	1.4±0.2	-	-	-	-
Prl	-	-	-	-	-	-	-	-	-	-	-	-	-	-	-	-	-
Qtz	32.5±0.8	44.4±1.0	28.7±0.6	38.0±1.0	51.6±1.0	55.1±1.1	61.2±1.1	57.5±0.9	60.7±1.1	39.8±0.7	11.2±0.6	35.4±0.7	28.6±0.7	35.8±0.7	35.7±0.8	49.0±0.6	47.1±0.8
Rt	-	0.6±0.3	1.4±0.2	0.6±0.3	0.9±0.3	0.7±0.3	-	0.4±0.2	-	0.9±0.2	0.7±0.3	0.9±0.3	1.4±0.2	0.9±0.3	0.9±0.3	-	0.8±0.2
Sd	-	-	-	-	-	-	-	-	-	-	-	-	-	-	-	-	-
Sp	-	-	-	-	-	-	-	-	-	-	4.9±0.5	-	-	-	-	-	-
Ttn	-	-	-	-	-	-	-	-	-	-	-	-	-	-	-	-	-
Errors of measurements (in %; XRD):																	
R_{wp}	6.39	8.20	7.04	8.16	8.72	12.04	10.38	10.32	12.10	7.72	8.47	6.78	8.47	6.72	7.40	5.76	8.06
R_{exp}	4.07	5.50	4.24	5.48	5.60	5.76	6.15	6.12	5.19	4.41	4.58	4.13	4.01	4.07	4.12	3.40	4.15

Notes: Alb = albite, ank = ankerite, ap = apatite, cal = calcite, chl = chlorite, dol = dolomite, ep = epidote, gn = galena, hem = hematite, hbl = hornblende, im = intermediate Na/K mica, kln = kaolinite, ms = muscovite, or = orthoclase, pg = paragonite, phn = phengite, py = pyrite, prl = pyrophyllite, qtz = quartz, rt = rutile, sd = siderite, sp = sphalerite, ttn = titanite, - = not detected.

	WT22-100	WT22-109	WT22-122	WT22-132	WT22-148	WT22-163	WT22-176	WT22-190	WT22-208	WT22-222	WT22-237	WT22-244	WT22-256	WT22-264	WT22-277	WT22-286	WT22-295
Major minerals (weight %; XRD):																	
Alb	19.8±1.1	18.8±0.9	19.4±1.0	29.8±1.0	38.4±1.1	22.0±1.3	21.0±1.4	27.8±1.1	-	5.8±0.8	-	-	-	-	-	-	-
Ank	-	-	-	-	-	-	-	-	-	-	-	-	-	-	-	-	-
Ap	-	-	-	-	-	-	-	-	-	-	-	-	-	-	-	-	-
Cal	4.6±0.4	8.1±0.5	0.6±0.2	3.3±0.3	1.3±0.3	1.6±0.3	1.4±0.3	2.7±0.3	-	1.6±0.3	-	-	-	-	-	-	1.3±0.3
Chl	14.4±0.8	4.5±0.5	13.8±0.7	5.2±0.6	2.5±0.6	21.5±0.9	19.5±1.0	3.4±0.7	14.6±0.9	11.8±0.8	13.1±0.8	1.8±0.7	6.1±0.9	2.2±0.5	-	-	-
Dol	-	-	-	-	-	-	-	-	-	-	-	-	-	-	-	-	5.6±0.5
Ep	16.5±0.8	4.0±0.7	-	-	-	-	-	-	-	-	-	-	-	-	-	-	-
Gn	-	-	-	-	-	-	-	-	-	-	-	-	-	-	-	-	-
Hem	-	-	-	-	-	-	-	-	-	-	-	-	-	-	-	-	-
Hbl	-	-	-	-	-	-	-	-	-	-	-	-	-	-	-	-	-
Im	-	-	-	-	5.3±2.2	-	2.4±0.5	-	-	-	-	-	-	-	-	-	2.7±0.6
Kln	-	-	-	-	-	-	-	-	-	-	-	-	-	-	-	-	-
Ms	-	14.7±1.2	26.0±1.1	23.9±1.1	12.7±1.3	8.2±0.9	8.4±0.9	19.2±0.8	13.8±0.9	25.9±1.3	34.0±1.1	33.3±0.8	46.4±1.1	38.3±0.9	36.2±1.1	68.8±0.9	36.8±1.2
Or	-	-	-	-	-	-	-	-	-	-	-	-	-	-	-	-	-
Pg	5.0±0.7	3.1±0.5	-	-	6.1±1.6	3.7±0.7	7.3±0.8	6.2±0.6	10.0±0.8	3.0±0.6	-	-	-	-	-	-	8.7±0.7
Phn	-	-	-	-	-	-	-	-	-	-	-	-	-	-	-	-	-
Py	2.6±0.2	6.1±0.2	14.2±0.4	12.7±0.4	14.8±0.4	13.8±0.5	13.8±0.5	10.0±0.3	11.5±0.5	7.7±0.3	8.3±0.4	11.0±0.3	12.5±0.4	11.9±0.3	8.6±0.4	23.7±0.6	7.5±0.4
Prl	-	-	-	-	-	-	-	-	-	-	-	-	-	-	-	-	-
Qtz	37.1±0.9	40.7±0.8	26.0±0.7	25.1±0.7	18.7±0.6	28.1±0.8	24.7±0.8	29.5±0.8	48.6±1.0	43.6±1.0	44.0±0.9	53.2±0.8	35.0±0.9	47.1±0.7	54.7±1.0	6.4±0.5	37.0±0.9
Rt	-	-	-	-	0.2±0.1	1.1±0.4	1.5±0.3	1.2±0.3	1.5±0.3	0.6±0.2	0.6±0.3	0.7±0.2	-	0.5±0.2	0.5±0.3	1.1±0.3	0.4±0.3
Sd	-	-	-	-	-	-	-	-	-	-	-	-	-	-	-	-	-
Sp	-	-	-	-	-	-	-	-	-	-	-	-	-	-	-	-	-
Ttn	-	-	-	-	-	-	-	-	-	-	-	-	-	-	-	-	-
Errors of measurements (in %; XRD):																	
R_{wp}	7.54	6.74	7.31	7.73	6.96	8.86	8.91	8.76	10.92	8.66	10.32	7.51	10.20	8.01	13.41	9.84	10.36
R_{exp}	4.22	4.13	4.18	4.12	4.16	4.75	4.78	4.80	5.06	5.89	4.86	4.64	5.13	4.54	5.13	4.80	5.39

Notes: Alb = albite, ank = ankerite, ap = apatite, cal = calcite, chl = chlorite, dol = dolomite, ep = epidote, gn = galena, hem = hematite, hbl = hornblende, im = intermediate Na/K mica, kln = kaolinite, ms = muscovite, or = orthoclase, pg = paragonite, phn = phengite, py = pyrite, prl = pyrophyllite, qtz = quartz, rt = rutile, sd = siderite, sp = sphalerite, ttn = titanite, - = not detected.

	WT22-302	WT22-307	WT22-314	WT22-322	WT22-328	WT22-329	WT22-332	WT23-114	WT23-140	WT23-152	WT23-168	WT23-182	WT23-198	WT23-208	WT23-227	WT23-242	WT23-256
Major minerals (weight %; XRD):																	
Alb	45.5±1.1	44.9±0.9	41.0±1.1	52.0±1.0	26.0±0.8	11.0±0.7	7.6±0.7	37.2±1.1	30.8±0.9	22.3±0.9	35.3±1.1	24.3±1.1	17.8±1.0	17.1±0.9	-	14.3±0.8	36.1±1.3
Ank	-	-	-	-	-	1.1±0.4	1.0±0.4	-	-	-	-	-	-	-	-	-	-
Ap	-	-	-	-	-	-	-	-	-	-	-	-	-	-	-	-	-
Cal	2.8±0.3	4.3±0.3	4.8±0.3	3.4±0.5	0.9±0.3	-	-	2.0±0.3	-	0.4±0.2	1.2±0.3	1.4±0.3	2.3±0.3	1.5±0.3	5.2±0.5	4.2±0.3	3.6±0.4
Chl	10.0±0.8	-	11.8±0.8	9.6±0.8	16.3±1.7	6.1±0.8	12.3±0.8	22.5±1.8	22.7±1.3	34.3±1.5	32.4±1.5	39.9±1.7	35.0±1.0	9.9±0.6	6.1±0.8	36.9±1.8	28.7±1.2
Dol	-	-	-	-	-	-	-	-	-	-	-	-	-	-	-	-	-
Ep	-	-	1.5±0.9	-	-	-	-	10.9±0.7	23.2±0.8	17.4±0.7	24.3±0.9	17.0±0.9	23.6±0.8	-	65.2±1.1	22.7±0.9	11.3±0.9
Gn	-	-	-	-	-	-	-	-	-	-	-	-	-	-	-	-	-
Hem	-	-	1.1±0.2	2.0±0.2	-	-	-	-	-	-	-	-	-	-	-	-	-
Hbl	-	-	-	-	-	-	-	10.0±0.7	2.2±0.5	12.3±0.7	1.5±0.5	7.1±0.6	5.7±0.6	-	5.1±0.8	-	-
Im	-	1.1±0.3	-	-	-	-	-	-	-	-	-	-	-	-	-	-	-
Kln	-	-	-	-	-	1.4±0.7	-	-	-	-	-	-	-	-	-	-	-
Ms	9.5±0.8	5.1±0.7	6.3±0.8	3.8±0.8	25.7±1.0	56.9±1.2	33.4±1.1	-	-	-	-	-	-	-	-	-	8.3±2.3
Or	-	-	-	-	-	-	-	-	-	-	-	-	-	3.6±0.5	-	-	-
Pg	2.4±0.7	3.6±0.6	-	-	-	-	-	-	-	-	-	-	-	-	-	-	-
Phn	-	-	-	-	-	-	-	-	-	-	-	-	-	13.5±1.2	-	-	-
Py	-	4.9±0.3	-	-	0.4±0.1	-	-	-	-	-	-	-	-	-	-	-	-
Prl	-	-	-	-	-	-	-	-	-	-	-	-	-	-	-	-	-
Qtz	29.0±0.8	36.1±0.8	32.9±0.9	28.5±0.8	30.0±0.9	20.9±0.7	44.9±1.0	14.8±0.5	18.1±0.6	10.4±0.4	3.2±0.2	7.8±0.4	13.0±0.4	54.4±1.0	16.6±0.5	19.7±0.8	9.5±0.5
Rt	0.8±0.3	-	0.6±0.3	0.7±0.3	0.7±0.2	0.7±0.3	0.8±0.3	-	-	-	-	-	-	-	-	-	-
Sd	-	-	-	-	-	1.9±0.4	-	-	-	-	-	-	-	-	-	-	-
Sp	-	-	-	-	-	-	-	-	-	-	-	-	-	-	-	-	-
Ttn	-	-	-	-	-	-	-	2.6±0.5	3.0±0.5	2.9±0.5	2.1±0.4	2.5±0.4	2.6±0.4	-	1.8±0.6	2.2±0.5	2.5±0.6
Errors of measurements (in %; XRD):																	
R_{wp}	8.27	9.39	8.14	7.79	6.85	8.62	8.95	5.98	6.45	5.94	7.00	6.37	6.38	8.02	8.97	6.42	7.83
R_{exp}	5.25	4.70	5.21	4.99	4.11	5.34	5.40	4.03	4.13	3.76	3.79	3.84	3.96	4.32	4.20	4.01	3.73

Notes: Alb = albite, ank = ankerite, ap = apatite, cal = calcite, chl = chlorite, dol = dolomite, ep = epidote, gn = galena, hem = hematite, hbl = hornblende, im = intermediate Na/K mica, kln = kaolinite, ms = muscovite, or = orthoclase, pg = paragonite, phn = phengite, py = pyrite, prl = pyrophyllite, qtz = quartz, rt = rutile, sd = siderite, sp = sphalerite, ttn = titanite, - = not detected.

	WT23-261	WT23-282	WT23-295	WT23-322	WT23-343	WT23-368	WT23-391	WT23-399	WT23-406	WT23-411	WT23-416	WT23-422	WT23-430	WT23-436	WT23-443	WT23-450	WT23-455
Major minerals (weight %; XRD):																	
Alb	3.5±0.5	19.8±0.9	28.7±1.1	16.6±0.9	26.6±0.8	10.2±0.8	25.5±0.8	17.2±0.9	-	2.1±0.5	48.8±1.0	51.2±1.0	37.5±0.8	42.9±0.8	54.7±1.1	57.2±0.9	36.5±1.0
Ank	-	-	-	-	-	-	-	-	-	-	-	-	-	-	-	-	-
Ap	-	-	-	-	-	-	-	-	-	-	-	-	-	-	-	-	-
Cal	5.1±0.4	4.2±0.4	4.7±0.5	1.4±0.3	0.6±0.2	2.5±0.3	4.4±0.4	3.7±0.3	5.5±0.4	6.0±0.5	5.0±0.5	1.5±0.3	1.6±0.3	2.1±0.3	4.4±0.4	4.5±0.3	2.4±0.2
Chl	3.4±0.4	31.5±1.7	36.2±1.7	7.1±0.5	9.9±0.6	5.5±0.5	5.4±0.6	6.8±0.5	8.1±0.6	13.2±1.0	8.2±0.7	15.6±0.7	9.2±0.6	6.1±0.6	7.6±0.6	8.1±0.7	8.4±0.6
Dol	-	-	-	-	-	-	-	-	-	-	-	-	-	-	-	-	-
Ep	13.2±0.6	25.0±1.0	14.3±0.8	3.9±0.6	9.5±0.6	-	6.3±0.5	10.5±0.6	1.0±0.3	-	1.4±0.5	1.8±0.6	5.0±0.6	5.8±0.6	1.7±0.4	4.6±0.8	-
Gn	-	-	-	-	-	-	-	-	-	-	-	-	-	-	-	-	-
Hem	-	-	-	-	-	-	0.4±0.1	-	1.1±0.2	-	3.7±0.3	4.7±0.3	3.1±0.3	4.5±0.3	-	1.9±0.2	-
Hbl	-	-	-	-	-	-	-	-	-	-	-	-	-	-	-	-	-
Im	-	-	-	-	-	-	-	-	-	4.2±0.7	-	-	-	-	-	-	-
Kln	-	-	-	-	-	-	-	-	1.3±0.7	-	-	-	-	-	-	-	-
Ms	-	-	-	-	-	-	11.8±0.9	19.0±1.2	18.9±1.4	14.4±1.2	7.7±1.1	10.8±1.0	17.2±0.9	3.3±0.6	-	-	3.1±0.6
Or	-	-	-	1.6±0.6	-	-	-	-	-	-	-	-	-	-	-	-	-
Pg	-	-	-	-	-	-	-	4.9±0.6	11.0±0.7	14.4±0.5	-	-	-	0.7±0.2	9.0±1.4	-	14.2±1.7
Phn	28.8±0.8	-	-	22.6±1.0	9.7±0.9	30.2±0.8	-	-	-	-	-	-	-	-	-	-	-
Py	-	-	-	-	-	-	-	-	-	-	-	-	-	-	-	-	0.3±0.1
Prl	-	-	-	-	-	-	-	-	-	-	-	-	-	-	-	-	-
Qtz	46.0±0.8	17.1±0.6	14.5±0.6	46.8±0.9	43.7±0.8	51.6±0.8	45.9±0.8	37.9±0.8	52.4±1.0	45.7±0.9	24.6±0.6	13.7±0.5	25.9±0.6	33.9±0.7	22.6±0.6	22.8±0.6	34.7±0.9
Rt	-	-	-	-	-	-	0.3±0.2	-	0.7±0.2	-	0.6±0.2	0.7±0.3	0.5±0.2	0.7±0.2	-	0.9±0.2	0.4±0.2
Sd	-	-	-	-	-	-	-	-	-	-	-	-	-	-	-	-	-
Sp	-	-	-	-	-	-	-	-	-	-	-	-	-	-	-	-	-
Ttn	-	2.4±0.5	1.6±0.5	-	-	-	-	-	-	-	-	-	-	-	-	-	-
Errors of measurements (in %; XRD):																	
R_{wp}	7.60	6.49	6.50	7.66	6.70	8.05	6.97	7.07	8.92	8.67	7.14	7.11	6.70	6.86	6.65	8.19	6.54
R_{exp}	4.55	4.01	4.01	4.35	4.27	4.63	4.45	4.05	4.43	4.21	4.11	3.93	4.07	4.01	4.17	4.00	4.18

Notes: Alb = albite, ank = ankerite, ap = apatite, cal = calcite, chl = chlorite, dol = dolomite, ep = epidote, gn = galena, hem = hematite, hbl = hornblende, im = intermediate Na/K mica, kln = kaolinite, ms = muscovite, or = orthoclase, pg = paragonite, phn = phengite, py = pyrite, prl = pyrophyllite, qtz = quartz, rt = rutile, sd = siderite, sp = sphalerite, ttn = titanite, - = not detected.

	WT23-460	WT23-477	WT23-488	WT23-505	WT24-115	WT24-137	WT24-155	WT24-167	WT24-182	WT24-196	WT24-219	WT24-231	WT24-239	WT24-266	WT24-290	WT24-300	WT24-318
Major minerals (weight %; XRD):																	
Alb	-	-	-	-	34.4±0.8	71.6±0.7	41.7±1.1	35.7±1.1	41.5±1.1	1.3±0.5	41.3±1.1	47.0±1.2	47.6±1.1	5.7±0.5	9.4±0.9	58.1±0.8	29.6±1.0
Ank	-	-	-	-	-	-	-	-	-	-	-	-	-	-	-	-	-
Ap	-	-	-	-	-	-	-	-	-	-	-	-	0.7±0.2	-	-	-	-
Cal	-	1.2±0.3	-	-	1.3±0.2	1.2±0.3	0.6±0.2	0.5±0.3	4.1±0.4	10.7±0.5	1.6±0.3	3.1±0.3	1.4±0.3	2.7±0.3	1.9±0.2	0.6±0.3	4.6±0.4
Chl	8.4±0.8	-	-	6.0±0.7	8.6±0.6	8.5±0.6	24.8±1.0	35.1±1.6	25.2±1.0	5.7±0.5	39.8±1.3	24.9±1.6	30.9±1.3	5.1±0.5	10.6±0.6	11.3±0.7	30.4±0.9
Dol	-	-	-	-	-	-	-	-	-	-	-	-	-	-	-	-	-
Ep	-	-	-	-	-	-	9.5±0.6	5.3±0.6	19.5±0.9	-	6.6±0.7	2.3±0.5	-	-	7.2±0.6	-	17.2±0.7
Gn	-	-	-	-	-	-	-	-	-	-	-	-	-	-	-	-	-
Hem	-	-	-	-	-	-	-	-	-	-	-	-	-	-	-	-	-
Hbl	-	-	-	-	-	-	12.8±0.7	11.4±0.7	-	-	-	-	-	-	-	-	-
Im	5.0±0.9	-	-	-	-	-	-	-	-	-	-	-	-	-	-	-	-
Kln	-	-	-	-	-	-	-	-	-	-	-	-	-	-	-	-	-
Ms	5.1±0.8	39.2±1.0	33.6±1.0	30.7±1.0	-	-	-	-	4.1±0.9	-	-	-	-	-	-	-	-
Or	-	-	-	-	-	-	-	-	-	-	-	-	-	-	-	-	-
Pg	15.8±0.8	-	-	-	-	-	-	-	-	-	-	-	-	-	-	-	-
Phn	-	-	-	-	16.7±0.9	-	-	-	-	36.6±0.9	-	-	-	27.5±0.8	19.7±0.9	-	-
Py	17.3±0.4	11.1±0.4	10.3±0.3	21.4±0.4	-	-	-	-	-	0.5±0.2	-	-	-	-	-	-	-
Prl	-	-	-	-	-	-	-	-	-	-	-	-	-	-	-	-	-
Qtz	47.6±0.8	47.3±1.0	55.2±0.9	41.4±0.7	39.0±0.7	18.7±0.5	7.7±0.3	9.1±0.4	4.6±0.4	45.2±0.8	7.2±0.3	19.1±0.6	15.5±0.5	59.0±0.8	51.2±1.0	30.0±0.6	16.0±0.5
Rt	0.8±0.3	1.2±0.3	0.9±0.3	0.5±0.2	-	-	-	-	-	-	-	-	-	-	-	-	-
Sd	-	-	-	-	-	-	-	-	-	-	-	-	-	-	-	-	-
Sp	-	-	-	-	-	-	-	-	-	-	-	-	-	-	-	-	-
Ttn	-	-	-	-	-	-	2.9±0.5	2.9±0.5	1.0±0.3	-	3.5±0.4	3.6±0.5	3.9±0.4	-	-	-	2.2±0.5
Errors of measurements (in %; XRD):																	
R_{wp}	7.99	8.98	9.40	8.40	7.25	8.21	6.32	6.29	8.11	8.26	6.74	6.58	6.70	8.01	7.31	8.27	6.66
R_{exp}	5.12	5.45	5.43	4.91	4.09	3.96	3.86	3.86	3.84	4.57	3.88	3.86	3.83	4.72	4.36	3.95	4.03

Notes: Alb = albite, ank = ankerite, ap = apatite, cal = calcite, chl = chlorite, dol = dolomite, ep = epidote, gn = galena, hem = hematite, hbl = hornblende, im = intermediate Na/K mica, kln = kaolinite, ms = muscovite, or = orthoclase, pg = paragonite, phn = phengite, py = pyrite, prl = pyrophyllite, qtz = quartz, rt = rutile, sd = siderite, sp = sphalerite, ttn = titanite, - = not detected.

	WT24-327	WT24-351	WT24-356	WT24-370	WT24-383	WT24-393	WT24-396	WT24-405	WT24-415	WT24-433	WT24-441	WT24-456	WT24-470	WT24-488	WT24-497	WT24-516	WT24-534
Major minerals (weight %; XRD):																	
Alb	8.4±0.5	9.3±0.8	32.0±0.8	56.6±0.9	41.5±1.3	31.3±0.8	2.9±0.5	57.1±1.0	51.2±1.4	36.0±1.1	33.3±0.8	35.2±0.9	36.2±0.9	13.6±1.3	40.8±0.9	-	-
Ank	-	-	-	-	-	-	-	-	-	-	-	-	-	-	-	-	-
Ap	-	-	-	-	-	-	-	-	-	-	-	-	-	-	-	-	-
Cal	2.9±0.3	3.3±0.3	3.8±0.3	2.0±0.3	1.9±0.2	4.5±0.4	1.3±0.3	3.3±0.3	1.4±0.3	1.0±0.2	0.4±0.2	0.8±0.3	1.7±0.3	4.1±0.4	3.9±0.3	6.2±0.5	-
Chl	14.2±0.6	5.1±0.5	7.1±0.5	6.6±0.6	11.3±2.3	7.2±0.6	8.0±0.6	6.6±0.7	10.4±0.9	20.4±1.9	6.2±0.6	11.6±0.7	11.4±0.7	3.3±0.6	4.8±0.7	4.4±0.9	-
Dol	-	-	-	-	-	-	-	-	-	-	-	-	-	-	-	-	-
Ep	-	-	9.2±0.6	7.4±0.7	3.4±0.6	6.3±0.6	-	3.6±0.6	5.8±0.7	2.3±0.5	19.9±0.6	6.0±0.7	4.3±0.7	15.7±0.8	4.4±0.7	-	-
Gn	-	-	-	-	-	-	-	-	-	-	-	-	-	-	-	-	-
Hem	-	-	-	2.9±0.3	2.8±0.2	-	-	3.4±0.3	3.3±0.3	-	0.9±0.2	2.5±0.2	1.1±0.2	-	-	-	-
Hbl	-	-	-	-	-	-	-	-	-	-	-	-	-	-	-	-	-
Im	-	-	-	-	-	-	-	-	-	-	-	-	-	7.2±0.6	-	5.9±0.6	-
Kln	-	-	-	-	-	-	-	-	-	-	-	-	-	-	-	-	-
Ms	-	-	18.2±0.9	-	6.1±0.9	20.7±1.0	-	4.1±1.1	4.5±2.3	5.2±0.6	3.4±1.1	16.8±1.0	10.5±1.1	3.8±0.8	2.3±0.4	12.7±0.9	43.3±1.1
Or	-	-	-	-	-	-	-	-	-	-	-	-	-	-	-	-	-
Pg	-	-	-	-	-	-	-	-	-	-	-	-	-	11.4±0.8	-	15.2±0.8	-
Phn	30.4±0.8	25.6±0.8	-	-	-	-	34.9±0.8	-	-	-	-	-	-	-	-	-	-
Py	-	-	-	-	-	-	-	-	-	0.2±0.1	-	-	-	2.6±0.3	1.5±0.2	5.0±0.4	11.3±0.4
Prl	-	-	-	-	-	-	-	-	-	-	-	-	-	-	-	-	-
Qtz	43.5±0.8	56.7±0.9	29.7±0.6	24.1±0.5	32.4±1.1	30.0±0.7	52.3±0.8	21.5±0.5	22.8±0.8	34.4±1.1	35.5±0.7	26.0±0.6	34.1±0.8	38.3±1.0	42.3±0.9	50.0±1.0	44.3±0.9
Rt	0.6±0.2	-	-	0.4±0.2	0.6±0.2	-	0.6±0.3	0.4±0.2	0.6±0.2	0.5±0.2	0.4±0.2	1.1±0.2	0.7±0.2	-	-	0.6±0.3	1.1±0.3
Sd	-	-	-	-	-	-	-	-	-	-	-	-	-	-	-	-	-
Sp	-	-	-	-	-	-	-	-	-	-	-	-	-	-	-	-	-
Ttn	-	-	-	-	-	-	-	-	-	-	-	-	-	-	-	-	-
Errors of measurements (in %; XRD):																	
Rwp	7.99	7.76	7.00	7.45	6.71	7.01	8.35	7.23	7.08	7.04	6.95	6.87	7.45	8.43	8.00	11.91	11.08
Rexp	4.38	4.63	4.27	4.08	4.01	4.22	4.44	3.87	3.80	3.92	4.21	3.85	3.89	4.31	4.06	5.22	5.22

Notes: Alb = albite, ank = ankerite, ap = apatite, cal = calcite, chl = chlorite, dol = dolomite, ep = epidote, gn = galena, hem = hematite, hbl = hornblende, im = intermediate Na/K mica, kln = kaolinite, ms = muscovite, or = orthoclase, pg = paragonite, phn = phengite, py = pyrite, prl = pyrophyllite, qtz = quartz, rt = rutile, sd = siderite, sp = sphalerite, ttn = titanite, - = not detected.

	WT25-97	WT25-110	WT25-126	WT25-139	WT25-162	WT25-174	WT25-198	WT25-228	WT25-242	WT25-265	WT25-280	WT25-296	WT25-318	WT25-328	WT25-339	WT25-357	WT25-372
Major minerals (weight %; XRD):																	
Alb	27.9±1.0	33.2±1.0	55.9±0.8	45.5±0.9	10.5±0.8	27.5±0.8	36.6±1.2	19.7±1.0	24.0±1.0	26.7±1.3	23.5±1.0	22.2±1.3	-	-	22.3±1.3	1.3±0.5	51.4±1.0
Ank	-	-	-	-	-	-	-	-	-	-	-	-	-	-	-	-	-
Ap	-	-	-	-	-	-	-	-	-	-	-	-	-	-	-	-	0.3±0.2
Cal	2.4±0.3	3.6±0.3	4.5±0.4	2.9±0.4	2.4±0.2	1.0±0.2	1.3±0.2	6.5±0.5	3.8±0.4	1.9±0.3	1.9±0.3	1.4±0.2	4.7±0.4	3.4±0.3	6.5±0.6	4.1±0.4	7.5±0.5
Chl	36.5±1.0	7.9±1.4	9.6±0.6	14.7±0.8	5.0±0.5	5.4±0.6	34.6±1.9	29.9±1.7	23.8±1.7	32.8±2.6	27.6±1.7	33.3±2.7	5.9±0.6	2.7±0.5	24.8±4.2	4.4±0.5	19.9±0.8
Dol	-	-	-	-	-	-	-	-	-	-	-	-	-	-	-	-	-
Ep	16.3±0.8	4.6±0.6	-	5.9±0.7	11.0±0.6	22.7±0.7	7.8±0.7	22.7±0.9	24.0±0.9	30.0±1.5	21.2±0.8	19.3±1.1	-	-	-	-	-
Gn	-	-	-	-	-	-	-	-	-	-	-	-	-	-	-	-	-
Hem	-	-	-	-	-	-	-	-	-	-	-	-	-	-	-	-	-
Hbl	-	-	-	-	-	-	-	-	-	-	11.3±0.7	3.9±0.6	-	-	-	-	-
Im	-	-	-	-	-	-	-	-	-	-	-	-	-	-	-	-	-
Kln	-	-	-	-	-	-	-	-	-	-	-	-	-	-	-	-	-
Ms	-	-	-	-	-	-	-	-	5.9±1.3	-	-	-	-	-	-	-	-
Or	-	-	-	-	-	-	-	-	-	-	-	-	-	-	-	-	-
Pg	-	-	-	-	-	-	-	-	-	-	-	-	-	-	-	-	-
Phn	-	22.1±1.2	-	-	20.0±0.9	13.7±1.1	-	-	-	-	-	-	31.6±0.9	38.7±0.7	18.6±2.0	31.1±0.8	-
Py	-	-	-	-	-	-	-	-	-	-	-	-	-	-	-	-	-
Prl	-	-	-	-	-	-	-	-	-	-	-	-	-	-	-	-	-
Qtz	13.8±0.4	28.6±0.8	28.4±0.6	28.7±0.6	48.9±0.8	28.8±0.6	19.7±0.8	19.7±0.7	17.2±0.7	6.9±0.4	12.3±0.5	18.0±0.9	57.8±0.8	55.2±0.7	27.8±1.7	59.1±0.8	19.1±0.5
Rt	-	-	-	-	-	-	-	-	-	-	-	-	-	-	-	-	-
Sd	-	-	-	-	-	-	-	-	-	-	-	-	-	-	-	-	-
Sp	-	-	-	-	-	-	-	-	-	-	-	-	-	-	-	-	-
Ttn	3.1±0.4	-	1.6±0.5	2.3±0.5	2.2±0.6	0.9±0.4	-	1.5±0.5	1.3±0.4	1.7±0.5	2.2±0.3	1.9±0.5	-	-	-	-	1.8±0.6
Errors of measurements (in %; XRD):																	
Rwp	6.57	7.05	7.33	7.52	6.40	6.30	7.07	6.85	6.58	7.08	6.21	6.99	8.34	8.39	6.82	8.43	7.45
Rexp	3.91	4.28	4.15	3.92	4.29	4.31	3.77	4.22	4.16	4.14	4.05	4.89	4.55	4.56	3.93	4.63	3.96

Notes: Alb = albite, ank = ankerite, ap = apatite, cal = calcite, chl = chlorite, dol = dolomite, ep = epidote, gn = galena, hem = hematite, hbl = hornblende, im = intermediate Na/K mica, kln = kaolinite, ms = muscovite, or = orthoclase, pg = paragonite, phn = phengite, py = pyrite, prl = pyrophyllite, qtz = quartz, rt = rutile, sd = siderite, sp = sphalerite, ttn = titanite, - = not detected.

	WT25-386	WT25-401	WT25-408	WT25-417	WT25-418	WT25-423	WT25-428	WT25-434	WT25-441	WT25-444	WT25-458	WT25-478	WT29-133	WT35-306	WT35-309	WT35-310	WT35-312
Major minerals (weight %; XRD):																	
Alb	11.6±0.6	20.8±0.9	13.2±0.8	94.0±0.5	45.7±1.0	31.8±1.1	-	-	16.9±3.3	-	-	-	-	58.9±1.3	92.3±0.7	29.0±0.7	49.6±1.0
Ank	-	-	-	-	-	-	-	-	-	-	-	-	-	-	-	-	-
Ap	-	-	-	-	-	-	-	-	-	-	-	-	-	-	-	-	-
Cal	1.4±0.3	5.6±0.4	1.2±0.2	2.6±0.3	8.3±0.5	3.1±0.4	7.9±0.5	6.5±0.5	1.3±0.3	4.3±0.4	-	-	17.2±0.5	1.4±0.3	2.6±0.3	2.2±0.2	5.2±0.5
Chl	14.2±0.7	5.8±0.6	11.2±0.6	-	8.5±0.6	10.2±0.7	8.1±0.8	8.1±0.8	2.7±0.7	2.9±1.1	-	5.6±0.8	3.1±0.5	6.8±0.7	1.3±0.6	4.0±0.6	1.9±0.6
Dol	-	-	-	-	-	-	-	-	-	-	-	-	-	-	-	-	-
Ep	-	-	-	-	-	-	-	-	-	-	-	-	-	-	-	-	1.4±0.7
Gn	-	-	-	-	-	-	-	-	-	-	-	-	-	-	-	-	-
Hem	-	-	-	2.0±0.2	-	-	-	-	-	-	-	-	-	-	2.6±0.2	0.3±0.1	5.0±0.3
Hbl	-	-	-	-	-	-	-	-	-	-	-	-	-	-	-	-	-
Im	-	-	-	-	-	-	-	-	6.0±1.0	8.5±0.6	10.1±0.8	-	-	-	-	-	1.2±0.4
Kln	-	-	-	-	-	-	-	-	-	-	-	-	-	-	-	-	-
Ms	-	-	-	-	-	32.3±1.2	29.8±0.9	18.7±0.8	5.2±0.8	8.5±0.9	28.0±1.2	43.8±1.1	9.9±0.6	7.9±1.8	-	-	18.6±1.0
Or	-	-	-	-	-	-	-	-	-	-	-	-	-	-	-	-	-
Pg	-	-	-	-	-	-	5.5±0.7	7.0±0.7	12.7±1.0	12.1±0.8	4.3±0.5	-	9.8±0.5	-	-	-	9.8±0.6
Phn	39.1±1.0	34.8±0.9	33.3±0.9	-	8.6±1.1	-	-	-	-	-	-	-	-	-	-	-	-
Py	0.9±0.2	-	-	-	-	-	-	-	9.4±0.5	12.2±0.4	9.1±0.4	11.1±0.4	-	-	-	-	-
Prl	-	-	-	-	-	-	-	-	-	-	-	-	-	-	-	-	-
Qtz	32.1±0.7	32.6±0.7	40.5±0.7	1.4±0.2	28.9±0.7	21.5±0.7	47.8±1.0	58.9±1.0	44.7±1.7	50.1±1.1	46.7±1.0	38.5±0.8	60.0±0.8	25.0±0.7	0.6±0.2	64.5±0.8	6.7±0.4
Rt	0.7±0.3	0.4±0.2	0.6±0.2	-	-	1.1±0.2	0.9±0.3	0.8±0.4	1.1±0.4	1.4±0.3	1.8±0.3	1.0±0.3	-	-	0.6±0.3	-	0.6±0.2
Sd	-	-	-	-	-	-	-	-	-	-	-	-	-	-	-	-	-
Sp	-	-	-	-	-	-	-	-	-	-	-	-	-	-	-	-	-
Ttn	-	-	-	-	-	-	-	-	-	-	-	-	-	-	-	-	-
Errors of measurements (in %; XRD):																	
Rwp	8.36	7.41	7.24	8.85	7.76	7.86	9.61	9.82	8.48	9.33	9.88	8.72	7.85	7.59	8.49	7.35	7.27
Rexp	4.03	4.34	4.15	4.06	4.05	5.36	5.69	5.49	5.59	5.58	5.70	5.57	4.46	4.03	4.12	4.31	4.18

Notes: Alb = albite, ank = ankerite, ap = apatite, cal = calcite, chl = chlorite, dol = dolomite, ep = epidote, gn = galena, hem = hematite, hbl = hornblende, im = intermediate Na/K mica, kln = kaolinite, ms = muscovite, or = orthoclase, pg = paragonite, phn = phengite, py = pyrite, prl = pyrophyllite, qtz = quartz, rt = rutile, sd = siderite, sp = sphalerite, ttn = titanite, - = not detected.

	WT2-280											WT2-338					
	1	2	3	4	5	6	7	8	9	10	11	1	2	3	4	5	6
Major elements (weight %; EMP):																	
SiO_2	46.37	49.34	49.55	49.45	47.07	49.44	49.55	47.23	49.10	50.57	53.43	47.90	48.61	48.30	45.78	48.21	47.54
TiO_2	0.08	0.45	0.28	ND	0.31	ND	0.06	1.12	0.15	0.10	0.38	0.18	0.47	0.43	0.20	1.33	0.42
Al_2O_3	35.32	32.65	30.54	30.59	32.66	31.53	31.89	34.92	30.52	27.72	27.30	31.95	31.67	30.97	35.58	31.14	34.86
Cr_2O_3	ND	0.11	ND	ND	ND	ND	ND	ND	ND	0.05	ND	ND	0.09	0.07	ND	0.05	0.09
FeO	2.02	1.31	2.37	2.49	2.63	2.13	2.02	1.16	2.59	4.46	2.50	1.69	2.23	3.16	1.30	2.54	0.16
V_2O_3	ND	0.09	ND	ND	ND	ND	ND	ND	ND	ND	0.07	ND	ND	ND	ND	0.09	0.72
MnO	0.07	ND	0.16	ND	0.06	ND	ND	0.07	0.05	0.09	ND	ND	ND	0.06	ND	ND	ND
MgO	0.61	1.99	2.19	2.17	1.76	2.12	1.59	1.21	2.30	2.64	2.14	1.78	1.87	2.08	0.41	1.70	1.32
CaO	ND	ND	ND	ND	ND	ND	ND	ND	ND	ND	0.12	ND	ND	ND	ND	ND	ND
BaO	0.34	0.25	0.19	0.29	ND	0.13	0.07	ND	ND	0.34	0.07	0.31	0.37	0.15	0.09	0.19	ND
Na_2O	0.43	0.34	0.06	0.09	0.52	0.15	0.32	0.33	0.13	0.10	1.56	0.30	0.21	0.18	0.37	0.23	0.40
K_2O	10.79	10.53	10.78	11.03	9.73	11.65	10.91	10.88	11.41	10.89	8.27	10.65	10.88	10.68	10.74	10.80	10.61
F	0.14	0.11	0.11	0.12	0.16	0.23	0.11	ND	0.20	0.18	0.11	0.26	0.32	0.26	0.09	0.31	0.22
Cl	ND	ND	ND	ND	ND	ND	ND	ND	ND	ND	ND	ND	ND	ND	ND	ND	ND
H_2O^+	4.44	4.54	4.47	4.46	4.39	4.45	4.50	4.58	4.41	4.42	4.53	4.34	4.37	4.37	4.42	4.36	4.46
-O≡F	0.06	0.05	0.05	0.05	0.07	0.10	0.05	ND	0.08	0.08	0.05	0.11	0.13	0.11	0.04	0.13	0.09
-O≡Cl	ND	ND	ND	ND	ND	ND	ND	ND	ND	ND	ND	ND	ND	ND	ND	ND	ND
Total	100.55	101.67	100.65	100.63	99.23	101.73	100.97	101.50	100.78	101.48	100.43	99.25	100.96	100.60	98.94	100.82	100.71
Number of atoms (apfu):																	
Si	6.17	6.44	6.57	6.57	6.32	6.51	6.53	6.19	6.53	6.73	7.00	6.43	6.44	6.44	6.15	6.41	6.24
Al^{IV}	1.83	1.56	1.43	1.43	1.68	1.49	1.47	1.81	1.47	1.27	1.00	1.57	1.56	1.56	1.85	1.59	1.76
Al^{VI}	3.71	3.46	3.34	3.36	3.48	3.40	3.48	3.58	3.31	3.08	3.21	3.49	3.39	3.31	3.79	3.29	3.64
Ti	0.01	0.04	0.03	ND	0.03	ND	0.01	0.11	0.02	0.01	0.04	0.02	0.05	0.04	0.02	0.13	0.04
Cr	ND	0.01	ND	ND	ND	ND	ND	ND	ND	0.01	ND	ND	0.01	0.01	ND	0.01	0.01
Fe^{2+}	0.22	0.14	0.26	0.28	0.30	0.23	0.22	0.13	0.29	0.50	0.27	0.19	0.25	0.35	0.15	0.28	0.02
V	ND	0.01	ND	ND	ND	ND	ND	ND	ND	ND	0.01	ND	ND	ND	ND	0.01	0.08
Mn^{2+}	0.01	ND	0.02	ND	0.01	ND	ND	0.01	0.01	0.01	ND	ND	ND	0.01	ND	ND	ND
Mg	0.12	0.39	0.43	0.43	0.35	0.42	0.31	0.24	0.46	0.52	0.42	0.36	0.37	0.41	0.08	0.34	0.26
Ca	ND	ND	ND	ND	ND	ND	ND	ND	ND	ND	0.02	ND	ND	ND	ND	ND	ND
Na	0.11	0.09	0.02	0.02	0.14	0.04	0.08	0.08	0.03	0.03	0.40	0.08	0.05	0.05	0.10	0.06	0.10
K	1.83	1.75	1.82	1.87	1.67	1.96	1.83	1.82	1.94	1.85	1.38	1.82	1.84	1.82	1.84	1.83	1.78
Ba	0.02	0.01	0.01	0.02	ND	0.01	< 0.01	ND	ND	0.02	<0.01	0.02	0.02	0.01	<0.01	0.01	ND
F	0.06	0.05	0.05	0.05	0.07	0.10	0.05	ND	0.08	0.08	0.05	0.11	0.13	0.11	0.04	0.13	0.09
Cl	ND	ND	ND	ND	ND	ND	ND	ND	ND	ND	ND	ND	ND	ND	ND	ND	ND
OH	3.94	3.95	3.95	3.95	3.93	3.90	3.95	4.00	3.92	3.92	3.95	3.89	3.87	3.89	3.96	3.87	3.91

Notes: Formulas are calculated on the basis of 22 oxygen equivalents. All iron is given as ferric iron. H_2O^+ is calculated. ND = not detected.

	WT2-338			WT9A-254													
	7	8	9	1	2	3	4	5	6	7	8	9	10	11	12	13	14
Major elements (weight %; EMP):																	
SiO_2	49.02	48.88	48.13	46.75	43.16	47.31	44.89	46.83	45.92	46.31	46.78	44.43	44.63	46.81	43.45	46.65	47.62
TiO_2	0.40	0.25	0.62	ND	ND	ND	ND	ND	ND	ND	ND	0.07	0.05	ND	0.13	0.05	ND
Al_2O_3	31.21	30.62	30.14	37.49	41.51	35.68	38.87	34.72	34.49	33.63	36.84	39.09	36.89	36.44	36.72	34.65	32.98
Cr_2O_3	ND	0.07	ND	ND	ND	ND	ND	ND	ND	ND	0.05	ND	ND	ND	ND	ND	ND
FeO	2.30	2.36	2.64	0.88	0.61	1.55	1.22	1.68	1.58	1.96	1.03	0.97	1.43	0.96	0.87	1.64	1.48
V_2O_3	ND	ND	ND	ND	ND	ND	ND	ND	ND	ND	ND	ND	0.18	ND	ND	0.08	ND
MnO	ND	ND	ND	ND	ND	ND	ND	ND	ND	ND	ND	ND	ND	ND	ND	ND	ND
MgO	2.03	2.00	1.79	0.34	0.20	0.71	0.40	0.88	0.56	0.98	0.47	0.39	0.47	0.52	0.34	0.71	0.97
CaO	ND	ND	ND	0.15	3.30	0.16	1.55	0.06	0.11	0.08	0.36	1.27	0.76	0.29	0.72	0.06	0.07
BaO	0.19	0.34	0.26	0.62	0.37	0.60	0.77	1.06	0.69	0.84	0.49	0.67	0.83	0.30	0.85	0.61	0.29
Na_2O	0.14	0.21	0.25	3.93	3.75	2.15	2.97	1.65	1.96	1.17	3.06	3.93	1.99	2.44	2.97	1.24	0.94
K_2O	11.18	10.95	10.44	4.20	2.45	6.92	5.00	7.95	7.34	8.23	5.27	3.72	7.01	6.05	4.87	8.19	8.58
F	0.25	0.34	0.26	0.12	0.12	0.16	0.19	0.24	0.21	0.31	0.20	0.17	0.20	0.22	0.14	0.24	0.32
Cl	ND	ND	ND	ND	ND	ND	ND	ND	ND	ND	ND	ND	ND	ND	ND	ND	ND
H_2O^+	4.41	4.33	4.30	4.52	4.56	4.47	4.49	4.38	4.31	4.27	4.46	4.48	4.38	4.43	4.30	4.35	4.29
-O≡F	0.11	0.14	0.11	0.05	0.05	0.07	0.08	0.10	0.09	0.13	0.08	0.07	0.08	0.09	0.06	0.10	0.13
-O≡Cl	ND	ND	ND	ND	ND	ND	ND	ND	ND	ND	ND	ND	ND	ND	ND	ND	ND
Total	101.02	100.20	98.72	98.95	99.98	99.65	100.27	99.35	97.09	97.65	98.93	99.12	98.74	98.37	95.31	98.37	97.40
Number of atoms (apfu):																	
Si	6.49	6.53	6.52	6.13	5.61	6.23	5.87	6.25	6.24	6.29	6.15	5.84	5.98	6.19	5.96	6.26	6.44
Al^{IV}	1.51	1.47	1.48	1.87	2.39	1.77	2.13	1.75	1.76	1.71	1.85	2.16	2.02	1.81	2.04	1.74	1.56
Al^{VI}	3.36	3.35	3.34	3.91	3.96	3.78	3.87	3.71	3.76	3.67	3.87	3.90	3.80	3.88	3.90	3.74	3.69
Ti	0.04	0.03	0.06	ND	ND	ND	ND	ND	ND	ND	ND	0.01	0.01	ND	0.01	0.01	ND
Cr	ND	0.01	ND	ND	ND	ND	ND	ND	ND	ND	0.01	ND	ND	ND	ND	ND	ND
Fe^{2+}	0.25	0.26	0.30	0.10	0.07	0.17	0.13	0.19	0.18	0.22	0.11	0.11	0.16	0.11	0.10	0.18	0.17
V	ND	ND	ND	ND	ND	ND	ND	ND	ND	ND	ND	ND	0.02	ND	ND	0.01	ND
Mn^{2+}	ND	ND	ND	ND	ND	ND	ND	ND	ND	ND	ND	ND	ND	ND	ND	ND	ND
Mg	0.40	0.40	0.36	0.07	0.04	0.14	0.08	0.17	0.11	0.20	0.09	0.08	0.09	0.10	0.07	0.14	0.20
Ca	ND	ND	ND	0.02	0.46	0.02	0.22	0.01	0.02	0.01	0.05	0.18	0.11	0.04	0.11	0.01	0.01
Na	0.04	0.05	0.07	1.00	0.94	0.55	0.75	0.43	0.52	0.31	0.78	1.00	0.52	0.63	0.79	0.32	0.25
K	1.89	1.87	1.80	0.70	0.41	1.16	0.83	1.35	1.27	1.43	0.88	0.62	1.20	1.02	0.85	1.40	1.48
Ba	0.01	0.02	0.01	0.03	0.02	0.03	0.04	0.06	0.04	0.04	0.03	0.03	0.04	0.02	0.05	0.03	0.02
F	0.10	0.14	0.11	0.05	0.05	0.07	0.08	0.10	0.09	0.13	0.08	0.07	0.08	0.09	0.06	0.10	0.14
Cl	ND	ND	ND	ND	ND	ND	ND	ND	ND	ND	ND	ND	ND	ND	ND	ND	ND
OH	3.90	3.86	3.89	3.95	3.95	3.93	3.92	3.90	3.91	3.87	3.92	3.93	3.92	3.91	3.94	3.90	3.86

Notes: Formulas are calculated on the basis of 22 oxygen equivalents. All iron is given as ferric iron. H_2O^+ is calculated. ND = not detected.

	WT9A-254																
	15	16	17	18	19	20	21	22	23	24	25	26	27	28	29	30	31
Major elements (weight %; EMP):																	
SiO_2	43.86	47.16	44.98	46.43	45.43	46.40	42.80	45.59	46.34	46.32	47.77	47.24	44.89	43.46	46.52	45.51	43.10
TiO_2	ND	0.06	ND	ND	ND	ND	0.07	ND	ND	ND	ND	ND	ND	ND	ND	ND	0.06
Al_2O_3	39.53	37.07	39.87	33.99	34.23	38.92	38.89	35.21	35.90	33.92	33.19	35.91	37.60	40.10	35.27	36.75	40.24
Cr_2O_3	ND	ND	ND	ND	ND	ND	ND	ND	ND	ND	ND	ND	ND	ND	ND	ND	ND
FeO	0.66	1.19	0.56	1.71	1.77	0.63	0.53	1.63	1.42	1.97	1.59	1.26	1.02	0.69	1.16	0.96	0.74
V_2O_3	0.40	ND	ND	0.05	ND	0.11	ND	0.18	ND	ND	ND	0.22	0.06	0.07	0.20	ND	ND
MnO	ND	ND	ND	ND	ND	ND	ND	ND	ND	ND	ND	ND	ND	ND	ND	ND	ND
MgO	0.18	0.40	0.17	0.81	0.73	0.20	0.24	0.70	0.67	0.87	0.89	0.64	0.31	0.23	0.57	0.37	0.30
CaO	2.40	0.39	2.00	0.17	0.22	1.00	2.30	0.16	0.38	ND	ND	0.31	1.25	2.80	0.07	0.26	3.50
BaO	0.62	0.79	0.38	0.57	0.71	0.41	0.32	1.00	0.70	1.08	0.48	0.59	0.71	0.52	0.41	0.45	0.54
Na_2O	3.71	2.43	4.07	1.45	1.33	4.92	3.96	1.58	2.43	1.02	1.07	2.07	3.31	3.71	2.30	3.44	3.41
K_2O	2.93	6.30	2.48	8.01	7.99	2.29	2.67	7.77	6.08	8.62	8.29	7.29	4.34	2.70	6.82	4.98	2.51
F	0.12	0.18	0.13	0.29	0.27	0.12	0.14	0.17	0.25	0.22	0.28	0.25	0.11	0.15	0.18	0.11	0.15
Cl	ND	ND	ND	ND	ND	ND	ND	ND	ND	ND	ND	ND	ND	ND	ND	ND	ND
H_2O^+	4.50	4.51	4.54	4.29	4.26	4.58	4.39	4.37	4.39	4.32	4.32	4.45	4.45	4.49	4.39	4.43	4.49
-O≡F	0.05	0.08	0.05	0.12	0.11	0.05	0.06	0.07	0.11	0.09	0.12	0.11	0.05	0.06	0.08	0.05	0.06
-O≡Cl	ND	ND	ND	ND	ND	ND	ND	ND	ND	ND	ND	ND	ND	ND	ND	ND	ND
Total	98.86	100.41	99.13	97.65	96.82	99.53	96.25	98.28	98.45	98.25	97.76	100.12	98.01	98.86	97.82	97.21	98.98
Number of atoms (apfu):																	
Si	5.77	6.15	5.86	6.28	6.21	6.00	5.76	6.15	6.17	6.27	6.43	6.21	5.98	5.71	6.23	6.09	5.67
Al^{IV}	2.23	1.85	2.14	1.72	1.79	2.00	2.24	1.85	1.83	1.73	1.57	1.79	2.02	2.29	1.77	1.91	2.33
Al^{VI}	3.90	3.85	3.97	3.70	3.73	3.94	3.93	3.75	3.80	3.69	3.70	3.77	3.88	3.93	3.80	3.89	3.90
Ti	ND	0.01	ND	ND	ND	ND	0.01	ND	ND	ND	ND	ND	ND	ND	ND	ND	0.01
Cr	ND	ND	ND	ND	ND	ND	ND	ND	ND	ND	ND	ND	ND	ND	ND	ND	ND
Fe^{2+}	0.07	0.13	0.06	0.19	0.20	0.07	0.06	0.18	0.16	0.22	0.18	0.14	0.11	0.08	0.13	0.11	0.08
V	0.04	ND	ND	0.01	ND	0.01	ND	0.02	ND	ND	ND	0.02	0.01	0.01	0.02	ND	ND
Mn^{2+}	ND	ND	ND	ND	ND	ND	ND	ND	ND	ND	ND	ND	ND	ND	ND	ND	ND
Mg	0.04	0.08	0.03	0.16	0.15	0.04	0.05	0.14	0.13	0.18	0.18	0.13	0.06	0.05	0.11	0.07	0.06
Ca	0.34	0.05	0.28	0.02	0.03	0.14	0.33	0.02	0.05	ND	ND	0.04	0.18	0.39	0.01	0.04	0.49
Na	0.95	0.61	1.03	0.38	0.35	1.23	1.03	0.41	0.63	0.27	0.28	0.53	0.85	0.95	0.60	0.89	0.87
K	0.49	1.05	0.41	1.38	1.39	0.38	0.46	1.34	1.03	1.49	1.42	1.22	0.74	0.45	1.17	0.85	0.42
Ba	0.03	0.04	0.02	0.03	0.04	0.02	0.02	0.05	0.04	0.06	0.03	0.03	0.04	0.03	0.02	0.02	0.03
F	0.05	0.07	0.05	0.12	0.12	0.05	0.06	0.07	0.11	0.09	0.12	0.10	0.05	0.06	0.08	0.05	0.06
Cl	ND	ND	ND	ND	ND	ND	ND	ND	ND	ND	ND	ND	ND	ND	ND	ND	ND
OH	3.95	3.93	3.95	3.88	3.88	3.95	3.94	3.93	3.89	3.91	3.88	3.90	3.95	3.94	3.92	3.95	3.94

Notes: Formulas are calculated on the basis of 22 oxygen equivalents. All iron is given as ferric iron. H_2O^+ is calculated. ND = not detected.

	WT9A-254								WT22-109								
	32	33	34	35	36	37	38	39	1	2	3	4	5	6	7	8	9
Major elements (weight %; EMP):																	
SiO_2	45.28	42.14	47.51	45.77	44.67	46.50	43.43	44.74	46.46	47.21	48.22	48.14	47.45	47.63	47.88	47.17	47.02
TiO_2	0.08	0.10	0.05	ND	ND	ND	0.09	ND	0.07	0.11	ND	ND	ND	0.09	0.09	ND	0.05
Al_2O_3	38.45	40.24	34.49	36.87	39.73	37.16	38.13	36.27	37.26	37.75	37.69	37.45	36.83	36.78	35.68	36.42	38.08
Cr_2O_3	ND	ND	ND	ND	ND	ND	ND	ND	ND	ND	ND	ND	0.05	ND	0.07	ND	ND
FeO	1.14	0.68	1.72	1.10	0.72	1.04	0.92	0.99	1.33	0.71	0.69	0.74	0.67	0.85	0.95	0.76	0.47
V_2O_3	0.11	ND	ND	ND	ND	ND	ND	0.08	ND	ND	ND	0.13	0.09	ND	0.07	0.06	ND
MnO	ND	ND	ND	ND	ND	ND	ND	ND	ND	ND	ND	ND	ND	ND	0.12	0.12	ND
MgO	0.40	0.20	1.08	0.56	0.22	0.46	0.38	0.34	0.85	0.34	0.41	0.45	0.50	0.42	0.72	0.47	0.51
CaO	0.75	2.48	0.08	0.69	1.57	0.88	1.44	0.46	0.49	0.61	0.22	0.22	0.13	ND	0.08	0.47	0.60
BaO	0.75	0.66	0.69	0.57	0.50	0.68	0.79	0.49	0.37	0.18	ND	0.18	0.20	0.25	0.30	0.34	0.24
Na_2O	3.18	3.96	1.07	2.65	4.32	3.11	2.98	3.44	2.08	2.33	2.44	1.97	1.16	1.01	1.13	1.81	2.62
K_2O	5.45	2.94	8.37	5.62	2.68	4.74	4.79	4.68	7.07	6.68	6.91	7.66	9.23	9.46	9.24	7.30	6.37
F	0.17	0.15	0.37	0.19	0.15	0.15	0.14	0.12	ND	ND	ND	0.06	0.11	0.07	0.07	ND	ND
Cl	ND	ND	ND	ND	ND	ND	ND	ND	ND	ND	ND	ND	ND	ND	ND	ND	ND
H_2O^+	4.50	4.43	4.35	4.42	4.52	4.49	4.39	4.36	4.59	4.62	4.67	4.63	4.55	4.57	4.55	4.56	4.63
-O≡F	0.07	0.06	0.16	0.08	0.06	0.06	0.06	0.05	ND	ND	ND	0.03	0.05	0.03	0.03	ND	ND
-O≡Cl	ND	ND	ND	ND	ND	ND	ND	ND	ND	ND	ND	ND	ND	ND	ND	ND	ND
Total	100.19	97.92	99.62	98.36	99.01	99.15	97.42	95.92	100.57	100.54	101.25	101.61	100.92	101.10	100.92	99.48	100.59
Number of atoms (apfu):																	
Si	5.93	5.62	6.30	6.08	5.84	6.11	5.84	6.07	6.07	6.12	6.19	6.19	6.19	6.21	6.26	6.20	6.09
Al^{IV}	2.07	2.38	1.70	1.92	2.16	1.89	2.16	1.93	1.93	1.88	1.81	1.81	1.81	1.79	1.74	1.80	1.91
Al^{VI}	3.86	3.94	3.69	3.85	3.96	3.86	3.89	3.88	3.80	3.89	3.90	3.87	3.85	3.85	3.76	3.85	3.90
Ti	0.01	0.01	<0.01	ND	ND	ND	0.01	ND	0.01	0.01	ND	ND	ND	0.01	0.01	ND	<0.01
Cr	ND	ND	ND	ND	ND	ND	ND	ND	ND	ND	ND	ND	0.01	ND	0.01	ND	ND
Fe^{2+}	0.12	0.08	0.19	0.12	0.08	0.11	0.10	0.11	0.15	0.08	0.07	0.08	0.07	0.09	0.10	0.08	0.05
V	0.01	ND	ND	ND	ND	ND	ND	0.01	ND	ND	ND	0.01	0.01	ND	0.01	0.01	ND
Mn^{2+}	ND	ND	ND	ND	ND	ND	ND	ND	ND	ND	ND	ND	ND	ND	0.01	0.01	ND
Mg	0.08	0.04	0.21	0.11	0.04	0.09	0.08	0.07	0.17	0.07	0.08	0.09	0.10	0.08	0.14	0.09	0.10
Ca	0.11	0.35	0.01	0.10	0.22	0.12	0.21	0.07	0.07	0.08	0.03	0.03	0.02	ND	0.01	0.07	0.08
Na	0.81	1.02	0.28	0.68	1.09	0.79	0.78	0.91	0.53	0.59	0.61	0.49	0.29	0.26	0.29	0.46	0.66
K	0.91	0.50	1.42	0.95	0.45	0.79	0.82	0.81	1.18	1.10	1.13	1.26	1.54	1.57	1.54	1.22	1.05
Ba	0.04	0.03	0.04	0.03	0.03	0.03	0.04	0.03	0.02	0.01	ND	0.01	0.01	0.01	0.02	0.02	0.01
F	0.07	0.06	0.16	0.08	0.06	0.06	0.06	0.05	ND	ND	ND	0.02	0.05	0.03	0.03	ND	ND
Cl	ND	ND	ND	ND	ND	ND	ND	ND	ND	ND	ND	ND	ND	ND	ND	ND	ND
OH	3.93	3.94	3.84	3.92	3.94	3.94	3.94	3.95	4.00	4.00	4.00	3.98	3.95	3.97	3.97	4.00	4.00

Notes: Formulas are calculated on the basis of 22 oxygen equivalents. All iron is given as ferric iron. H_2O^+ is calculated. ND = not detected.

	WT22-109	WT22-163		WT22-222							WT22-256						
	10	1	2	1	2	3	4	5	6	7	8	9	1	2	4	5	6
Major elements (weight %; EMP):																	
SiO_2	46.00	46.53	46.66	47.13	46.96	47.71	46.62	46.47	47.76	46.51	47.12	47.14	45.91	48.81	46.34	44.75	46.22
TiO_2	ND	0.08	0.09	0.11	0.12	0.14	0.21	0.12	0.08	0.12	0.05	0.13	0.14	ND	0.16	0.13	0.12
Al_2O_3	37.58	36.83	36.95	38.59	36.24	36.64	36.58	36.49	36.02	36.80	35.46	37.38	36.11	36.21	35.69	35.58	35.54
Cr_2O_3	ND	ND	ND	ND	ND	ND	0.05	ND	ND	ND	0.07	ND	ND	ND	ND	0.05	ND
FeO	0.72	0.84	0.64	0.25	0.46	0.30	0.55	0.38	0.31	0.36	0.39	0.38	0.29	0.64	0.47	0.57	0.12
V_2O_3	ND	ND	0.05	ND	ND	0.08	0.07	0.06	0.07	ND	0.15	ND	ND	ND	ND	0.10	ND
MnO	ND	0.07	0.10	ND	ND	ND	ND	ND	ND	ND	0.05	ND	ND	ND	ND	0.12	ND
MgO	0.42	0.97	0.53	0.53	0.78	0.61	0.96	0.55	0.83	0.57	0.99	1.04	0.73	1.05	1.06	3.36	0.84
CaO	0.51	0.19	0.15	0.19	0.05	ND	0.10	0.17	ND	0.09	0.15	ND	ND	0.13	ND	0.16	ND
BaO	0.13	0.26	0.36	0.19	0.19	0.23	0.20	0.16	0.13	0.24	0.26	0.23	0.31	0.22	0.07	0.25	0.12
Na_2O	1.23	3.01	2.52	3.41	1.26	1.58	1.86	2.60	1.18	2.99	1.16	1.65	0.68	0.66	0.68	0.72	0.69
K_2O	8.76	5.66	7.38	6.18	9.33	9.30	7.94	6.90	9.54	6.37	9.24	8.96	10.28	9.22	9.91	8.95	10.16
F	0.07	0.18	0.16	0.22	0.26	0.20	0.25	0.26	0.30	0.06	0.32	0.13	0.17	0.26	0.34	0.32	0.26
Cl	ND	0.15	ND	ND	ND	ND	ND	0.07	ND	0.05	ND	ND	ND	ND	ND	ND	ND
H_2O^+	4.52	4.44	4.50	4.56	4.43	4.52	4.44	4.38	4.44	4.50	4.38	4.57	4.40	4.52	4.34	4.35	4.35
-O≡F	0.03	0.08	0.07	0.09	0.11	0.08	0.11	0.11	0.13	0.03	0.13	0.05	0.07	0.11	0.14	0.13	0.11
-O≡Cl	ND	0.03	ND	ND	ND	ND	ND	0.02	ND	0.01	ND	ND	ND	ND	ND	ND	ND
Total	99.91	99.10	100.02	101.27	99.97	101.22	99.73	98.49	100.54	98.62	99.66	101.55	98.95	101.61	98.92	99.27	98.31
Number of atoms (apfu):																	
Si	6.06	6.12	6.12	6.06	6.19	6.20	6.13	6.16	6.25	6.14	6.23	6.11	6.14	6.30	6.18	5.97	6.20
Al^{IV}	1.94	1.88	1.88	1.94	1.81	1.80	1.87	1.84	1.75	1.86	1.77	1.89	1.86	1.70	1.82	2.03	1.80
Al^{VI}	3.89	3.82	3.83	3.90	3.81	3.82	3.80	3.86	3.80	3.87	3.76	3.81	3.83	3.81	3.79	3.56	3.82
Ti	ND	0.01	0.01	0.01	0.01	0.01	0.02	0.01	0.01	0.01	<0.01	0.01	0.01	ND	0.02	0.01	0.01
Cr	ND	ND	ND	ND	ND	ND	0.01	ND	ND	ND	0.01	ND	ND	ND	ND	0.01	ND
Fe^{2+}	0.08	0.09	0.07	0.03	0.05	0.03	0.06	0.04	0.03	0.04	0.04	0.04	0.03	0.07	0.05	0.06	0.01
V	ND	ND	0.01	ND	ND	0.01	0.01	0.01	0.01	ND	0.02	ND	ND	ND	ND	0.01	ND
Mn^{2+}	ND	0.01	0.01	ND	ND	ND	ND	ND	ND	ND	0.01	ND	ND	ND	ND	0.01	ND
Mg	0.08	0.19	0.10	0.10	0.15	0.12	0.19	0.11	0.16	0.11	0.20	0.20	0.15	0.20	0.21	0.67	0.17
Ca	0.07	0.03	0.02	0.03	0.01	ND	0.01	0.02	ND	0.01	0.02	ND	ND	0.02	ND	0.02	ND
Na	0.31	0.77	0.64	0.85	0.32	0.40	0.47	0.67	0.30	0.77	0.30	0.41	0.18	0.17	0.18	0.19	0.18
K	1.47	0.95	1.24	1.01	1.57	1.54	1.33	1.17	1.59	1.07	1.56	1.48	1.75	1.52	1.69	1.52	1.74
Ba	0.01	0.01	0.02	0.01	0.01	0.01	0.01	0.01	0.01	0.01	0.01	0.01	0.02	0.01	<0.01	0.01	0.01
F	0.03	0.07	0.07	0.09	0.11	0.08	0.10	0.11	0.12	0.03	0.13	0.05	0.07	0.11	0.14	0.13	0.11
Cl	ND	0.03	ND	ND	ND	ND	ND	0.02	ND	0.01	ND	ND	ND	ND	ND	ND	ND
OH	3.97	3.89	3.93	3.91	3.89	3.92	3.90	3.88	3.88	3.96	3.87	3.95	3.93	3.89	3.86	3.87	3.89

Notes: Formulas are calculated on the basis of 22 oxygen equivalents. All iron is given as ferric iron. H_2O^+ is calculated. ND = not detected.

	WT22-256					WT22-277							WT22-322				
	7	8	9	10	11	1	2	3	4	5	6	7	1	2	3	4	5
Major elements (weight %; EMP):																	
SiO_2	46.65	45.61	45.82	46.99	46.89	46.18	46.95	46.18	46.82	46.28	46.76	47.20	44.60	46.14	46.13	49.08	45.95
TiO_2	0.09	0.10	0.10	0.09	0.09	0.05	ND	ND	ND	0.05	ND	ND	0.18	0.07	0.22	0.25	0.17
Al_2O_3	36.78	35.27	37.34	35.55	37.03	37.30	37.96	37.37	37.97	37.48	37.64	38.03	34.98	35.36	34.47	33.91	35.21
Cr_2O_3	ND	ND	ND	ND	ND	ND	ND	ND	ND	0.06	ND	0.05	ND	ND	ND	ND	ND
FeO	0.11	0.26	0.20	0.31	0.13	0.89	0.34	0.41	0.45	0.20	0.39	0.34	5.10	2.69	3.29	2.23	3.00
V_2O_3	0.06	ND	0.10	0.09	ND	0.05	0.09	ND	0.07	0.06	0.15	ND	0.07	0.06	0.05	ND	0.17
MnO	ND	ND	0.10	ND	0.06	ND	ND	ND	ND	ND	0.09	ND	0.10	ND	0.09	ND	ND
MgO	0.64	1.03	0.64	1.00	0.74	0.27	0.27	0.23	0.28	0.21	0.31	0.32	1.09	0.49	0.50	0.51	0.52
CaO	ND	ND	0.24	ND	ND	ND	0.07	0.25	0.05	0.05	0.09	0.09	0.07	ND	ND	0.06	ND
BaO	ND	0.11	0.25	0.05	0.13	0.13	0.22	0.05	0.12	0.17	0.13	0.09	0.48	0.33	0.28	0.19	0.21
Na_2O	0.75	0.71	0.90	0.72	0.77	1.19	1.04	1.05	1.03	0.96	1.00	0.97	1.27	1.15	1.12	2.22	1.09
K_2O	10.49	9.86	9.99	9.95	10.32	9.31	9.28	9.16	9.45	9.58	9.41	9.28	8.22	9.67	9.83	8.40	9.66
F	0.29	0.27	0.20	0.30	0.25	0.19	0.17	0.13	0.13	0.09	0.12	0.17	0.32	0.38	0.33	0.30	0.34
Cl	ND	ND	ND	ND	ND	ND	0.06	0.05	ND	ND	ND	ND	ND	ND	ND	ND	ND
H_2O^+	4.41	4.30	4.45	4.38	4.46	4.45	4.51	4.46	4.54	4.50	4.53	4.54	4.32	4.33	4.33	4.46	4.34
-O≡F	0.12	0.11	0.08	0.13	0.11	0.08	0.07	0.05	0.05	0.04	0.05	0.07	0.13	0.16	0.14	0.13	0.14
-O≡Cl	ND	ND	ND	ND	ND	ND	0.01	0.01	ND	ND	ND	ND	ND	ND	ND	ND	ND
Total	100.15	97.40	100.25	99.30	100.77	99.93	100.88	99.28	100.86	99.65	100.57	101.01	100.67	100.51	100.50	101.48	100.52
Number of atoms (apfu):																	
Si	6.15	6.18	6.05	6.23	6.14	6.09	6.12	6.11	6.10	6.11	6.12	6.13	5.98	6.14	6.16	6.40	6.12
Al^{IV}	1.85	1.82	1.95	1.77	1.86	1.91	1.88	1.89	1.90	1.89	1.88	1.87	2.02	1.86	1.84	1.60	1.88
Al^{VI}	3.86	3.80	3.85	3.79	3.85	3.89	3.94	3.94	3.94	3.94	3.92	3.95	3.51	3.68	3.59	3.61	3.65
Ti	0.01	0.01	0.01	0.01	0.01	<0.01	ND	ND	ND	<0.01	ND	ND	0.02	0.01	0.02	0.02	0.02
Cr	ND	ND	ND	ND	ND	ND	ND	ND	ND	0.01	ND	0.01	ND	ND	ND	ND	ND
Fe^{2+}	0.01	0.03	0.02	0.03	0.01	0.10	0.04	0.05	0.05	0.02	0.04	0.04	0.57	0.30	0.37	0.24	0.33
V	0.01	ND	0.01	0.01	ND	0.01	0.01	ND	0.01	0.01	0.02	ND	0.01	0.01	0.01	ND	0.02
Mn^{2+}	ND	ND	0.01	ND	0.01	ND	ND	ND	ND	ND	0.01	ND	0.01	ND	0.01	ND	ND
Mg	0.13	0.21	0.13	0.20	0.14	0.05	0.05	0.05	0.05	0.04	0.06	0.06	0.22	0.10	0.10	0.10	0.10
Ca	ND	ND	0.03	ND	ND	ND	0.01	0.04	0.01	0.01	0.01	0.01	0.01	ND	ND	0.01	ND
Na	0.19	0.19	0.23	0.19	0.20	0.30	0.26	0.27	0.26	0.25	0.25	0.24	0.33	0.30	0.29	0.56	0.28
K	1.76	1.70	1.68	1.68	1.72	1.57	1.54	1.55	1.57	1.61	1.57	1.54	1.41	1.64	1.68	1.40	1.64
Ba	ND	0.01	0.01	<0.01	0.01	0.01	0.01	<0.01	0.01	0.01	0.01	<0.01	0.03	0.02	0.01	0.01	0.01
F	0.12	0.12	0.08	0.13	0.10	0.08	0.07	0.05	0.05	0.04	0.05	0.07	0.14	0.16	0.14	0.12	0.14
Cl	ND	ND	ND	ND	ND	ND	0.01	0.01	ND	ND	ND	ND	ND	ND	ND	ND	ND
OH	3.88	3.88	3.92	3.87	3.90	3.92	3.92	3.93	3.95	3.96	3.95	3.93	3.86	3.84	3.86	3.88	3.86

Notes: Formulas are calculated on the basis of 22 oxygen equivalents. All iron is given as ferric iron. H_2O^+ is calculated. ND = not detected.

	WT22-322					WT22-329										WT24-327	
	6	7	8	9	10	1	2	3	4	5	6	7	8	9	10	1	2
Major elements (weight %; EMP):																	
SiO_2	46.06	45.97	44.55	46.63	45.69	46.91	46.18	45.39	45.40	46.27	45.30	45.64	45.50	46.51	46.28	48.87	49.07
TiO_2	0.18	0.15	1.75	0.20	0.17	0.21	0.26	0.14	0.33	0.15	0.25	0.23	0.24	0.19	0.07	0.38	0.31
Al_2O_3	35.62	35.91	34.63	34.95	35.57	34.40	34.60	35.80	34.60	35.37	34.58	33.90	34.92	34.07	35.15	32.59	32.75
Cr_2O_3	0.06	ND	ND	ND	ND	ND	ND	ND	ND	0.07	ND	ND	ND	ND	ND	0.10	ND
FeO	2.88	2.76	2.80	2.91	2.90	3.14	2.26	2.16	2.67	2.32	3.23	2.50	2.75	2.43	2.08	1.49	1.52
V_2O_3	ND	ND	ND	ND	ND	ND	ND	ND	ND	0.07	ND	ND	ND	ND	ND	ND	ND
MnO	0.07	ND	ND	0.09	0.05	0.09	ND	ND	ND	ND	ND	ND	ND	ND	ND	ND	ND
MgO	0.42	0.42	0.40	0.51	0.43	0.86	0.61	0.41	0.57	0.60	0.60	0.57	0.55	0.52	0.57	1.22	1.38
CaO	0.06	0.05	0.07	ND	ND	ND	ND	ND	ND	ND	ND	ND	ND	ND	ND	ND	ND
BaO	0.32	0.28	0.23	0.19	0.37	0.35	0.34	0.50	0.60	0.36	0.25	0.23	0.23	0.59	0.29	0.21	0.19
Na_2O	1.23	1.19	1.10	0.97	1.13	0.67	0.68	0.91	0.67	0.72	0.74	0.84	0.76	0.88	0.88	0.28	0.34
K_2O	9.62	9.44	9.69	9.84	9.84	10.48	10.00	9.92	9.78	10.00	9.87	9.70	10.02	9.98	9.89	10.59	10.86
F	0.31	0.38	0.26	0.32	0.26	0.23	0.22	0.07	0.24	0.16	0.19	0.09	0.14	0.23	0.21	0.27	0.30
Cl	ND	ND	ND	ND	ND	ND	ND	ND	ND	ND	ND	0.09	ND	ND	ND	ND	ND
H_2O^+	4.38	4.34	4.33	4.37	4.38	4.43	4.36	4.44	4.32	4.44	4.35	4.34	4.39	4.36	4.39	4.40	4.41
-O≡F	0.13	0.16	0.11	0.13	0.11	0.10	0.09	0.03	0.10	0.07	0.08	0.04	0.06	0.10	0.09	0.11	0.13
-O≡Cl	ND	ND	ND	ND	ND	ND	ND	ND	ND	ND	ND	0.02	ND	ND	ND	ND	ND
Total	101.08	100.73	99.70	100.85	100.68	101.67	99.42	99.71	99.08	100.46	99.28	98.07	99.44	99.66	99.72	100.29	101.01
Number of atoms (apfu):																	
Si	6.10	6.10	6.00	6.18	6.09	6.20	6.20	6.09	6.14	6.15	6.12	6.21	6.12	6.25	6.18	6.47	6.46
Al^{IV}	1.90	1.90	2.00	1.82	1.91	1.80	1.80	1.91	1.86	1.85	1.88	1.79	1.88	1.75	1.82	1.53	1.54
Al^{VI}	3.66	3.71	3.50	3.65	3.67	3.56	3.67	3.74	3.66	3.69	3.63	3.65	3.66	3.64	3.72	3.55	3.54
Ti	0.02	0.01	0.18	0.02	0.02	0.02	0.03	0.01	0.03	0.01	0.03	0.02	0.02	0.02	0.01	0.04	0.03
Cr	0.01	ND	ND	ND	ND	ND	ND	ND	ND	0.01	ND	ND	ND	ND	ND	0.01	ND
Fe^{2+}	0.32	0.31	0.32	0.32	0.32	0.35	0.25	0.24	0.30	0.26	0.36	0.28	0.31	0.27	0.23	0.16	0.17
V	ND	ND	ND	ND	ND	ND	ND	ND	ND	0.01	ND	ND	ND	ND	ND	ND	ND
Mn^{2+}	0.01	ND	ND	0.01	0.01	0.01	ND	ND	ND	ND	ND	ND	ND	ND	ND	ND	ND
Mg	0.08	0.08	0.08	0.10	0.09	0.17	0.12	0.08	0.11	0.12	0.12	0.12	0.11	0.10	0.11	0.24	0.27
Ca	0.01	0.01	0.01	ND	ND	ND	ND	ND	ND	ND	ND	ND	ND	ND	ND	ND	ND
Na	0.32	0.31	0.29	0.25	0.29	0.17	0.18	0.24	0.18	0.19	0.19	0.22	0.20	0.23	0.23	0.07	0.09
K	1.63	1.60	1.67	1.66	1.67	1.77	1.71	1.70	1.69	1.70	1.70	1.68	1.72	1.71	1.69	1.79	1.82
Ba	0.02	0.01	0.01	0.01	0.02	0.02	0.02	0.03	0.03	0.02	0.01	0.01	0.01	0.03	0.02	0.01	0.01
F	0.13	0.16	0.11	0.13	0.11	0.10	0.09	0.03	0.10	0.07	0.08	0.04	0.06	0.10	0.09	0.11	0.12
Cl	ND	ND	ND	ND	ND	ND	ND	ND	ND	ND	ND	0.02	ND	ND	ND	ND	ND
OH	3.87	3.84	3.89	3.87	3.89	3.90	3.91	3.97	3.90	3.93	3.92	3.94	3.94	3.90	3.91	3.89	3.88

Notes: Formulas are calculated on the basis of 22 oxygen equivalents. All iron is given as ferric iron. H_2O^+ is calculated. ND = not detected.

	WT24-327				WT24-488												
	3	4	5	6	1	2	3	4	5	6	7	8	9	10	11	12	13
Major elements (weight %; EMP):																	
SiO_2	44.54	46.09	49.53	46.43	45.45	45.05	45.05	45.89	44.33	44.36	43.36	46.19	45.98	45.86	44.29	45.14	43.73
TiO_2	0.28	0.24	0.18	0.19	ND	ND	ND	0.06	0.06	ND	0.05	0.10	0.08	0.07	ND	ND	ND
Al_2O_3	32.97	33.52	30.64	34.30	36.01	40.59	40.01	36.65	37.96	38.39	38.29	36.15	36.25	38.67	40.03	38.83	41.24
Cr_2O_3	ND	ND	0.07	ND	ND	ND	ND	ND	ND	ND	ND	ND	ND	ND	ND	ND	ND
FeO	3.77	1.52	1.53	1.46	0.55	0.31	0.63	0.52	0.55	0.40	0.41	0.74	0.66	0.68	0.49	0.39	0.38
V_2O_3	0.05	ND	ND	ND	0.08	ND	ND	ND	ND	ND	ND	ND	ND	ND	0.20	0.08	0.16
MnO	0.12	ND	ND	ND	0.06	ND	ND	ND	ND	ND	ND	ND	ND	ND	ND	ND	ND
MgO	2.55	1.31	1.34	1.15	0.40	0.10	0.11	0.24	0.12	0.12	0.12	0.26	0.31	0.35	0.19	0.09	0.10
CaO	ND	ND	ND	ND	0.43	2.27	1.73	0.45	0.54	0.56	0.95	0.19	0.23	0.39	0.17	0.17	1.83
BaO	0.17	0.37	0.15	0.23	0.10	0.08	0.11	0.14	0.07	0.16	0.16	0.06	0.11	0.10	ND	0.06	0.08
Na_2O	0.32	0.34	0.30	0.42	4.69	4.24	4.67	4.94	6.02	5.83	5.09	3.11	3.03	4.38	5.66	5.89	3.84
K_2O	9.83	10.79	9.98	10.79	2.68	2.31	2.21	2.54	1.03	1.81	1.86	5.27	5.46	4.01	2.21	1.54	3.38
F	0.25	0.28	0.18	0.15	ND	0.10	0.06	0.09	ND	ND	ND	ND	ND	ND	0.05	0.06	0.05
Cl	ND	ND	ND	ND	0.05	ND	ND	ND	ND	ND	ND	ND	ND	ND	ND	ND	ND
H_2O^*	4.28	4.29	4.37	4.40	4.42	4.59	4.59	4.44	4.46	4.49	4.42	4.47	4.47	4.59	4.54	4.51	4.58
-O≡F	0.11	0.12	0.08	0.06	ND	0.04	0.03	0.04	ND	ND	ND	ND	ND	ND	0.02	0.03	0.02
-O≡Cl	ND	ND	ND	ND	0.01	ND	ND	ND	ND	ND	ND	ND	ND	ND	ND	ND	ND
Total	99.03	98.64	98.20	99.46	94.91	99.60	99.14	95.92	95.14	96.12	94.71	96.54	96.58	99.10	97.81	96.73	99.35
Number of atoms (apfu):																	
Si	6.07	6.24	6.66	6.22	6.15	5.82	5.85	6.14	5.96	5.93	5.88	6.19	6.17	5.99	5.82	5.97	5.70
Al^{IV}	1.93	1.76	1.34	1.78	1.85	2.18	2.15	1.86	2.04	2.07	2.12	1.81	1.83	2.01	2.18	2.03	2.30
Al^{VI}	3.36	3.60	3.52	3.64	3.90	4.00	3.98	3.92	3.98	3.98	4.00	3.91	3.91	3.94	4.02	4.02	4.03
Ti	0.03	0.02	0.02	0.02	ND	ND	ND	0.01	0.01	ND	0.01	0.01	0.01	0.01	ND	ND	ND
Cr	ND	ND	0.01	ND	ND	ND	ND	ND	ND	ND	ND	ND	ND	ND	ND	ND	ND
Fe^{2+}	0.43	0.17	0.17	0.16	0.06	0.03	0.07	0.06	0.06	0.04	0.05	0.08	0.07	0.07	0.05	0.04	0.04
V	0.01	ND	ND	ND	0.01	ND	ND	ND	ND	ND	ND	ND	ND	ND	0.02	0.01	0.02
Mn^{2+}	0.01	ND	ND	ND	0.01	ND	ND	ND	ND	ND	ND	ND	ND	ND	ND	ND	ND
Mg	0.52	0.26	0.27	0.23	0.08	0.02	0.02	0.05	0.02	0.02	0.02	0.05	0.06	0.07	0.04	0.02	0.02
Ca	ND	ND	ND	ND	0.06	0.31	0.24	0.06	0.08	0.08	0.14	0.03	0.03	0.05	0.02	0.02	0.26
Na	0.08	0.09	0.08	0.11	1.23	1.06	1.18	1.28	1.57	1.51	1.34	0.81	0.79	1.11	1.44	1.51	0.97
K	1.71	1.86	1.71	1.85	0.46	0.38	0.37	0.43	0.18	0.31	0.32	0.90	0.93	0.67	0.37	0.26	0.56
Ba	0.01	0.02	0.01	0.01	0.01	<0.01	0.01	0.01	<0.01	0.01	0.01	<0.01	0.01	0.01	ND	<0.01	<0.01
F	0.11	0.12	0.08	0.06	ND	0.04	0.02	0.04	ND	ND	ND	ND	ND	ND	0.02	0.03	0.02
Cl	ND	ND	ND	ND	0.01	ND	ND	ND	ND	ND	ND	ND	ND	ND	ND	ND	ND
OH	3.89	3.88	3.92	3.94	3.99	3.96	3.98	3.96	4.00	4.00	4.00	4.00	4.00	4.00	3.98	3.97	3.98

Notes: Formulas are calculated on the basis of 22 oxygen equivalents. All iron is given as ferric iron. H_2O^* is calculated. ND = not detected.

	WT24-488					WT25-434								
	14	15	16	17	18	19	20	21	1	2	3	4	5	6
Major elements (weight %; EMP):														
SiO_2	42.70	46.86	43.74	44.60	44.80	45.09	45.57	46.10	47.44	45.01	46.95	46.21	44.92	44.66
TiO_2	ND	0.11	ND	ND	ND	ND	ND	ND	0.11	0.06	0.05	0.09	0.09	0.09
Al_2O_3	41.00	37.61	39.95	40.44	39.70	39.46	37.88	39.34	35.36	35.15	35.85	34.87	35.78	34.86
Cr_2O_3	ND	ND	ND	ND	ND	ND	ND	ND	0.06	ND	ND	ND	ND	ND
FeO	0.33	0.82	0.38	0.40	0.57	0.41	0.49	0.55	1.91	2.57	1.05	2.92	2.69	3.13
V_2O_3	ND	0.06	ND	0.16	0.13	ND	0.07	0.24	ND	ND	ND	ND	ND	ND
MnO	ND	ND	ND	ND	ND	ND	ND	ND	ND	ND	ND	0.05	ND	ND
MgO	0.14	0.36	0.06	0.11	0.18	0.10	0.24	0.25	0.85	1.29	0.56	1.17	0.95	1.35
CaO	2.78	0.15	2.10	2.08	0.70	1.60	0.73	1.56	0.16	0.18	0.19	0.22	0.21	0.13
BaO	0.06	0.17	0.05	0.18	0.16	0.10	0.15	0.05	0.56	0.52	0.21	0.45	0.58	0.67
Na_2O	4.28	2.79	4.28	4.35	4.03	4.29	4.23	4.00	1.79	2.13	3.14	1.95	1.76	1.59
K_2O	2.02	6.34	2.38	2.50	4.18	2.42	3.35	3.21	7.68	6.76	5.43	6.82	7.66	7.63
F	0.05	ND	0.05	0.07	0.07	ND	0.09	ND	0.27	0.26	0.25	0.18	0.26	0.21
Cl	ND	ND	ND	ND	ND	ND	ND	ND	ND	ND	ND	ND	ND	ND
H_2O^+	4.52	4.60	4.51	4.59	4.55	4.58	4.48	4.65	4.44	4.32	4.40	4.41	4.35	4.33
-O≡F	0.02	ND	0.02	0.03	0.03	ND	0.04	ND	0.11	0.11	0.11	0.08	0.11	0.09
-O≡Cl	ND	ND	ND	ND	ND	ND	ND	ND	ND	ND	ND	ND	ND	ND
Total	97.86	99.87	97.48	99.45	99.04	98.05	97.25	99.95	100.51	98.14	97.98	99.27	99.14	98.56
Number of atoms (apfu):														
Si	5.63	6.11	5.78	5.79	5.86	5.91	6.04	5.95	6.23	6.07	6.23	6.16	6.03	6.05
Al^{IV}	2.37	1.89	2.22	2.21	2.14	2.09	1.96	2.05	1.77	1.93	1.77	1.84	1.97	1.95
Al^{VI}	4.00	3.90	4.00	3.98	3.99	4.00	3.95	3.93	3.70	3.66	3.83	3.64	3.69	3.61
Ti	ND	0.01	ND	ND	ND	ND	ND	ND	0.01	0.01	<0.01	0.01	0.01	0.01
Cr	ND	ND	ND	ND	ND	ND	ND	ND	0.01	ND	ND	ND	ND	ND
Fe^{2+}	0.04	0.09	0.04	0.04	0.06	0.04	0.05	0.06	0.21	0.29	0.12	0.33	0.30	0.35
V	ND	0.01	ND	0.02	0.01	ND	0.01	0.02	ND	ND	ND	ND	ND	ND
Mn^{2+}	ND	ND	ND	ND	ND	ND	ND	ND	ND	ND	ND	0.01	ND	ND
Mg	0.03	0.07	0.01	0.02	0.04	0.02	0.05	0.05	0.17	0.26	0.11	0.23	0.19	0.27
Ca	0.39	0.02	0.30	0.29	0.10	0.22	0.10	0.22	0.02	0.03	0.03	0.03	0.03	0.02
Na	1.09	0.71	1.10	1.09	1.02	1.09	1.09	1.00	0.46	0.56	0.81	0.50	0.46	0.42
K	0.34	1.06	0.40	0.41	0.70	0.40	0.57	0.53	1.29	1.16	0.92	1.16	1.31	1.32
Ba	<0.01	0.01	<0.01	0.01	0.01	0.01	0.01	<0.01	0.03	0.03	0.01	0.02	0.03	0.04
F	0.02	ND	0.02	0.03	0.03	ND	0.04	ND	0.11	0.11	0.10	0.08	0.11	0.09
Cl	ND	ND	ND	ND	ND	ND	ND	ND	ND	ND	ND	ND	ND	ND
OH	3.98	4.00	3.98	3.97	3.97	4.00	3.96	4.00	3.89	3.89	3.90	3.92	3.89	3.91

Notes: Formulas are calculated on the basis of 22 oxygen equivalents. All iron is given as ferric iron. H_2O^+ is calculated. ND = not detected.